Alexander von Humboldt
Stiftung/Foundation

2nd North African Conference on Computational Physics and Chemistry Humboldt Kolleg

NACCPC 2010

December 12th - 14th, 2010 - Oran -

University Of Sidi Bel-Abbès, Algeria

Conference Objectives

This conference, organized by the L2MSM laboratory of the Faculty of Sciences, University Djillali Liabes of Sidi Bel Abbès, Algeria, will bring together an international network of chemists and physicists interested in computational physics and chemistry methods in molecular, nano and material sciences. Since it is organized with the collaboration of the Alexander von Humboldt foundation (Bonn, Germany), the Conference in this field should attract participation of a number of Humboldtians from neighbouring countries and of researchers from various application areas who are pioneering advanced application of computational methods to sciences such as physics and chemistry.
The emphasis will be on innovative theory, computational realization and application. The present call concerns particularly young scientists among PhD students and post-docs whishing to present original research works either as oral contribution or poster.

Technical Topics Area

NAC-CPC'10 covers the following major thematic sessions:

*(Topic1): **Theoretical physics**
* (Topic2): **Theoretical chemistry**
* (Topic3): **Simulation and molecular modelling methods**
* (Topic4): **Material Science (Condensed matter, electronic structure, ab initio calculations, Molecular Dynamics, nanostructure)**
* (Topic5): **Molecular Structure and Spectroscopy**
* (Topic6): **Electrochemistry, large molecules**
* (Topic7): **Biological physics, drug design, bioinformatics, QSAR**
* Other fields **(especially for Humboldtians)**

President of the Conference
Prof. M. Sekkal-Rahal

Co-President of the Conference
Prof. A. Kadoun

Honored President
Prof. A. Tou

Honored Members
Prof. Aourag Hafid (Univ. Tlemcen, Algeria)

Prof. Mesli Abderrezak (Univ. S.B.A, Algeria)

Scientific Committee

International Members

Prof. Philippe Derreumaux (Univ. Paris VII, France)
Prof. Michael Springborg (Univ. Sarrlandes, Saarbruechen, Germany)
Prof. Manuel Dauchez (Univ. Reims, France).
Prof. Philip Bunker (NRC, Ottawa, Canada).
Prof. Cenk Selcuki (Aegean Univ., Izmir, Turkey).
Prof. Daniel Bougeard (USTL - Lille1, France)
Prof. Eric Monflier (Univ. D'Artois, France)
Prof. Adnane Abdelghani (Univ. El Manar, Tunisia)
Prof. Tangour Bahaouddine (Univ-Tunis, Tunisia)
Prof. Ellouze Mohammed (Univ-Sfax, Tunisia)
Prof. Abdelhadi Soudi (Univ. Rabat, Morocco)
Prof. Waheed.A. Badaoui (Univ. Cairo, Egypt)
Prof. Christian Mathieu (Univ. d'Artois, France)
Dr. Adlane Sayede (Univ. d'Artois, France)
Dr. Amal Maurady (Univ. Tanger, Morocco)

National Members

Prof. Abdelghani Krallafa (Univ. Es-Senia Oran)
Prof. Ali Rahmouni (Univ . Saida)
Prof. Redjem Hadef (Univ. Oum El Bouaghi)
Prof. Nasredine Chabane-Sari (Univ. Tlemcen)
Prof. Boumediène Benyoucef (Univ. Tlemven)
Prof. Boucif Abdeslem (Centre Univ. Aïn Témouchent)
Prof. Berrezoug Belgoumène (Univ. Saida)
Prof. Majda Sekkal-Rahal (Univ. Sidi Bel Abbès)
Prof. Abd-Ed-Daim Kadoun (Univ. Sidi Bel Abbès)
Prof. Kadour Guemra (Univ. Sidi Bel Abbès)
Prof. Zineb. Benamara (Univ. Sidi Bel Abbès)
Prof. Ghaouti Bassou (Univ. Sidi Bel Abbès)
Prof. Bachir Bouhafs (Univ. Sidi Bel Abbès)
Prof. Boucif Abbar (Univ. Sidi Bel Abbès)
Dr. Omar Benhelal (Univ. Sidi Bel Abbès)
Dr. I.N. Taleb-Mokhtari (Univ. S.B.A, Algeria)

Organizing Committee

Dr. I.N. Taleb-Mokhtari
Dr. N. Yousfi (Univ. S.B.A, Algeria)
Dr. O. Benhelal (Univ. S.B.A, Algeria)
Dr. A. Lazreg (Univ. S.B.A, Algeria)
Dr. O. Mansour (Univ. S.B.A, Algeria)
Dr. Y. Mahmoud (Univ. S.B.A, Algeria)
Dr. M. Bendahmene (Univ. S.B.A, Algeria)
Mr. A. Taalbi (Univ. S.B.A, Algeria)
Mr. M. Bouterfas (Univ. S.B.A, Algeria)
Mr. M.H. Gaffour (Univ. S.B.A, Algeria)
M^{rs} S.N. Derrar (Univ. S.B.A, Algeria)
M^{rs} R. Fodil (Univ. S.B.A, Algeria)
M^{rs} N. Méçabih (Univ. S.B.A, Algeria)
M^{rs} K. Sail (Univ. S.B.A, Algeria)
M^{rs} R. Khatir (Univ. S.B.A, Algeria)
Mr. M. Rezki (Univ. S.B.A, Algeria)

List of participants

Plenary lectures

P. A. Bopp	On the Motions of Water in Chabazite, a Molecular Dynamics Study
D. Bougeard	Modeling and vibrational spectroscopy applied to the study of the dynamics in aluminosilicates
M. Dauchez	Molecular modeling of EBP-Elastin Binding Protein: docking of different ligands
P. Derreumaux	Protein and rna computer simulations
A. Kadri	Built-in strain, electric field, and spin polarization effects in wide bandgap semiconductor materials and nano-devices
C. Schmidt	Shear-Induced Structures in Lyotropic Liquid Crystals Investigated by NMR Spectroscopy
E. Spohr	Molecular Dynamics Modeling of Proton Discharge at the Aqueous / Metallic Interface
M. Springborg	Determining and Analyzing the Structure of Clusters

Contributed Oral Presentations

A. H. Abadi	Computational Insight: Oral Phosphodiesterase 5 Inhibitors for Erectile Dysfunction
A. Abdelghani	Advanced Apparatus for Pathogen Detection
A. Al-Ajlouni	Kinetics and DFT studies on the Catalytic Epoxidation of Olefins by η^5-Cyclopentadienyl Molybdenum Catalysts
Y. A. Al-Soud	Synthesis Approaches And Pharmacological Importance of 1,2,4-Triazoles
A. Arhrib	CP Violation in Fourth Generation Quark Decays

W. A. Badawy	Application of nanotechnology in solar cell fabrication – Future perspectives
N. Benghozlen	Ultrasonic guided waves in functionally graded piezoelectric hetero structure
E. Bruyer	Multiferroic behaviour of $(SrTiO_3)_n$-$(BiFeO_3)_m$ heterostructures predicted from first-principles calculations
L. Belkhiri	Complexes of lanthanide and actinides. Between theoretical challenges and contributions of DFT/ZORA relativistic method!
F. Benmouna	Effects of Crosslinker and Porogen on Microfluidic Properties of Polymer Based Monolithic Systems
A. Bendounan	Electronic properties of low dimensional structures
B.A. Cheba	Laser Biomedical Physics:Principles and Applications
S. Chatti	Elaboration of new biopolymers based on sugar diols and characterization by NMR and MALDI-TOFs
M. El-khateeb	Spectroscopic and computational analysis [FeFe]-Hydrogenase Models with Bridging Moieties Containing (S, Se) and (S, Te)
A. El-Azhary	Conformational and Vibrational analysis of Crown Ethers
M. Ellouze	Properties of iron substituted manganese $La_{0.67}Sr_{0.33}Fe_xMn_{1-x}O_3$ nano-manganites oxide
Y. Hannachi	DFT study of the interaction of iron dimer with benzene
A. Idrissi	On the characterization of cluster distribution in supercritical fluids: A molecular dynamics and data mining approaches
S. Lakhdar	Mechanisms in Aminocatalysis
B. Lasri	NEW OF SCHWINGER VARIATIONNAL PRINCIPLE FOR K-SHELL EXCITATION OF $Ca^{18+}(1S^2)$ ions by impact of various atoms at 8.6 MeV/amu
A. Mazzah	Surface modification of plasma-treated polyethylene with fluorinated alcohols using chlorinated phosphazenes as coupling agents
C. Misbah	Modeling blood flow and cell motility: a physicist view
A. Selmi	Magnetism and technology

M. Said	Optical performances of InAs/GaSb/InSb short-period superlattice laser diode for mid-infrared emission
C. Selcuki	Computational Investigation of Metal Ion-Peptide Interactions
A. Souifi	Transistors à un électron à température ambiante : une revue
A. Sayede	Multiferroic behaviour of $(SrTiO_3)_n$-$(BiFeO_3)_m$ heterostructures predicted from first-principles calculations
B. Tanguour	New behavior of molecules confined in carbon nanotubes

Posters Session1

F.Z. Aoumeur	Structural and Dynamical properties of SrO in the Rock-salt phase
F. Azza	Interaction electron-gas in an HPSEM: Application to CO_2 and comparison with H_2 and H_2O
R. Becharef	EBIC microscopy investigations on microelectronic devices
R. Bellatreche	Radial Confinement Study of the Taylor Couette Flow
B. Benaffane	Full-potential study of structural and electronic properties of β-ZrNX (X = Cl,Br and I)
F. Benharrats	Computational Studies of Optoelectronic Properties of ZnO/MgO/CdO Nanostructures
O. Benhelal	First-principles calculations of the structural and electronic properties of semiconducting intermetallics compounds $RuGa_3$, and $OsGa_3$ in the $FeGa_3$-type structure
K. Benkabou	Tight Binding calculation Of Electronic Properties Of Ternary Alloy ZnS_xSe_{1-x}
N.H. Benmansour	The Importance of the Resonance in the Calculation of Relative Intensities of Emission of Ion FE^{+16}
A. Boutasta	Structural Study of the Neurotransmitter by the Ab-initio Methods and Spectroscopy
M.Z. Chekroun	Etude des résonances plasmons dans les Nano-fils en Ag

S. Dergal	Electronic and Elastic Properties of Hypothetical Zinc Blende $Sc_xIIIA_{1-x}N$ (IIIA= Al, Ga and In): Empirical Pseudopotential Methode Calculation
A. Djellal	Ab-initio and *k.P* simulations of $In_xGa_{1-x}N/Mg_yZn_{1-y}O$ and $In_xAl_{1-x}N/Mg_yZn_{1-y}O$ Quantum Nanostructured Lasers
M. Djermouni	LDA+U+SOC Ab-initio Study of Magnetic Behavior and Electronic Structure of RE5Ge3 Intermetallics Compounds
Z. Dridi	Study of the origin of ferromagnetism in $Ga_{1-x}Gd_xN$
A. Dekhira	Development of software for photonic crystal simulation and analysis using FDTD and PWE methods
M. Gallouze	Atomistic Study of Hydrogen Absorption FeAl BULK
A. Hallouch	First-principles prediction of electronic and magnetic properties of REPtBi (RE= Rare Earth Element) half-Heusler by LSDA+U calculations
N. Iles	Orientation effect on ferroelectric surface stability of $BaTiO_3$
S. Laksari	Full-potential study of structural and electronic properties of MB_2-type metal diborides (M=Be, Mg and Ca)
A. Lazreg	First-principles study of the magnetic properties of $Al_{1-x}Gd_xN$
S. Lecheheb	Analytical approach of the Graëtz heat exchanger in MHD
F. Litimein	Structural, electronic and thermodynamic properties of Bi_2O_3 from First Principles Calculations
O. Mansour	Electrons beam behavior in a gas mixture under low voltage in the environmental SEM
H. Mazari	Evolution of physical properties according to the stoichiometric coefficient x of the alloy $In_xGa_{1-x}N$ intended for photovoltaic devices
H. M. A. Mazouz	First principles lattice dynamics and thermodynamical study of Thallium-V compounds
R. Mebsout	First-principles calculations of the structural and electronic properties of three semiconducting intermetallics compounds RuAl2, RuGa2 and OsAl2 in the TiSi2-type structure
S. Medina	Electronic and structural properties of the quaternary chalcopyrites $Cu_2FeAlSe_2$ and $CuFe_2AlSe_4$

S. Méziane	Ab-intio study of structural, electronic and mechanical properties of intermetallics of typeTM-Al
F. Mezrag	The effect of zinc concentration upon optical properties of $Cd_{1-x}Zn_xSe$
D. Missaoui	Conformational Study of Some α-ketophosphonates
A. Mokadem	Full-potential study of structural and electronic properties of metal nitride halide chlorides, β-MNCl (M = Ti,Zr and Hf)
M. Mostefaoui	Simulation of photovoltaic parameters of a solar cell
M. Naoui	Theoretical Studies of Structural Properties of the Complexes of Pd, Rh, Ru With Hemilabile Ligands (BPMO's)
K. Ouadah	DFT Calculations of the Structural and Electronic Properties of Spinosyns A and D
M. Ouali	Study of Non Linear Instability of Taylor in the Vicinity of its Appearance
L. Rabahi	Theoretical study of structural and thermal properties of Fe_2 (Zr, Nb) Laves alloys
K. Rahmoun	Vickers Indentation Method used for Elastic Properties Characterization of Porous Silicon Thin Films
K. Saïl	Polishing effect of samples on WDS microanalysis X
H. Sediki	Ab initio calculations and structures properties correlation of SiO2 polymorphs
A. Sekkal	Structural and thermoelastic properties of the B2–YX (X=Cu, Mg and Rh) intermetallic compounds
F. Serdouk	Determination of the density of states (DOS) of the amorphous semiconductors using Laplace Technics
N.Settouti	Computation and prediction of exchange and correlation energy in density functional theory using data mining methods
H. Si Abdelkader	First-principles calculations of Mo/ZrC interface and Re alloying effects on adhesion
K. Smail	Theoretical Study of the Structural and Electronic Properties of Luteolin
F.Smain	Effective interaction and structure of charge-stabilized colloidal suspension

H.Tabet-Derraz A Comparaison of Experimental and Theoretical Optical Constants of the ZnxCd1-xO (x=1-0.6 - 0.4 - 0) Thin Films

A. Taalbi Analysis of Channel Filter Based on Photonic Crystals Ring Resonator

N. Tayebi Electronic Band structure of $Ga_xIn_{1-x}As$

N. Tchouar Numerical Simulation of Thermodynamics, Structural and Transport Properties of Liquid Para-Hydrogen by the Quantum Molecular Dynamics

M. Y. Mahmoud Optical channel drop filter based on dual ring photonic crystal ring resonators, a wavelength division demultiplexer based on photonic crystal ring resonator

B. Zebentout Simulation and optimization of photovoltaic parameters in single and tandem junction thin film silicon solar cells

H. Zenasni First principle prediction of half-metallic ferrimagnetism in the Heusler alloys Mn2TiZ(Z=Al,As,Bi,Ga,Ge,Sb,Si,Sn) in high ordered structure

R. Zine El Kelma Electronic structure of the tetragonal ternary iron arsenide $BaFe_2As_2$: Contribution of itinerant Fe 3*d*-states to the Fermi Level

Posters Session2

S. Abdalla Theoretical study of tautomerization and iomerization of methylphosphino- and Phenylphosphino-substituted cyclic azaphospholines, oxphospholines and thiaphospholines in gas and aqueous phases

S. Abdelkrim Theoretical Study of the Reaction of Rearrangement of 1,3 DIAZA-CLAISEN

H. Aliouat Influence of Amino Acid Side Chain Preceding Azaprolyl Residue on β-turn Stabilization

A. Amar Theoretical Research of the Obtained Isomer in the Synthesis of New Derivative Pyrazolones: DFT Modelling

N. Bekhti-Bensalem. Harmonic dynamics of β-D- RHAMNOSE in the crystalline state.

O. Belaidi The Molecular Conformation of 2-Ethylhexyl Acrylate, an Infrared and Abinitio Study

O. Benali Correlation Between Molecular Structure and Inhibition Efficiency Against Corrosion of Two Tautomers of 2-Mercapto 1-Methyl Imidazole

M. Bendahmane Physicochemical properties, pollen spectra, and antimicrobial activity of few varieties of honeys harvested in western and central regions of Algeria

H. Benhassaini Contribution of microscopic techniques to anatomical and morphological knowledge on *Pistacia atlantica* Desf. ssp. atlantica in Algeria

M. Benmalti Theoretical Study and Car Parrinello Molecular Dynamics (CPMD) Calculation Of The ν_{O-H} IR Spectra for Acetic Acid Cyclic Dimers

D. Benrezkallah Molecular Dynamics Simulation of a Cold-adapted Enzyme

K. Bentayeb Spectrophotometric Studies of Complexes of Some Electron Donors with Ferric Chloride in Methanol

F. Berrahoui Theoretical Study of the [2+2]/ [4+2] Competitive Cycloaddition Pathways of Ketenes with Diazadienes

N. B. B. Bestaoui Relaxed energetic maps of kappa carrabiose: a dft study

A. Chouaih A Comparative X-ray Diffraction Study and Theoretical Calculation on a Nonlinear Optical Material

S. N. Derrar Design of Copolymeric Films Intended to be Employed in Nonlinear Optical Field: a DF study

A. Djedouani Structure, Theoritical And Electrochemical Study Of A New Zwitterionic Schiff Base Derivative From DHA

N. Drici Cys3 His-Zn2+ Interactions with SPC Water Molecules: Computational Study using GROMOS96 Force Field

F. Kateb Structure, dynamics and ligand binding of the DEAF-1 MYND domain by NMR

Z. Djelloul Prediction of New Solid Catalysts by the Technique of Datamining

M.H.Gafour	*ab initio* Conformational Maps for Lactulose in Gas Phase and Aqueous Solution
N. Guechtouli	Resentation du logiciel de calcul adf : application a l'etude de reaction d'interconvertion des isomeres du cluster $Fe_4N_2(CO)_{12}$.
Z. Haddadi	Modelling of the Diazepines' Synthesis by PM3 and DFT Methods
M. Hadj Ben Ali	Structure and Charge Distribution, Electronic and Vibrational (Hyper) Polarizabilities of Some Twist Intramolecular Charge Transfer Chromophores
D. Hammoutène	Quintet electronic states of N2
D Hannachi	Quantum chemistry study of lanthanide (iii) complexes with tri&bidentate oxygen ligands
A. Kadari	Theoretical Studies (DFT and TDDFT) on Structures and Spectroscopic Properties of Series of Novel iridium complexes
A. k. Nacereddine	A DFT study of the mechanism, regio- and stereoselectivity of 1,3-dipolar cycloaddition of phosphorylated nitrone with substituted alkenes
S. M. Messabih	Modeling stability conditions the different structures of Gas Hydrates
S. Moussi	Theoritical Studies of Phosphirine Polyanions Using Density Functional Theory DFT
A. Oughilas	Physico-chemical study Microbiological some varieties Of Local honey
C. Reguieg	Interactions Between κ-Carrabiose and Some Ions of Alkali Metals
B. Teyar	Theoretical Study of The Transition State of The Cyanidobis (Cyclooctatetraenyle) Compound in DFT / Zora Relativistic
N. Yousfi	Conformational DFT Study of κ-Carrabiose in gas phase and aqueous solution
S. Zaater	Sandwich Complex Containing Ge Atoms: Comparative Studies With Ferrocene

Summary

ABSTRACTS

Plenary Lectures

On the Motions of Water in Chabazite, a Molecular Dynamics Study

R.Chanajaree[1], S.Fritzsche[1], J.Kärger[2], Ph.A.Bopp[3]

[1] Institute of Theoretical Physics, Faculty of Physics and Geosciences, Universität Leipzig, Postfach 100920, DE-04009 Leipzig
[2] Institute of Experimental Physics I, Faculty of Physics and Geosciences, Universität Leipzig, Linéstrasse 5, DE-04103 Leipzig
[3] Department of Chemistry, University Bordeaux 1, 351 Cours de la Libération, FR-33405 Talence cedex, e-mail:philippe.bopp@u-bordeaux1.f

Introduction: The internal structure of the zeolite Chabazite consists of interconnected cavities with dimensions of a few molecular diameters (say, of water). The presence of aluminum ions in the zeolite lattice leads to an anionic character of the framework, which is neutralized by extra-framework ions, here calcium. The presence of these ions in the zeolite voids is an additional constraint on the motions of the guest molecules in these systems. We study here the translational self-diffusion, the librations, and the reorientations of water molecules at 300K and different loadings of the zeolite.

Method: We have performed Molecular Dynamics (MD) computer simulations of this zeolite at 300K and various loadings of water. Figure 1 shows a typical simulated system.

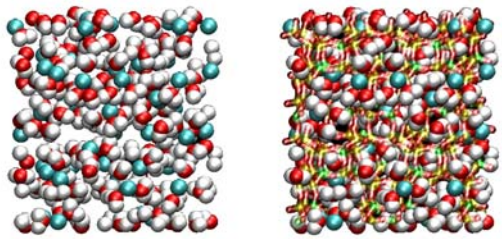

Figure 1: Simulation box: Left: Water molecules and extra-framework ions,; Right: Chabazite lattice (sticks), water, and ions.

The simulation boxes contained 864 lattice atoms (24 cavities) and, per cavity, on the average 2 calcium ions and from 2 to 13 water molecules. The zeolite lattice and the geometry of the water molecules were kept rigid during the simulations. The SPC/E water model was used together with compatible ion-water, ion-lattice, and water-lattice terms. Ewald summations were used for the electrostatic interactions. After lengthy initial equilibration the trajectories were sampled for 10 to 35 nanoseconds.

Results: (a) *translational self-diffusion*: The self-diffusion coefficients are of the order of 10^{-12} m^2 s^{-1}. The new results broadly confirm the conclusions drawn from previous simulations at higher temperatures (Jost 2007). The self-diffusion is found to be anisotropic (due to the internal structure of the zeolite), in keeping with experimental results (Bär 1998). It is also strongly dependent on the loading with a maximum around a load of 10 water molecules per cavity.

(b) Librations The librational motions are not unlike the ones found in liquid water and aqueous ionic solutions (Spohr 1988). However, following recent arguments (Laage 2008) the concept of rotational self-diffusion seems not to apply here.

(c) Reorientations The molecular reorientations are found to be much slower here than in liquids, with characteristic times of nanoseconds rather than picoseconds. In keeping with the findings for the librations, the reorientations are seen to occur in large jumps rather that in a continuous way.

In all three cases, the motions of the water molecules can be rationalized in terms of an almost immobile fraction, strongly hydrated to the extra-framework cations, and a more mobile fraction further away from these ions.

Acknowledgment: Financial support by Deutsche Forschungsgemeinschaft (DFG) was received through the IRTG 'Diffusion in Porous Materials'. Computer time was provided by Universität Leipzig and ZIH Dresden. PAB thanks University Bordeaux 1 for a sabbatical leave in 2009/2010. The Max Planck-Institut für Mathematik in den Naturwissenschaften (MPI-MIS), Leipzig, and The Department of Materials Chemistry, Uppsala University, are gratefully acknowlegded for their hospitality and support during this time. Financial support by the Wenner-Gren Foundation, Stockholm, is also acknowledged.

References:

Bär N.-K.; Kärger J., Schäfer H., Schmitz W., *Microporous Mesoporous Mater*. (1998) 22, 289-295

Jost S., Biswas P., Schüring A., Kärger J., Bopp Ph., Haberlandt R., Fritzsche S. (2007) *Journal of Physical Chemistry C*, 111, 14707-14712

Laage D., Hynes J.T. (2008) *Journal of Physical Chemistry B* 112 14230-14242

Spohr E., Pálinkás G., Heinzinger K., Bopp Ph. (1988) *Journal Physical Chemistry* 92, 6754-6761

Modeling and vibrational spectroscopy applied to the study of the dynamics in aluminosilicates

D. Bougeard[1]

[1] Laboratoire de Spectrochimie Infrarouge et Raman, Université des Sciences et Technologies de Lille, Cité Scientifique, Villeneuve d'Ascq Cedex 59655, FRANCE

Introduction: The importance of silicate minerals, the major components of the Earth's crust, in everyday's life can hardly be overestimated. Clays are indispensable as construction materials; crystalline and amorphous silicates find widespread applications as electronic devices; glasses, the most famous aluminosilicates, are ubiquitous. The properties of the materials are dictated by their structures, which can be obtained from simple basic units: TO_4 tetrahedra (T = Si, Al) and XO_6 octahedra (X = Al, Mg, Fe,…). Arrangement of the units by sharing corners or edges results in a variety of structures ranging from the dense crystalline silica polymorphs to open structures with two- and three-dimensional networks of cavities and channels. Such open structures, having voids of nanometric size, attract much attention due to their applications but they necessitate coupling of modeling with experimental methods to gat ride of their complexity.

Methods: The classical MD techniques rest on a classical description of a system of interacting particles and on a model of effective potentials representing the interatomic interactions. The phase space is explored by solving the classical equations of motion of particles. The quantities of interest (structural data, vibrational spectra, diffusional behavior) are obtained as the mean of their instantaneous values along the trajectory, i.e. as the average over time.

For the calculation of the vibrational spectra we developed a potential model for aluminosilicates which leads to a very good reproduction of the vibrational frequencies. It was extended to octahedral aluminium and magnesium (Arab et al. 2002, Bougeard et al. 2000, Ermoshin et al. 1996). The IR and Raman spectra were obtained by Fourier transformation of the auto-correlation function of the dipole moment and of the polarizability tensor, respectively (Berens et al., 1981). Using the bond polarizability model, the corresponding electro-optical parameters were derived for aluminosilicates from the data obtained in quantum-chemical calculations of small molecules (Smirnov et al. 2006).

Results: Several applications will be presented including the Raman spectra of glasses (Figure 1), the diffusion in clays (Figure 2) and in zeolites.

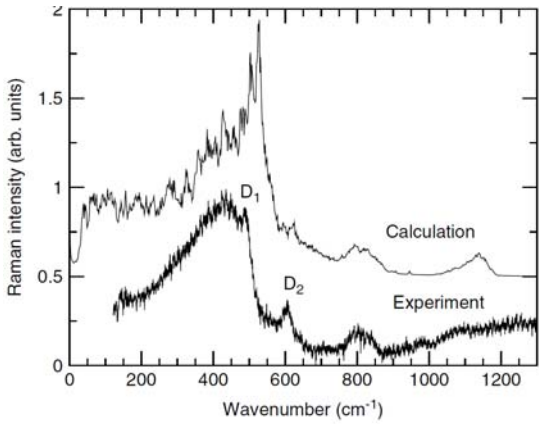

Figure 2: Raman spectra of amorphous silica (D_1 and D_2 bands are used in experiment for the characterization of glasses)

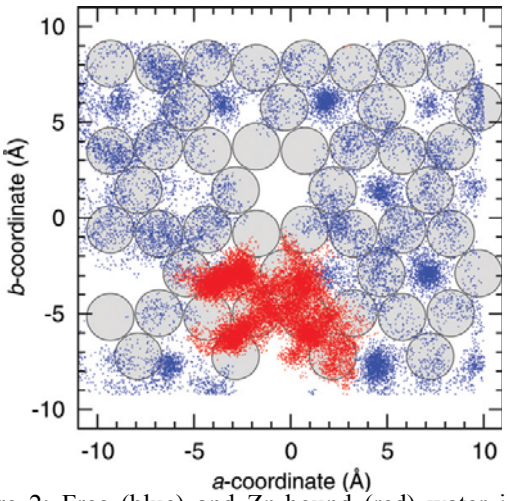

Figure 2: Free (blue) and Zn-bound (red) water in hydrated Zn-Vermiculite

References:

Arab, M., Bougeard, D., Smirnov, K. S. (2002) Physical Chemistry Chemical Physics, 4,1957, 2002.
Berens, P.H., White, S. R. , Wilson, K. R. (1981) Journal of Chemical Physics, 75, 515, 2000.
Bougeard, D., Smirnov, K. S., Geidel, E., (2000) Journal of Physical Chemistry B, 104, 9210, 2000.
Ermoshin, V. A., Smirnov, K. S., Bougeard, D. (1996) Chemical Physics, 209, 41, 1996.
Smirnov, K. S., Bougeard, D., Tandon, P., (2006) Journal of Physical Chemistry A, 110, 4516, 2006.

Shear-Induced Structures in Lyotropic Liquid Crystals Investigated by NMR Spectroscopy

C. Schmidt[1]

[1]Faculty of Science, Department of Chemistry, University of Paderborn,
Warburger Str. 100, D-33098 Paderborn, GERMANY
claudia.schmidt@uni-paderborn.de

Introduction: Concentrated aqueous solutions of surfactants often form liquid-crystalline phases. The application of shear to these mesophases can have pronounced effects on their orientation and structure, leading to rheological phenomena such as shear-thinning or shear-thickening. In order to better understand the rheological properties of surfactant systems, many studies combining rheological measurements with structural investigations have been performed. The majority of researchers have used light, x-ray or neutron scattering methods or direct optical observations by light microscopy [1]. Nuclear magnetic resonance (NMR) investigations are not yet very common in this field [2-4], although NMR spectrometers are often more easily accessible than large scale scattering facilities. Focusing on the shear-induced structural transitions of the lyotropic lamellar phase [1,5-11], this contribution will give an overview on how shear-induced changes of the structure of lyotropic-liquid crystals can be elucidated by NMR experiments.

Experimental: In situ NMR experiments under shear have been performed using home-built NMR probes that contain a shear cell of either cone-and-plate or cylindrical Couette geometry. The cell is surrounded by the NMR coil and driven by a motor located underneath the superconducting magnet. From the deuterium resonance of D_2O-enriched samples information on the sample orientation and structure is obtained. Often shear-induced structures are metastable and do not relax when shear is stopped. In this case, NMR methods which require longer measuring times, such as NMR diffusometry, can be applied.

Results: The lamellar phase under shear may consist of extended planar lamellae, which can assume different orientations with respect to the flow, or of close-packed multilamellar vesicles (MLV), also known as "onions" [5]. The stability regions of these structures as a function of shear rate and temperature can be readily obtained from the ^2H NMR line shapes of D_2O-enriched samples and mapped in a shear diagram. An analysis of the NMR line widths and of the diffusion properties can provide further structural details, such as the MLV size [7,8]. Not only steady-state structures but also transient processes under shear, such as the formation of MLVs from initially planar lamellae or the reverse process, can be followed. From time-dependent NMR experiments, performed on the nonionic surfactant system $C_{10}E_3/D_2O$, a fundamental difference depending on the direction of the transformation process has been found: the transition from planar lamellae to MLVs is a continuous transformation, whereas the opposite transition occurs via a "two-phase" region [6].

It has been suggested that an intermediate structure of multilamellar cylinders occurs during the shear-induced transformation from planar layers to MLVs [9,10]. ^1H NMR measurements of the water diffusion parallel to the velocity, the velocity gradient and the vorticity directions at various stages of the transformation process are consistent with such an intermediate structure [11].

References:

Koschorek, S., Fujii, S., Richtering, W. (2008) *Prog. Theor. Phys. Suppl.,* 175, 154-165.

Callaghan, P. T. (1999) *Rep. Prog. Phys.,* 652, 599-670.

Callaghan, P. T. (2006) *Current Opinion in Coll. Interface Sci.*, 11, 13-18.

Schmidt, C. (2006) In *Modern Magnetic Resonance*, Vol. 3, 1495-1501, Springer, New York.

Diat, O., Roux, D. Nallet, F. (1993) *J. Physique II,* 3, 1427-1452.

Medronho, B., Shafaei, S., Szopko, R., Miguel, M. G., Olsson, U., Schmidt, C. (2008) *Langmuir*, 24, 6480-6486.

Medronho, B., Schmidt, C., Olsson, U, Miguel, M. G. (2010) *Langmuir,* 26, 1477-1481.

Åslund, I., Medronho, B., Topgaard, D., Söderman, O., Schmidt, C., *Phys. Chem. Chem. Phys.*, submitted.

Zipfel, J., Nettesheim, F., Lindner, P., Le, T. D., Olsson, U., Richtering, W. (2001) *Europhys. Lett.*, 53, 335-341.

Nettesheim, F., Zipfel, J., Olsson, U., Renth, F., Lindner, P., Richtering, W. (2003), *Langmui*r, 19, 3603-3618.

Medronho, B., Brown, J., Miguel, M. G., Schmidt, C., Olsson, O., Galvosas, P., to be submitted to *Soft Matter*.

Molecular Dynamics Modeling of Proton Discharge at the Aqueous / Metallic Interface

E. Spohr[1]

[1] Lehrstuhl für Theoretische Chemie, Universität Duisburg-Essen
Universitätsstr. 5, 45141 Essen, GERMANY
eckhard.spohr@uni-due.de

Abstract

An empirical valence-bond (EVB) model is developed in order to describe the transfer of a proton from aqueous solution bulk to a (charged) metal electrode surface. Results of density functional calculations are used for parametrizing the model for the Pt(111) surface. The EVB model makes possible large scale molecular dynamics simulations for a metal/electrolyte solution including Grotthuss style proton transport [1]. We have systematically studied the rate of proton discharge on negatively charged surfaces in the range of medium to large surface charge densities. The mean rate of transfer was analysed for proton trajectories which were started in the bulk of a water film adsorbed on the electrode. The results indicate a transition between a reaction-dominated regime at moderate negative charges, where the rate constant increases exponentially, to a ``diffusion controlled'' regime where the transfer rate is almost independent of the surface charge density (at more negative surface charge densities) [2].

References:

A Model for Proton Transfer To Metal Electrodes, Wilhelm, F., Schmickler, W., Nazmutdinov, R. R., Spohr, E. (2008) *J. Phys. Chem*. C 112, 10814.

Proton Transfer to Charged Platinum Electrodes. A Molecular Dynamics Trajectory Study, Wilhelm, F., Schmickler, W., Spohr, E. (2010) *J. Phys. Cond. Matt*. 22, 175001

Determining and Analyzing the Structure of Clusters

M. Springborg[1]

[1]Physical and Theoretical Chemistry, University of Saarland, 66123 Saarbrücken, GERMANY
m.springborg@mx.uni-saarland.de

Introduction: One of the big challenges facing theoretical studies of clusters is to determine the structure of the global total-energy minimum. During the last couple of decades more different approaches have been proposed for tackling this problem and also applied to various systems in combination with more or less accurate descriptions of the total energy as a function of structure. As the result of such calculations one obtains first of all the nuclear coordinates and the total energies as functions of the size of the clusters. Another challenge is then to extract chemically or physically relevant information from this often very large amount of information.

In this presentation we shall give examples from our own work on the unbiased determination of the structure of different types of clusters. We have used different structure-optimization methods as well as approximate total-energy methods, and shall put special emphasis on the analysis of the results. This includes the identification of particularly stable clusters as well as the structural shape and similarity with various types of reference structures.

As examples we shall consider isolated metal clusters and metal clusters deposited or grown on metal surfaces. Also semiconductor clusters with one or more types of atoms shall be treated.

Methods: We use two different methods for calculating the total energy for a given structure. Both methods are approximate and have been developed specifically for the problem at hand. With one method, the embedded-atom method, the electronic degrees of freedom are not directly included in the calculations, which makes the method fast and most suitable for systems for which close packing is expected to be important (e.g., simple metals). The other method is a parameterized density-functional method with which also electronic properties are calculated whereby the study of systems with directional bonds is made possible.

In order to determine the global total-energy minimum we use either genetic algorithms or our own aufbau/abbau method. Both methods are unbiased structure-optimization methods and based on the idea of combining "keeping good building blocks" with randomness.

Systems: As a first example we discuss the properties of isolated Ni clusters with from 2 to 150 atoms. For those, we also present various approaches that we have developed in order to identify general properties. These properties include the total energy per atom from which a stability function can be derived with which particularly stable clusters can be identified. Structural properties can be quantified through a shape analysis as well as though the radial distances of the individual atoms. The positions of the atoms can also be used in identifying and quantifying structural similarities.

Subsequently, we study the properties of bimetallic clusters, as well as of clusters either grown or deposited on a surface. In all cases, the embedded-atom method has been used.

For nanostructured HAlO we show how the calculations can be used in providing experimentally relevant but hardly accessible information. To this end we consider isolated as well as two interacting clusters with up to 28 fornula units and apply the parameterized density-functional method.

Next we study various semiconductor clusters. This includes II-VI and III-V semiconductors for which either the zincblende or the wurtzite structure is found for the macroscopic systems. We study how this manifests itself for the nanoparticles. Also Si, Ge, and mixed Si-Ge clusters shall be studied. In all cases, we discuss a possible correlation between stability and optical properties, quantified through teh HOMO-LUMO energy gap.

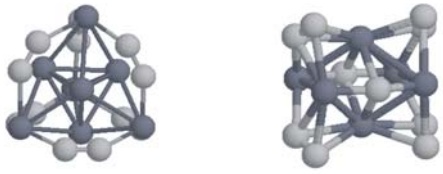

As a final example, we study the so-called metallocarbohedrenes ("metcars"). The Ti_8C_{12} metcar is the most famous example that has a particularly high and appealing symmetry. We compare this cluster with metcars with slightly more or less Ti and/or C atoms. As an example, the figure shows the optimized structures of Ti_8C_{12} and Ti_6C_{10}.

Molecular modeling of EBP-Elastin Binding Protein: docking of different ligands

S. Baud[1], N. Belloy[1], L. Duca[1], L. Debelle[1], L. Martiny[1], M. Dauchez[1]

1Laboratoire SiRMa, CNRS UMR MEDyC 6237, IFR 53 Biomolécules, Université de Reims Champagne-Ardennes, UFR Sciences Exactes et Naturelles, 51687 Reims Cedex 2, France

Elastin is the extracellular matrix protein responsible for the elasticity of tissues. Its degradation produces elastin peptides with biological activity which leads to proliferation, proteases synthesis or chemotaxis. These peptides are involved in diverse physiopathological processes through their binding to the elastin complex receptor.

Previous data have shown that both the structure of the peptide and the structure of the elastin binding (EBP, *Elastin Binding Protein*) sub-unit are key elements in the binding process : the first finding was that elastin peptides presenting the XGXXPG consensus sequence (such as VGVAPG) bind to EBP, the second finding was that EBP interacts with elastin peptides through a specific region of 32 residues (known as V32) which contains some important amino acids.

The aim of this work is to characterize thoroughly and from an atomistic point of view the binding process of elastin peptides to EBP. This computational study is divided into two main steps: we start with various sequences of elastin peptides and test their affinity for EBP through docking experiments.

We can then check if the predicted fixation site on EBP is always the same and if the orientation of the peptides on this site is similar from one peptide to another. Once the effect of the peptide sequence is described and characterized, we focus on the role of some few important amino acids located on the EBP. After we mutate these residues (modifications of the sidechain charge or length), we perform new docking experiment between the VGVAPG peptide and these new versions of EBP. Among other things, we demonstrate a potential role of the charges of the E137 and R107 amino acids.

The validation of all these results is performed : (i) using molecular dynamic simulations on the different systems. This way, we can check the stability of the binding using pressure, temperature and solvent conditions mimicking a biological environment, and (ii) confronting our *in silico* results to *in vitro* biological tests on cells.

Built-in strain, electric field, and spin polarization effects in wide bandgap semiconductor materials and nano-devices

A. Kadri[1]

[1]Laboratoire d'Etude des Matériaux Opto-électronique & Polymères (L. E. M. O. P.)
Department of Physics, University of Oran (Es-Senia), 31300 Oran, ALGERIA
kadri.lemop.uo@mail.com

Abstract

Advanced optoelectronics and electronics applications put increasing and stringent demands on new properties of new materials with new systems, and new devices. First of all, it becomes highly desirable to shrink the size of the devices down to the nanoscale (10^{-9}m). This is made so not only in order to make the devices smaller, smarter, chipper…, but it is done in the purpose of enhancing the quantum nature of materials properties, and revealing a set of new and very rich phenomena, unreachable neither at micro nor at macro scales. These issues are actually addressed by the evolving field of nanotechnologies and constitute the first part of my talk.

The second part of my talk addresses issues related to the necessity of finding new concepts and/or new phenomena to built new devices. I will focus on 3 such lines of interest: 1. built-in strain; 2. built-in polarization which leads to internal electric field and finally; 3. spin polarization. In each case, I'll give examples of works done by our teams at the LEMOP Laboratory at the University of Oran Es-Sénia.

Built-in strain results from the mismatch between different materials associated in hetero-structures. This kind of internal strain can be controlled at the nanoscale. As far as this strain does not exceed some critical value, it can modify very deeply the properties of hetero-structures and constituent materials as well. Materials properties as electronic, mechanical, optical, magnetic, … can be fine tuned in this way in a wide range to fit some desirable value of interest.

The internal electric fields which build up in nanostructures arise from spontaneous and/or piezoelectric polarizations effects. Such internal electric fields do also modify very dramatically the physical properties of nanostructures. They also can be controlled and tuned in a fine way, so that it can be possible to obtain a desired effect.

The control of spin polarization can be also achieved in nano-systems, because of the strong spin degeneracy lifting, as a result of both quantum and size effects. It can lead to very interesting phenomena, and more particularly, to the so-called ''spintronics'' which is of fundamental and practical importance in many applications as in quantum computations and memories for future computers.

Key words: nanomaterials, nanodevices, low dimensional systems, built-in strain, built-in electric field, spin polarization, ab-initio, DFT (FP-LAPW), **k.P**-theory, III-V Nitrides, II-VI oxydes , Lasers, Quantum Well heterostructures

References:

Zitouni, K., Kadri, A., Lefebvre, P., Gil, B. (2006) *Superlattices and Microstructures* 39, 91-96.

Benharrats, Zitouni, K., Kadri, A., Gil, B. (2010) *Superlattices and Microstructures*, 47, 592.

Djellal, A., Kadri, A., Gil, B., Breta-gnon, T., Zitouni, K. 4-10 July 2010 3rd International Symposium on Growth of III- Nitrides (ISGN3), Montpellier France

Djellal, A., Kadri, A., Gil, B., Breta-gnon, T., Zitouni, *accepted in Physica Status Solidi C*, Décembre 2010 .

PROTEIN AND RNA COMPUTER SIMULATIONS

Philippe Derreumaux[1]

[1]Laboratoire de Biochimie Théorique, UPR9080 CNRS, IBPC, 13 rue Pierre et Marie Curie, 75005, Paris, Université Paris 7 et Institut Universitaire de France

Folding proteins or RNA on computers using molecular mechanics force fields so as to reproduce closely or complement experimental data is very challenging. The surrounding water molecules must be treated, the quality of the underlying force field must high, and the sampling of the conformational space must be very efficient.

The shortest time for protein and RNA folding is, however, about tens of microsecond, and most all-atom simulations explore the 100-1000 ns timescale. In addition, the calculation of accurate folding pathways requires hundreds of molecular dynamics trajectories and even with the increase of computational power, enhanced conformational techniques of all-atom systems are hampered by very slow convergence towards equilibrium.

Due these limitations and because other phenomena of high medical interest, such as amyloid fibril formation, demand insights into much longer timescales, scientists are developing and improving coarse grained models.

In this talk, I shall present (1) OPEP coarse-grained simulations for predicting the native structures of mini-proteins and targeting amyloid soluble oligomers associated with Alzheimer's disease and (2) applications of the coarse-grained HiRE-RNA force field to RNA.

ABSTRACTS

Contributed Oral Presentations

Properties of iron substituted manganese $La_{0.67}Sr_{0.33}Fe_xMn_{1-x}O_3$ nano-manganites oxide

W. Cherif[1], M. Ellouze[1], F. Elhalouani[2], A-F. Lehlooh[3]

[1] Faculté des Sciences de Sfax, B. P. 1171 - 3000, TUNISIA
wajdi_cherif@yahoo.fr
mohamed.ellouze@fss.rnu.tn
[2] Ecole Nationale d'Ingénieurs de Sfax, B. P. W 3038, TUNISIA
foued.elhalouani@enis.rnu.tn
[3] Yarmouk University, 211-63 Irbid, JORDAN
aflehlooh@yu.edu.jo

Introduction: A metal–insulator transition and large negative magnetoresistance were discovered 50 years ago in alkaline-earth substituted perovskite-type rare earth manganese oxides of the type $La_{1-x}Ca_xMnO_3$ with La rare metals and Ca alkaline-earth metals [1, 2]. In recent years, these materials have regained great interest for research due to their particular microstructure and magnetic properties [3–8]. Colossal magnetoresistance (CMR) was found to be caused by the magnetic-field-driven shift of a first-order metal–insulator transition in the temperature window around the ferromagnetic ordering of the Mn charges and spins. The CMR materials have basically a perovskite-derived structure with rhombohedral or orthorhombic distortion. In the double exchange mechanism [9] for CMR the Mn–O–Mn bond distance and angle are considered to play an important role in controlling the CMR properties. The microstructure has also found to have a strong influence on physicochemical properties, such as the Curie temperatures.

In this work, we present structural and magnetic properties of $La_{0.67}Sr_{0.33}Fe_xMn_{1-x}O_3$ with $0 \leq x \leq 1$ samples. Powder samples have been elaborated by the mechanical alloying method. This powder samples have been elaborated by mixing precursors La_2O_3, MnO_2, Fe_2O_3 and SrO_2 up to 99.9 % purity in the desired proportion according to the following reaction:

$$0.67\ La_2O_3 + 0.33\ SrO_2 + 3\ x\ Fe_2O_3 + 3(1-x)\ MnO_2 \rightarrow 6\ La_{0.67}Sr_{0.33}Fe_xMn_{1-x}O_3.$$

We present in Fig. a SEM photo of the elaborated samples. The powder X-ray diffraction shows that the elaborated samples are single phase. Our magnetic investigations show that the samples exhibit a paramagnetic to ferromagnetic behaviour when the temperature decreases.

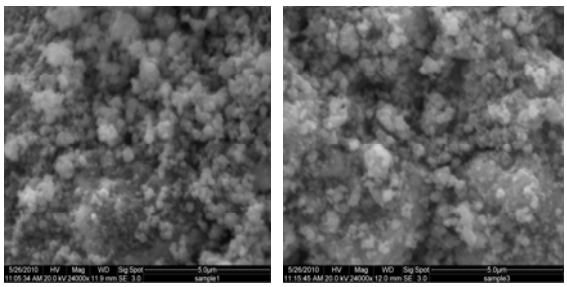

Figure: SEM photos of powder of $La_{0.67}Sr_{0.33}Fe_xMn_{1-x}O_3$ with $0 \leq x \leq 1$ milled by the ball milling.

References:

Jonker, G. H., Van Santen, J. H. (1950) *Physica XVI* 337.
Vogler, J. (1954) *Physica XX* 49.
Von Helmolt, R., Wecker, J., Holzapfel, B., Schultz, L., Samwer, K. (1993) *Phys. Rev. Lett*. 71 2331.
Wang, R. H., Gui, J. N., Zhu, Y. M., Moodenbaugh, R. (2000) *Phys. Rev. B* 61 11946.
Wang, R. H., Gui, J. N., Zhu, Y. M., Moodenbaugh, R. (2001) *Phys. Rev. B* 63 144106.
He, J. Q., Wang, R. H., Gui, J. N., Dong, C. (2002) *Phys. Stat. Sol. B* 229 1145.
Rao, R. A., Lavric, D., Nath, T. K., Eom, C. B., Wu, L., Tsai, F. (1999) *J. Appl. Phys*. 85 4794.
Ziese, M., Semmelhack, H. C., Han, K. H., S. P., Sena, Blythe, H.J. (2002) *J. Appl. Phys*. 91 9930.
Zener, C. (1951) *Phys. Rev*. 82 403.

Advanced Apparatus for Pathogen Detection

M. B. Mejri[1,4], H. Baccar[1,2], S.Helali[1], M.Aouni[4], E.Baldrich[3], J.Del Campo[3] ,A. Abdelghani[1,2*]

[1]Nanotechnology Laboratory, INSAT, Centre Urbain Nord, 1080 Charguia Cedex, TUNISIA
Corresponding author: tel: +216 71 703 829, fax: +216 71 704 329,
email:aabdelghan@yahoo.fr
[2]Unité de recherche de Physico-chimie des Matériaux Polymères, IPEST, TUNISIA
[3]Centro Nacional de Microelectrónica, Barcelona, SPAIN
[4]Laboratoire des maladies transmissibles et substances biologiquement actives (LR99ES27), Faculté de Pharmacie, 5000 Monastir, TUNISIA

Abstract: Currently available methods for bacteria detection are mostly based on classical methodological approaches such as selective culture, immuno-affinity testing (like enzyme linked immunosorbent assay, ELISA) and, more recently, polymerase chain reaction (PCR).. In the context of bacteria detection, biosensor development offers the possibility to perform faster, cheaper and simplified detection of multiple analytes, even in complex multicomponent matrices. In the present work, we compare the efficiency of phages as bioreceptors for bacteria biosensing, following their incorporation onto interdigitated gold microelectrodes by different funtionalization strategies. Impedance Spectroscopy and Surface Plasmon Resonance Imaging techniques were used for bacteria detection. The kinetic behavior, the detection limit and the reproductibility of the developed biosensor will be discussed.

Introduction: In spite of the medical advances occurred over the last decades, bacterial pathogens are still among the main cause of death in the world. The ability of microorganisms to evolve extraordinarily fast may partly account for this, but changes in the population cultural habits, as well as technological and medical advances, have deeply influenced pathogen prevalence and distribution.
In this work we demonstrate that EIS monitoring over time using bacteriophages for bacteria detection generates successive dual signals of opposite trend, enabling in-chip detection confirmation. In this respect, specific capture generates an initial increase in impedance, which is followed by an impedance decrease due to phage-induced lysis. These signals can be easily distinguished from those caused by non-specific adsorption and/or crossbinding.

.

Material and Methods: Interdigitated microelectrodes were produced by standard photolithographic techniques. *E. coli* K12 cells, provided by BioPhage Pharma (Montreal, Canada), were grown at 37ºC in Luria-Bertani (LB) liquid medium for 8-10 h. *Lactobacillus plantarum* cells were grown at 37ºC in MRS broth for 18-20 h. T4 phage, which specifically infects *E. coli*, was obtained from BioPhage Pharma (Montreal, Canada). *E. coli* K12 liquid culture, grown until the exponential phase was reached, was inoculated with 500 µl of a phage T4 stock solution

Results and discussions: The typical response of EIS immunosensors in the presence of target *E. coli* is illustrated in Figure 1. The curve shows the absolute variation of the impedance (ΔZ) versus the incubation time at fixed frequency (233 mHz). ΔZ is calculated as $|Z - Z_0|$, where Z is the value of the impedance module of the immunofunctionalised microelectrode after bacteria binding and Z_0 is the value of the impedance module of that immunofunctionalised microelectrode previous to bacteria capture.

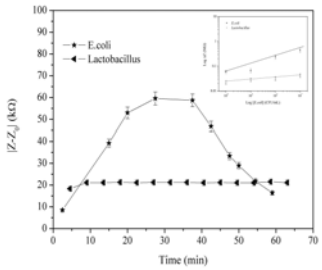

Figure.1: ΔZ registered at 233 mHz over time for phage-modified microelectrodes in the presence of 10^4 CFU mL^{-1} *E. coli*

References:

Rose, S. A., Stringer, M. F. eds (1989) *Immunological Methods* (New York: Elsevier)
Updike, S. J., Hicks, G. P. (1967) *The Enzyme Electrode Nature* 214**,** 986-8.
Mejri, M., Helali, S., Baccar, H., Baldrich, E., Del Campo, J., Gnanaprakasa, T., Simonian, A., Abdelghani, A. for Biosensors and Bioelectronics, *In Press*.

Acknowledgments:
This research is sponsored by NATO's Public Diplomacy Division in the Framework of "Science for Peace", project SfP.983115. The authors thank Biophage Pharma (Canada) for their collaborations.

Complexes of lanthanide and actinides Between theoretical challenges and contributions of DFT/ZORA relativistic method!

L. Belkhiri[1], S. Meskaldji[1], A. Zaiter[1], B. Teyar[1], M. Ephritikhine[2] and A. Boucekkine[3]

[1]Unité de Recherche Chimie de l'Environnement et Moléculaire Structurale (URCHEMS) Université Mentouri de Constantine, 25017 Constantine, ALGERIA
lotfi.belkhiri@umc.edu.dz
[2]CEA Saclay, DSM, IRAMIS, UMR 3299 CEA/CNRS SIS2M, 91191 Gif-sur-Yvette cedex .[3]UMR CNRS 6226 Sciences Chimiques de Rennes, Université de Rennes 1, Campus de Beaulieu 35042 Rennes Cedex, FRANCE

Abtsract: Organometallic compounds synthesized recently, with both lanthanides and actinides f elements and having interesting structural, electrochemical, optical and magnetic properties, have opened promising routes to technological applications such as heterogeneous catalysis (precursors, luminescence and / or nonlinear optics, medical imaging as contrast agents and for molecular electronics for storage of information [1].

The theoretical study of such systems is difficult (relativistic and electron correlation effects important) but essential to understand and analyze the binding mode of metal-ligand, the role of f orbitals, electronic structure and attempt to interpret / rationalize their physicochemical properties. The DFT method used in its relativistic framework ZORA (Zero Order Regular Approximation) using ADF code [2] led us to ground state properties in good agreement with experimental data.

We were interested, through some examples treated by our group in the contex of Lanthanide(III)/actinide(III) differentiation [3], to the crucial role of f orbitals in the metal-ligand and other electronic factors and/or steric which can affect this differentiation.

The magnetic behavior of polymetallic molecular compounds of actinides is currently the subject of intense study both experimentally and theoretically [4]. We performed DFT calculations according to the 'Broken Symmetry' (BS) approach in order to analyze the role of both bridging ligand and 5f orbitals in the electronic or magnetic communication between different metallic sites. The presence of the uranium 5f orbitals, much diffuse, also seems to be a determining factor for the charge transfer and metal-ligand spin delocalization through the bridging ligand.

References:

Ephritikhine, M., *Dalton Trans.* (2006) 2501. (b) Edelmann, F.T., *Coord. Chem. Rev.* 253 (2009) 343. Schelter, E. J. Veauthier J. M., Graves, C. R. John, Scott, K. D., Thompson, B. L., Tournear, J. D., Morris, J. A. P.-D., Kiplinger, D. E. J. L. (2008) *Chem. Eur. J.* 14 7782.
ADF, SCM; Theoretical Chemistry, Vrije University: Amsterdam, The Netherlands; http://www.scm.com
Arliguie, T. Belkhiri, L. Bouaoud, S.E. Thuéry, P. Villiers, C. Boucekkine, A. Ephritikhine, M.*Inorg.* (2009) *Chem.* 48 221.
Meskaldji, S., Belkhiri, L., Arliguie, T. Fourmigué, Ephritikhine, M., Boucekkine, M., A.*Inorg. Chem.* DOI: 10.1021/ic902135t.
Neese, F . (2009) *Coord. Chem. Rev*. 253 526.
Noh, E. A., Zhang, J. Mol. (2009) J.*Struct (theochem*) 896 54.
Rinehart, J. D. Harris, T. D.. Kozimor, S. A Bartlett, Long. B. M Inorg, J. R. *Chem*. 48 (2009) 3382.
Newell, B. S. Rappé, A. K. Shores. M. P. (2010) *Inorg. Chem.* 49 1595.
Schreckenbach, G. Shamov, G. A. (2010) *Acc. Chem .Res.* 43 19.

Elaboration of new biopolymers based on sugar diols and characterization by NMR and MALDI-TOF

S. Chatti[1], H.R.Kricheldorf[2]
[1] Institut National de Recherche et d'Analyse Physico-chimique (INRAP),
Technopôle Sidi Thabet 2020 Sidi Thabet, TUNISIA
saber.chatti@inrap.rnrt.tn
[2]Institut für Technische und Makromolekulare Chemie der Universität, Bundesstrasse 45,
D-20146 Hamburg, GERMANY

Abstract:

Utilization of carbohydrate derivatives for biopolymers syntheses has been paid much attention not only because of the huge abundance of resources but also of the promising biodegradability and biocompatibility of them (Stross and Hemmer, 1991).

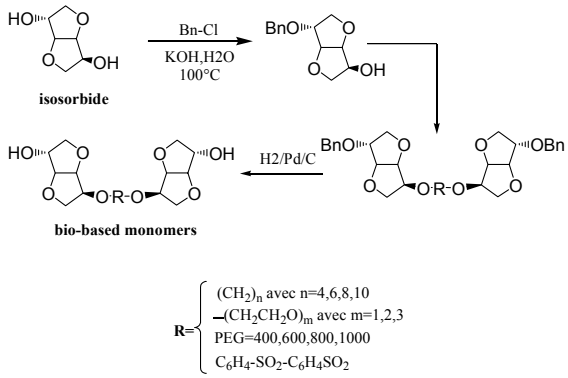

Figure 3: Synthesis of new diols from isosorbide

We have synthesed and characterized several bio-based sugar monomers (Chatti et al. 2000) (isosorbide and isomers) which can be used for the syntheses of novel biomaterials such as polycarbonates, polyesters, polyurethanes and poly(ether-sulfone)s (Chatti, 2006, 2009).

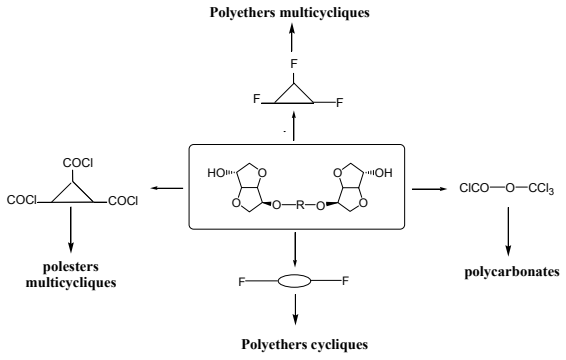

Figure 2: Biomaterials obtained by polycondensation of chirals diols with various difontionnalized agents

We have studied the influence of reaction conditions (reaction time, temperature, excess and stereochemistry of monomers) on the fraction of cyclic and linear chains of these biopolymers.

The resulting bio-based polymers has been characterized by NMR spectroscopy, MALDI-TOF mass spectrometry, SEC and DSC.

Sufficiently high molecular weights and glass transition temperature mean that such biopolymers could be useful as transparent engineering plastics, films and membranes (less sensitive to an attack of oil, gasoline and other organic solvent or liquid) and as bio-sensors (steroids, metals).

References:

Chatti, S.; Bortolussi, M. and Loupy, A. (2000) *Synthesis of diethers derived from dianhydrohexitols by phasetransfer catalysis under microwave.* Tetrahedron 2000, 56, 5877.

Chatti, S.; Kricheldorf, H.R. and Schwarz, G. (2006) *Cyclic and Noncyclic Polycarbonates of Isosorbide (1,4:3,6-Dianhydro-D-glucitol).* Macromolecules, 39, 9064-9070, 2006.

Chatti, S.; Hani, M. A.; Borhorst, K. and Kricheldorf, H.R. (2009). *Poly(ether-sulfone) of Isosorbide, Isomannide and Isoidide.* High Performance *Polymers Journal*, 21, 105-118, 2009.

Stross, P. and Hemmer, R. (1991). Advances in *Carbohydrate Chemistry & Biochemistry*. 1991, 49, 93.

Conformational and Vibrational analysis of Crown Ethers

N. A. Al-Jallal[1], A. A. El-Azhary[1] and A. Al-Kahtani[1]
Azhary60@hotmail.com
[1]Chemistry Department, Faculty of Science, King Saud University,
P.O. Box 2455, Riyadh 11451,
KINGDOM OF SAUDI ARABIA

Crown ethers are important class of molecules with wide applications. Some of the important crown ethers are 18-crown-6 (18c6) and 12-crown-4 (12c4) and their sulfur analogues, 18t6 and 12t4. Crown ethers are large ring molecules with large number of possible conformations. The aim of our research is to use computational and vibrational methods to determine in what conformations these molecules exit in. For this purpose, the CONFLEX method of the conformational search was used to determine the possible conformations of these molecules. To get better energy order of the predicted conformations, computations were done at higher levels of the ab initio methods as high as the MP2/6-31+G* level. The vibrational spectra of free 18c6 and 12c4 were measured and the experimental vibrational spectra were compared with the calculated vibrational spectra. The ab initio computations of 18c6 revealed that a new S6 conformation of 18c6 is the lowest energy conformation. The experimentally known Ci conformation is higher in energy by 1.84 kcal/mol at the MP2/6-31+G* level than the S6 conformation.

For 12c4, comparison between the calculated and vibrational spectra gave the evidence for the first time that 12c4 exists in the Ci conformation. This Ci conformation is higher by 2.61 kcal/mol at the MP2/6-31+G* level than the lowest energy S4 conformation. A rationalization was given why the S6 conformation of 18c6 and the S4 conformation of 12c4 are the lowest energy conformations. That is, both conformations have more number of hydrogen bonds and at shorter distances than any other predicted conformations of both molecules. A similar conformational and vibrational study of the complexes of 12c4 and 18c6 with alkali metal cations was performed. The study showed gave the proof for the first time that 12c4-alkali metal complexes exist in the C4 conformation, while confirmed the experimentally known structure of 18c6-alkali metal complexes. Currently, we are extending these computational and vibrational studies to 12t4 and 18t6 and their metal complexes.

Synthesis Approaches And Pharmacological Importance of 1,2,4-Triazoles

Y. A. Al-Soud[1]

[1]Department of Chemistry, College of Science, University of Al al-Bayt, Al-Mafraq, JORDAN

alsoud@rocketmail.com

Introduction: Recently, the short-lived reactive intermediates 1-aza-2-azoniaallene cations **1** (Figure 1) were used in the synthesis of various 1,2,4-triazole compounds *via* cycloaddition reaction with various unsaturated precursors in the presence of lewis acid. In my recent work, these cations have been utilized in the synthesis of new type of 1,2,4-triazole compound such as acyclic C-nucleosides, C-nucleosides of D-mannose, as well as attached to thymine, phthalimids, indols and quinolone, benzotriazoles, 3-triazolo-thymidine, piperazines and thiophenes.

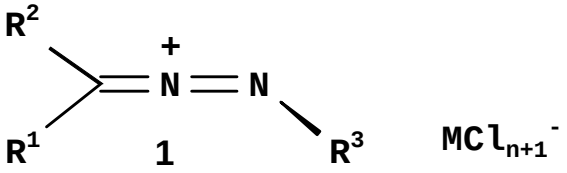

Figure 4

References:

Al-Soud, Y. A. (2008) Synthesis, structure and in vitro anti-HIV activity of new pyrazole, 1,2,4-thiadiazole and 1,2,4-triazole derivatives, *Phosphorus, Sulfur & Silicon***,** 183(10), 2621-2636.

Al-Soud, Y. A.(2007) Synthesis and anti-HIV Activity of Substituted 1,2,4-Triazolo thiophene Derivatives*, Heteroaom. Chemistry,* 18(4), 443-448.

Al-Soud, Y.A.; Al-Dweri, M.N. and Al-Masoudi, N.A. (2004) Synthesis, Antitumor and Antiviral Propreties of Some 1,5-Dialkyl- 1,2,4- riazoles-3-Substituted Hydrazides, 5-Mercapto-1,2,4-Triazoles, 1,3,4-Oxadiazole-2-thione and Indole, *IL Farmaco*, 59(10), 775-783.

Al-Soud, Y.A. and Al-Masoudi, N.A. (2004) DNA-Directed Alkylating Agents: Synthesis, Antitumor Activity and DNA Affinity of Bis-N,N'-Trisubstituted 1,2,4-Triazolo-Piprazines, *IL Farmaco*, 59(1), 41-46.

Al-Soud, Y.A.; Al-Masoudi, N.A. and Ferwanah, A. S. (2003) Synthesis and Properties of New Substituted 1,2,4-Triazoles: Potential Antitumor Agents, *Bioorg.& Med. Chem.*, 11(8), 1701-1708.

Al-Soud, Y.A.; Al-Masoudi, I. A.; Saeed, B.; Beifuß, U. and Al-Masoudi, N. I. A. (2006) Synthesis of New 1H-1,2,4-Triazolylcoumarins and Their Antitumor and Anti-HIV Activities, *Chemistry of Heterocyclic Compounds*, 42(5), 669-676.

Al-Soud,Y.A.; Qalalweh, M.N.A.; Al-Sa'doni, H.H. and Al-Masoudi, N.A. (2005) New Benzylpiperazine Derivatives Bearing Mono- and Bis-dialkyl Substituted 1,2,4-Triazoles*, Heteroaomt. Chemistry*, 16(1), 28-32.

Application of nanotechnology in solar cell fabrication - Future perspectives

Waheed A. Badawy[1]

[1]Chemistry Department, Faculty of Science, Cairo University, 12 613 Giza-EGYPT
e-mail: wbadawy@cu. edu. eg, wbadawy50@hotmail.com

Abstract:

Solar energy conversion with high efficiency and economically competitive solar cells represent the main task of many research groups [1, 2]. The fabrication of solar cells has passed through a large number of improvement steps. The first generation solar cells were based on Si wafers, mainly single crystals. Permanent researches on cost reduction and improved solar cell efficiency have led to the marketing of solar modules having 12-16% solar conversion efficiency. Application of polycrystalline Si and other forms of Si have reduced the cost but on the expense of the solar conversion efficiency. Some new ideas about the use of porous Si on Si to achieve higher solar conversion efficiencies are now in progress [2, 3]. The usefulness of the porous structure was extended to include Titania (TiO_2) and the technological applications were also extended to optoelectronics and medical applications [4].

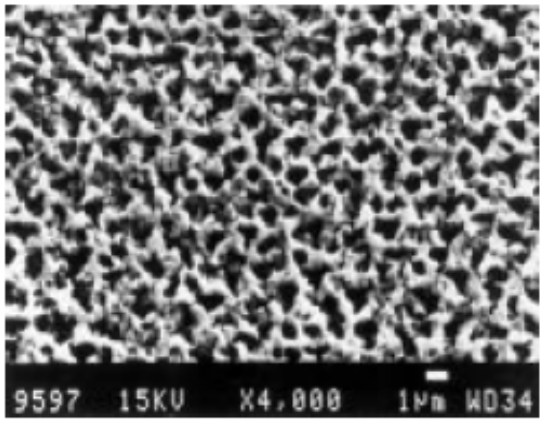

Porous Silicon of micropores

Polycrystalline Si panels

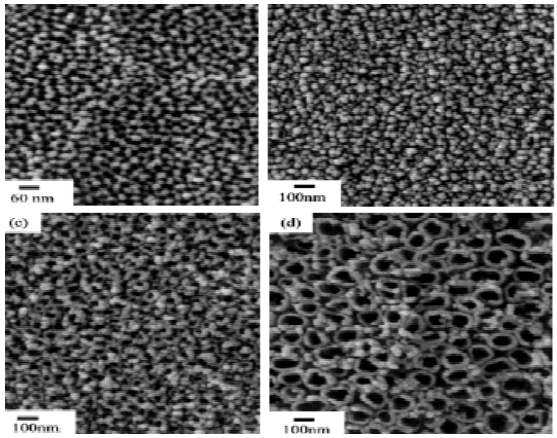

Porous Si and Porous Titania (TiO_2)
of different pore structures

Until now the main energy source of what is called the third world (developing or poor south) countries is the fossil fuels (oil, gas and coal). These countries represent about 85% of the world population. Unfortunately, the fossil fuels are not renewable and the reserves about to finish in near future if the production was kept constant as presented in the next tables. The environmental pollution problem is another issue.

World Oil Reserves 2006		
Thousand milB	**%of World**	**R/P Ratio**(y)
1208.2	**100**	**40.5**
World Gas Reserves 2006		
Trillion cubic ft	**% of World**	**R/P Ratio**(y)
6405.5	**100**	**63.3**

Based on thin film technology, a second generation solar cells have been developed. Materials like amorphous Si, CIS (copper-indium-selinide) and t-Si were used and efficiencies of about 12% have been achieved with a remarkable cost reduction due to less consumption of materials.

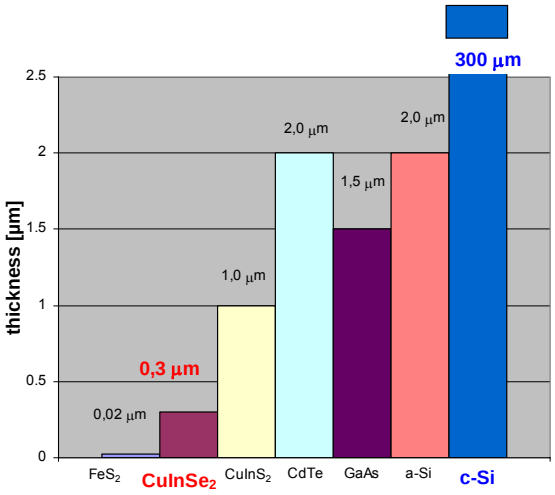

Theoretical thickness of PV materials

In the last decade, a third generation solar cells based on nano-porous materials and quantum dots have been developed [5, 6]. In Kansas State University, a research group has developed solar cells based on GaAs nanoparticles. An advanced photovoltaic cell, originally developed for satellites with solar conversion efficiency of 37.3%, based on concentration of the solar spectrum up to 400 suns was developed. It is based on extremely thin concentration cells.

New synthetic strategies have been developed to design nanostructure architectures of semiconductors, metals, polymers and light harvesting assemblies. Some examples have unique optical, photocatalytic and photoelectrochemical properties of nanostructures. New sensitizer or semiconductor systems are necessary to broaden the photoresponse in solar spectrum. Hybrides of solar and conventional devices may provide an interim benefit in seeking economically valuable devices [5]. In 2008 new quantum dot solar cells based on CdSe-TiO_2 architecture have been developed [6]. With increasing demand for clean energy alternatives an increasing interest from private sector and venture capitalist investment could be achieved, where major breakthroughs in developing economically viable solar energy conversion devices are expected.

More efficient conversion of solar energy into electricity by recent developments in nanotechnology found potential applications in Saudi Arabia, where a whole sunny climate all over the year is ideally suited for such application. The new devices based on nano-sized particles are expected not only to have higher conversion efficiencies compared to conventional solar cells, but are most likely to bring the costs to compete with electricity generated from fossil fuels [7].

References:

Saadoun, M., Ezzaouia, H., Bessais, B., Boujmil, M. F., Bennaceur; R., *Solar Energy Materials and Solar Cells*, 59 (1999) 377-385.

Waheed A. Badawy; *J. Alloys and Compounds*; 464 (2008) 347-351.

Waheed A.Badawy, Rabab M..El-Sherif and Shaaban A.Khalil; Electrochim. Acta; *In Press*. Available on line on Aug. 6, 2010. doi:1016/j.electacta.2010.07.057.

Rabab A. El-Serief, Sahar A. Fadl-allah and Waheed A. Badawy, Modern Trends; in Physics *Research, American Institute of Physics* (AIP Conference Proceedings, Volume 888, Melville, New York, 2007, Pages 110-122.

Kamat; P. V. *J. Phys. Chem*. C, 111 (2007) 2843-2860.

Kongkanan, A., Tvrdy, K., Takechi, K., Kuno, M., Kamat; P. V., *J. Am. Chem. Soc*., 130 (2008) 4007-40015.

International J. Nanomanufacturing, 4 (2009)117. http://inderscience.metapress.com/app/home/

Multiferroic behaviour of $(SrTiO_3)_n$-$(BiFeO_3)_m$ heterostructures predicted from first-principles calculations

E. Bruyer[1,2,3], A. Sayede[1,2,3], R. Desfeux[1,2,3]

[1] Univ. Lille Nord de France, F-59000, Lille, FRANCE
[2]UArtois, UCCS, Faculé des Sciences Jean Perrin, 62300 Lens, FRANCE
[3]CNRS, UMR 818, FRANCE

Introduction:

The development of new multifunctionnal materials is in growing interest in the recent years. In particular, multiferroic materials, which exhibit both electronic and magnetic properties, are very useful for applications in memory devices, especially when deposited in thin films.

Recently, much attention has been focused on the elaboration of artificial heterostructures : indeed, controlling the strain and the composition of ferroelectric superlattices allows the tuning of structural and electronic properties like the spontaneous polarization.

In this work, first-principles calculations were performed to describe the structural, electronic, magnetic and ferroelectric properties of $(SrTiO_3)_n$-$(BiFeO_3)_m$ heterostructures with potentially enhanced multiferroic properties, using density functional theory within the generalized gradient approximation (GGA) and the GGA+U method, as implemented in the Vienna Ab-initio Simulation Package (VASP) code.

These superlattices consist in an alternation of $BiFeO_3$ (rhombohedral, R3c) and $SrTiO_3$ (cubic, Fd3m) unit cells along the [001] direction. For each heterostructure, the atomic positions and lattice constants were optimized and the electronic ground-state properties are calculated. Spontaneous polarization of each heterostructure was described using the Berry-phase method. The influence of the in-plane strain on the multiferroic properties of these superlattices is also investigated.

Structural optimizations were performed on $(STO)_2(BFO)_2$ and $(STO)_4(BFO)_4$ heterostructures, with an initial in-plane parameter equal to the equilibrium lattice constant of STO.

The first results reveal that the in-plane lattice constant takes an intermediate value between the equilibrium lattice constants of $SrTiO_3$ and $BiFeO_3$. Moreover, we observed an elongation of each superlattice along the *c* axis, due to a pronounced elongation of the layers at the interface STO/BFO, while outer layers undergo a slight compression along the *c* axis.

The effect of the epitaxial strain imposed by a cubic substrate (like STO), by varying the in-plane lattice constant, with a ranging from a0 -5% and a0 + 5% in steps of 1 %, allowing all atomic positions and the out-of-plane lattice constant to relax fully until the energy is minimized, has also been studied.

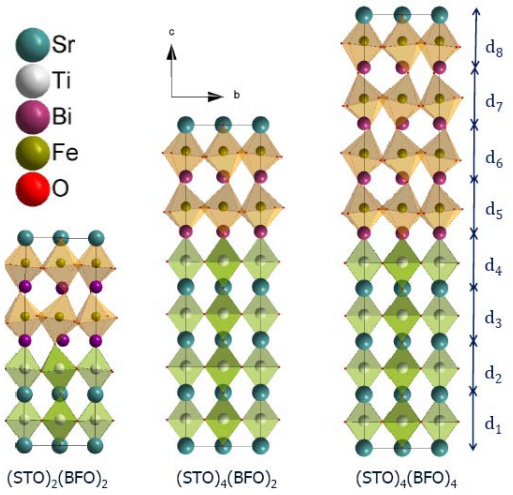

Figure 1: Crystal structure of the $(STO)_n$-$(BFO)_n$ heterostructures

Optical performances of InAs/GaSb/InSb short-period superlattice laser diode for mid-infrared emission

M. Said[1], M. Debbichi[1], S. Ben Rejeb[1]

[1]Unité de recherche de Physique des Solides, Département de Physique, Faculté des Sciences de Monastir, 5019 Monastir, TUNISIA

moncef_said@yahoo.fr

New kind of antimonide-based InAs/GaSb/InSb short-period superlattice (SPSL) laser diode on GaSb substrate for mid-infrared emission has been modelled by an accurate eight-band k.p model. By using a realistic graded and asymmetric interface profile, calculated energy gap between the electron and heavy-hole miniband shows good agreement with our experimental data. Optical gain and threshold current density are then presented and compared with experimental results of SPSL laser diodes operating in pulsed regime. Analysis of the optical performances obtained at room temperature is made.

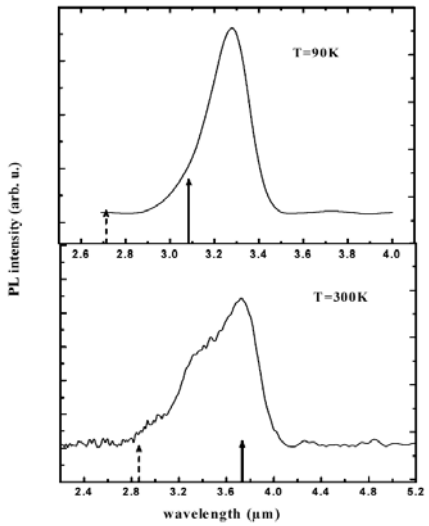

Figure 5: PL spectra from the SPSL structure at 90K and 300K compared with the calculated wavelength values: dashed arrows for the abrupt profile and solid arrows for the segregated profile.

Fig.1 displays PL spectra obtained for the designed SPSL structure at 90K and 300K, exhibiting a peak at 3.27μm and 3.75 μm, respectively. Dashed arrows show the calculated wavelength assuming perfectly abrupt interfaces (InAs-GaSb and GaSb-InAs) and solid arrows for the segregated profile. One can see that in the case of abrupt profile the transition energies are extremely overestimated by 70-90 meV. However, by using appropriate segregated interface profiles, good agreement is obtained between the modelling results and experimental PL spectra.

To fit the experimental values, we have taken into account the effects of interface by introducing an interface layer that comprises 2MLs of material with graded composition, of which 1ML was taken from GaSb and another from InAs. This material is the quaternary $Ga_xIn_{1-x}As_{1-y}Sb_y$, where x and y may be independent. For simplicity, we have used $(InAs)_x(GaSb)_{1-x}$ as interface layer. This interface layer is constructed on the basis of different dominating interface-disorder mechanisms for the two interfaces GaSb on InAs and InAs on GaSb.

References:

Ben Rejeb, S., Debbichi, M., Said, M., Gassenq A., Tournié, E., Christol, P. (2010) *J. Phys. D: Appl. Phys.* 43 325102

Ben Rejeb, S., Debbichi, M., Said, M., Gassenq A., Tournié, E., Christol, P., *Accepted in journal of applied physics*.

Multiband coupling and electronic structure of InAs/GaSb/InSb short-period superlattices

M. Debbichi[1], S.Ben Rejeb[1] and M. Said[1]

[1]Unité de recherche de Physique des Solides, Département de Physique, Faculté des Sciences de Monastir, 5019 Monastir, TUNISIA.
mourad_fsm@yahoo.fr ; moncef_said@yahoo.fr

The antimonide-based system provides great potential for photonic devices in a wide wavelength range, including the useful 3-5 µm mid-infrared atmospheric window. In combination with InAs binary, antimonides (Sb) can form type-II with broken-gap band alignment (also called type-III). These types of heterostructures are particularly relevant because of the expected suppression of non-radiative Auger recombinations in such design [1]. One material system that shows promise for emission at ambient temperature is $(InAs)_n/(GaSb)_m$ superlattices (SLs) on GaSb substrate [2]. The use of these superlattices for mid-infrared lasers and photodetectors depends on the successful growth of the periodic structures but also to the accurate design of their band gaps. Indeed, in the InAs/GaSb SLs, the heterointerface presents a type-II broken gap alignment wherein the valence band of GaSb is about 150 meV above the conduction band of InAs [3], making interband optical transitions between the confined electron and hole miniband states possible.

In order to reduce the natural tensile strain of the InAs layer on GaSb, it is well known that intentional insertion of highly-strained (ε=6.3%) InSb layer in each SPSL's period has to be considered [4] for the fabrication of high quality samples.

In the present work the electronic band-structure and optical gain of InAs/GaSb/InSb short-period superlattice laser diode on GaSb substrate are numerically investigated with an accurate 8x8 **k.p** model. By using a realistic graded and asymmetric interface profile based on experimental measurements, we obtain a good agreement on band gap energy with the experimental data extracted from laser emission performed on laser diode. The optical performance in term of optical gain is then calculated for the laser structure and we demonstrate the utility of interface design to model short-period superlattice structures.

References:

Bürkle, L., Fuchs, F., Henini, M., Razeghi, M. (2002) (Eds), *Handbook of Infrared detection Technologies*, *Elsevier*, UK, p. 159

Deguffroy, N., Tasco, V., Gassenq, A., Cerutti, L., Trampert A., Baranov, A.N., Tournié, E. (2007) *Elect. Lett.* 43, 1285-1286

Surface modification of plasma-treated polyethylene with fluorinated alcohols using chlorinated phosphazenes as coupling agents

Mazzah[1], R. De Jaeger[1]

[1]Université de Lille1 des Sciences et Technologies, Laboratoire de Spectrochimie Infrarouge et Raman, UMR – CNRS 8516, 59655 Villeneuve d'Ascq, FRANCE
ahmed.mazzah@univ-lille1.fr

Abstract

Surface functionalization is a useful technique to modify materials properties such as wettability, biocompatibility, adhesion, flame resistance, optical response, surface conductivity, tribology and catalytic activity, while maintaining bulk properties of functionalized substrates.

Low temperature plasma treatment of polymeric materials brings about several effects on their surfaces, such as cleaning, chain scission, volatilization of smaller polymer fragments and formation of radicals, which may lead to crosslinking, chemical incorporation and formation of oxidized species upon re-exposure of the treated material to atmosphere.

Chlorophosphazenes are compounds of general formula (NPCl2)n, existing both as high molecular weight linear polymers (n=10,000-15,000) and as cyclic oligomers (n=3,4). P-Cl units of these compounds can react with a great variety of nucleophiles, e.g. alcohols, phenols, and primary or secondary amines, leading to the formation of strong covalent P-OR, P-NR2 or P-NHR bonds, respectively.

In the present work a general three-step strategy was devised for the surface functionalization of high density polyethylene (HDPE) plates, by exploiting chlorophosphazenes as coupling agents. The polymeric substrate is first treated with low pressure cold Ar plasma and subsequently exposed to the atmosphere to form oxidized species (e.g. OH, OR, COOH, COOR, etc.) on the surface. Hydroxy groups thus formed were then reacted in the second step with hexachlorocyclophosphazene (HCCP) or, alternatively, with polydichlorophosphazene (PDCP), by simple immersion of the plasma-treated HDPE samples in solutions of HCCP and PDCP.

During reaction, only part of the chlorines of the phosphazenes were utilized to graft the molecules onto the HDPE plates surface. The remaining P-Cl moieties were exploited in the third step of the procedure, where they were reacted with 2,2,2-trifluoroethanol or 1,1-H-heptadecafluorononanol according to classic phosphazene chemistry[3], again by immersion of the substrates in solutions of the alcoholates of fluorinated nucleophiles. The obtained materials were characterized by ATR-IR, contact angle, XPS and SEM techniques. They present potentially interesting applications as biocompatible materials.

It is worth stressing that the character of the presented procedure leading to the modification of surface properties of the samples is completely general. Thanks to the versatility of phosphazene chemistry, in fact, the introduction of an almost unlimited variety of nucleophiles onto the substrate surface can be achieved, granting a series of different properties to be obtained. Moreover, surface activation through plasma can be in principle extended to other substrates, thus opening even wider perspectives for the proposed surface functionalization strategy.

References

H.R.Allcock, *Appl. Organomet Chem*. (1998), 12, 659

S. Guruvenket et al., *Appl. Surf. Sci*. (2004), 236, 278

M.Gleria, R. De Jaeger Eds. Phosphazenes. A Worldwide Insight, NOVA Science Publishers, Hauppauge, New York, USA, (2004).

Modeling blood flow and cell motility: a physicist view

C. Misbah[1]

[1]Univérsité de Grenoble et CNRS, Laboratoire Interdisciplinaire de Physique, 140 rue de la physique, BP87, 38402 Saint Martin d'Hères, FRANCE
chaouqi.misbah@ujf-grenoble.fr

Red blood cells (RBCs) occupy approximately 45% of the total blood volume, whereas other blood corpuscles including white cells compose less than 1%. The remaining blood volume consists of plasma. RBCs are the most common type of blood cells found in vertebrate organisms. Their main function is to transport oxygen from the lungs to bodily tissues via the microcirculatory system (the arterioles and capillaries).

To date blood flow has been described by means of phenomenological continuum models that require many assumptions which are difficult both to justify and to validate. Furthermore, the modern view of complex fluids has highlighted the intimate coupling between the dynamics of the microscopic suspended entities (RBCs in the example of blood) and the flow at the global scale. This implies that the macroscopic law of blood flow should carry information on the microscopic scale, such as the orientation of the cells, their individual and collective dynamics, their local concentration (hematocrit), and so on...

I will discuss questions pertaining to blood cells dynamics. The first focus will be directed towards blood flow. Several types of methods are used: (i) analytical, (ii) boundary integral formulation, (iii) level set and phase field, and (vi) Lattice Boltzmann methods. We present results of a single cell under shear flow, and then under a parabolic flow (this type of flow is relevant to blood flow). Under shear flow cells may undergo a variety of dynamics (tank-treading, vacillating-breathing, tumbling, kayaking…), and these dynamics have a direct impact on the overall blood flow properties (rheology). We will then address the question of why do red blood cells adopt a non symmetric shape (called a slipper shape) even in a symmetric flow ? The adoption of this shape is shown to result from instability of the symmetric shape. It will further be shown that by adopting a slipper shape the red cell acquires a better flow efficiency. In addition the slipper favors mixing of the internal fluid, and may thus help blood flow transport and oxygen delivery.

In the second part I will address the notion of cell motility assisted by actin-driven polymerization (actin is a protein found in the cell cytoplasm). It will be shown that the cell can undergo a spontaneous symmetry breaking leading to polarization (Figure 2). Some biomimetic experiments will be presented showing that even a bead on which actin polymerization can take place may undergo a spontaneous symmetry breaking and acquires a motion. I will show how these kinds of biological simplifications offer a fruitful terrain for building a firm basis on elementary processes that are decisive in real life.

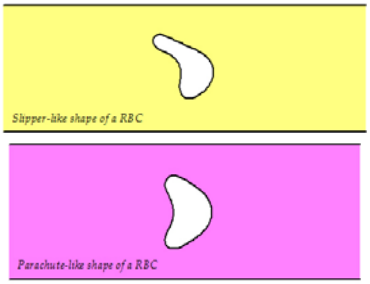

Figure 6: Top: slipper shape. Bottom parachute shape

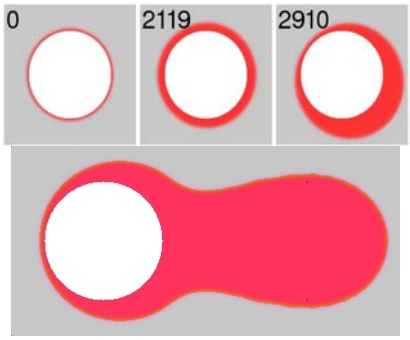

Figure 2 : In red actin gel growing on bead (white) and undergoing spontaneous symmetry breaking

References:

Fung Y.C., *Biomechanics* (Springer, New York, 1990).
Larson, R.., *The structure and rheology of complex fluids*, Oxford (1999).
Misbah, C. (2006), *Phys. Rev. Lett.* , 96, 028104.
Biben, T.., Misbah C., preprint soumis à *Phys. Rev. E.*
Danker, G., Misbah, C., (2007) *Phys. Rev. Lett.* , 98, 088104.
Kaoui, B., Biros, G., & Misbah, C. (2009), *Phys. Rev. Lett.* 103, 188101-188104 .
John K. et al. (2008), *Phys. Rev. Lett.* 100, 068101

Computational Investigation of Metal Ion-Peptide Interactions

E. Terzioglu[1], M. U. Kahveci[2], Z. P. Cakar[1, 2, 3], N. Acar[4], C. Kopruluoglu[5], A. Kara[6], C. Selcuki[5]

[1]Molecular Biology Genetics and Biotechnology Programme, Institute for Graduate Studies in Science and Enginnering, Istanbul Technical University, 34469 Maslak/Istanbul/TURKEY
[2]Department of Molecular Biology and Genetics, Istanbul Technical University, 34469 Maslak/Istanbul/TURKEY
[3]Dr. Orhan Ocalgiray Molecular Biology-Biotechnology and Genetics Research Center, Istanbul Technical University, 34469 Maslak/Istanbul/TURKEY
[4]Ege University Faculty of Science Department of Chemistry, 35100 Bornova/Izmir/TURKEY
[5] Ege University Faculty of Science Department of Biochemistry, 35100 Bornova/Izmir/TURKEY
[6]Ege University Institute for Nuclear Sciences, 35100 Bornova/Izmir/TURKEY

Some metal ions are essential for living cells as co-factors for metalloproteins; but, they are also potentially toxic. Therefore, some proteins in the cell act as metal transporters and metal chaperons. Copper is one of these essential metals whose damage should also be avoided by copper chaperones. Saccharomyces cerevisiae is the yeast that has been commonly studied to determine the complex pathways of copper trafficking. One of these pathways includes Atx1 protein, copper chaperon for Ccc2 which is a P-type ATPase cation transporter. Atx1 copper chaperone's functional homologues were identified in organisms varying from bacteria to humans. These polypeptides are small, consisting of approximately 70 amino acids and have a common MXCXXC motif, where M is methionine, C is cysteine and X is any amino acid. Atx1 is thought to bind copper via the two cysteine residues.

In this part, the structure of MXCXXC motif will be investigated by computational methods. HyperChem software will be used for computations. Initially, threonine is chosen for the first X residue and small amino acids (i.e. glycine) for the other X residues. In the following step, small amino acids will be used in different combinations for the three X residues. Thus, it is aimed to clarify if these X residues may provide selectivity for copper binding. We will also focus on the understanding of the exact mechanism of copper binding. The calculations will be repeated with quantum mechanics by using the Density Functional Theory methods (DFT) methods implemented in Gaussian series of programs.

A plasma membrane protein complex consisting of a multicopper ferroxidase enzyme and a ferric iron permease is responsible for high affinity iron uptake in fungi. In S.s cerevisiae, Ftr1p is the permease component of the high affinity iron-uptake complex, namely Fet3p–Ftr1p complex. Ftr1 is considered to be a multi-pass transmembrane protein with seven transmembrane segments, which contain two REXLE sequence motifs that are essential for ferric iron (Fe3+) binding and uptake. In this part, we will investigate the binding site, REXLE motif, using molecular mechanics (CHARMM). Seven different amino acids (G, L, V, A, C, S and T) are used for X, and comparative conformational analyses will be performed in the presence or absence of Fe3+. Furthermore, same analysis will be carried out for REXXE motif using the same seven amino acids. The preliminary comparative results indicated that the most possible two sequences playing role in iron binding were REGLE and RECLE.

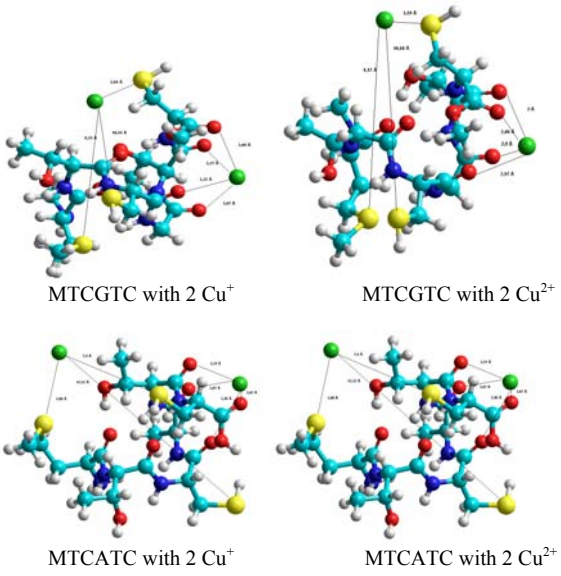

Figure 7: Some structures obtained for MXCXXC-Cu interactions

This work is supported by TUBITAK Grant No: 109T616 as part of the COST Action CM0902 "Molecular machineries for ion translocation across biomembranes".

HyperChem 8.0, HyperCube Inc., USA.
Gaussian 03 Version C02., Frisch M. et al. Gaussian Inc., USA.

Spectroscopic and computational analysis [FeFe]-Hydrogenase Models with Bridging Moieties Containing (S, Se) and (S, Te)

M. El-khateeb[1], M. Harb[1]

[1] Chemistry Depeartment, Faculty of Sciences, JUST PO Box 3030 Irbid JORDAN
kateeb@just.edu.jo

Introduction: The natural energy resources are diminishing, and their continued use has become more harmful for the environment. Therefore, efforts to develop alternative energy resources and fuels have become major goals for the scientific community. Dihydrogen is one of the future fuels that causes no deleterious products for the environment. Efficient production of dihydrogen in good yield has become a challenge, and there has been much research aimed at overcoming this challenge. Biomimetic catalysts are based on the active site of [FeFe]-hydrogenases.[1, 2] Recently, diiron complexes containing diselenolato ligands have been prepared and substituted. More recently, we prepare a series of model complexes containing dithiolato, diselenolato, ditellerrolato and mixed chalcogenio ligand. Spectroscopic and theoretical investigation of these complexes are reported.[3]

Content: [FeFe]-hydrogenase-active-site models containing larger chalcogens such as Se or Te have exhibited greater electron richness at the metal centers and smaller gas-phase ionization energies and reorganization energies relative to molecules containing S atoms. Diiron complexes related to the much-studied molecule [Fe2(μ-SC3H6S)(CO)6] (**1**) have been prepared with one S atom replaced either by one Se atom to give [Fe2(μ-SC3H6Se)(CO)6] (**2**) or by one Te atom to give [Fe2(μ-SC3H6Te)(CO)6] (**3**).[4,5] The molecules have been characterized by use of mass spectrometry and $^{13}C\{^{1}H\}$ NMR, $^{77}Se\{1H\}$ NMR, IR, and photoelectron spectroscopic techniques along with structure determination with single-crystal X-ray diffraction, electrochemical measurements, and DFT calculations. He I photoelectron spectra and DFT computations of **2** and **3** show a lowering of ionization energies relative to those of the all-sulfur complex **1**, indicating increased electron richness at the metal centers that favors electrocatalytic reduction of protons from weak acids to produce H2. However, chalcogen substitution from S to Se or Te also causes an increase in the Fe–Fe bond length, which disfavors the formation of a carbonyl-bridged "rotated" structure, as also shown by the photoelectron spectra and computations. This "rotated" structure is believed to be important in the mechanism of H2 production. As a consequence of the competing influences of increased electron richness at the metals with less favorable "rotated" structures, the catalytic efficiency of the Se and Te molecules **2** and **3** is found to be comparable to that of molecule **1**.[3,5]

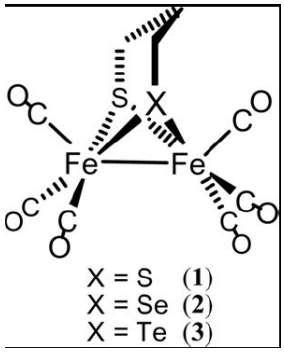

Figure 8: Structure of Complexes

References:

Frey, M. *ChemBioChem* 2002, *3*, 153–160.
Vignais, P. M., Billoud, B. *Chem. Rev.* 2007, *107*, 4206–4272.
Harb, M. K., Niksch, T., Windhager, J., Görls, H., Holze, R., Lockett, L. T., Okumura, N., Evans, D. H., Glass, R. S., Lichtenberger, D. L., El-khateeb, M. Weigand, W. (2009)*Organometallics*, *28*, 1039–1048.
Song, L. C., Gai, B., Wang, H.-T., Hu, Q. M. (2009) *J. Inorg. Biochem.*, *103*, 805–812.
Harb, M. K., Windhager, J., Daraosheh, A., Görls, H., Lockett, L. T., Okumura, N., Evans, D. H., Glass, R. S., Lichtenberger, D. L., El-khateeb, M., Weigand, W. (2009) *Eur. J. Inorg. Chem*, 3414–3420.

Molecular dynamics simulations of amphiphilic inclusion complexes formed by β-Cyclodextrin and sorbitol esters

A. Sayede[1,2,3], M. Bouterfas[1,2,3,4], C. Machut[1,2,3], S. Menuel[1,2,3], M. Sekkal[4] and E. Monflier[1,2,3]

[1] Univ. Lille Nord de France, F-59000, Lille, FRANCE
[2]UArtois, UCCS, Faculé des Sciences Jean Perrin, 62300 Lens, FRANCE
[3]CNRS, UMR 818, France
[4]L2MSM, Faculté des Sciences, Université Djilali Liabes, 22000, Sidi Bel Abbes, ALGERIA

Introduction:

Force-field-based atomistic simulations of host−guest supramolecular complexes between β-cyclodextrin (β-CD) and two sorbitol esters have been analyzed with respect to relative orientation and interaction energies, explicitly considering solvent (water) molecules. The guest molecules were sorbitol esters of oleic acid (1) or stearic (2) . The studied host-guest complexes are sketched in Figure 1. The initial configuration of β-CD was obtained from the crystal structure of a β-CD hydrate [1] whereas the geometries of guest molecules were built with Gausview software [2].

prevent molecules from being artificially split when one of the atoms was inside and another was outside the atom-based cutoff. The correct density of the system was checked by performing a relaxation run under isobaric−isothermal conditions at a temperature of 298 K, which left the box size unchanged.

Constant temperature MD simulations were performed with a time step of 1 fs applying the Verlet velocity algorithm. The overall simulation time of a single run ranged from 1 to 10 ns. For the whole simulation procedure the Amber10 suite of program [3] were used using the general force field

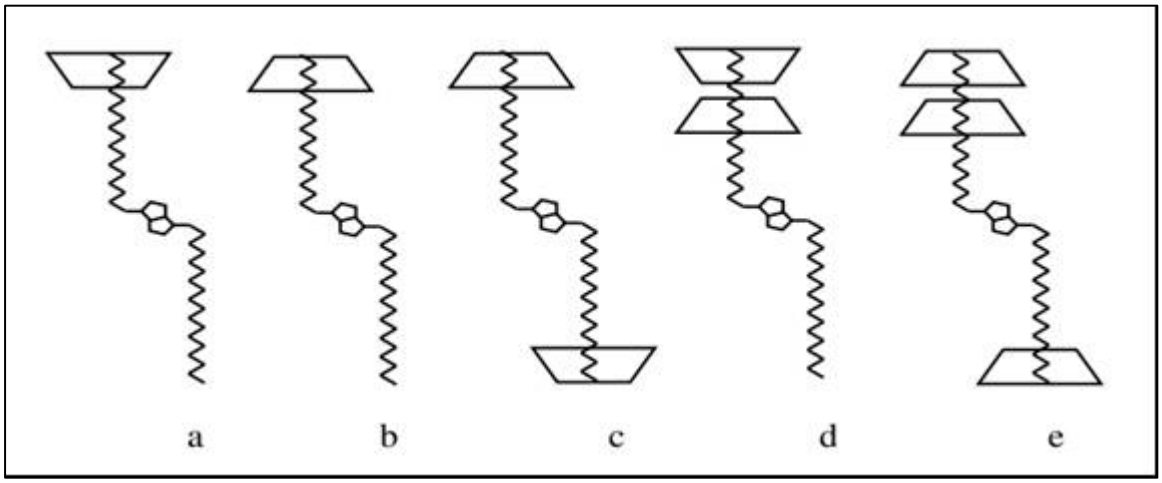

Figure 1. The different studied Host-Geust complexes formed by sorbitol ester (1) or (2) and one (two or three) β-CDs

The molecular dynamics (MD) simulation of a single host−guest complex in aqueous solution was carried out in a parallelepiped box with periodic boundary conditions in all directions. The simulation box contain one (two or three) β-CDs and one guest molecule, (**1**) or (**2**), and up to 2500 water molecules corresponding to a density of 1 g/cm3, characteristic of ambient temperature (298 K). The box was large enough that any interactions between a molecule and its periodic images was avoided, thus correctly simulating an infinitely diluted solution. For the nonbonding interactions, charge groups were used to

parameters (GAFF) [4] and TIP3P water model [5]. Atomic charges for guest molecules were obtained by the restrained electrostatic potential (RESP) methodology, electrostatic potentials were generated at DFT (B3LYP) level with 631G* basis set. For β-CD the charges were taken from reference [6] . The DFT calculations were performed with Gaussian03 software [7]. The obtained MD trajectories were used to estimate the binding free energies (ΔG_{bind}) of the Host:Guest complexes using the molecular mechanics Poisson Boltzmann surface area (MM-PBSA) method.

For both sorbitol esters, the calculations revealed different stable orientations within one or more β-CDs. In addition, the binding free energies calculation indicates that the the apolar contributions ($\Delta e_{vdW}+\Delta G_{nonpolar}$) are the driving forces for binding in theses complexes. The results show also that inclusion complexes formed by (**2**) and β-CDs are more stable due to the presence of more flexible chains. The higher rotational degrees of freedom of (**2**) leads to a more favorable complexation entropy, where more of the hydrophobic chains can fit properly into the β-CD cavity.

References:

Lindner, K., Saenger, W. (1982) *Carbohydrate Research* 99 103.

Dennington II, R., Keith, T., Millam, J., Eppinnett, K., Hovell, W.L., Gilliland, R. (2003) GaussView, Version 3.09, *Semichem*, Inc., Shawnee Mission, KS.

Case, D.A., Darden, T.A., Cheatham, T.E.,III, Simmerling, C.L., Wang, J., Duke, R.E., Luo, R. Walker, R.C., Zhang, W., Merz, K.M., Roberts, B.P., Wang, B., Hayik, S., Roitberg, A., Seabra, G., Kolossváry, I., Wong, K.F., Paesani, F., Vanicek, J., X. Wu, S.R. Brozell, T. Steinbrecher, H. Gohlke, Q. Cai, , Wang, Hsieh, X. Ye., J., M. J., Cui, G., Roe, D.R., Mathews, D.H., Seetin, M.G., Sagui, C., Babin, V., Luchko, T., Gusarov, S., Kovalenko, A., Kollman, P.A. (2010), AMBER 11.

Cornell, W.D., Cieplak, P., Bayly, C.I., Gould, I.R., Merz, K.M., Ferguson, Jr.,D.M., Spellmeyer, D.C., Fox, T., Caldwell, J.W., Kollman, P.A. (1995) *J. Am. Chem. Soc*. 117 5179.

Jorgensen, W. L., Chandrasekhar, J., Madura, J. D. (1983) J. *Chem. Phys*. 79 926.

Bonnet, Jaime, P., C., Morin-Allory, L., (2001*) The Journal of Organic Chemistry* 66 689.

Gaussian 03, Revision C.02, Frisch, M. J., Trucks, G. W., Schlegel, H. B., Scuseria, G. E., Robb, M. A., Cheeseman, J. R., Montgomery, J. A., Vreven, Jr., T.,K. Kudin, N., Burant, J. C., Millam, J. M., Iyengar, S. S., Tomasi, J., Barone, V., Mennucci, B., Cossi, M., Scalmani, G., Rega, N., Petersson, G. A., Nakatsuji, H., Hada, M., Ehara, M., Toyota, K., Fukuda, R., Hasegawa, J., Ishida, M., Nakajima, T., Honda, Y., Kitao, O., Nakai, H., Klene, M., Li, X., Knox, J. E., Hratchian, H. P., Cross, J. B., Bakken, V., Adamo, C., Jaramillo, J., Gomperts, R., Stratmann, R. E., Yazyev, O., A. Austin, J., Cammi, R., Pomelli, C., Ochterski, J. W., Ayala, P. Y. , Morokuma, K., Voth, G. A., Salvador, P., Dannenberg, J. J., Zakrzewski, V. G., Dapprich, S., Daniels, A. D., Strain, M. C., Farkas, O., Malick, D. K., Rabuck, A. Raghavachari, D., K., Foresman, J. B., Ortiz, J. V., Cui, Q., Baboul, A. G., Clifford, S., Cioslowski, J., Stefanov, B. B., Liu, G., Liashenko, A., Piskorz, P., Komaromi, I., Martin, R. L., Fox, D. J., Keith, T., Al-Laham, M. A., Peng, C. Y., Nanayakkara, A., Challacombe, M., Gill, P. M. W., Johnson, B., Chen, W., Wong, M. W., Gonzalez, C., Pople, J. A. (2004) Gaussian, Inc., Wallingford CT,.

Electronic properties of low dimensional structures

A. Bendounan[1,2]

[1] Experimentelle Physik II, Universität Würzburg, Am Hubland, D-97074 Würzburg, GERMANY

[2] Synchrotron SOLEIL, Saint-Aubin, BP48, F-91192 Gif-sur-Yvette Cedex, FRANCE
azzedine.bendounan@synchrotron-soleil.fr

Abstract: Many physical properties of materials, concerning for example the transport, are directly connected to theirs electronic band structures and are mainly controlled by the behavior of electronic states located in the vicinity of the Fermi level. Exotic phenomena about the behavior of electrons inside the solid were a long time ago predicted by the quantum mechanic physics and are only recently experimentally proved, in particular for systems of extremely reduced dimensions. Perhaps on can refer to the superconductivity as the most prestigious phenomenon thoroughly investigated over the last decades in order to draw a clear picture of the underlying physics. Much interest has also been devoted to the behavior of the surface states, which were successfully used as a model system to explore many-body-effect through different electronic interactions in the solid (electron-electron, electron-phonon and electron-defect) and have also recently opened up the way for new spintronic developments. Here, I will give an overview of recent experimental observations of fundamental effect concerning spectroscopic properties of low energy electronic states close to the Fermi level studied by angle resolved photoemission and band structure calculations.

DFT study of the interaction of iron dimer with benzene

Z. Guennoun[1], J. Mascetti[1], Y. Hannachi[1]

[1]Groupe de Spectroscopie Moléculaire de l'Institut des Sciences Moléculaires
Université de Bordeaux 1, CNRS, UMR5255
351, cours de la Libération 33405 Talence Cedex
y.hannachi@ism.u-bordeaux1.fr

As part of our starting project on the interaction of iron atom and iron clusters with polycyclic aromatic hydrocarbons (PAHs), a theoretical study the Fe_2(benzene) system have been conducted using density functional method with various combinations of exchange and correlation functionals.

Three types of coordination modes were used as starting point for geometry optimisation, namely an η^6 and η^2 coordination mode (perpendicular) and a parallel configuration. Spin states ranging from singlet (S=0; open shell) to S=4 have been characterized. For all spin state the perpendicular configuration is more stable than the parallel one (see Table 1). The ground state structure corresponds to an η^6 coordination mode with a septet (S=3) spin multiplicity with all used combination of functionals (see Figure 1 and Table 2). The calculated vibrational spectra of the obtained lowest energy structure agrees well with that observed by Ball et al. [1] in argon matrix. Comparison is made with a very recent theoretical study of Parker [2] and Valencia et *al.* [3].

Table 1: Calculated bonding energies (eV) of different coordination mode and spin states of η^6 Fe_2-Benzene complexes

Spin state	perpendicular	parallel
singlet	-0.77	-
triplet	-0.73	+0.33
quintet	-0.25	+0.09
septet	-0.85	-0.46
nonet	-0.17	0.07

Table 2: Calculated relative energies (eV) of different spin states of η^6 Fe_2-Benzene complexes.

Spin state	*MPW1PW91*	*B3LYP*
singlet	0.08	0.09
triplet	0.12	0.19
quintet	0.60	0.64
septet	0.00	0.00
nonet	0.69	dissociates

References:

Ball, D. W., Kafafi, Z. H, Hauge, R. H.; Margrave, J. L. (1986) *J. Am. Chem. Soc*. 108, 6621.
Parker, S. F. (2010) *J. Phys. Chem*. A, 114 1657.
Valencia, I., Castro, M. 2010 *Phys. Chem. Chem. Phys*., , 12, 7545–7554

Figure 9: h^o coordination mode of Fe_2-benzene complex.

Efficient Methods for Micro- and Mesoscopic Time- and Length-Scales in Classical Particle Simulations on Massively Parallel Computers

G. Sutmann[1]

[1]Institute for Advanced Simulation (IAS)
Jülich Supercomputing Centre (JSC)
Research Centre Jülich, GERMANY
E-mail: g.sutmann@fz-juelich.de

Simulation of complex particle systems, such as biomolecular or soft matter systems, by means of classical force field methods is a very demanding task. Due to the presence of a variety of time scales ranging from femto- to micro-seconds or longer, all-atom simulations of solvated molecules are restricted to relatively small scales, both in time and length.

Considering classical force fields one can nevertheless optimise the methods and algorithms in such a way that the computational complexity becomes optimal, i.e. O(N). Furthermore one can try to perform a seperation of time scales, e.g. intra- vs intermolecular motions or hydrodynamic modes. Finally, parallelization is often key to tackle problems on extended scales.

In the talk, several optimal methods for intermolecular interactions, including methods for short- and long range interactions, such as optimised list techniques or hierarchical methods for electrostatics are presented. Also methods based on time scale seperation are discussed, including the coupling between microscopic and mesoscopic medium descriptions, leading to mesoscopic hydrodynamics, which can be modelled e.g. by stochastic particle collisions.

Finally, parallelisation of particle simulation methods is addressed and it is demonstrated, which gain may be achieved by using supercomputers for the simulation of complex systems.

Kinetics and DFT studies on the Catalytic Epoxidation of Olefins by η^5-Cyclopentadienyl Molybdenum Catalysts

A. Al-Ajlouni[1]

[1]Department of Applied Chemical Sciences, Jordan University of Science and Technology, Irbid 22110,

JORDAN

aajlouni@just.edu.jo

Abstract:

η^5cyclopentadienyl(tricarbonyl)methylmolybdenum(II) (**1**) is oxidized by *tert*-butylhydroperoxide (TBHP) to yield in the first step η^5-cyclopentadienyl(dioxo)methyl molybdenum(VI) (**2**). This compound further reacts with excess of TBHP to form η^5-cyclopentadienyl(oxo)-(peroxo)methyl molybdenum(VI) (**3**). The solid state structure of this compound has been determined by X-ray crystallography. Compounds **2** and **3** are unable to epoxidize olefins when used in stoichiometric amounts in the absence of TBHP, and decompose, but addition of TBHP leads, in both cases, to olefin epoxidation. The conversion of compound **2** to **3** competes with the formation of an active species **C**, able to catalyze the olefin epoxidation. Compound **3** also leads to an active species **I**, which is, however, less active than that formed from compound **2**. DFT calculations indicate that intermediates **C** and **I** both display end-on bound alkyl peroxo ligands, and activation.

Computational Insight: Oral Phosphodiesterase 5 Inhibitors for Erectile Dysfunction

Ashraf H. Abadi[1]

[1]Pharmaceutical Chemistry Department, Faculty of Pharmacy and Biotechnology, German University in Cairo, 11835 Cairo, EGYPT

The talk will highlight the mechanisms by which different phosphodiesterase 5 inhibitors interact with the enzyme and the shortcomings of some current co-crystallized proteins with the inhibitors.

In view of the docking and in vitro binding studies of novel tadalafil analogues a plausible explanation of the steric and stereochemical aspects involved in the interaction and new potential types of interaction will be revealed and discussed.

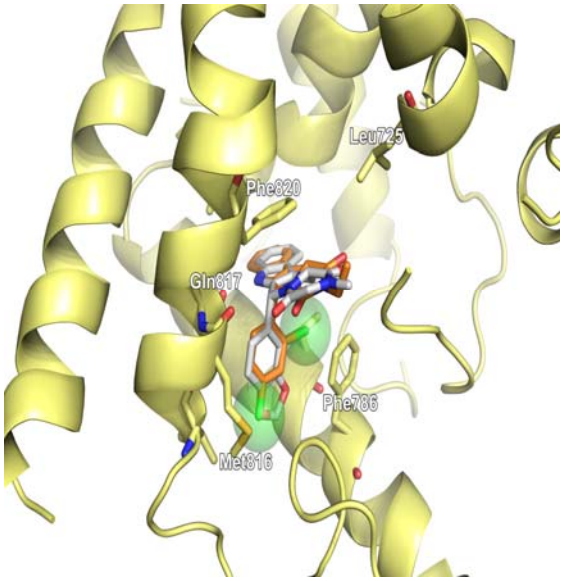

Figure 1: Docked pose of a new active compound (orange) in the cavity of 1UDU superimposed on tadalafil (white) featuring van-der-Waals spheres on the chlorine atoms

NEW OF SCHWINGER VARIATIONNAL PRINCIPLE FOR K-SHELL EXCITATION OF $Ca^{18+}(1S^2)$ IONS BY IMPACT OF VARIOUS ATOMS AT 8.6 MeV/amu

B. Lasri[1, 2], M. Bouamoud[1], J. Hanssen[3]

[1]Laboratoire de Physique Théorique, Département de Physique, Faculté des Sciences, Université Abou-Bekr-belkaïd , B.P 119 Tlemcen, ALGERIA
[2]Université D[r] Tahar Moulay. B.P 138 El-Nasr, Saïda (20000), ALGERIA
lasribo@yahoo.fr
[3]Laboratoire de Physique Moléculaire et des Collisions, Université de Metz, 1 Bd Arago, 57078, Cedex 3, Metz, FRANCE

Abstract:

A new variational impact parameter approach to the process of direct electronic excitation of atoms by impact of ions at intermediate velocities regimes was shown to be very successful in predicting the saturation of cross sections when the projectile charge is increased. In our approach, this new procedure is based on the fractional form of the Schwinger variational principle and applied to study *K*-shell excitation of Ca^{18+} ($1s^2$) ions impinging at 8.6 MeV/amu on various gases (H_2, He, N_2, O_2, Ne, Ar, Kr, Xe). The excitation cross sections are compared with the Glauber and the Plane wave Born approximation. All obtained results stay in good agreement with experimental data of Xiang-Yuan et al [1].

In the present study, the target propagator G_T^+ has been expanded on the whole discrete spectrum of the target and the contribution of the continuum has been taken into account using an analytical continuation which consists to evaluate the part close to ionisation threshold [2-5].

Initially, the excitation of $Ca^{18+}(1s^2)$ to the levels (1s, nl) was made with a set of 5 orbitals : $B_1 = B_2 = \{1s, ns, np_0, np_{+1}, np_{-1}\}$ where $n = 2, 3$. This procedure was called the Schw55. In our new approach, and in order to refine this varaiational procedure, the calculations are performed and the wave functions $\left|\psi_\alpha^+\right\rangle$ and $\left|\psi_\beta^-\right\rangle$ are expended on fourteen-states basis set as $B_1 = B_2 = \{1s , 2s , 2p_0 , 2p_1 , 2p_{-1} ,3s , 3p_0, 3p_1, 3p_{-1}, 3d_0, 3d_1, 3d_{-1}, 3d_2, 3d_{-2}\}$ which is called Schw1414 [2,5].

Experimentally, the excitation cross sections were determined from coincidence measurements between projectile *K* x-ray and the projectile charge state fraction which had not undergone charge exchange in passage through the target. [1].

The total excitation cross sections of the level (1s,*nl*) of $Ca^{18+}(1s^2)$ by various gases of nuclear charges Zp, are plotted as function of Zp. Finally, it should be noted that an good agreement is observed between the present calculation (Schw55, Schw1414) and the experimental data of Xiang-Yuan et al [1].

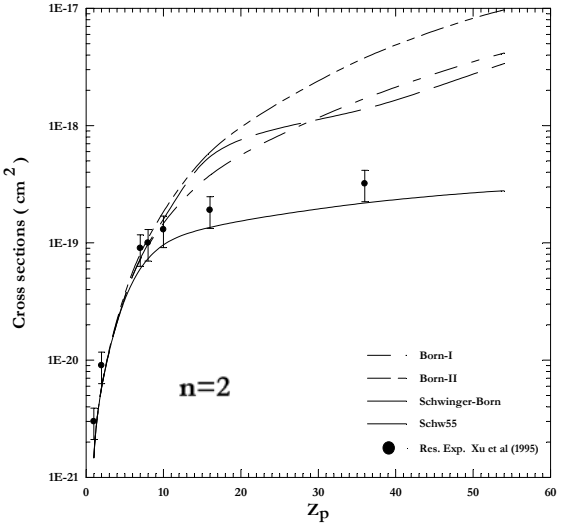

Figure: Excitation Cross sections of the n=2 level of Ca^{18+} ($1s^2$) impinging at an energy 8.6 MeV/u on various target of nuclear charge Z_P indicated in the abscise

References :

Xiang-Yuan Xu, Montenegro, E.C., Anholt, R., Danzmann, K., Meyerhof, W.E., Schlachter, A.S., Rude, B. S., McDonald, R.J. (1988) *Physical Review A*, Vol 38, 4, 1848.

Lasri, B., Bouamoud M., Gayet, R. (2004) *Physical et Chemical News Journal*, 20, p12-17.

Lasri, B., Bouamoud M., Gayet, R. (2006) *Physical et Chemical News Journal*, 28, p97-102.

Lasri, B., Bouamoud M., Gayet, R. (2006) *Nucl. Instr. and Meth.B* 251, 66-72.

Lasri, B., Bouamoud M., Hanssen, J. (2007) *Journal of Electron Devices,* Vol. 5, pp. 127-131.

On the characterization of cluster distribution in supercritical fluids: A molecular dynamics and data mining approaches

A. Idrissi[1], I. Vyalov[1,2], M. Kiselev[2]
nacer.idrissi@univ.lille1.fr

[1]Université de Lille1 des Sciences et Technologies, Laboratoire de Spectrochimie Infrarouge et Raman, UMR – CNRS 8516, 59655 Villeneuve d'Ascq, FRANCE
[2]Institute of Solution Chemistry of the RAS, Akademicheskaya st.1, 153045 Ivanovo, RUSSIA

Abstract

One of the most important properties of supercritical fluids (SCF) is the density inhomogeneity (the radial and mutual orientation distributions of molecules when approaching the critical point). From the microscopic point of view the formation of inhomogeneities in the fluid is associated with the compressibility behavior which increases drastically near the critical point. As a consequence, the properties of supercritical fluids can be varied continuously and markedly from gas-like to liquid-like values with a small change in pressure or/and temperature. This feature makes SCF attractive alternatives to liquid solvents for the use in the developments of new chemical processes. In several previously reported experimental and theoretical studies the importance of density inhomogeneity distribution in the determination of SCF properties has been clearly underlined.

In this contribution, we offer a new method to analyze the inhomogeneity distributions of particles in sub and supercritical conditions. This method combines numerical methods and data mining approaches. The probability distributions of molecules are evaluated using algorithm relaying on the density based clustering. When this algorithm is used to calculate the probability distribution of domains, one is faced with the choice of the minimum number of atoms in the density-domains and the spatial extent of these density-domains. In principal the choice of these parameters is arbitrary. However, in order to rationalize the choice of these parameters, we propose to use the radial nearest neighbors approach which allows to determine the two input parameters based on the value of the average density for the calculation of the probability distribution of the number of density-domains and the number of particles in each density-domain.

CP Violation in Fourth Generation Quark Decays

A. Arhrib[1]

[1]Faculté des Sciences et Techniques, B.P 416 Tangier, MOROCCO

Motivations: The 4th generation is troubled by the electroweak precision test (EWPT) S parameter. However, this severe constraint is softened when one allows some t'–b' mass splitting that contributes to T parameter. With the LHC, we finally have a machine that can discover or rule out the 4th generation once and for all by direct search [1]. There is in fact renewed interest at the Tevatron. CDF has searched for t' and b', setting the 95% C.L. limits of $m_{t'} > 311$ GeV and $m_{b'} > 325$ GeV, respectively.

Moreover, 4th generation could enhance the invariant CPV measure of Jarlskog by a factor of 10^{15} [2], and perhaps could satisfy the CPV part of the Sakharov conditions for baryogenesis in the early Universe.

Motivated by the BSM source of CPV, and with heightened direct search activity, we ask: What can the direct discovery of the b' and t' quarks do for the quest of CPV? We find the best case to be flavor changing neutral current (FCNC) $b' \to s$ decays, with b' around and above the tW threshold (see Fig. 1).

Mechanism of CPV: CPV requires two interfering amplitudes $\mathcal{M} = \mathcal{M}_1 + \mathcal{M}_2$, and the CP asymmetry is

$$A_{\rm CP} = \frac{2|\mathcal{M}_1||\mathcal{M}_2|\sin\delta\sin\phi}{|\mathcal{M}_1|^2 + |\mathcal{M}_2|^2 + 2|\mathcal{M}_1||\mathcal{M}_2|\cos\delta\cos\phi}, \quad (1)$$

which vanishes unless both the weak *and* "strong" phase differences $\phi \equiv \phi_2 - \phi_1$ and $\delta \equiv \delta_2 - \delta_1$ are nonzero.

The u quark effect in Fig. 1 is suppressed by a tiny $V^*_{ub}V_{ub'}$. Alternatively, $q = c$, u are effectively massless, and provide a GIM subtraction to the t and t' amplitudes via $V^*_{qs}V_{qb'} + V^*_{ts}V_{tb'} + V^*_{t's}V_{t'b'} = 0$, giving

$$\mathcal{M}_{b'\to s} = V^*_{ts}V_{tb'}\,\Delta(t,0) + V^*_{t's}V_{t'b'}\,\Delta(t',0), \quad (2)$$

with $\Delta(a,b) = f(m_a) - f(m_b)$, and f the loop function.

Let us consider the CP conserving phase difference δ between $\Delta(t,0)$ and $\Delta(t',0)$. Having both t', b', and even the top rather heavy, enriches the strong phase difference $\sin\delta$ in Eq. (2). For b' below tW (hence $t'W$) threshold, both the t and t' effects are dispersive, the strong phase difference between GIM-subtracted t and t' contributions are subdued. But as the tW threshold (illustrated by the cut in Fig. 1) is approached, the dispersive t amplitude gets affected, and $\sin\delta$ starts to grow. Above tW threshold, the behavior of $\sin\delta$ depends on $m_{t'}$, e.g. whether it is correlated with $m_{b'}$ due to electroweak constraints. It also depends on the process. Note that the processes $b' \to b$, the $t' \to t$, c, and the $t \to c$ transitions all turn out to be dominated by a single amplitude, and, according to Eq. (1), cannot generate much $A_{\rm CP}$.

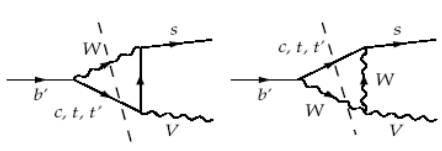

Fig. 1: $b' \to s$ loop transition, where the cut is for c and t.

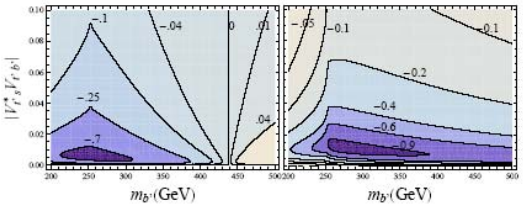

Fig. 2: Contour plots of $A_{\rm CP}$ for $b' \to sZ$ (left) and $b' \to s\gamma$ (right) in $m_{b'}$–$|V^*_{t's}V_{t'b'}|$ plane, with $m_{t'} = m_{b'} + 50$ GeV, with $\arg(-V^*_{t's}V_{t'b'}) = 70°$, and $V^*_{ts}V_{tb'} = -0.01\,e^{i\,10°}$, $V_{tb'} = 0.1$

From Eq. (2), we see that $b' \to s$ transitions are controlled by $V^*_{t's}V_{t'b'}$.

CPV in $b' \to s$ Transitions The contours of $A_{\rm CP}$ in the plane of $m_{b'}$ and $|V^*_{t's}V_{t'b'}|$ is plotted in Fig. 2 for $b' \to sZ$ and $b' \to s\gamma$ decays, with $m_{t'} = m_{b'} + 50$ GeV. One sees clearly that the largest $A_{\rm CP}$ occurs around tW threshold, and for $|V^*_{t's}V_{t'b'}|$ approaching $V^*_{ts}V_{tb'}$ in strength. We see from Fig. 2 that maximal $A_{\rm CP}$ occurs for $|V^*_{t's}V_{t'b'}|$ not far from $|V^*_{ts}V_{tb'}|$, as can be understood from Eq. (1).

We see that $A_{\rm CP}(b' \to sZ)$ can in principle go up to more than 70%, especially if $m_{t'}$, $m_{b'} \lesssim 350$ GeV or so (and $m_{b'} > m_{t'}$ would be better). Larger asymmetries are possible for $b' \to s\gamma$, and extending to high $m_{b'}$.

Conclusion In conclusion, the best scenario for CPV studies at high energy collider is for $b' \to s$ decays. One would first have to discover the 4th generation, preferably around 300 GeV or so. After sorting out the dominant decays, one would have to identify $b' \to sZ$ or $b' \to s\gamma$ channels, and then tag the other $\bar{b}'$.

References

[1] A. Arhrib and W.S. Hou, JHEP **07**, 009 (2006).

[2] W.S. Hou, Chin. J. Phys. 47 (2009) 134.

Laser Biomedical Physics: Principles and Applications

B.A. Cheba[1]

[1] Department of Biotechnology, Faculty of Sciences, University of Sciences and Technology -USTO, Oran, ALGERIA

c31b28@maktoob.com

Abstract: Due to its unique properties, laser light can be used in wide range of different applications. All biomedical laser applications are based on the interaction of laser light with biological substances, such interaction causes a broad spectrum of effects. In the simplest case, low intensity laser light is absorbed, reflected or reradiated as fluorescence by the substance without any change, such interactions form the basis of laser diagnostics in biology and medicine, both for diagnosis at the atomic or molecular level (micro-diagnosis) and at the level of cells and organs (macro-diagnosis).In the other hand laser light can interact with bio-maters through photothermal,photoablation and photochemical effects which find practical applications in photo-medicine and surgery. In this review we will discuss the effects of lasers on biosubstances and their applications in biology and medicine as diagnostic, therapeutic and surgical tool.

Keywords: laser, bio-medicine, biosubstance, effect, applications .

References:

Alfano, R.R. (ed). (1982). Biological events probed by ultra fast laser spectroscopy. (Academic .NEW YORK.).

Anderson, E. M., Angyal, G.N., Weaver, C.N., Felkner, I. C,. Wolf, W.F. and Worthy, B.E. (1993). Potential application micro bioassay technology for determining water soluble vitamins in foods. *J-AOAC- int.* 76(3): 682-690

Babajev, K. B; Babajev, O.G. and Korepanov, V. I. (1991). Treatment of cutaneous leishmaniasis using a corbon dioscid laser. *Bulletin of the world health organization* 69 (1): 103-106.

Bedwell, J.; Holton, J,; Vaira, D.; Macrobert, A.J. and Bown, S.G. (1990). In vitro killing of Helicobacter pylori with photodynamic therapy. *The lancet* 335: 1287.

Berns, M.W; Olson, R.S. and Rounus, D.E. (1969). In vitro production of chromosomol lesions with an argon laser microbeam. *Nature* 221: 74-75.

Berns, M.W. et al (1981). Laser microsurgery in cell and developmental biology. *Science* 213: 505-513.

Braun, A.; Little, DP. Reuter, D.; Muller –Mysok. B. and Koster, H. (1997). Improved analysis of micro satellites using mass spectrometry. *Genomics*. 46 (1): 18-23 (abst).

Bridges, T.J.; Patel, C.K.; Strand, A.R and Wood, O. R (1983). Syneresis of vitreous by carbon dioscide laser radiation. *Science*. 219: 1217-1219.

Carson, S; Cohen, A.S; et al (1993). DNA sequencing by capillary electraphoresis. *Analytical. Chemistry*. 65 (22): 3219-3227.

Chopra, S. and Chawla, H.M. (1992). Laser chemical and biological sciences wiley eastern limited, New Delhi PP: 2-182.

Dobrov, N.E.; ARBieva, KH.Z; Timonfeva, K.E; Esenaliv, O.R; Oraevsky, A.A. and Nikogosyan, N.D. (1989). UV laser induced RNA- protein crosslinks and RNA chain breaks in Tabacco Mosaic Virus RNA in situ. *photochem- photobiol*. 49 (5): 595-

Dougherty, T.J.; Thoma, R.E; Boyle, D.G. and Weishaupt, K.P. (1980). Laser in photomedicine and biology (eds pratesi, R. and sacchi, C.A). (springes, berlin) PP 67-75.

Duguid, J.; Bloom-field, VA.; Benevides, J. and Thomas. G.J. (1993). Raman spectroscopy of DNA-metal complesces. I. interactions and conformational effects of the divalent cations: Mg, Ca, Sr, Ba, Mn, Co, Ni, Cu, Pd and Cd. *Biophys-J*. 65 (5): 1916-1928.

Foultier, M.T; Patrice, T.; Tanielian, C; Wolff, C; Yactayo, Berrada, A. and combre, A. (1991). Photosensitization of L 1210 leukaemic cells by argon laser irradiation after incubation with haematoporphyin derivative and rhodamine 123, *J. photochem. photobiol. B. Biol*. 10: 119-132.

Houben, A., Ralf, G.K., Hein, V., Hermann, H, Jones, N.R and Fester, W.J. (1996). Molecular cytogenetic characterization of the hetero chromatic segment of the B- chromosome of rye (secale cereale) *Chromosoma*. 105: 97-103.

Transistors à un électron à température ambiante : une revue

A. SOUIFI[1]
[1]Institut des Nanotechnologies de Lyon, UMR CNRS 5270
INL – INSA de Lyon, 7 av. Jean Capelle, 69621 Villeurbanne cedex, FRANCE
Abdelkader.souifi@insa-lyon.fr

Résumé :

Ces dernières années, plusieurs équipes explorent différentes stratégies pour augmenter la température de fonctionnement des transistors à un électron (Single Electron Transistors : SETs) compatibles avec la technologie CMOS. Dans ces dispositifs qui utilisent le mécanisme de blocage de Coulomb, la condition de fonctionnement repose sur l'énergie de charge d'un l'îlot conducteur ou semi-conducteur placé entre la source et le drain qui doit être bien supérieure à l'énergie thermique. La problématique étant d'augmenter l'énergie de charge $E_C = e^2/C_{\Sigma}$, où C_{Σ} représente la capacité totale vue par l'îlot du SET, il s'agit d'étudier les moyens technologiques de réduire cette dernière.

Indépendamment du caractère métallique où semi-conducteur de l'îlot, la réduction de la capacité C_{Σ} passe soit par la réduction de la taille de l'îlot, soit par la réduction de toutes les capacités de liaison avec les électrodes de source, de drain, de grille et de substrat. Le cas idéal consistant à réduire à la fois la dimension de l'îlot et toutes les capacités îlot/électrodes. Nous présentons ici une revue des résultats les plus marquants publiés récemment [1-4] qui répondent aux mêmes critères : (i) reproductibilité, (ii) compatibilité avec un procédé CMOS et (iii) fonctionnement à haute température.

Réf.	Volume Ilot	C_{Σ}	E_C	Contrôle
[1]	2nm-Si dot (4.2nm^3)	0.42 aF	0.377 eV	Oxydation
[2]	10nm-Au dot (523 nm^3)	4.42 aF	0.037 eV	Fonctionnalisation
[3,4]	Ti - 2x10x60 (1200 nm^3)	0.35 aF	0.455 eV	CMP

L'analyse des résultats obtenus dans les différentes approches montre que l'utilisation d'îlots métalliques permet de « relaxer » la dimension de ces derniers sans forcément dégrader la capacité totale. Dans ce cas, il semble que la forme de l'îlot et par suite les surfaces des jonctions tunnel sont plus importantes que le volume total. Ceci explique comment il est possible d'obtenir de très grandes énergies de charge, et par suite, un fonctionnement à hautes températures.
Après avoir présenté les avantages et inconvénients de chaque approche technologique en fonction des applications visées (Mémoire et/ou Logique), nous présenterons les principaux critères qui permettent de faire un choix : vitesse de commutation, sensibilité aux charges parasites, effets des interconnexions, effets du couplage aux couches CMOS, souplesse des modèles compacts pour la conception.

References:

" Si-based ultrasmall multiswitching single-electron transistor operating at room-temperature" , S. J. Shin, C. S. Jung, B. J. Park, T. K. Yoon, J. J. Lee, S. J. Kim, J. B. Choi, Y. Takahashi, and D. G. Hasko, *APPLIED PHYSICS LETTERS* 97, 103101 (2010)
" CMOS-compatible fabrication of room temperature single-electron devices", VISHVA RAY, RAMKUMAR SUBRAMANIAN, PRADEEP BHADRACHALAM, LIANG-CHIEH MA, CHOONG-UN KIM AND SEONG JIN KOH, *NATURE NANOTECHNOLOGY* **3**, 603 (2008)
"Single-electron transistors with wide operating temperature range", C. Dubuc, J. Beauvais, and D. Drouin, *APPLIED PHYSICS LETTERS* 90, 113104 (2007);

NEW BEHAVIOR OF MOLECULES CONFINED IN CARBON NANOTUBES

B. TANGOUR[1]

[1]Unité de Recherche de Chimie Théorique et Réactivité, IPEIEM, Université de Tunis- El Manar

Carbon nanotubes (CNT) are representative of nanosystemes. Regardless of their chirality, which affects their electrical properties, their diameters are measured in nanometers and thus allow to confine molecules in their interior. They are composites by inclusion noted molecule@CNT. Carbon nanotubes may be sufficient, as a simple role of material carrier in particular the anticancer drug carboplatin. This role involves a diameter much larger than that of the free molecule to prevent any chemical interaction between the molecule and the nanotube. However, In other situations, weak interactions between the substrate and the nanotube are hoped to reveal a new behavior as in the case of controlling the conformation of the molecule TIBO, an anti-HIV, to follow the mutation virus and reverse the effects of drug resistance that severely limit the effectiveness of the drug.

In the case where the energy of encapsulation is important, so containment replaces an increase in temperature or pressure. Finally, if the atoms of the molecule are chemically bonded to carbon atoms of the nanotube, new coordinators have stabilized and opening the way for a new chapter in chemistry.

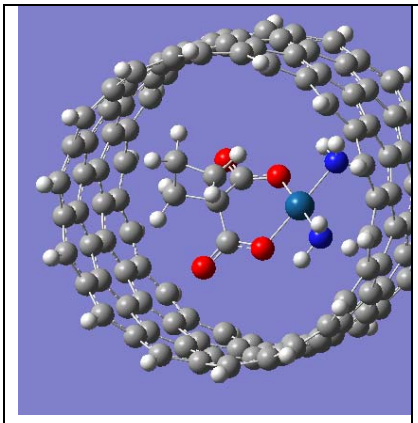	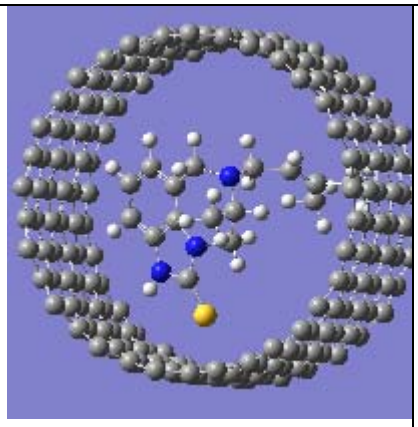	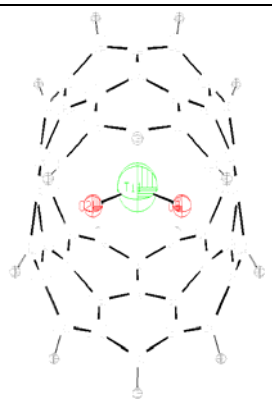
Carboplatine@(11,11)	TIBO@(16,0)	TiO_2@(8,0)

Mechanisms in Aminocatalysis

S. Lakhdar[1], H. Mayr[1]

[1]Department Chemie der Ludwig-Maximilians-Universität München Butenandtstr. 5-13, 81377 München, GERMANY

sami.lakhdar@cup.uni-muenchen.de

Extensive studies of the reactions of carbocations and Michael acceptors with *n*-, π-, and σ-nucleophiles have shown that the rates of these reactions can be described by eq. 1, where electrophiles are characterized by one parameter (*E*), while nucleophiles are characterized by the solvent-dependent nucleophilicity parameter *N* and the slope-parameter *s* [1]

$$\lg k20°C = s(E+N) \quad (1)$$

This type of reaction is involved in many organocatalytic reaction cycles, e. g., the iminium-catalyzed reactions depicted in Scheme 1.

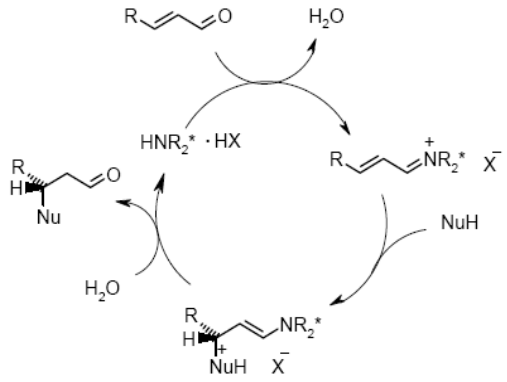

Figure 1: Iminium catalysis in nucleophilic additions to unsaturated aldehydes

By studying the kinetics of the reactions of iminium ions with ketene acetals (reference nucleophiles), we have determined the *E* parameters of the iminium ions depicted in Scheme 2. In this contribution, we will show how these data can be employed for analyzing scope and selectivities of iminium-catalyzed reactions [2, 3].

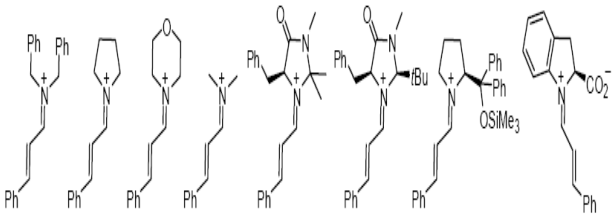

Figure 2: Cinnamaldehyde-derived iminium ions.

Applications of the reactivity parameters *N*, *s,* and *E* to analyze mechanistic aspects of enamine catalysis [3] and Baylis-Hillman type reactions will be discussed

References:

H. Mayr, M. Patz, *Angew. Chem. Int. Ed. Engl.* 1994, *33*, 938-957; b) H. Mayr, B. Kempf, A. R. Ofial, *Acc. Chem. Res.* 2003, *36*, 66-77; c) H. Mayr, A. R. Ofial, *J. Phys. Org. Chem.* 2008, *21*, 584-595.

S. Lakhdar, T. Tokuyasu, H. Mayr, *Angew. Chem. Int. Ed.* 2008, *47*, 8723-8726. b) S. Lakhdar, R. Appel, H. Mayr, *Angew. Chem. Int. Ed.* 2009, *48*, 5034-5037; c) S. Lakhdar, H. Mayr, *Chem. Commun*. 2010, in press. 3) Review: S. Lakhdar, A. R. Ofial, H. Mayr, *J. Phys. Org. Chem.* 2010, 23, 886-892.

Ultrasonic guided waves in functionally graded piezoelectric hetero structure

H. M. Ben Ghozlan

Université de Sfax, TUNISIA

A numerical matrix method relative to the propagation of ultrasonic guided waves in functionally graded piezoelectric material is given in order to make a comparative study with the respective performances of analytical methods proposed in literature. The preliminary obtained results show a good agreement, however numerical approach has the advantage of conceptual simplicity and flexibility brought about by the stiffness matrix method. The propagation behaviour of Love waves in a functionally graded piezoelectric material (FGPM) is investigated in this article. It involves a thin FGPM layer bonded perfectly to an elastic substrate. The inhomogeneous FGPM hetero structure has been stratified along the depth direction, hence each layer can be considered as homogeneous and the ordinary differential equation method is applied.

The obtained solutions are used to study the effect of an exponential gradient applied to physical properties. Such numerical approach allows applying different gradient variation for mechanical and electrical properties. For this case, the obtained results reveal opposite effects. The dispersive curves and phase velocities of the Love wave propagation in the layered piezoelectric film are obtained for electrical open and short cases on the free surface, respectively. The effect of gradient coefficients on coupled electromechanical factor, on the stress fields, the electrical potential and the mechanical displacement are discussed, respectively. Illustration is achieved on the well known hetero structure PZT-5H/SiO2, the obtained results are especially useful in the design of high-performance acoustic surface devices and accurately prediction of the Love wave propagation behaviour.

ABSTRACTS

Posters1
Physics

OPTICAL CHANNEL DROP FILTER BASED ON DUAL RING PHOTONIC CRYSTAL RING RESONATORS

M. Youcef Mahmoud[1], G. Bassou[1], A. Taalbi[1], Z. M. Chekroun[1]

[1]laboratory of Microanalysis, Microscopy and Molecular Spectroscopy, Physics Department, Faculty of Science, Djilalli Liabes, University of Sidi Bel Abbes, ALGERIA
mahmoudhamoud@yahoo.com

Abstract: we present an optical channel drop filter based dual ring on photonic crystal ring resonators. Its spectral information including intensity, dropped efficiency affected by different physical parameters were numerically analyzed with 2D finite-difference time domain technique

Introduction: The optical add-drop filter (ADF) is one of the fundamental building blocks for optical add-drop multiplexers (OADMs), reconfigurable OADMs, optical modulators, and optical switches needed for silicon photonics, photonic integrated circuits (PICs), and wavelengthdivision multiplexed (WDM) optical communication systems. Significant progress has been made on ADF based devices in the areas of compactness, high spectral selectivity, wide spectral tunability, fast switching, and low-power switching. One of the most promising designs for waveguided ADFs is the strip-based (or rib-based) micro-ring resonator, wherein a circulating mode in the ring is excited by the coupling of the forward propagating wave in a nearby bus waveguide. Very high spectral selectivity can be achieved due to the high resonator quality factor Q and the ring's intrinsic single mode nature.

Dual-ring photonic crystal ring resonators

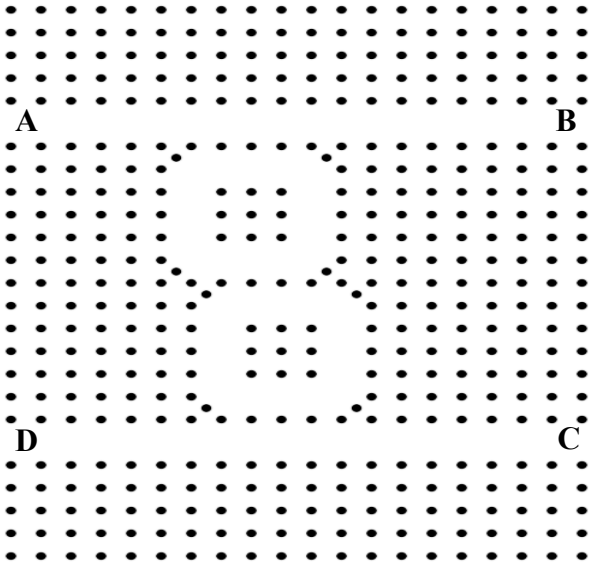

Figure 10: Dual-ring photonic crystal ring resonators

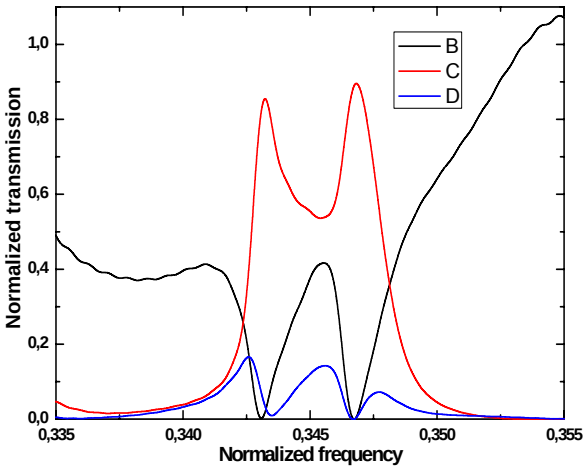

Figure 2: Normalized transmission spectra

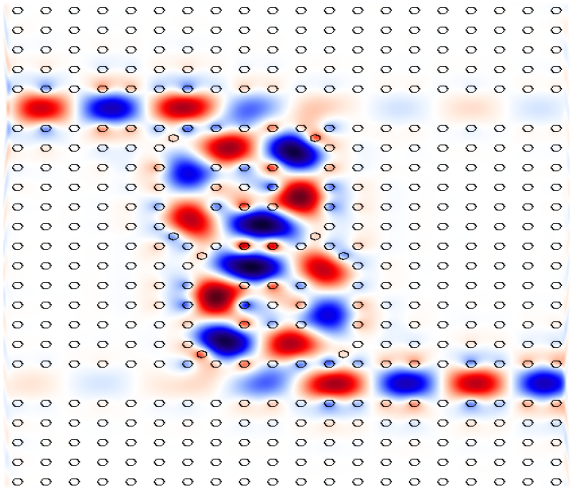

Figure 3: Electric filed intensity of the dual ring resonator's resonant wavelength

References:

For a review, see Kunz, K. S., Luebbers, R. J. (1993) *The Finite-Difference Time-Domain Methods* (CRC Press,Boca Raton.

Qiang, Z., Zhou, W., Soref, R. A. (2007) *Optical add-drop filters based on photonic crystal ring resonators, Opt. Express* 15, 1823-1831.

Qiang, Z., Zhou, W., Soref, R. A., Ma, Z. (2008) *Characteristics of ultra-compact polymer modulators based on silicon photonic crystal ring resonators, J. Nanophotonics* 2, 02350

ANALYSIS OF CHANNEL FILTER BASED ON PHOTONIC CRYSTALS RING RESONATOR

A. Taalbi[1], G. Bassou[1], M. Youcef Mahmoud[1], Z. M. Chekroun[1]

[1]laboratory of Microanalysis, Microscopy and Molecular Spectroscopy, Physics Department, Faculty of Science, Djillali Liabes, University of Sidi Bel Abbes, ALGERIA
taalbi_a@yahoo.fr

Abstract: in the present paper, we present a complete analysis of channel filter based on photonic crystals ring resonator. The normalized transmission spectra have been investigated by using the two-dimensional finite-difference time-domain (FDTD) technique in a square lattice dielectric-rod photonic crystal structure. With the introduction of four scatters at the corners of quasi-square ring, high wavelength selectivity and close to 100% drop efficiency can be obtained. We investigate parameters which affects resonant frequency in this channel filter. Theses parameters include dielectric constant of coupling rods and whole rods of the structure as well as radius of the coupling rods and scatter rods.

Introduction: Photonic crystal structures are considered for using in integrated nanophotonic circuits. One of the most important devices for ultra-dense integrated circuits is channel-drop filter (CDF). CDFs, which extract one channel from wavelength multiplexed signals and pass through other channels undisturbed, are useful and essential elements for photonic integrated circuits. Various CDFs exist, such as fiber Bragg gratings, Fabry-Perot filters, and arrayed waveguide gratings. Resonant CDFs, which involve waveguide–cavity interaction, are other attractive applicants for this intention. In this paper, such a CDF is devised in two-dimensional photonic crystal with a ring resonator instead of point-defect cavity, where the ring used realizes channel drop operation.

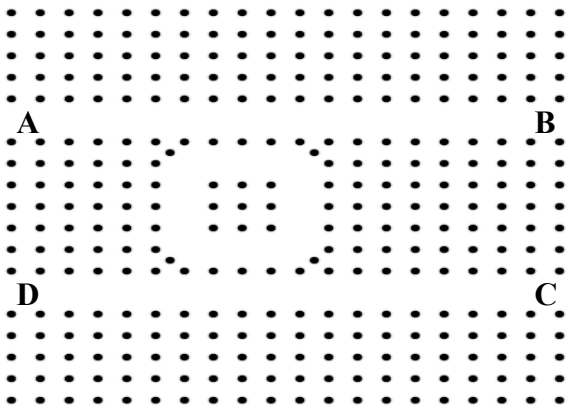

Figure 11: Channel drop-filter based on photonic crystals ring resonator

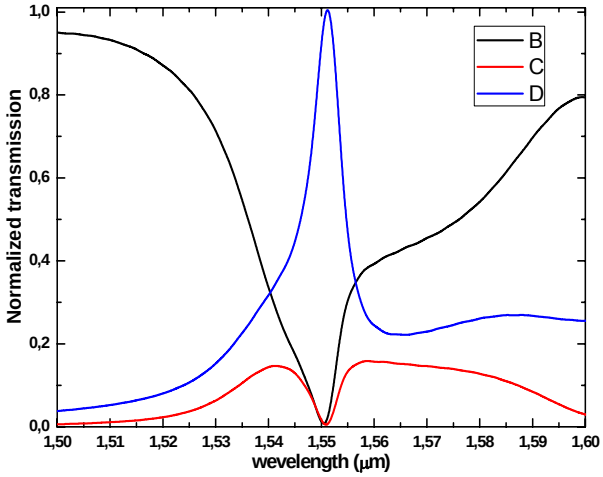

Figure 2: Normalized transmission spectra

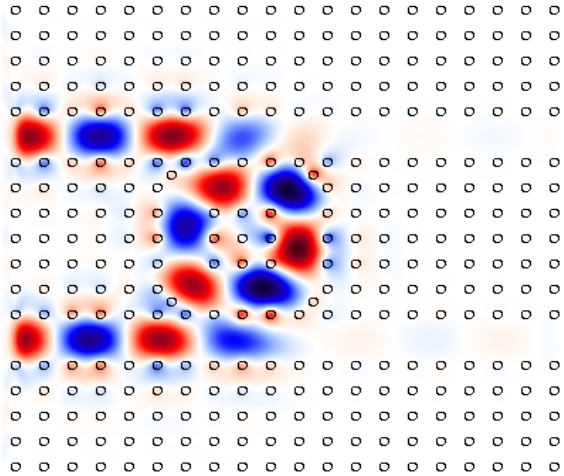

Figure 3: Electric filed intensity of the ring resonator's resonant wavelength at 1500 nm

References:

For a review, see Kunz, K. S., Luebbers, R. J. (1993) *The Finite-Difference Time-Domain Methods* (CRC Press,Boca Raton.

Chen, J. C., Microw, K. Li. (1995) *Opt. Technol. Lett*. 10, 319

Qiang, Z., Zhou, W., Soref, R. A. (2007) *Optical add-drop filters based on photonic crystal ring resonators Opt. Express* 15, 1823–1831.

Interaction electron-gas in an HPSEM: Application to CO_2 and comparison with H_2 and H_2O

F. Azza[1], O. Mansour[1], A. Kadoun[1]

[1]laboratory of Microanalysis, Microscopy and Molecular Spectroscopy, Physics Department, Faculty of Science, Djilali Liabes University of Sidi Bel-Abbes, ALGERIA
azza.faiza@ymail.com

Abstract: The High Pressure Scanning Electron Microscope (HPSEM) is a SEM instrument able to operate at several thousand Pa in it's specimen chamber. The collision of the electron beam with the gas atoms or molecules generates positive ions which neutralize the negative surface charge, thereby facilitating the observation of non conductive materials. Various gases can be used (air, nitrogen, helium, water vapour). However, the electron beam profile is modified by the presence of the gas so that only a fraction of the beam remains unscattered, leading to a beam spreading also called "skirt". [Danilatos, Kadoun, Mathieu]. The aim of this work is to compare the behaviour of the electron beam in CO_2, H_2 and H_2O respectively. To do this, we implemented Monte Carlo calculations based upon the modelling of electron-gas interactions. As it can be seen in Figs 1 and 2, helium, gas appears to be the best one since the unscattered fraction of the electron beam remains quite high and the skirt is approximately independent of pressure and remains low. However in special cases, one should need the use of CO_2 or H_2O. CO_2 seems to be less favorable and the pressure effect is more pronounced for this gas than for water vapor. However for pressures below 100 Pa (Fig.2), the skirt is drastically reduced for CO_2. Consequently CO_2 gas could be used in variable pressure SEM (VPSEM) where working distance is usually as high as 1,5 cm and where the pressure can be consequently lowered to small values.

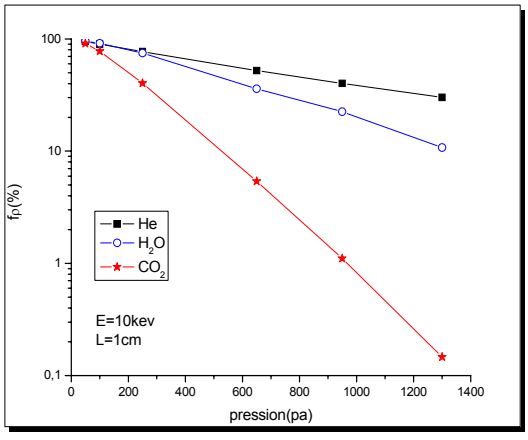

Figure 1: Non scattered fraction of the electron beam versus the chamber pressure

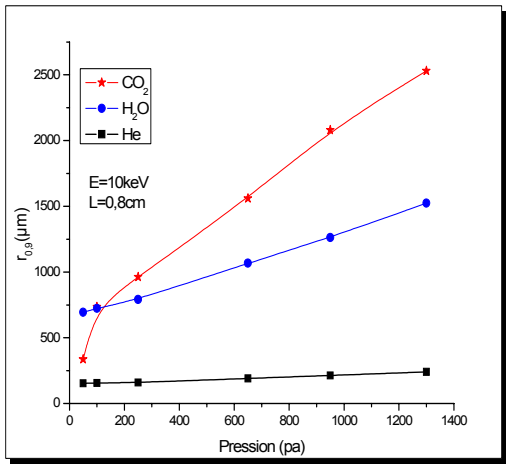

Figure 2: Skirt radius versus the chamber pressure

References:

Danilatos, G.D. (1988). Foundations of environmental scanning electron microscopy. *Advances in electronics and electron physics*, 71, 109-250.

Kadoun, A., Belkorissat, R., Khelifa, B., Mathieu, C. (2003). Comparative study of electron beam-gas interaction in an SEM operating at pressures up to 300 Pa. *Vacuum*, 21, 537-543.

Mathieu, C., Khouchaf, L., Kadoun, A., (2007) Exploring the high pressure SEM. *Modern Research and Educationnal Topics in Microscopy, (Microscopy Book Series N°3– Edition 2007)* 2,.779-786.

A WAVELENGTH DIVISION DEMULTIPLEXER BASED ON PHOTONIC CRYSTAL RING RESONATOR

M. Youcef Mahmoud[1], G. Bassou[1], A. Taalbi[1], Z. M. Chekroun[1]

[1]laboratory of Microanalysis, Microscopy and Molecular Spectroscopy, Physics Department, Faculty of Science, Djillali Liabes, University of Sidi Bel Abbes, ALGERIA
mahmoudhamoud@yahoo.com

Abstract: we demonstrate a new type of two-dimensional photonic crystal wavelength division demultiplexers based on ring resonators that can be applicable to photonic integrated circuits. The proposed structure mechanism is performed based on coupling between a waveguide and a ring resonator. FDTD method concludes output efficiency close to 100%.

Introduction: Photonic crystals (PCs) have inspired great interest recently because of their potential ability to control light wave propagation. Wavelength multiplexers are essential components in wavelength division multiplexing for use in point-to-point core networks. Dense-WDM (DWDM) systems require highly accurate wavelength control of the WDM light source and the wavelength multiplexer–demultiplexer.

WAVELENGTH DIVISION DEMULTIPLEXER

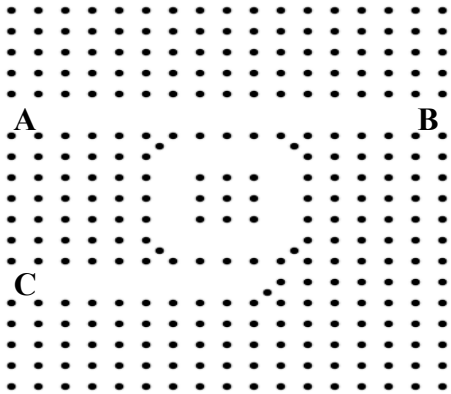

Figure 12: A fundamental element of WDM

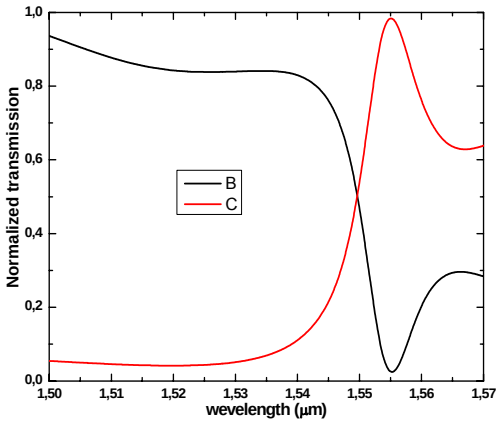

Figure 2: Normalized transmission spectra

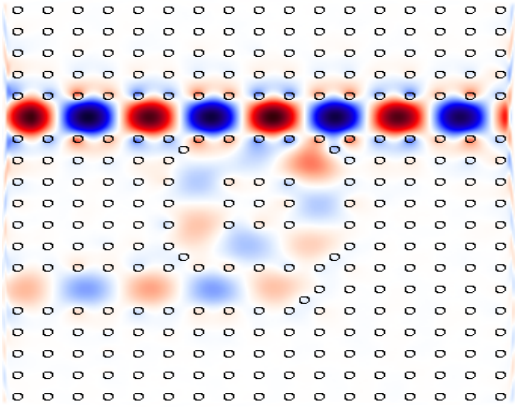

Figure 3: Electric filed intensity of the ring resonator's nonresonant wavelength at 1500nm

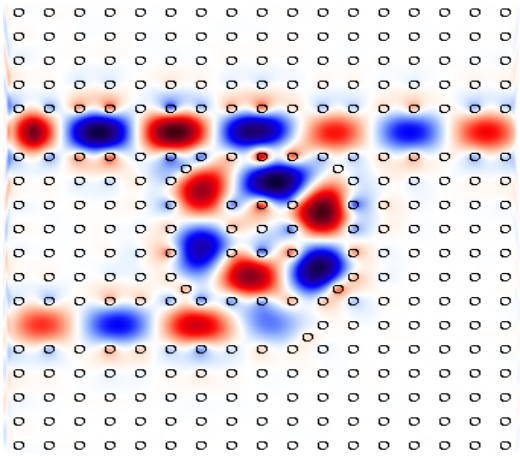

Figure 4: Electric filed intensity of the ring resonator's switching wavelength at 1550nm

References:

Taflove, A., Computational Electrodynamics: The Finite-Difference Time- Domain Method, third ed, Artech House, 2005.

Qiang, Z., Zhou, W., Soref, R. A., Ma, Z. (2008) *Characteristics of ultra-compact polymer modulators based on silicon photonic crystal ring resonators, J. Nanophotonics* 2, 023507.

Berenger, J.P. (1994) *J. Comput. Phys*. 114 185.

Electronic structure and ferromagnetism of Mn-substituted CuGaS2

A. Chahed[1], O. Benhelal[1]
[1] Faculté des Sciences, Laboratoire LMSSM, Université Djillali Liabes de Sidi Bel Abbès, B.P.89, Sidi Bel Abbès, 22000, ALGERIA
cha_abbes@yahoo.fr

Abstract: We present *ab initio* density functional theory calculations for the electronic and magnetic structure of Mn-containing $CuGaS_2$ chalcopyrite semiconductors. We find that the substitution of Ga sites results in the formation half-metallic ferromagnetic band, resulting from hybridization of Mn-3d and nearest-neighboring S-3p orbitals. These materials offer a potential for spintronic applications at room temperature.

1. Introductiont: Semiconductor spintronics, i.e., the use of electron spin as an additional degree of freedom in electronic devices, is emerging as an exciting new class of electronics with novel functionality [1]. Specifically, much recent work has focused on dilute magnetic semiconductors (DMS), where a magnetic element is introduced into a non-magnetic semiconductor. By far the best studied DMS is MnxGa1–xAs [2], but many other binary semiconductor-based DMS have been investigated both experimentally and theoretically [3]. Ternary $A^{I}B^{III}X^{VI2}$ chalcopyrite compounds, which crystallize in the chalcopyrite type structure (s.g.I-42d), were proposed as a new class of ferromagnetic semiconductors [4]. By ab initio calculations it was found, that the ferromagnetic state is strongly favoured. Curie temperatures of 100–150 K and ~160 K [5] were predicted for CuGaSe2 and CuGaS2 substituted with Mn on the Ga-site. Also the Curie temperature should be higher by employing other materials with smaller lattice constant. Calculations on CuAl1–xMnxS2 estimated Tc are 10% or more higher than that of $CuIn_{1-x}Mn_xSe2$ [6].

2. Details of calculations: The equilibrium structural parameters were calculated using the Vienna package WIEN2K [7]. This is an implementation of a hybrid full-potential (linear) augmented plane-wave plus local orbitals (L/APW+lo) method within the density-functional theory [8]. We use 64-atom supercells, (16Cu, 15Ga, 1Mn and 16S atoms) placing one Mn in various lattice positions. All atomic positions and lattice constants are relaxed by minimizing the total energy.

3. Results and discussion: Fig.1 and 2 show respectively the spin-dependent total and partial (3d of Mn) density of states of (DOS) of $CuGaMnS_2$ systems at its equilibrium lattice constant.

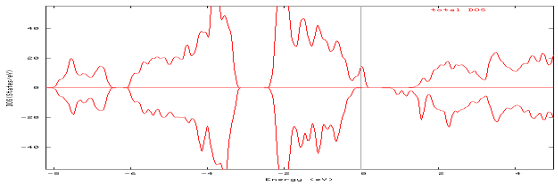

Figure 13: spin-dependent total density of states of (DOS) of $CuGaMnS_2$

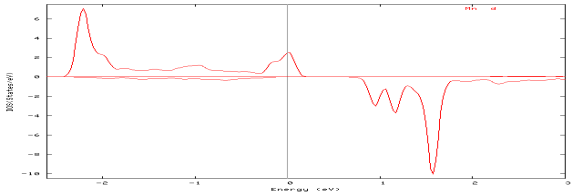

Figure 2: spin-dependent partial density of states of (DOS) of $CuGaMnS_2$ (Mn-3d)

Fig.1 shows the spin-dependent total density of states (DOS). It is clear that there is a large exchange splitting between the majority spin (spin-up) DOS and the minority spin (spin-down) DOS around the Fermi level and the majority spin electrons are metallic while there is an energy gap at the Fermi energy in the bands of the minority spin electrons.

We note from Fig.2 that the upper valence band complex has Mn-d character, which differ widely for spin up and spin down, i.e. the majority-spin DOS around the Fermi level (EF) mainly originates from the Mn-d. Near the Fermi level, however, the majority-spin channel has a narrow band, while the minority-spin channel exhibits a clean band gap. Such an electronic structure is a typical signature of a half-metallic ferromagnetic semiconductor.

References:

Awschalom, D.D., Loss, D. (2002) *Semiconductor Spintronics and Quantum Computation*.
Ohno, H. (1998) *Science* 281, 951.
Furdyna, J. (1988*) J. Appl. Phys*. 64, R29.
Zhao,Y-J., Freeman, A. (2002) *J. Magn. Magn. Mater*. 246, 145.
Jansen, H. Freeman, A. (1984) *Phys. Rev. B* 30, 561.
Schorr,S., Hoehne, R. Korzun, B. (2006) *phys. stat. sol. (a)* 203, No. 11, 2783– 2787
Blaha, P., Schwarz, K., Madsen, G.K.H., Kvasnicka, Luitz, D. (2001) WIEN2k, Vienna University of Technology, Vienna, Austria

Structural and Dynamical properties of SrO in the Rock-salt phase

F.Z. Aoumeur-Benkabou

Faculté des Sciences, Laboratoire L2MSM, Université Djillali Liabes de Sidi Bel Abbès,
Sidi Bel Abbès, 22000, ALGERIA
aoumeurf@yahoo.fr

Abstract:

We present a molecular dynamics study of structural and thermodynamic properties of SrO in the rock-salt structure.

Based on a three-body potential, our results are in agreement with experimental measurements and ab initio calculations. The transferability of this potential model is tested by simulating the Rock-salt phase of SrO for varying temperature.

Various thermodynamic properties including the Debye temperature, heat capacity, linear thermal coefficient and melting point are predicted. Calculations are extended to simulate also the liquid phase in the rock-salt phase.

References:

W.A. Harrisson, Electronic Tructure and the Properties of solids, Freemann, New York,. (1980).
J. Tersoff (1988) Phys. Rev. B 37 , 6991.
F.Z. Aoumeur, Kh. Benkabou, B. Belgoumene, (2003) Physica B 337, 292.
G. Cappelleni, F. Finocchi, S.Bouette-Russo (2001) Comput. Mater. Sci. 20, 401.
M.J. Mehl, (1993), Phys. Rev. B 47, 2493.
W. Sekkal, A. Laref, A. Zaoui, H. Aourag, M. Certier (1999). Solid. State. Commun.112, 49.

Tight Binding calculation Of Electronic Properties Of Ternary Alloy ZnS_xSe_{1-x}

K. Benkabou
Faculté des Sciences, Laboratory of Applied materials, Université Djillali Liabes de Sidi Bel Abbès, B.P.89, Sidi Bel Abbès, 22000, ALGERIA
kbenkabou@yahoo.fr

Introduction : In semiconductors alloys the band gap value and the lattice parameter are among the most important physical parameters, since these parameters control the band offset and the mismatching in the different devices.
To further enhance our understanding of the electronic properties of ZnS_xSe_{1-x} ternary alloy for device application we have carried out an empirical tight binding (TB) band structure on this alloy coupled with an improved virtual crystal approximation (VCA).. We introduce an empirical correction factor in the VCA in order to take into account the non-linear dependence with the concentration.

Method : The TB method describe quite well the dispersion of the valence bands of the binary compounds, as well as the lower conduction band edge in the high symmetry point after the inclusion of the s* state (Vogl (1983)). For the ternary alloy AB_xC_{1-x}, the TB parameters are calculating using the VCA and are given by the weighted averages of the corresponding end-point parameters :

$$\overline{E}_{\mu\nu} = xE^{AB}_{\mu\nu} + (1-x)E^{AC}_{\mu\nu}$$ Where

$E^{j}_{\mu\nu}(\mu,\nu = s,p^3,s^*)$ are TBPs of the j compound (j=AB,AC).
Then assuming that for ternary alloys the non linear behaviour of Eg(x) comes from the biggest shift of the conduction bands, compared with the corresponding valence band edge and from the fact that the s-on site parameters locate in energy the conduction band minimum at Γ, D. Olguin et al. (1999) Suggest a correction to the VCA expression for the s on-site TBPs.

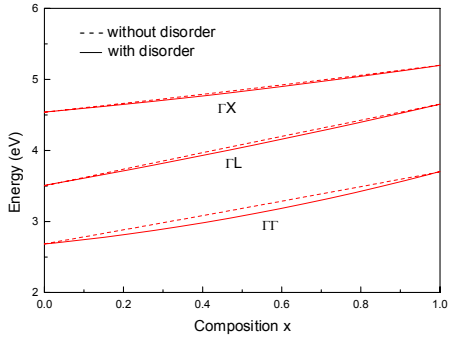

Figure 1: Energy band gap of ZnS_xSe_{1-x}

In this new model we substitute the VCA expression for the s on-site TBPs with an expression that include an empirical bowing parameter :

.

$$\overline{E}_{s\nu}(x,b) = \overline{E}_{s\nu}(x) + b_\nu x(1-x) \qquad \nu = a,c$$

Where the $\overline{E}_{s\nu}(x)$ is the corresponding VCA average for the s on-site TBPs and b_ν the empirical bowing parameter and is given by :

$$b_\nu = \pm k \frac{\left|E^{AB}_{s\nu} - E^{AC}_{s\nu}\right|^{\lambda}}{\left|V^{AB}_{ss} - V^{AC}_{ss}\right|} \qquad \nu = a,c$$

The sign + (-) is used for the cation (anion) substitution. λ and k are free parameters used to fit Eg(x). For the ternary alloy ZnS_xSe_{1-x} we use λ = 1.0 and k=1.04. the results obtaining are shown on figure 1 for the energy band gap and figure 2 for the band structure of $ZnS_{0.5}Se_{0.5}$ .The bowing factor obtained by (TBM) when including the correction term (ba= -2.83) is b_Γ = 0.46. This value of the bowing parameter of direct band gap is in good agreement with the experimental result .

References

Bernard J. E.,. Zunger A (1987) Phys. Rev B 36, 6, 3199.
Ebina A., Fukunaga E., Takabashi T. (1974) .Phys. Rev. B10 (6) .
Olguin, D. (1999) Rev. Mex. Fis. 45, 271.
Vogl P., Hjalmarson H. P. and J. D. Dow (1983) J. Phys. Chem. Solis, 44, 365.

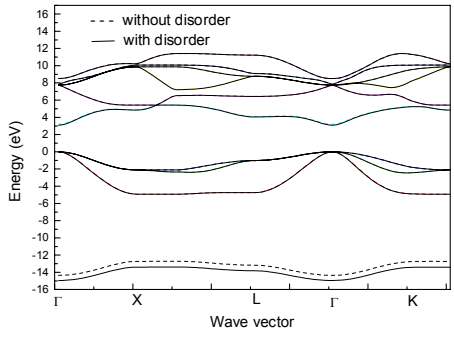

Figure 2: Band structure of $ZnS_{0.5}Se_{0.5}$

Study of the origin of ferromagnetism in $Ga_{1-x}Gd_xN$

Z. Dridi[1] , A. Lazreg[1], B. Bouhafs[1]
[1]Modelling and Simulation in Materials Science Laboratory, Physics Department, University of Sidi Bel-Abbes, 22000 Sidi Bel-Abbes, ALGERIA
zoulidridi@yahoo.fr

ABSTRACT

First-principles calculations of the electronic structure and magnetic interaction of substitutional europium rare-earth impurity in cubic GaN have been performed using density functional theory within the LSDA approach (local spin density approximation). The $Ga_{1-x}Gd_xN$ is shown to be semiconductors, where the filled *f* states are located at the top of the valence bands and the empty ones at the bottom of the conduction bands. The magnetic interaction of the rare-earth ion with the host states at the valence and conduction band edges has been investigated and found to be weak in comparison with Mn impurities.
PACS number (s): 71.27.+a , 71.55.Eq, 75.50. Pp.
Keywords: Rare-earth; GaN; ferromagnetism.

1. Introduction

Nitride semiconductors such as GaN and AlN have emerged as new materials for light-emitting and laser diodes and now prevailed as most important semiconductors in optoelectronics . Recently, ferromagnetic behaviours at well above room temperature have been reported for Gd doped GaN **[1-3]**, offering a new stage for interactions among charge, spin, and light. Further, the colossal magnetic moment of 4000 μ_B per Gd atom has been observed in epitaxial Gd-doped GaN, so the clarification of the microscopic origins for the ferromagnetic state in GaN is imperative.
In this work, the electronic structure and magnetic interaction of gadolinium substituting in cubic AlN are studied. We have reported the density of states and have calculated the exchange splitting parameters.
The present paper is organized as followed: Section 2 presents details of our calculations. Results and discussion are presented in Sec. 3, and Sec. 4 summarizes our conclusion.

2. Calculation

The calculations are based on the density-functional theory in the local spin-density approximation (LSDA). The first-principles band-structure approach applied in this work is the scalar relativistic full-potential linear-augmented-plane-wave plus local orbital (FPLAPW+lo) method (Wien2k implementation **[4]**). Basis functions were expanded as combinations of spherical harmonic functions inside non-overlapping spheres around the atomic sites (muffin-tin spheres) and in Fourier series in the interstitial region. In the muffin-tin (MT) spheres, the *l*-expansion of the non-spherical potential and charge density was carried out up to l_{max}=10. In order to achieve energy eingenvalues convergence, the wavefunctions in the interstitial region were expanded in plane waves with a cutoff of $k_{max} = 7/R_{mt}$ (where R_{mt} is the average radius of the MT spheres). Our calculations were performed in the zinc-blende ferromagnetic phase, at the concentration $x = 0.25$. The Brillouin-zone integration were performed using $2 \times 2 \times 2$ Mokhorst-Pack special *k*-points **[5]**.

2. Results and discussion

For GaGdN alloys, we have calculated the total and partial density of states (DOS) at the equilibrium lattice constant. The spin direction (↑ and ↓) is taken as the direction of the rare-earth spin (majority ↑ and minority spin ↓ direction).
The partial densities of states shown in fig. 1 for $Ga_{0.75}Gd_{0.25}N$ are given for Gd-4*f*, Gd-5*d*, and N-2*p* states. For majority spin, we note a peak corresponding to the filled *f*-states located at the top of valence band. For minority spin, the Gd-4*f* states are unoccupied and located for the CBM. For majority spin, Gd-4*f* states at the valence band maximum (VBM) hybridize with the N-2*p* and Gd-5*d* states. For minority spin, the VBM shows a highest contribution of the N-2*p* states, which hybridize with Gd-5*d* states. The latter are high in energy in the conduction band, and thus are fully unoccupied for both spin directions.
To study the magnetic interaction of the rare-earth with the host band states, we have calculated the exchange splitting of the band states at the VBM and CBM. The sign of the spin-splitting at the top of the valence band is positive and is estimated to 0.03 eV, so the VBM states tend to align with gadolinium spin. At the conduction band minimum, the spin-splitting has been estimated to -0.11 eV.
The spin-splitting at the VBM obtained in the present work for gadolinium is smaller in comparison to

those of Mn in GaN **[6]**. Theoretical studies **[7, 8]** have reported also a weak magnetic interaction of Gd ion with the host states at the valence and conduction band edges in comparison with Mn-doped GaN **[6]**. Experimental **[2]** and theoretical **[7]** results strongly suggest that defects play an important role in ferromagnetism in GaN:Gd. Liu *et al.* **[9]**, using the FP-LAPW method, reported that most of the measured magnetic moment of GaN:Gd must come from holes present in the GaN host, such as Ga vacancies. This model was argued to be unlikely, by Mitra and Lambrecht **[10]**, because Ga vacancies have a high energy of formation in the neutral charge state that carries magnetic moment. They propose that interstitial nitrogen and oxygen in octahedral sites support magnetic moments and ferromagnetic coupling in semi-insulating conditions.

3. Conclusion

The electronic structure and magnetic interaction in cubic GaN:Gd have been investigated. In this work, we conclude that for GaN:Gd it is unlikely that the gadolinium dopant by itself may induce room temperature ferromagnetism. The role of the interaction of the rare-earth with other defects must be investigated.

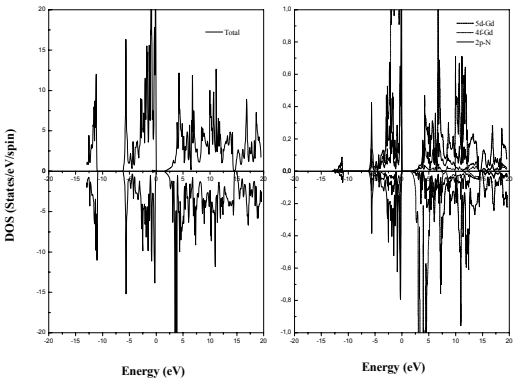

Figure 1: Total and partial spin-polarized density of states of $Ga_{1-x}Gd_xN$ with x =0.25. The zero of energy is placed at the VBM.

Reference

N. Teraguchi, A. Suzuki, Y. Nanishi, Y.-K. Zhou, M. Hashimoto and H. Asahi, Sol. State Comm. 122 (2002) 651.

S. Dhar, O. Brandt, M. Ramsteiner, V. F. Sapega, K. H. Ploog, Phys. Rev. Lett. 94 (2005) 037205.

H. Asahi, Y. K. Zhou, M. Hashimoto, M. S. Kim, X. J. Li, S. Emura, and S. Hasegawa, J. Phys. Condens. Matter 16 (2004) S5555.

P. Blaha, K. Schwarz, G. K. H. Madsen, D. Kvasnicka, and J. Luitz, WIEN2k, An Augmented Plane Wave + Local Orbitals Program for Calculating Crystal Properties (Technische Universität Wien, Austria, 2001).

H. J. Monkhorst and J. D. Pack, Phys. Rev. B 13 (1976) 5188.

T. C. Schulthess, W. M. Temmerman, Z. Szotek, W. H. Bulter, G. Malcolm Stocks, Nat. Mater. 4 (2005) 838.

A. Svane, N. E. Christensen, L. Petit, Z. Szotek, W. M. Temmerman, Phys. Rev. B 74 (2006) 165204.

G. M. Dalpian and S.-H. Wei, Phys. Rev. B 72 (2005) 115201.

L. Liu, P. Y. Yu, Z. Ma, S. S. Mao, PRL 100 (2008) 127203.

C. Mitra and Walter. R. L. Lambrecht, Phys. Rev. B 80 (2009) 081202 (R).

Full-potential study of structural and electronic properties of *M*B_2-type metal diborides (M=Be, Mg and Ca)

S. Laksari[1], R. Khatir[1], O. Benhelal[1], A. Chahed[1], R. Mebsout[1], B. Bouhafs[1]
[1]Modelling and Simulation in Materials Science Laboratory (LMSSM), Physics Department, University of Sidi Bel-Abbes, 22000 Algeria.
Lak_sor@yahoo.com
KHATIR_RAJAA@HOTMAIL.FR

Abstract

Structural, electronic and bonding properties of BeB_2 and CaB_2 were studied using the full-potential linearized augmented plane-wave (FP-LAPW) method, based on the density functional theory, implemented in the Wien2K code and are compared with those of the isostructural superconductor MgB_2. The exchange and correlation potential energies are treated using the local density approximation (LDA); the results are compared with available theoretical and experimental data. Our results are found in good agreement with the experiment. We also evaluate the electronic structure of BeB_2 in order to obtain further insight into its surprising difference from the superconducting MgB_2 and therefore attempt to predict the nature of CaB_2, one of the interesting candidates for the higher T_c.

Keywords: DFT, FP-LAPW, LDA, Electronic structure.

References:

Blaha, K. Schwarz, G.K.H. Madsen, D. Kvasnicka, J. Luitz, WIEN2k, An Augmented Plane Wave Plus Local Orbitals Program for Calculating Crystal Properties, Vienna University of Technology, Vienna, Austria, (2001). Cava, Nature 410, 23 (2001). Chen, Q. Y. Tu, L. Dai, Y. P. Xu, Modern Phys. Lett. B 16, 73 (2002). Felner, physica C 353, 11-13 (2001).
Fjellstedt, A. E. W. Jarfors, L. Svendsen, J. Alloys Compd. 283, 192 (1999). Hohenberg, W. Kohn, Phys. Rev. B 136, 864 (1964). Hyoung Joon Choi, Steven G. Louie and Marvin L. Cohen 0906.2613v1, cond-mat, (2009). Islam, F. N. Islam, M. S. Iqbal, Abraham F. Jalbout, Ludwik Adamowicz Solid State Communications 139, 315–320 (2006). Kohn, L.J. Sham, Phys. Rev. A 140, 1133 (1965). Madsen, P. Blaha, K. Schwarz, E. Sjostedt, L. Nordstrom, Phys. Rev. B64 195134 (2001). Medvedeva, J. E. Medvedeva, A. L. Ivanovskii, V. G. Zubkov, and A. J. Freeman, Pis'ma Zh. Eksp. Teor. Fiz. 73, 378 (2001) [JETP Lett. 73, 336 (2001). Mokhorst and J.D. Pack, Phys. Rev. B 13, 5188 (1976).
Nagamatsu, N. Nakagawa, T. Muranaka, Y. Zenitani, Nature 410, 63 (2001). Okatov, A. L. Ivanovskii, Y. E. Medvedeva, and N. I. Medvedeva, Phys. Status Solidi B 225, R3 (2001). Oguchi, J. Phys. Soc. Jpn. 71, 1495 (2002). Pereira, C. A. Perottoni, J. A. H. DaJoronda, J. M. Leger, J. Haines, J .Phys. Condens. Matter 14, 10615 (2002). Ravidran, P. Vajeeston, R. Vidya, A. Kjekshus, H. Fjellvag, Phys. Rev B63, 224509 (2001). Sight, Phys.Rev.Lett.87, 087004 (2001). Sjostedt, L. Nordstrom, D.J. Singh, Solid State Commun. 114, 15 (2000).

First-principles study of the magnetic properties of $Al_{1-x}Gd_xN$

A. Lazreg[1] , Z. Dridi[1], and B. Bouhafs[1]
[1]Modelling and Simulation in Materials Science Laboratory, Physics Department, University of Sidi Bel-Abbes,
22000 Sidi Bel-Abbes, ALGERIA
aeklazreg@yahoo.fr

ABSTRACT

First-principles calculations of the electronic structure of substitutional gadolinium rare-earth impurity in cubic AlN have been performed using density functional theory within the LSDA approach (local spin density approximation). The $Al_{1-x}Gd_xN$ is shown to be semiconductors, where the filled *f* states are located at the top of the valence bands and the empty ones at the bottom of the conduction bands. The magnetic interaction of the rare-earth ion with the host states at the valence and conduction band edges has been investigated and found to be relatively weak in comparison with Mn impurities.

PACS number (s): 71.27.+a , 71.55.Eq, 75.50. Pp.
Keywords: Rare-earth; AlN; magnetism.

1. Introduction

In the past few years, considerable research activity has taken place in the field of doping of wide gap semiconductors with magnetic impurities. They are expected to be room temperature ferromagnetic materials for spin electronics and luminescent materials for optoelectronic applications. Rare-earth (RE) ions are unique dopants, because they are magnetically and optically active in the semiconductor host crystals. Ferromagnetism has been observed in $Ga_{1-x}Gd_xN$, with Curie temperature larger than 400 K **[1-3]**, and at room temperature in $Al_{1-x}Gd_xN$ **[4]**. Further, photoluminescence in the visible has been observed in RE-doped GaN **[5-7]** and RE-doped AlN **[8-10]**, and several light emissions used as primary colors in screen displays **[11-13]**.

In this work, the electronic structure and magnetic interaction of gadolinium substituting in cubic AlN are studied. We have reported the density of states and have calculated the exchange splitting parameters.

The present paper is organized as followed: Section 2 presents details of our calculations. Results and discussion are presented in Sec. 3, and Sec. 4 summarizes our conclusion. *2. Calculation*

The calculations are based on the density-functional theory in the local spin-density approximation (LSDA). The first-principles band-structure approach applied in this work is the scalar relativistic full-potential linear-augmented-plane-wave plus local orbital (FPLAPW+lo) method (Wien2k implementation **[14]**). Basis functions were expanded as combinations of spherical harmonic functions inside non-overlapping spheres around the atomic sites (muffin-tin spheres) and in Fourier series in the interstitial region. In the muffin-tin (MT) spheres, the *l*-expansion of the non-spherical potential and charge density was carried out up to l_{max}=10. In order to achieve energy eingenvalues convergence, the wavefunctions in the interstitial region were expanded in plane waves with a cutoff of $k_{max} = 7/R_{mt}$ (where R_{mt} is the average radius of the MT spheres). Our calculations were performed in the zinc-blende ferromagnetic phase, at the concentration $x = 0.25$. The Brillouin-zone integration were performed using $2 \times 2 \times 2$ Mokhorst-Pack special *k*-points **[15]**.

2. Results and discussion

For AlGdN alloys, we have calculated the total and partial density of states (DOS) at the equilibrium lattice constant. The spin direction (↑ and ↓) is taken as the direction of the rare-earth spin (majority ↑ and minority spin ↓ direction).

The partial densities of states shown in fig. 1 for $Al_{0.75}Gd_{0.25}N$ are given for Gd-4*f*, Gd-5*d*, and N-2*p* states. For majority spin, we note a peak corresponding to the filled *f*-states located at the top of valence band. For minority spin, the Gd-4*f* states are unoccupied and located for the CBM. For majority spin, Gd-4*f* states at the valence band maximum (VBM) hybridize with the N-2*p* and Gd-5*d* states. For minority spin, the VBM shows a highest contribution of the N-2*p* states, which hybridize with Gd-5*d* states. The latter are high in energy in the conduction band, and thus are fully unoccupied for both spin directions.

To study the magnetic interaction of the rare-earth with the host band states, we have calculated the exchange splitting of the band states at the VBM and CBM. The sign of the spin-splitting at the top of the

valence band is positive and is estimated to 0.04 eV, so the VBM states tend to align with gadolinium spin. At the conduction band minimum, the spin-splitting has been estimated to -0.46 eV.
The spin-splittings obtained in the present work for gadolinium are weak in comparison to those of Mn-doped GaN **[16]**. So, for AlN:Gd, it is unlikely that the rare-earth dopant by itself may induce room temperature ferromagnetism, perhaps by introducing defects as the case of GaN:Gd in which high temperature ferromagnetism and giant magnetization amplifications have been observed.

3. Conclusion

First-principles study of the magnetism in cubic AlN:Gd has been investigated. For majority spin, the filled *f* states are located at the top of the valence bands, and for minority spin the empty ones are located at the bottom of the conduction bands. The magnetic behaviour of Gd in AlN appears to be different from that of Mn: the effect of the exchange interaction of the gadolinium ion with the host states at the valence band maximum and conduction band minimum is weaker.

Reference

[N. Teraguchi, A. Suzuki, Y. Nanishi, Y.-K. Zhou, M. Hashimoto and H. Asahi, Sol. State Comm. 122 (2002) 651.
S. Dhar, O. Brandt, M. Ramsteiner, V. F. Sapega, K. H. Ploog, Phys. Rev. Lett. 94 (2005) 037205.
H. Asahi, Y. K. Zhou, M. Hashimoto, M. S. Kim, X. J. Li, S. Emura, and S. Hasegawa, J. Phys. Condens. Matter 16 (2004) S5555.
S. W. Choi, Y. K. Zhou, S. Emura, X. J. Lee, N. Teraguchi, A. Suzuki, H. Asahi, Physica Status Solidi C, 3 (2006), 2250.
J. D. MacKenzie, C. R. Abernathy, S. J. Pearton, U. Hömmerich, J. T. Seo, R. G. Wilson, Appl. Phys. Lett. 72 (1998) 2710.
N. A. Sobolev, V. V. Lundin, V. I. Sakharov, I. T. Serenkov, A. S. Usikov, A. M. Emel'yanov, Semiconductors 33 (1999) 624.
Y. Q. Wang and A. J. Steckl, Appl. Phys. Lett. 82 (2003) 402.
K. Gurumurugan, H. Chen, G. R. Harp, W. M. Jadwisienczak, H.-J. lozykowski, Appl. Phys. Lett. 74 (1999) 3008.
V. I. Dimitrova, P. G. Van Patten, H. Richardson, M. E. Kordesch, Appl. Phys. Lett. **77** (2000) 478.
V. I. Dimitrova, P. G. Van Patten, H. Richardson, M. E. Kordesch, Appl. Surf. Sci. 175/176 (2001) 480.
A. J. Steckl, J. Heikenfeld, M. Garter, R. Birkhahn, D. S. Lee, Compound Semicond. 6 (2000) 48; U. Hömmerich, E. E. Nyein, J. Heikenfeld, A. J. Steckl, J. M. Zavada, Mater. Sci. Eng. B 105 (2003) 91.
A. J. Steckl and J. M. Zavada, Mat. Res. Soc. 24 (1999) 33.
L. C. Chao, B. K. Lee, C. J. Chi, J. Cheng, T. Chyr, A. J. Steckl, Appl. Phys. Lett. 75 (1999) 1833; L. C. Chao, B. K. Lee, C. J. Chi, J. Cheng, T. Chyr, A. J. Steckl, J. Vac. Sci. Technol. B 17 (1999) 2791.
P. Blaha, K. Schwarz, G. K. H. Madsen, D. Kvasnicka, and J. Luitz, WIEN2k, An Augmented Plane Wave + Local Orbitals Program for Calculating Crystal Properties (Technische Universität Wien, Austria, 2001).
H. J. Monkhorst and J. D. Pack, Phys. Rev. B 13 (1976) 5188.
T. C. Schulthess, W. M. Temmerman, Z. Szotek, W. H. Bulter, and G. Malcolm Stocks, Nat. Mater. 4 (2005) 838.

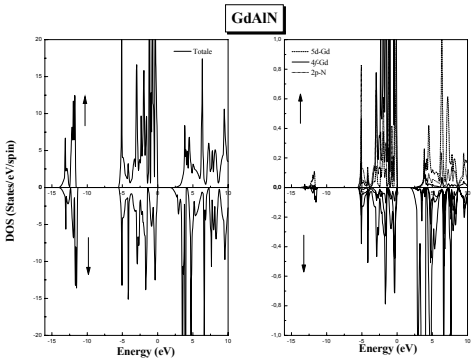

Figure 1: Total and partial spin-polarized density of states of $Al_{1-x}Gd_xN$ with x =0.25. The zero of energy is placed at the VBM.

Structural, electronic and thermodynamic properties of Bi_2O_3 from First Principles Calculations

F. Litimein[1], K. Bougherara, H. Belkhalfa[1], D. Rached[1], F. Miloua[2]

[1] Laboratoire des Matériaux Magnétiques, Département De Physique,
Université de Sidi Bel Abbés, Sidi Bel Abbes, 22000 – Algerie
flitimein@gmail.com
[2] Laboratoire de Microscopie, Microanalyse et Spectroscopie Moléculaire Faculté des Sciences,
Université Djillali Liabès, Sidi-Bel-Abbès, ALGERIA

Abstract:

Bi_2O_3 oxidic compound is characterised by significant values of refractive index, polarizability of Bi3+ cation [Gobrecht (1969), Dolocan et al. (1981), Clapham et al. (1967), Nikolov et al.(1975), Leontie (1998)], and a remarkable photosensitivity. Also, its energy gap is close to that of CdS, which is considered an outstanding candidate for solar cells Luonite (1998).

We have carried out a first-principles total energy calculations of the structural and the electronic properties of Bi_2O_3 in its tetragonal phase. We have applied the full-potential linearized augmented plane waves (FP-LAPW) method based on the density functional theory (DFT) using the local-density approximation (LDA) Blaha et al. (2001).

For the first time through the quasi-harmonic Debye model Blanco et al. (2004), in which the phononic effects are considered, the dependences of relative volume V/V_0 on pressure P, cell volume V on temperature T, and Debye temperature θ and specific heat C_V on pressure P are successfully obtained. The variation of the thermal expansion α with temperature and pressure is investigated, which shows the temperature has hardly any effect on the thermal expansion α at higher pressure.

Keywords: Bi_2O_3, FP-LAPW, quasi-harmonic Debye Model.

References:

Blaha, P. Schwarz, K. Madsen, G. K. H. Kvasnicka, D. and Luitz, J. (2001) WIEN2k, An Augmented Plane Wave Plus Local Orbitals Program for Calculating Crystal Properties, Vienna University of Technology, Vienna, Austria.

Blanco, M.A. Francisco, E. Luana, V. (2004) Comput. Phys. Commun. 158, 7.

Clapham P.B., Br. (1967) J. Appl. Phys. 18 363.

Dolocan V., and Iova F., (1981) Phys. Stat. Sol. A 64 755.

Gobrecht H., Seeck S., Bergt H.-E., Märtens A., Kossmann K., (1969) Phys. Stat. Sol. 33, 599.

Leontie L., Doctoral Thesis, "Al. I. Cuza" University, Iassy, (1998).

Nikolov T.S., Aroyo M., Klein E., and Ikonopisov K., (1975) Thin Solid Films 30 37.

First-principles calculations of the structural and electronic properties of three semiconducting intermetallics compounds RuAl2, RuGa2 and OsAl2 in the TiSi2-type structure

R. Mebsout[1], O. Benhelal[1], A. Chahed[1], R. Khatir[1], B. Bouhafs[1]
[1]Modelling and Simulation in Materials Science Laboratory (LMSSM), Physics Department,
University of Sidi Bel-Abbes, 22000 ALGERIA
mebsoutrezki@yahoo.fr
22ouioui@live.fr

Abstract:

We report structural and electronic properties of the compounds known as Nowotny chimney-ladder (CL) phases RuAl2, RuGa2 and OsAl2 using the full potential linearized augmented plane wave (FP-LAPW) method. For treating the exchange-correlation potential term, we have chosen the generalized gradient approximation (GGA). The total energy approach is used to determine the equilibrium volume. The energy gap is found to be indirect for all our compounds. Results on electronic properties such as band structures, density of states and electronic charge densities are presented and interpreted.

Keywords: DFT, FP-LAPW, LDA, Electronic structure of semiconducting.

References:

Lars-Erik Edshammar - Acta Chemica Scandinavica 20. 427-431. 1966.

Mat. Ress. Bull. Vol.19, pp. 1177-1180. Printed In the USA. (1984). Michael Springborgy and Rüdiger Fischerz - J. Phys.: Condens. Matter 10 701–716. Printed in the UK. (1998).

M. Weinert and R. E. Waston. Vol 58, Number 15. Physical Review B, 9732 - 9740. (1998).

Serdar Ögüt and Karin M. Rabe. Vol 54, Number 12. Physical Review B. 8297 - 8300. (1996).

Y.Imai , A ,Watanabe . Intermetallics 13. 233-241. (2005).

Polishing effect of samples on WDS microanalysis X

K. Saïl[1], G. Bassou[1]

[1]Microscopy Microanalysis and Molecular Spectroscopy laboratory L2MSM, Physics Department, Faculty of Science, Djilalli Liabes University of Sidi Bel Abbes, ALGERIA
B.P.89, Sidi Bel Abbès, 22000, ALGERIA
Sailkari7@yahoo.com

Abstract :

The Scanning Electron Microscope (SEM) is an essential tool for characterization in most scientific laboratories and particularly when it is equipped with an X-ray detector. The apparatus on which we carried out our investigations is a SX100, a Cameca mark SEM, coupled to four wavelength dispersion spectrometers. The sample studied in this paper is ores. It is calcic apatite would also contain oolites and coprolithes. Analyzes on these polished and nonpolished samples were carried out in order to highlight the role of polishing

Metallographic preparation

The operation of polishing requires a preparation which consists in coating the ore powders some in an epoxy resin appearing itself as two liquids characterized by a very good fluidity as well as a very good hardness and a good chemical resistance to solvents and acids. After polymerization at a temperature about 80°C mechanical polishing is carried out in three stages as indicated on table 1

polishing	***Pré-polishing***	***Fine***	***Finition***
Support	paper	self-adhesive cloths, compressed, metal	Polyurétane cloths
Abrasives, Composition, size	SiC	Diament de 45 à 0.25µm aérosol, suspension ou pâte	SiO_2 0.05µm
Lubrifiant	water	Alcool Base huileuse	water
speed Trs/mn	300 and +	150 à 250	150 à250

Table 1 : Polish stages.

The last stage is the cleaning which is obtained by a washing with alcohol then with water plus liquid soap using an ultrasound tank and finally a rinsing and drying with the compressed air.

Results

The comparison between spectra of the polished and no polished samples shows clearly the relative increase in x-emission in the case as of polished samples. The figure1 represents an example of this increase.

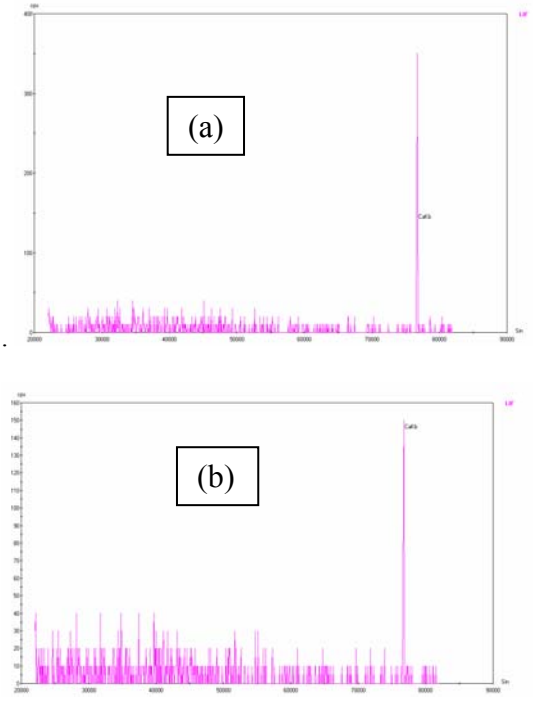

Fig. 2: Ores spectra (a) polish (b) no polish

References:

J.L.Pouchou (2008), Les méthodes de quantification en microanalyse X, Microscopie électronique à balayage et microanalyses. P 465-467.
J.Ruste, (2008) la microanalyse quantitative en WDS des éléments très légers. Microscopie électronique à balayage et microanalyses. p 473-474.
R. Wilmotte, J. Benezech " (1975),Pratique et Théorie des Traitement des Surfaces : tome 1 Décapage et Dégraissage" ,: Editions B. P. J.

Electronic Band structure of $Ga_xIn_{1-x}As$

N. Tayebi Larbi[1], K. Benkabou[1]
[1]Faculté des Sciences, Laboratory of Applied materials, Université Djillali Liabes de Sidi Bel Abbès, B.P.89, Sidi Bel Abbès, 22000, ALGERIA
Tayebinadjia@yahoo.fr

Introduction:

The $Ga_xIn_{1-x}As$ is a key component in the active regions of high speed electronic devices , infrared lasres , and long-wavelength quantum cascade lasers. The III-V ternary alloy semiconductor $Ga_xIn_{1-x}As$ is a very interesting terahertz -radiation material system . It is expected to exhibits properties physically related to both binary systems InAs and GaAs. Moreover, the bad gap of $Ga_xIn_{1-x}As$ can be tuned from 0.36 to 1.42 eV by variation of the Ga mole fraction x from 0 to 1 .

Method: In this communication, we present a theoretical study of band structure of ternary alloy $Ga_xIn_{1-x}As$ based on tight binding method and virtual crystal approximation. The result obtained are shown on figure 1 for band structure of $Ga_{0.64}In_{0.36}As$ and figure 2 for $Ga_xIn_{1-x}As$ ($0 \le x \le 0.64$).The results agree well with the experimental data of reference 4 when we introduce a correction to the VCA using Lee et al. formalism .

References

Driad R. et al. (1998) Appl. Phys. Lett. 73, 665.
Capasso F. et al. (1997) solid state commun. 102, 231.
Lam Y., Loehr J.P. and Singh J. (1992) IEEE J. Quantum Electron 28, 1248.
Lee S.J.et al. (1990) J. Phys.: Condens. Matter 2 3253 .
Levinshtein M. et al. (1996) Hand book series on semiconductor parameter (world Scientific, Singapor.
Youngok, K. et al. (2008) Phys. Rev. B 78, 035201.

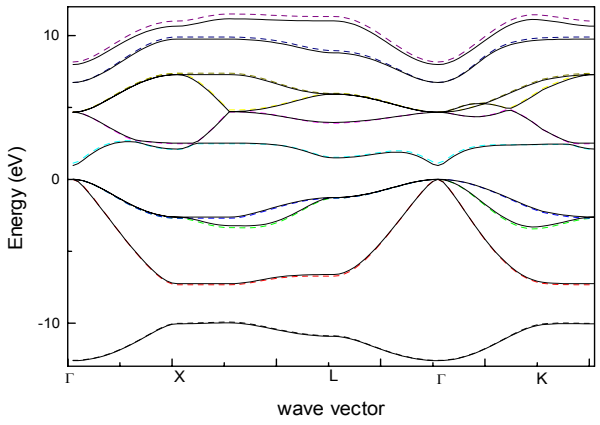

Figure 1: band structure of $Ga_{0.64}In_{0.36}As$

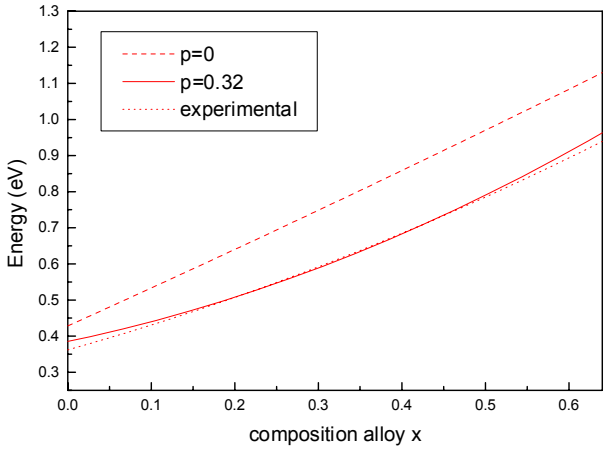

Figure 2: Direct Band gap of $Ga_xIn_{1-x}As$

EBIC microscopy investigations on microelectronic devices

R. BECHAREF[1], G. BASSOU[1], Z. SOUAR[2]
1: Laboratory of Microscopy, Microanalysis of the matter and Molecular Spectroscopy, Science Faculty, Djillali Liabès University of Sidi-Bel-Abbès, ALGERIA
2: Dept of Electrical Engineering Moulay Tahar University of Saida.

Introduction: In

this paper, we will give the principle of the EBIC (Electron Beam Induced Current) method as well as the characterization of bipolar transistors. The micrographs carried out in EBIC mode, were exploited quantitatively. Measures of the minority carrier diffusion length on the base were thus carried out.

EBIC mode:

In EBIC mode, the sample is such a detector or 'collector' of carriers. Thus, the charge carriers generated by the electron beam can move under the influence of the electric field and produce a measurable signal being able to be detected in an external circuit. This current constitutes the EBIC signal and can be used for the formation of an image. Currently, the EBIC remains a technique valid for the characterization and the analysis of the defects in materials and devices semiconductors.

Measurements EBIC and application to the junction base/emitter of a transistor

Current EBIC is measured by an external circuit where a Faraday cage is used for the collect of the electron beam. Theoretically, all the electrons of the beam will be collected and constitutes thus a reference.

We present an investigation on bipolar transistor pnp not encapsulated (realized at ENIE company in Sidi-Bel-Abbes (Algeria)), in order to use this technique in this configuration.

Secondary electron image (SEI) of the bipolar structure is shown in fig.1, where we see micro welding of the base and the emitter. Under the same conditions, we carried out an image in EBIC mode of the structure given by Fig.2.

From the curve given in fig.3, it was possible to deduce the diffusion length in the base from the transistor which is about 1.2 µm. For the same type of transistor, C.H.Wang and S.E.Swirhun give value diffusion length L_P = 0.90-3 µm.

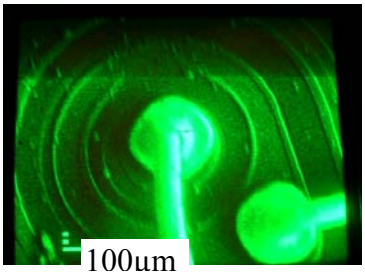

Fig1. SEI of the bipolar transistor

Fig.2: EBIC micrograph of the transistor with connection of the junction base-emitter

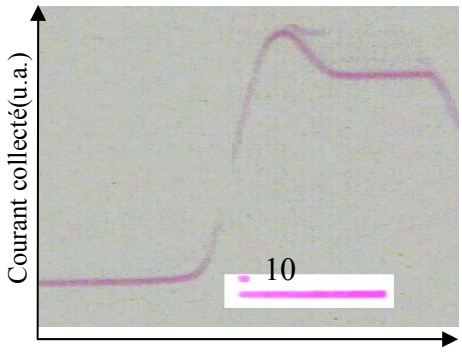

Fig.3 EBIC line scan above junction E-B

References:

A.Boudjani, G.Bassou, T.Benbakhti, M. Beghdad and Belmekki. "Direct measurment of minority carrier diffusion lengh in planar devices", (1994).

M.-G. Han, Y.Zhu, K. Sasaki, T. Kato C. A.J. Fisher , T. Hirayama, Solid-State Electronics (2010) 'Direct measurement of electron beam induced currents in p-type silicon'

Radial Confinement Study of the Taylor Couette Flow

R. Bellatreche[1], M. Ouali[1], A. Bouabdallah[1]

[1] Faculté de Physique, Laboratoire LTSE, Université des Sciences et de Technologie Houari Boumediene, Alger
BP EL ALIA 16111 – Bab Ezzouar - ALGER, ALGERIA
bellatreche_randa@yahoo.fr

Introduction:

In order to expand and study the dynamics of instabilities in fluid mechanics from a numerical point of view and especially between two coaxial cylinders, which's the inner cylinder, rotates and the outer one kept fixed, our choice is focused on code calculation called Fluent. We will structure the Taylor Couette flow and study the various changes produced by the effect of the geometry and setting system speeds.

Layout:

To study the effect of radial confinement on the outbreak of the first instability in cylindrical Couette Taylor flow has been proposed several structures of the flow system for different values of radial clearance δ was chosen more than three configurations thin intermediate and large values of radial clearance δ follows: 0.15, 0.25, 0.35, 0.40. The procedure followed in fluent is to vary the angular velocity of a quasi-static instability characterize the first start with low speed until the appearance of the axial wave. The exploitation of results is made by the representation of the contours of axial velocity and static pressure in the vicinity of the axial wave Tc1 (Figure 1). We note from these results that the case was thin-checked the critical value of the first theoretical instability evaluated by **A. Bouabdallah [1]**, and that the appearance of the axial wave is delayed with the increasing value of radial clearance δ

We compared our results obtained by numerical simulation of various gaps δ: 0.10 to 0.40 with the results of **A. Recktenwald** et **al. [2]** And **M. E. Ali [3]** they proved very successful in the graph in Figure 2, it demonstrated the correlation between the three results. The error on the present results with the results mentioned above is 0.6%. We note that the size of Taylor cell for fixed δ does not change along the annulus in the vicinity of the wave for different axial annular space. The evolution of the axial wave number in function of the gap δ shows us that whenever we increase the value of radial clearance, the axial wave number n decreases.

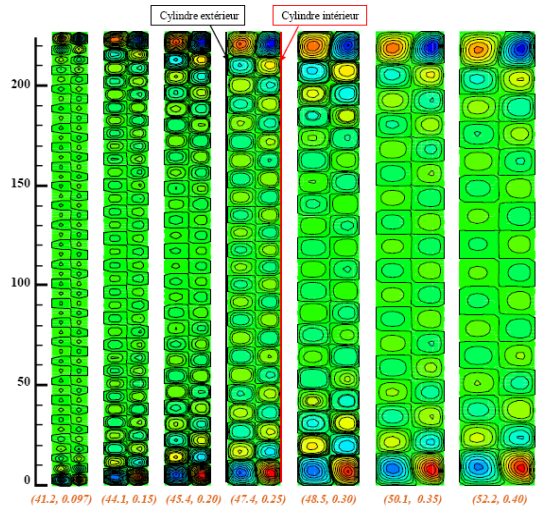

Figure 14: Representation of the axial velocity in Taylor Couette flow for different values of radial clearance (Ta, δ) near the critical state Tc_1

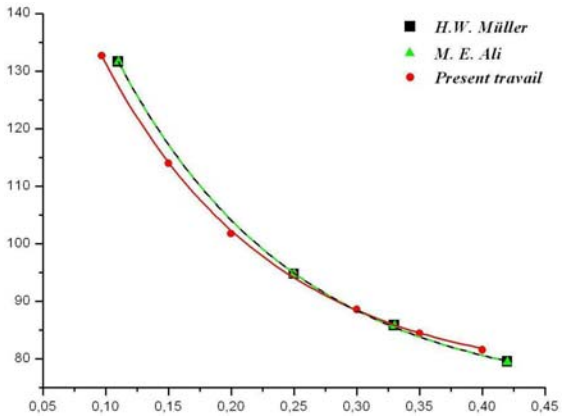

Figure 2: Evolution of the Reynolds number Re as a function of gap δ in the vicinity of the onset of the first instability Ta = Tc_1

References:

Bouabdallah, A. (1980) Instabilités et turbulence dans l'écoulement de Taylor-Couette, *Thèse Docteur ès Sciences*.

Recktenwald, A., Lücke, M. and Müller, H. W. (1993) *Phys. Rev. E48, 4444*

Ali, M.E., Mitra, D., Schwille, J.A., and Lueptow, R.M. (2002) Hydrodynamic stability of a suspension in cylindrical Couette flow, *Phys. Fluids 14, 1236; doi:10.1063/1.1449468.*

Computational Studies of Optoelectronic Properties of ZnO/MgO/CdO Nanostructures

. Benharrats[1], A. Djellal[1], K. Zitouni[1], A. Kadri[1]

1Laboratoire d'Etude des Matériaux Opto-électronique & Polymères" (L.E.M.O.P.)
Department of Physics, University of Oran (Es-Sénia), 31100, Oran, ALGERIA
Farah.lemop@yahoo.fr

M. Djermouni[2], A. Hallouche[2], A. Zaoui[1], B. Bouhafs[2]
[2]Laboratoire de Modélisation et Simulation en Sciences des Matériaux (L . M . S . S . M .)
Department of Physics, University Djillali Liabes of Sidi-Bel-Abbès, 22000, Sidi Bel Abbes, AlGERIA

Abstract: In this work, we present a theoretical study of electronic and optoelectronic properties of II-VI wide band gap semiconductor ZnO,MgO and CdO materials and their nano-heterosystems ZnO/ $Mg_xZn_{1-x}O$ and ZnO/$Cd_xZn_{1-x}O$. These materials and nanostructures are very interesting because of their potential applications in optoélectronics as semiconductor based Lasers emitting in the visible (green) to Ultra-violet range.

This study is based on numerical computations performed jointly through ab-initio and ***k.P*** theories [1]. We study structural and energy band parameters of these two different materials: binary end materials ZnO, MgO et CdO, as well as their ternary alloys $Mg_xZn_{1-x}O$ et $Cd_xZn_{1-x}O$.

In this work we choose to combine ab-initio theory with the ***k.P*** method. The ab-initio calculations were performed with the help of a Wien-2k software package 2009 version, and ***k.P*** theory computations were performed with the help of computer programs written under matlab and fortran languages by ourselves at LEMOP Laboratory.

The ab-initio simulations give us the possibility to determine structural, energy band, optical, and other parameters of ZnO/MgO/CdO nanosystems. The ***k.P*** theory computations allow to study fine properties around energy band extrema directly involved in electron transport and optical transitions of bulk as well as low dimensional ZnO/ZnMgO and ZnO/ZnCdO nanostructures used as optoelectronic light emitting devices.

We show that the interest of combining these two kind of theoretical approches the ab-initio theory with ***k.P*** computational method lies in their complementarity. Structural and energy band parameters which are determined by ab-initio method are readily injected into the ***k.P***. computations so that it is possible to avoid in this way the use of empiric and less accurate paramétrisation.

In both cases, we compare our results with other similar calculations and with experimental results available in literature.

Particular attention is paid here of some very special effects characterizing the hexagonal Würtzite crystal structure of this ZnO materials family, namely, polarisation effects [2] and built-in strain effects, which have dramatic influence on optoelectronic devices based on these ZnO/ $Mg_xZn_{1-x}O$ and ZnO/$Cd_xZn_{1-x}O$.

Key words: ab-initio, ***k.P***, nanosystems, ZnO, MgO, CdO, $Mg_xZn_{1-x}O$, $Cd_xZn_{1-x}O$, ZnO/MgO, ZnO/CdO, Visible-UV Lasers.

References:

Benharrats F., Zitouni K., Kadri A., Gil B., (2010), Superlattices and Microstructures, 47, 592, (2010).

Zitouni K., Kadri A., Lefebvre P., Gil B., (2006), Superlattices and Microstructures 39, 91-96, (2006).

First-principles calculations of the structural and electronic properties of semiconducting intermetallics compounds $RuGa_3$, and $OsGa_3$ in the $FeGa_3$-type structure

O. Benhelal[1], S. Laksari[1], A. Chahed[1], R. Khatir[1]

[1]Modelling and Simulation in Materials Science Laboratory (LMSSM), Physics Department, University of Sidi Bel-Abbes, 22000 ALGERIA
Benhelalomar@yahoo.com

Electronic structure of $RuGa_3$ and $OsGa_3$ with the crystal structures belonging to the space group of P42/mnm (No. 136), which is usually referred to as the $FeGa_3$-type structure, have been calculated using a full potential linearized augmented plane wave (FP-LAPW) method based on the density-functional theory within the local density approximation (LDA) and with the generalized gradient correction (GGA). The total energy approach is used to determine the equilibrium volume. Results on electronic properties such as band structures, density of states and electronic charge densities are presented and interpreted.

The intermetallic compounds offer an interesting alternative to modify optical or transport properties of various devices and moreover their properties will prove to lie in between those of metals and traditional semiconductors. Notably, they will be found to have small bands gaps and excellent transport properties.

Keywords: DFT, FP-LAPW, LDA, Electronic structure.

References:

Amagai, Y., Yamamoto, A., Iida, T., Takanashi, Y. (2004) *J Appl Phys*; 96, 5644.

Amato, A. (1997) Rev. *Mod. Phys*. 69 1119.

Lue, C.S., Kuo, Y.-K. (2002 *Phys. Rev. B* 66, 085121.

Lue, C.S., Lai, W.J., Chen, C.C., Kuo, Y.-K. (2004) *J. Phys.: Condens. Mat*. 16, 4283.

Dasarathy, C., Hume-Rothery,W. (1965) Proc R Soc Lond Ser A, 141 (286).

Blatt, F.J., Schroeder, P.A., Foiles, C.L., Greig, D. (1976) *Thermoelectric Power of Metals, Plenum Press*, New York,.

Imai, Y., Watanabe, A., Mukaida, M. (2003) *J Alloys Compd* 358, 257.

Ivashchenko VI, Shevchenko VI. (2001) *Appl Surf Sci* 184, 137.

Evers, J., Oehlinger, G., Meyer, H. (1984) *Mater. Res. Bull* 19, 1177.

Lue, C. S., Lai, W. J., Kuo, Y. K. J (2005) *Alloys Compd* 392, 72.

Payne, M. C., Teter, M. P., Allan, D. C., Arias, T. A., Joannopoulos, J. D. (1992) *Rev Mod Phys* 64, 1045.

Schubert, K., Lukas, H. L., Meissner, H. G., Bhan, S. (1959) Zeit Metallkunde 50, 534–9.

Ogut, S., Rabe, K. M., (1995) *Phys. Rev. B* 51, 10443.

Tao-Fan, C., Ching-Kwei, L. (1966) *Chin J Phys* 22, 952.

Haussermann, U., Bostrom, M., Viklund, P., Rapp, O., Bjornangen, T. (2002) *J. Solid State Chem*. 165, 94.

Vanderbilt, D. (1990) *Phys Rev* 41, 7892.

Aeppli, Z.G., Fisk, Z. (1992) *Comments Condens. Mat. Phys*. 16, 155.

The Importance of the Resonance in the Calculation of Relative Intensities of Emission of Ion FE^{+16}

N.H. Benmansour [1], M.K. Inal[1]

[1] Laboratoire Physique Théorique -B.P 119 Chetouane 13000 Tlemcen, ALGERIA
1 nour_mansour1@yahoo.fr

Abstract:

We have performed calculations of intensity ratios of lines due to $2p^53d \rightarrow 2p^6\ ^1S_0$ and $2p^53s \rightarrow 2p^6\ ^1S_0$ transitions, emitted in the wavelength range 15–17Å by neon-like Fe^{16+} ions from Maxwellian hot plasmas. The populations of the upper levels of the considered lines required in the line intensity calculations were determined by solving a set of rate equations in the collisional-radiative model, where 89 levels of Fe^{16+} were included, those originating from the configurations $2s^22p^6$, $2s^22p^53l$ (l=0–2), $2s^22p^54l$ (l=0–3), $2s2p^63l$ (l=0–2), $2s2p^64l$ (l=0–3). We have taken into account the collisional excitation from the ground level as well as from the metastable $2p^53s\ ^3P_0$ and $^3P_2$ levels, and radiative cascades in calculating the level populations. Several line intensity ratios have been computed as a function of the electron temperature between 2 and 10×10^6 K and for various values of the electron density in the range 10^{12} – 10^{14} cm^{-3}. Comparisons have been made with experimental results obtained by English researchers on tokamak plasmas and temperature diagnostics have been performed for these plasmas.

References:

M. Arnauld and J. Raymond, Astrophys. J. 398 (1992) 394.
P.F. Winkler and *al*, Astrophys. J. 246 (1981) L27.
K.J.H. Phillips and *al*, Astrophys. J 256 (1982) 774.
P.W. Vedder and C.R. Canizares, Astrophys. J. 270 (1983) 666.
S.M. Kahn, F.D. Seward and T. Chlebowski, Astrophys. J. 283 (1984) 286.
S.D. Loch, M.S. Pindzola, C.P. Ballance and D.C. Griffin, J. Phys. B: At. Mol. Opt. Phys. 39 (2006) 85.
K.J.H. Phillips and *al*, Astron. Astrophys. 324 (1997) 381.
A.K. Bhatia and G.A. Doschek, At. Data Nucl. Data Tables 85 (2003) 1.
K.M. Aggarwal, F.P. Keenan and A.Z. Msezane, Astrophys. J. Suppl. 144 (2003) 169.
B.W. Smith, J.C. Raymond, J.B. Mann and R.D. Cowan, Astrophys. J. 298 (1985) 898.

Structural Study of the Neurotransmitter by the Ab-initio Methods and Spectroscopy

A. Boutasta [1], A. Benosman[1]

[1] Laboratoire Physique Théorique -B.P 119 Chetouane 13000 Tlemcen, AlGERIA
aboutasta@yahoo.fr

Abstract:
Spectroscopic studies (infrared or Raman) allow to obtain information on the conformation of amino acids. The information obtained through the modes of vibration whose intensity and the wave number depends on their conformation.
These results provide a better interpretation of the vibration of an amino acid and a better understanding of its structure. In parallel with these experimental studies (which involve modes of vibration), the theoretical methods (ab initio, semi-empirical and empirical) have continued to grow since the first program "Gaussian" in 1970. The results of these theoretical methods are encouraging and motivate many authors to choose this line of research that may be designated by "molecular modeling", which allowed the determination of structural properties with great precision.
In our work we have performed calculations of the geometry optimization and harmonic force field of GABA and taurine which are amino acid neurotransmitters.
For methods of ab initio calculations based on DFT/B3LYP and close as possible to the theoretical frequencies to experimental frequencies we used a second program: Redongqui is based on a transformation of the space constants in Cartesian coordinates a space in internal coordinates.
To validate the theoretical level used, we compared our results with those obtained by infrared spectroscopy and Raman scattering.

References:

A.D. Becke, Rev. Phys. A 38, 3098 (1988).
Alloche and Pourcin J. *spectrochim. Acta*, part A49 571 (1993).
G. Lee, W. Yang and R.G. Parr *Phys. Rev*. B 37 , 785 (1988) .
N. Leullio et M. Ghomi, Etude des propriété structurales des acides.
W.J. Heher, W.A. Lathan, M.D. Neuton, R. Ditch_eld, J.A. Polpe, Gaussian 70, *quantum chem*.

Electronic and Elastic Properties of Hypothetical Zinc Blende $Sc_xIIIA_{1-x}N$ (IIIA= Al, Ga and In): Empirical Pseudopotential Methode Calculation

S. Dergal [1], A. E. Merad[1, 2]

[1]Equipe Physique de l'état solide, LPT, Département de Physique, Faculté des Sciences, Université de Tlemcen, BP 13000 Tlemcen, ALGERIA
Samiha_der@yahoo.fr
[2]Le Abdus Salam ICTP, Strada Costiera 11 I-34014 Trieste, ITALY

Introduction:

Transition metal nitrides constitute a diverse class of materials with many technological applications. Because of their great strength and durability, they have been used traditionally at extreme conditions of temperature and pressure. Their hardness has given them applications in cutting tools, golf shoe spikes, and snow tires. In ferrous alloys they are the components responsible for the toughness of steels [1]. However, they also have interesting optical, electronic and magnetic properties and have been used for optical coatings [2], electrical contacts [3] and diffusion barriers [4].

For this, we are interested to the electronic and elastic properties and some related properties of AlN, GaN, InN, ScN and their hypothetical semiconductor alloys $Sc_xAl_{1-x}N$, $Sc_xGa_{1-x}N$ and $Sc_xIn_{1-x}N$ in their hypothetical zinc-blende structure; using the empirical pseudo-potential method (EPM) within the virtual crystal approximation (VCA) combined with the Harrison bond-orbital model. Elastic constants and sound velocity were calculated as a function of the scandium (Sc) concentration x. Agreement between the present results and the available data has been found. Our results for $Sc_xIIIA_{1-x}N$ (IIIA= Al, Ga and In) at $0 < x < 1$ constitutes a predictions for a future experimental investigation. In this abstract, we give some preliminary results.

Elastic properties:

The dependences of the elastic constants C_{11} on the *Sc* concentration x over the range 0–1, without including the compositional disorder effect are shown in figures 1.

We note that for $Sc_xAl_{1-x}N$ and $Sc_xGa_{1-x}N$ the trend in going from x= 0 to 1 (with a 0.1 steps) is the decrease of C_{11} but for $Sc_xIn_{1-x}N$, it increase.

The origin and the magnitude of the nonlinear corrections to this parameter cannot be easily explained in terms of the endpoint values of the parameters peculiar to the binary compounds. Hence, one can believe that the nonlinearity of the C_{11} value versus the *Sc* concentration x arises from order effects which exist already in a fictitiously periodic alloy.

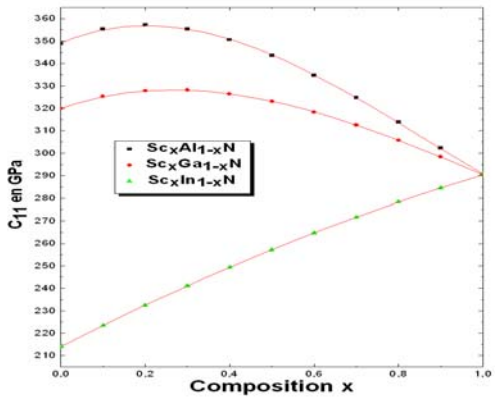

Figure 1 : Elastic constant C_{11} of $Sc_xAl_{1-x}N$, $Sc_xGa_{1-x}N$ and $Sc_xIn_{1-x}N$ as a function of the composition x

References:

Oyama.S.T. (1996),' the chemistry of transition metal carbides and nitrides', Blackie academic and professional.

Erola. M, Keinonen. J, Anttilla. A and. Koskinen. J (1986). Solar Energy Mater. 12, 353

Ernsberger. C, Miller. A and Banks. D (1985), J. Vac. Sci. Technol. A, 3, 2303

Suni. I (1983), J. Electrochem. Soc., 130, 1215

Ab-initio and *k.P* simulations of $In_xGa_{1-x}N/Mg_yZn_{1-y}O$ and $In_xAl_{1-x}N/Mg_yZn_{1-y}O$ Quantum Nanostructured Lasers

A. Djellal[1], F. Benharrats[1], K. Zitouni[1], A. Kadri[1]

[1]Laboratoire d'Etude des Matériaux Opto-électronique & Polymères (L. E. M. O. P.)
Department of Physics, University of Oran (Es-Senia), 31300 Oran, ALGERIA
djellal_abdellah@yahoo.fr

M. Djermouni[2], A. Hallouche[2], A. Zaoui[2], B. Bouhafs[2]
[2] Laboratoire de Modélisation et Simulation en Sciences des Matériaux (L . M . S . S . M .)
Department of Physics, University Djillali Liabes of Sidi-Bel-Abbès, 22000, Sidi Bel Abbes, ALGERIA

Abstract:
In this work**,** we use the ab-initio Density Functional Theory (DFT) and the ***k.P*** method in order to determine various physical properties of these hybrid quantum nanostructured systems consisting of the combination of two different types of wide bandgap semiconductor materials: the III-V nitride materials as $In_xGa_{1-x}N$ and $In_xAl_{1-x}N$ with the II-VI Oxydes as: $Mg_yZn_{1-y}O$. We perform this study in a wide range of alloy compositions x-contents of In and y-contents of Mg.

The ab-initio DFT calculations were based on the full potential linearized and augmented plane waves method (FP-LAPW) (*Wien2k* code, 2009 issue), and we used two approximations : the generalized gradient approximation (GGA) and the local density approximation (LDA).

The ***k.P*** theory computations were made with the help of our own made computer programming softwares written under matlab and fortran systems.

The use of the ab-initio DFT theory allowed us to determine various physical properties of these compound semiconductor materials : structural, optical and electronic properties in various phases such as Würzite, Zinc-Blende and Rocksalt ones. We are more particularly interested in the following properties and their variations as a function of alloy composition : the lattice a and c parameters, internal parameter u, the compressibility coefficient B, the total energy E_{tot}, the Fermi Energy E_F and the total and partial densities of states.

These parameters which are obtained through the ab-initio DFT computations are of paramount importance for our nanostrutures :

1. They give the possibility to determine in turn some very important parameters of our quantum nano-heterostructures $In_xGa_{1-x}N/Mg_yZn_{1-y}O$ and $In_xAl_{1-x}N/Mg_yZn_{1-y}O$ such as the energy band offsets at the interface and, consequently the associated carrier quantum confinement effects.

2. They also give straightforward and accurate determination of some very useful input parameters for the ***k.P*** computations of quantum confined subband states which are otherwise taken from rough semi-empirical interpolations.

Thanks to this accurate and fine study of physical parameters of our $In_xGa_{1-x}N/Mg_yZn_{1-y}O$ and $In_xAl_{1-x}N/Mg_yZn_{1-y}O$ nastructures, we were then able to determine the behavior of the main optical transitions, the Laser gain and the current threshold densities as a function of alloy composition.

We finally perform a comparative study of Laser performance of the two different types of nanostructures, and we could find the selected range of alloy compositions in each case.

Key words: ab-initio, DFT (FP-LAPW), **k.P**-theory, III-V Nitrides, ZnMgO, Lasers, Quantum Well heterostructures.

References:

Djellal A., Kadri A., Gil B., Bretagnon T., Zitouni K., (2010), 3rd International Sympo-sium on Growth of III-Nitrides(ISGN3),
4-10 July 2010, Montpellier France

Djellal A., Kadri A., Gil B., Bretagnon T., Zitouni K., (2010), accepted in Physica Status Solidi C Décembre 2010.

LDA+U+SOC Ab-initio Study of Magnetic Behavior and Electronic Structure of RE5Ge3 Intermetallics Compounds

M. Djermouni[1], S. Kacimi[1], A. Zaoui[1], B. Bouhafs[1]

[1]Modeling and Simulation in Materials Science Laboratory, Physics Department, University of Sidi Bel-Abbes, 22000 Sidi Bel-Abbes, ALGERIA

djermouni_mostefa@yahoo.fr

Abstract

A series of binary rare-earth metal germanides RE5Ge3 (RE= La, Ce, Pr, Nd and Pm) adopting the Mn5Si3-type hexagonal structure [Fig.1] was investigated. Recently these intermetallic phases show a complex magnetic behavior [1]. The electronic and magnetic properties of RE5Ge3 compounds have been studied by using local-density approximation (LSDA) [2]. The spin orbit coupling was treated using a scalar relativistic basis and the second variational method (LSDA+U+SOC) [3, 4]. The magnetic stabilities; bonding characters; total and partial densities of state and band structures were analyzed and compared with experiments. The effect of the Hubbard correction and the spin-orbit interaction are investigated and are found to be a necessary requirement for the accurate description of correct state of these compounds. We confirm the results of recently synthesized intermetallic compounds RE5Ge3 [Phy. Rev. B 79, 014425 (2009)].

Keywords: Intermetallics compounds, magnetic properties, FP- LAPW method, LDA+U+SOC.

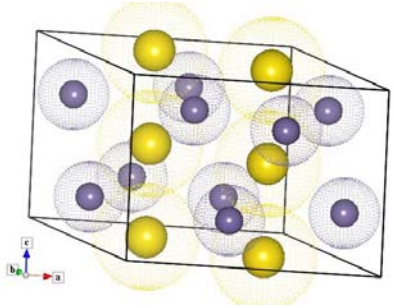

Fig.1. RE (Yellow sphere) and Ge (purple sphere)

References:

Devang A. Joshi, A. Thamizhavel, and S. K. Dhar, Phy. Rev B 79 014425 (2009).

J. P. Perdew, Y. Wang, Phys. Rev. B 45, 13244 (1992).

V. I. Anisimov, J. Zaanen, and O. K. Andersen, Phys. Rev. B 44, 943 (1991).

V. I. Anisimov and O. Gunnarsson, Phys. Rev. B 43, 7570 (1991).

Atomistic Study of Hydrogen Absorption FeAl BULK

M. Gallouze[1], A. Kellou[1], M. Drir[1]

[1]Theoretical Physics Laboratory, Physics Faculty USTHB, BP 32 El Alia, 16111 Bab Ezzouar, Algiers, ALGERIA

Abstract: The FeAl alloys are interesting materials for structural application. In particular, as these materials are sensitive to quench-in vacancies, the interaction of hydrogen atom with vacancies has not been fully addressed and is of a particular interest.

It is well known that the concentration of certain point defects (vacancies, interstitials, impurities, etc.,) affect the behavior of dislocations in crystals, and hence their mechanical properties. The vacancy is one of the simplest defects in crystal structure and so represents a benchmark for experimental and theoretical understanding.

The B2 FeAl phase has ClCs structure and has three types of interstitial sites, one tetrahedral (T) and two octahedral (O^{Fe}, O^{Al}). All tetrahedral are equivalents with the same chemical environment around the site. The O^{Fe} is an octahedral formed by four iron atoms in its base capped with two aluminum atoms, while the O^{Al} has four aluminum atoms in its base capped with two iron atoms. In elementary cell we found 12 tetrahedral sites, 3 octahedral Fe and 3 octahedral Al, and then the T sites have a smaller size then the O sites. This size effect stimulate that the T sites was the most favorable then another ones.

In this work we propose to study the effects of hydrogen in bulk FeAl and the interaction effect with different defect sites using the Density Functional Theory (DFT) implemented in the pseudo-potential plane wave self-consistent field (PWSCF) ab initio package. The generalized-gradient approximation (GGA) functional of Perdew, Burke and Ernzerhof (PBE) was employed in spin-polarized scheme (SP). The ultra soft pseudo-potentials (USPP) of Vanderbilt are used with non-linear core corrections.

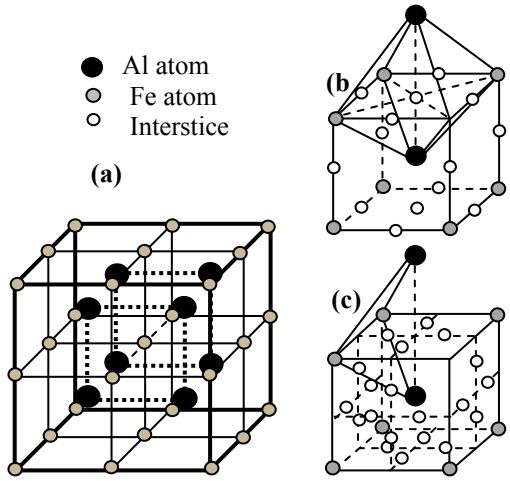

Figure 1: **(a)** The Fe_8Al_8 supercell used in the calculations of bulk structure. (b) and (c) the interstitial sites in a bcc lattice.

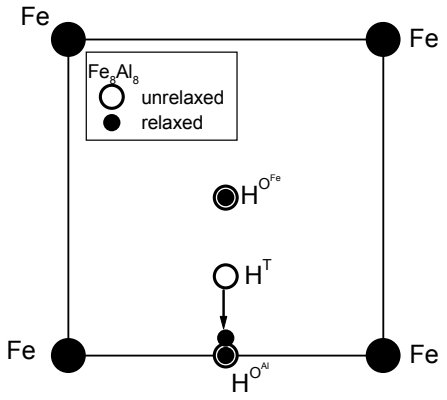

Figure 2: Hydrogen positions in different interstitials sites in Fe_8Al_8 bulk before and after relaxation.

References:

Balasubramaniam R., J Alloys Comp 2002;330–332:506–10.

Jiang DE., Carter EA., Acta Mater 2004;52:4801–7.

Kellou A., H. Feraoun, T. Grosdidier, C. Caddet and H. Aourag, Acta Mater 52 (2004) 3263-3271.

McKamey CG., DeVan JH, Tortorelli PF, Sikka VK., J Mater Res 1991; 6:1779–805.

Semenova O., Krachler R., Ipser H. A., Solid State Sci 2008;10: 1236–44.

First-principles prediction of electronic and magnetic properties of REPtBi (RE= Rare Earth Element) half-Heusler by LSDA+U calculations

A. Hallouch[1], S. Kacimi[1], A. Zaoui[1], B. Bouhafs[1]

[1]Modeling and Simulation in Materials Science Laboratory,
Physics Department, University of Sidi Bel-Abbes, 22000 Sidi Bel-Abbes, ALGERIA
hallouche_a22@yahoo.fr

Abstract

First principles calculations results of a new RE-based half-Heusler *RE*PtBi (*RE*=Rare Earth Element) were presented. The calculations are based on the density functional theory (DFT) within local spin density approximation (LSDA) [1]. The spin orbit coupling was treated using (LSDA+U+SOC) [2, 3] method. The electronic character of the compound is determined by the 4*f* electronic states of rare earth atoms. *f*-states of bismuth atom were also included in calculations although it has no distinct effect on electronic structure. Here, we predict that *RE*PtBi are possible half-Heusler with an energy gap in the minority spin and a completely spin polarization at the Fermi level. We discuss and compare [4] in the present study the electronic and magnetic properties of these materials which may provide a rich platform for novel quantum phenomena.

Keywords: Half-Heusler; magnetic properties; FP- LAPW method; LDA+U+SOC.

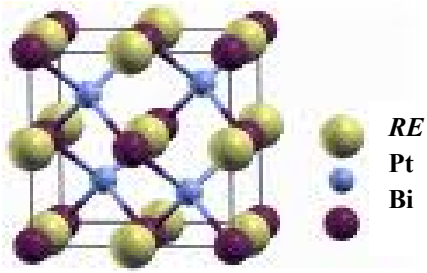

Figures: Crystal structure of half-Heusler com-pound *RE*PtBi in the *F*-43 m space group.

References:

J. P. Perdew, Y. Wang, Phys. Rev. B 45, 13244 (1992).
V. I. Anisimov, J. Zaanen, and O. K. Andersen, Phys. Rev. B 44, 943 (1991).
V. I. Anisimov and O. Gunnarsson, Phys. Rev. B 43, 7570 (1991).

Orientation effect on ferroelectric surface stability of $BaTiO_3$

N. Iles[1], K. Driss Khodja[1]

[1]Laboratoire de Physique des Couches Minces et Matériaux pour l'Electronique
Université d'Oran Es Sénia
Oran 31100, ALGERIA
n_ilesdz@yahoo.fr

Introduction:I

in the few last decades, ABO_3 perovskites oxides were intensively investigated for their interesting physical properties. The most important is the spontaneous polarisation which appears below Curie temperature. Barium titanate $BaTiO_3$ is a prototypical ferroelectric perovskite. It undergoes a structural transition from a paraelectric cubic phase to ferroelectric tetragonal phase at Tc=408 K. This property is largely used to carry out new generation of ferroectric memories FeRAM (*Setter et al.).* Integration of this kind of ternary oxides for this new component requires reaching a nanometre scale of these multilayered systems. At this stage, ferroelctricty is very sensitive to interface quality (Junquera *and Ghosez*). The surface is the first interface between a given material and ambient, it can be extended to few monolayers and present properties different than the bulk material (*Iles et al*).

Along the three equivalent (001) directions, the paraelectric $BaTiO_3$ surface can have two possible terminations BaO or TiO_2. For the ferroelectric surface, two different orientations are possible. The first one, along the polar axis (001) and the second along the non polar axis (100) with BaO and TiO_2 termination displaying atomic displacements of Ti and O atoms of the tetragonale structure (see Fig. 1). Which one of these surfaces is the most stable, a necessary question that needs to be answered because it can have consequences on molecules adsorption on this kind of surfaces (*Rakotovelo ; Wang*).

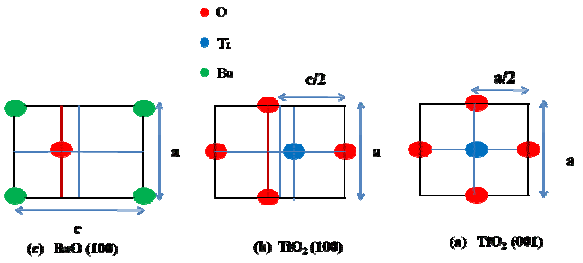

Figure 15: Topmost surface layer for ferroelectric $BaTiO_3$ (a)TiO_2 termination along the polar axis (001), (b) TiO_2 and (c) BaO termination for the non polar (100) surfaces.

In this theoretical work, we used *ab initio* calculations, in the framework of the Density Functional Theory (DFT), in order to study the thermodynamic stability of the paraelectric and ferroelectric (001) and (100) $BaTiO_3$ surfaces. The surface free energy of our surfaces is calculated as a function of the excess in Oxygen to be closer to the experimental annealing conditions. The polar (001) is the most stable surface compared to the non polar (100) and the cubic surface (See fig. 2). This result can have important implications on molecular species adsorption on such polar surfaces.

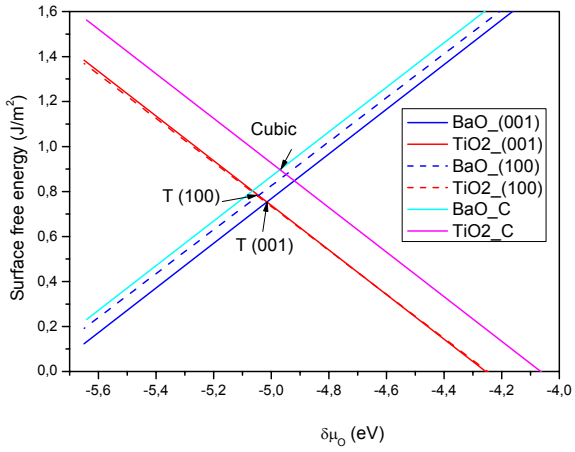

Figure 2: Surface free energy with respect to the oxygen excess, for the cubic and tetragonal (T) (001) and (100) surface terminations.

References:

Iles, N., Finocchi, F., Driss Khodja, K. (2010) J. Phys.: Condens. Matter 22, 305001.
Junquera, J. and Ghosez P. (2003) Nature 22, 506.
Rakotovelo, G., et al. (2009) Surf. Sci. 603, 1221-1228.
Setter, N., et al. (2006) J. Appl. Phys. 100, 051606.
Wang, R.V., et al. (2009) Phys. Rev. Lett. 102, 047601.

Analytical approach of the Graëtz heat exchanger in MHD

S. Lecheheb[1], M. Zizi[1], A. Bouabdallah[1]

[1] Faculté de Physique, Laboratoire de Thermodynamique et des Systèmes Énergétiques, Université des Sciences et de Technologie Houari Boumediene d'Alger,
USTHB, ALGERIA
lecheheb.sabrina@gmail.com

Introduction:

In the methods of transfer, the Graëtz heat exchanger is a key to operate the control and energy management. It is established that a large proportion (90%) of thermal energy used in industrial processes passes at least once by a heat exchanger of this type, both in the processes themselves as in recovery systems thermal energy. It is found mainly in the process industries (steel, plastic materials and energy production), it is accepted that to have a suitable and properly sized heat exchanger achieves a significant performance gain.

In particular, it proposes to undertake the study of the heat exchanger of Graëtz with parallel plans (Figure 1) submitted to the simultaneous influence of the temperature and magnetic fields to assess the performance of heat transfer in the conditions imposed which are close to the industrial reality.

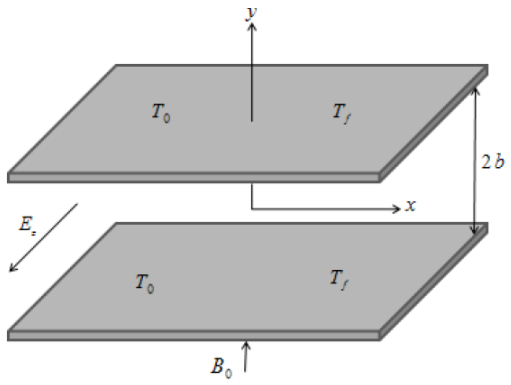

Figure 1: Graëtz heat exchanger description

A viscous, incompressible and electrically conducting fluid or liquid metal flows through a long two parallel-plate channel with laminar regime. We are interested in the part of the heat exchanger for which the flow is fully developed. The velocity profile component in the axial direction x for this flow is the well-known Hartmann profile:

$$u(\eta) = \frac{2}{3}\frac{U_x(y)}{U_m} = \frac{2}{3}\frac{(ch(Ha) - ch(Ha\eta))}{\left(ch(Ha) - \left(\frac{sh(Ha)}{Ha}\right)\right)}$$

The channel walls are maintained at temperature T_0 for $x \leq 0$ and T_f for $x > 0$ (as shown in Figure 1).
All fluid properties are assumed to be constant. The free convection caused by the temperature difference is negligible.

In this study, we solve the equation governing the temperature field θ coupled with the influence of a uniform magnetic field imposed transverse to the parallel plates and direction of flow. Using a variational technique, the Galerkin method, we are led to establish an eigenvalues problem for connecting the flow sensitive parameters, the Brinkman number, the Hartmann number and the Peclet number, depending on the characteristics of the fluid (ρ, ν, σ, μ etc. ...) and geometry considered and estimating the local and global Nusselt number Nu provides interesting information on the performance and effectiveness of this type of heat exchanger.

References:

A.Bouabdallah, Doctorat es Science, Institut Polytechnique de Loraine / Nancy.France 1980.
J. Lahjomri, A. Oubarra, A. Alemany, Heat transfer by laminar Hartmann flow in thermal entrance region with a step change in wall temperatures: The Graëtz problem. J. Heat and mass transfer 45(2002) 1127-1148.
J.P. Hartnett and W.J. Minkowycz, Semi analytical solution to the Cartesian Graetz problem: results for the entrance region. Int. Comm. Heat Mass Transfer, Vol.31, No.5, pp.733-740, 2004.
L.Graëtz. Über die warmeleitungsfahigkeit von Flüssigkeiten, Ann. Phy. Chem. 25 (1885) 337-357.
R.C. Lecroy, A.H. Eraslan, The solution of temperature development in the entrance region of an MHD channel by the B.G. Galerkin method. J. Heat transfer C 91 (1969) 212-220.

Evolution of physical properties according to the stoichiometric coefficient x of the alloy $In_xGa_{1-x}N$ intended for photovoltaic devices

H. Mazari[1], Z. Benamara[1], M. Mostefaoui[1], N. Benseddik[1], K. Ameur[1], N. Zougagh[1]

[1]Laboratoire de Microélectronique Appliquée, Département d'électronique, Faculté de l'Ingénieur, Université Djillali Liabès de Sidi Bel-Abbes,
BP 89, 22000 Sidi Bel-Abbes, ALGERIA
h_mazari2005@yahoo.fr

Abstract

The InGaN alloy has a great potential in the manufacture of the photovoltaic devices.
A simple optimized junction InGaN can reach an conversion efficiency from > 20%, comparable with that reached by the best cells of die CISGS. Because the band gap of InGaN can be modified from 0,7 eV to 3,4 eV by increasing the gallium content with multi-junction cells, it is theoretically possible to achieve the record performance (70%) with this only material system, whereas the theoretical record in technology GaAs multi-junctions is less than 50%.
To study a solar cell single-junction, containing the alloy InGaN, it is significant to know the physical properties of this material and in particular the evolution of its last according to the stoichiometric coefficient x.

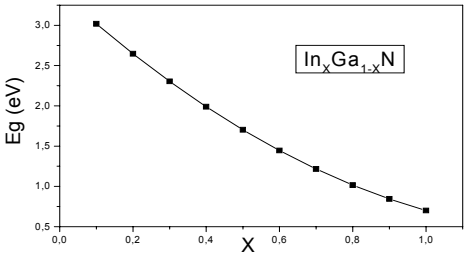

Figure 1: Evbolution of E_G to the x [1]

We present in this work the variations of certain parameters like the energy of the band gap (Fig.1), the absorption coefficient α (Fig.2), the mobility μ, the effective mass m,
etc...., according to the stoichiometric coefficient x.
The interest is in the choice of x that gives us the best photovoltaic parameters for achieving the best possible conversion efficiency.

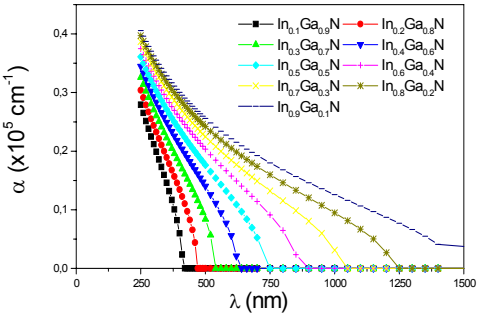

Figure 2: Evolution of α to the λ for different values of x

The best conversion efficiency η is obtained for x=0.6 and values 24.3 % for a simple junction (Figure.3).

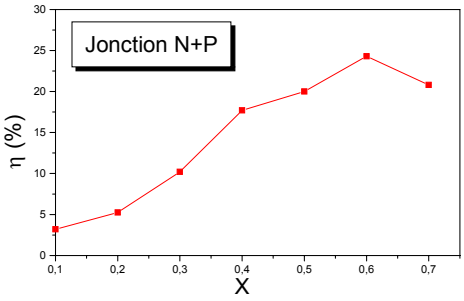

Figure 3: Evolution of η to the x

References :

F. Languy , 2007, Thèse, Fac. Univ. Notre-Dame de la Paix, Faculté des Sciences de Namur, 2007.
W. J. Aziz, K. Ibrahim, 2010, Int. J. Nanoelectronics and Materials 3 43-52, 2010.

First principles lattice dynamics and thermodynamical study of Thallium-V compounds

H. M. A. Mazouz[1], A. Belabbes[2] , M. Ferhat[2]

[1] Faculté des Sciences, Département de Physique, Université M'Hamed Bougara, Boumerdes , ALGERIA
mazouz_moulay@yahoo.fr

[2] Faculté des Sciences Département de Physique, Université des Sciences et de la Technologie d'Oran, BP 1505 El Mnaouer, ALGERIA

Abstract:

We have performed an ab initio calculation in order to investigate the structural, the electronic, the lattice-dynamical and the thermodynamical properties of zinc blend thallium-V compounds: TlAs, TlP and TlN. The ground-state parameters, i.e., lattice constant and the bulk modulus and the electronic structure are calculated using the plane wave pseudopotential approach to the density functional theory within local density approximation. Phonon dispersion spectra are derived from linear-response to density-functional theory. Thermodynamical properties are also reported by using the quasi harmonic approximation.

The structural properties including the lattice parameter and the bulk modulus are calculated using the pseudopotential approach to the density functional theory within local density approximation in a plane wave basis. The core–valence electron interaction is described by Vanderbilt ultrasoft pseudopotentials[1], as implemented in the PWscf code[2], with Perdew–Zunger (PZ)[3], for the exchange–correlation functionals. Integration in Brillouin zone are performed using a 8×8×8 k-point mesh for the zinc blende phase. The phonon frequencies are calculated within the framework of the selfconsistent density-functional perturbation theory DFPT[4] which allows the calculation of the Born effective charge tensor Z_B and the dielectric constant, in polar semiconductors and insulators, for each inequivalent atom in the unit cell.

In particular, eight dynamical matrices were calculated for a 4×4×4 k-points mesh of Monkhorst and Pack[5]. These matrices were then Fourier interpolated to obtain the phonon dispersion curves. The results for the ground state and the electronic properties are in good agreement with available theoretical studies. We have highlighted the main features of the predicted phonon dispersion curves of these materials compared with the other III–V compounds. We have also reported thermodynamical results (the specific heats and entropies) concerning the Thallium-V compound considered.

References:

D. Vanderbilt (1985), Phys. Rev. B 32 8412.

S. Baroni, A. Dal Corso, S. de Gironcoli, P. Giannozzi, C. Cavazzoni, G. Ballabio, S. Scandolo, G. Chiarotti, P. Focher, A. Pasquarello, K. Laasonen, A. Trave, R. Car, N. Marzari, A. Kokalj, http://www.pwscf.org.

J. P. Perdew and A. Zunger . (1981) Phys. Rev. B 23 5048.

S. Baroni, de S. Gironcoli, A. Dal Corso and P. Giannozzi (2001), Rev. Mod. Phys., 73 515.

H. J. Monkhorst and J. D. Park (1976), Phys. Rev. B 13 5188.

Electrons beam behavior in a gas mixture under low voltage in the environmental SEM

O. Mansour[1, 2] A. Kadoun[1], K.Aidaoui[1], C.Mathieu[3]

[1] Faculté des Sciences, Laboratoire L2MSM, Université Djillali Liabes de Sidi Bel Abbès, B.P.89, Sidi Bel Abbès, 22000, ALGERIA
[2] Faculté des sciences et de technologie, Université Ziane Achour de Djelfa 17000 ALGERIA
[3] Centre de calcule et de modélisation, Université de Lens, Université d'Artois, faculté des sciences, FRANCE

Content:

The effects of various gas environment used in high pressure SEM inside the specimen chamber were investigated using Monte Carlo simulation **[1]**, **[2]**.In order to improve the signal to noise ratio for the electron detection, we suggest using helium gas-based mixture. The Helium gas is well known to reduce the skirt effect due to its low elastic scattering cross-section **[3]**, **[4]**. The addition of an ionizing gas such as hydrogen or nitrogen is proposed to increase the inelastic scattering cross section which is mainly responsible for the ionization process taking place during the beam-gas interactions.

Results:

In order to compare the influence of the gas environment, we have plotted the skirt radius $r_{0,9}$ vs. the pressure (Figs.1 and 2). It appears that for He, the variation of the skirt radius does not depend on the pressure in the investigated range from 1 to 100 Pa at 5 kV (Figs.1).

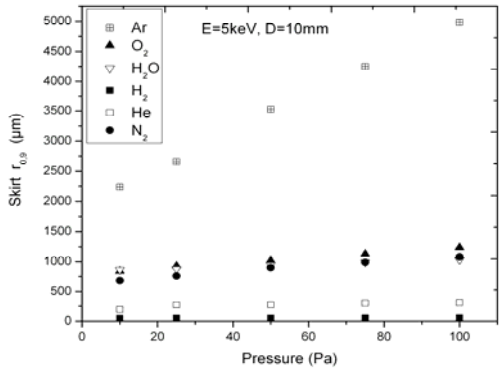

Figure 16: Variation of the skirt radius vs. the pressure

Figs.2 show that for all the mixtures (except He-Argon), the skirt is slightly modified with the increase of the pressure. For the BSE detection, the signal to noise can remain high and gives a good contrast in imaging. Moreover, the presence of an ionizing gas will favor the ionizing process which is very important in beam-based electron detection. In this case, an increase of the signal to noise ratio can be expected.

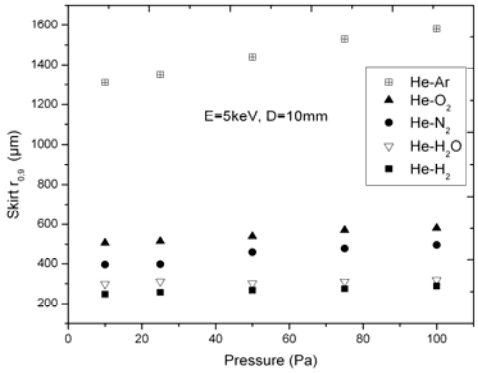

Figure 2: Variation of the skirt radius vs. the pressure of gas mixtures constituted from 90% of pure helium

Conclusion:

In order to improve the signal to noise ratio for the electron detection, we suggest to use helium gas based mixture. For all the mixtures (except He-Argon), the main results show that the skirt is slightly modified with the increase of the pressure. For the BSE detection, the signal to noise can remain high and gives a good contrast in imaging. Moreover, the presence of an ionizing gas will favor the ionizing process which is very important in beam–based electron detection. In addition, the presence of such ionizing gas leads to work at lower pressure, which reduces the beam skirt phenomena. In this case, an increase of the signal to noise ration can be expected.

References:

A.Kadoun, R.Belkorissat, B.Khelifa and C.Mathieu, J Trace Microprobe Tech 21 (2003), pp. 229–238.
A.Kadoun, R.Belkorissat, B.Khelifa and C.Mathieu, Vacuum 69 (2003), pp. 537–543.
R.Belkorissat, A.Kadoun, B.Khelifa and C.Mathieu, Micron 35 (2004), pp. 543–547.
E.Oho, A.Akai, I.E.O.Sukehiro, A.Natsuki and I.Sukehiro, J. Electron Microscopy 49 (2000), pp. 761–763.

Electronic and structural properties of the quaternary chalcopyrites $Cu_2FeAlSe_2$ and $CuFe_2AlSe_4$

S. Medina[1], B. Bouhafs[1]

[1]Modelling and Simulation in Materials Science Laboratory
Djillali Liabès University of Sidi Bel-Abbès, Sidi Bel-Abbès 22000, ALGERIA
smedinadz@yahoo.fr

Abstract: In recent years, chalcopyrites semiconductors have attracted much attention because of their potential application in non-linear optics, photovoltaic and spintronics devices.

Our aim is to searching novel chalcopyrites promising for these applications, in particular, we treated the I_2–II–III–VI_4 and I-II_2-III-VI_4 quaternary compounds with (I=Cu, II=Fe, III=Al, VI=Se) synthesized through cation cross substitution in ternary I-III-VI_2 systems.

We investigated the structural and electronic properties of quaternary chalcopyrites by means of a first-principles density functional total energy calculation within the local density approximation (LDA), using the all electron full-potential linear augmented plane wave method (FP-LAPW). The equilibrium lattice constants, bulk modulus, band structures and density of states have been given in detail, analyzed and compared with previous calculations.

Introduction:

The compounds with ternary structures of the chalcopyrite family Cu-III-Se_2 (III=Al, Ga, In) form an wide group of semiconductor materials with diverse optical and electrical properties. Recently, the formation of some member with compositions Cu-Fe-III-S_3 (x=1/2), Cu-Fe_2-III-Se_4 (x=2/3) and Cu_2-Fe-III-Se_5 (x=1/3) have been reported. Much attention has been focused on the fabrication of nanoscale metal chalcogenide semiconductors, which can exhibit fascinating chemical and physical properties and have many potential applications.

Chalcogenide compounds such as the chalcopyrite, $CuFeSe_2$, which belong to the I–III–VI_2 family, usually exhibit chalcopyrite structure. $CuFeSe_2$ is an antiferromagnetic semiconductor with a very small band gap and exhibits novel electrical, optical and magnetic properties. Because of both ferromagnetism and the electronic transport properties of magnetic semiconductors, they have been used as suitable materials for spintronics applications.

Calculation:

The calculations are based on the density-functional theory in the local spin-density approximation (LSDA) with additional Hubbard correlation terms describing on-site electron–electron repulsion associated with the 4*f* narrow bands (LSDA+U approach). The crystal structure of the chalcogenide compounds (Fig. 1), were characterized using the X-ray powder diffraction data for both compounds. Both compounds crystallize in the tetragonal space group.

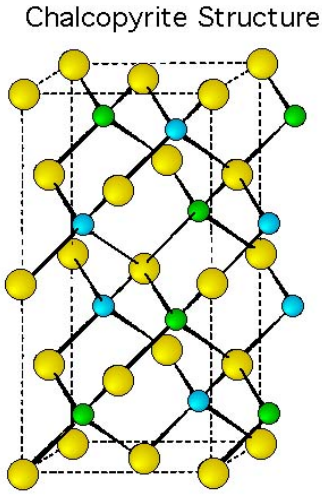

Figure 17: The $CuFeSe_2$ chalcopyrite structure.

References:

Delgado, G.E., Mora, A.J., Contreras, J.E., Grima-Gallardo, P., Durán, S., Muñoz, M. and Quintero, M. (2009) Crystal structure characterization of the quaternary compounds $CuFeAlSe_3$ and $CuFeGaSe_3$, Cryst. Res. Technol. 44, 548–552.

Sato, K., Harada, Y., Taguchi, M., Shin, S. and Fujimori, A. (2009) Characterization of Fe 3d states in $CuFeS_2$ by resonant X-ray emission spectroscopy, Physica Status Solidi A 206, 1096–1100.

Lamazares, J., Gonzalez-Jimenez, F., Jaimes, E., D'Onofrio, L., Iraldi, R., Sanchez-Porras, G., Quintero, M., Gonzalez, J., Woolley, J.C. and Lamarche, G. (1992) Magnetic, transport, X-ray diffraction and Mössbauer measurements on $CuFeSe_2$, Journal of Magnetism and Magnetic Materials 104-107, 997-998.

Ab-intio study of structural, electronic and mechanical properties of intermetallics of typeTM-Al

S.Méziane[1], H.Aourag[1], H.I.Faraoun[1]

Laboratoire d'Etude et Prédiction des Matériaux, Unité de Recherche Matériaux et Energies Renouvelables, Université A. Belkaid, Tlemcen, ALGERIA
msouheyr@yahoo.fr ; h_aourag@univ-tlemcen.dz, h_faraoun@mail.univ-tlemcen.dz

Abstract:

The intermetallic compounds, in particular the Transition Metal Aluminides TM-Al [1], have significant potentialities like materials at high temperature. A certain number of their characteristics (microstructural stability, creep, ductility…) are directly related to their crystallographic structures like with their electronic configurations and are thus conditioned by the properties of distribution of their atoms. However, their use remains currently very limited because of their practically non-existent intrinsic ductilities to ambient temperature [2].

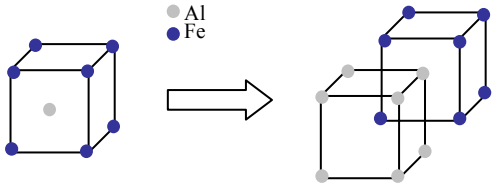

Figure 1: Example of cubic cell of FeAl.

This study has for main goal to predict the mechanical properties of these materials in various configurations: simple copounds the intermetallic ones, structures in layers and alloys of substitutions. With this intention, we used calculations ab- initio with the technique of super-cell. Calculations are carried out in the framework of the theory of the functional calculus of density DFT and the approximation of the pseudo-potentials. We used the potentials of the ultrasoft type (of Vanderbilt) included in code VASP [3].

We considered the case of TiAl, FeAl, CoAl and NiAl. ¶Our calculations make it possible to conclude that the solid solution Fex Ti1- x Al for x = 0.5 in the B2 (CsCl) phase has best ductility, whereas the structure in FeAl/CoAl layers has the highest rigidity.¶

References:

James R. Morris, Yiying Ye, Young-Bin Lee, Bruce N. Harmon, Karl A. Gschneidner Jr., Alan M. Russell; "Ab initio calculation of bulk and defect properties of ductile rare-earth intermetallic compounds". Acta Materialia, volume 52, pages 4849-4857, September 2004.

Zbigniew Witczak, Valeria A. Goncharova, Przemyslaw Witczak; "Elastic properties of a plycrystalline sample of the L12 Al5CrTi2 intermetallic compound under hydrostatic pressure up to 1GPa at room temperature". Journal of Alloys and Compounds, volume 337, pages 58-63, May 2002.

Georg Kresse and Jürgen Furthmüller; "VASP the GUIDE". Institut für Materialphysik, Universität Wien, Sensengasse 8, A-1130 Wien, Austria.

The effect of zinc concentration upon optical properties of $Cd_{1-x}Zn_xSe$

F. Mezrag[1], W. Kara Mohamed[2], N. Bouarissa[3]

[1]Physics Department, Faculty of Science and Engineering, University of M`sila, 28000 M`sila , ALGERIA
[2]Centre Universitaire de Bordj-Bou-Arreridj, El-Anasser, 34265 Bordj-Bou-Arreridj, ALGERIA
[3]Department of Physics, Faculty of Science, King Khalid University, Abha, P.O.Box 9004, SAUDI ARABIA

Abstract

Theoretical investigations of the optical properties of $Cd_{1-x}Zn_xSe$ with zinc-blende crystal structure are reported. The calculations are mainly based on the pseudopotential framework within the virtual crystal approximation in which the effect of compositional disorder is involved. A meaningful agreement with known data is only obtained when the disorder effect is included in the calculation. The zinc concentration dependence of the selected features of $Cd_{1-x}Zn_xSe$, such as energy band gaps, and refractive index, has been examined. All studied quantities are found to vary monotonically with zinc concentration x. The refractive index has been scaled with the zinc concentration. Such scaling showed that the variation of the refractive index versus Zinc concentration exhibits a non-linear behavior.

Keywords: Optical properties; II-VI ternary alloys; CdZnSe

Conformational Study of Some α-ketophosphonates

D. MISSAOUI[1], O. BENSAID[2], A. RAHMOUNI[1], N. BENBRAHIM[1, 3]

[1] Laboratoire de modélisation et de méthodes de calcul, université de Saida, B.P. 138, Cité En-Nasr 20002 Saida, Algérie
[2] Laboratoire de Chimie Organique Substances Naturelles et Analyse (COSNA) Université Abou Baker Belkaid Tlemcen Faculté des Sciences Département de Chimie BP 119 Tlemcen 13000 ALGERIA
[3]Département de pharmacie, Faculté de médecine, Université de SBA, ALGERIA
missaoui_chem@yahoo.fr

Abstract:
The α-ketophosphonates such as $(RO)_2P(O)C(O)R'$ possess interesting and varied biological activities[1]. Their corresponding α–hydroxyphosphonates obtained by reduction are used in the constitution of antibacterial, antiviral, and antibiotics [2]. The biological activities of these α-ketophosphonates depend on the conformation which they adopt when they approach the active site. The aim of this work is a determination of the most stable conformations of the α- ketophosphonates such as $[(CH_3O)_2P(O)C(O)R]$ with R=(Me, Et, Pr) [3]. The energetic variation with varying the dihedral angle $\angle O_1C_1PO_2$ was studied.

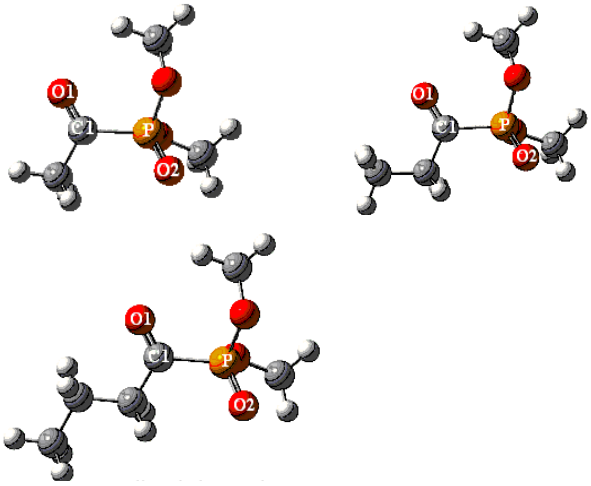

The quantum chemical calculations used are at HF/6-31G*, B3LYP/6-31G* and MP2/6-31G* levels. The obtained graphs reveal that the most stable conformations are intermediate between the Cisoïde and the Transoïde shape.

Keywords: α-ketophosphonates, HF, B3LYP, MP2, Cisoïde, Transoïde.

References:

T. Oshikawa, and M. Yamashita. (1990) Chem. Soc. Jpn. 63pp 2728.
K. Afarinkia, and M. Vinader. (1995) The Synthesis of Acyl Phophorus, -Arsenic,Antimony or Bismuth Functions, In Organic Functional Group Transformations Moody, 393-407.
K. Afarinkia, J. Echenique and S. C. Nyburg. (1997) Tetrahedron Letters, Vol. 38, No. 9, pp. 1663-1666.

Simulation of photovoltaic parameters of a solar cell

H. Mazari[1], M. Mostefaoui[1], N. Benseddik[1], K. Ameur[1],
Z. Benamara[1], N. Zougagh[11]Laboratoire de Microélectronique Appliquée, Département d'électroniqueFaculté de l'Ingénieur, Université Djillali Liabès de Sidi Bel-Abbes, BP 89, 22000 Sidi Bel-Abbes, ALGERIA
rayce-82@hotmail.fr

Abstract: III-V nitrides (GaN, AlN, InN) are semiconductor wide bandgap particularly attractive for applications in optoelectronics and microelectronics.GaN alloys exhibit a direct gap adjustable hence their use in photovoltaics. Among these alloys nitrided, is interested in the InGaN, a material that has great potential.The sensitivity of the photovoltaic parameters such as current short-circuit I_{CC}, the conversion efficiency η, the open circuit voltage V_{CO} and the form factor FF and the spectral response as a function of stoichiometric coefficient x of the alloy $In_xGa_{(1-x)}N$ has been studied by the software Pc1D.

Introduction: The goal of achieving photovoltaic conversion efficiencies of 50% or higher not only attributes as a scientific achievement and aids specialized applications, but can also reduce the cost of large-scale solar electric generation. The maximum reported photovoltaic efficiency of 39% at 236 suns is achieved by a triple-junction GaInPGaInAs-Ge tandem solar cell [1]. While the achievable efficiency of triple-junction tandem solar cells is restricted to about 40%, modeling results show that a tandem solar cell of five junctions or greater, or an equivalent structure, is required to achieve practical efficiencies of greater than 50% under an AM1.5.

InGaN material system: The III-Nitride semiconductor system, which includes AlN, GaN, InN and its alloys provides all band gaps needed to construct solar cells with response above 2.4 eV. The nitrides also have high charge velocities and strong light absorption. InGaN LEDs are relatively insensitive to high dislocation densities and have unusual polarization and piezoelectric properties .The III-N material system has undergone remarkable development due to the use of GaN and InxGa1-xN for blue LEDs and laser diodes [2]. MOCVD has emerged as the leading candidate for commercial growth of high band gap InGaN due to its large scale manufacturing potential. A major challenge for the MOCVD growth of InGaN is to reduce its band gap and achieve efficient light emission in the blue green region. This material can be used as the highest band gap material in a solar cell with five-junctions or greater. InN and In-rich low-band gap InGaN are commonly grown by MBE. Recently the band gap of InN was shown to be lower than previously thought;low band gap InGaN is a subject of fundamental study.

Simulation resultas: The described model is incorporated in the source-code of PC1D. The simulation results of a test structure (Figure 1) are presented and discussed.

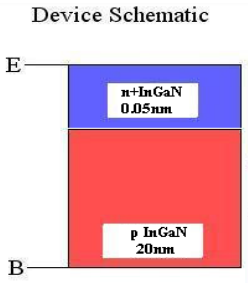

Figure 1: Schematic of simulated device.

Optimization at summer made for each value of x (going from 0.1 to 0.9) for all the sizes (N_A ,N_D X_f ,X_b, S_n , S_p ,τ_n,τ_n) (Figure2).

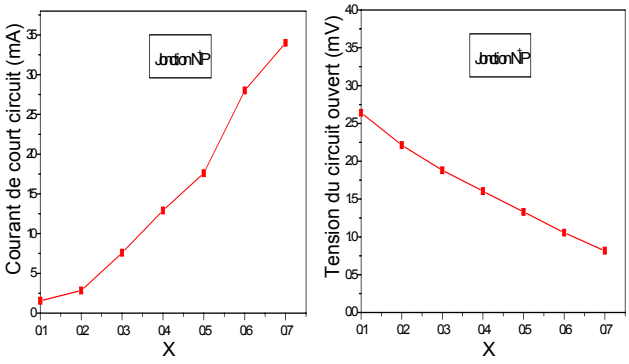

Figure 2: Photovoltaic parameters according to the stoechiometric coefficient

References:

O. Jani, C. Honsberg, A. Asghar, D. Nicol, I. Ferguson,A. Doolittle, S. Kurtz, "Characterization and Analysis of InGaN Photovoltaic Devices," Proceedings of the 31st IEEE PVSC, 2005, pp. 37-42.
Y. Nanishi, Y. Saito and T. Yamaguchi, "R-F MolecularBeam Epitaxy Growth and Properties of InN and RelatedAlloys", *Jpn. J. Appl. Phys.*, **42**, 5A, 2003, pp. 2549-2559.

Theoretical Studies of Structural Properties of the Complexes of Pd, Rh, Ru With Hemilabile Ligands (BPMO's)

M. NAOUI[1] , A. RAHMOUNI[1]

Laboratory of modeling and method of calculation LMMC, University Dr .MOULAY TAHAR of Saida,P.B 138, En-Nasr 20002 Saida, ALGERIA
naouimed@gmail.com ;
naouifet@yahoo.fr

Introduction:

In general, ligand design is somewhat like a fine art, requiring an individual, often intuitive approach for each catalytic system. The right choice of a ligand for a metal-catalyzed homogeneous reaction can be as critical as the choice of the metal itself. (1)

Great interest has been devoted to transition metal complexes containing the so-called hemilabile ligands, with both soft and hard nucleophilic centers within one molecule. Due to their potential application as homogeneous catalysts, bis-phosphine monoxides (BPMOs) of the general formula R1R2P-Y-P(O)R3R4, where Y is a divalent spacer, constitute an important class of hemilabile ligands. The combination of a soft phosphino group with a hard phosphoryl one in the same molecule enables biphosphine monoxide ligands (BPMOs) to have different coordination modes depending on the transition metal involved and can stabilize various transition metals in low and high oxidation states. Also, BPMOs often form labile metal chelates which can easily generate reactive, coordinatively unsaturated species. Consequently, the weak BPMO chelation provides low activation energy paths to various transformations at the metal center, such as ligand exchange, isomerization, oxidative addition, migratory insertion, reductive elimination, and so forth. The structural properties of those complexes determined with theoretical methods are very important due to there large applications and expensive characterisation with classic methods.

The aim of our work consists in carrying out a theoretical study of structural properties of the complexes of Pd, Rh, Ru (Palladium, Rhodium, Ruthenium) with hemilabile ligands (BPMOs) . With this intention, we carried out optimizations of geometry of some configurations of these complexes. All calculations were performed with the Gaussian03 program packages. (2). The density functional calculations (DFT) with the B3LYP and B3PW91 functionals employed a basis set of double-ζ quality, which is denoted LANL2DZ in Gaussian. For the heavy elements (*e.g.* Pd,Rh and Ru) effective core potentials (ECPs) with the corresponding basis set were used while the light elements (C, H, O, Cl) were described by a 6-31G* basis set. Geometries were fully optimized

References:

vladimir V.grushin, Chem. Rev. 2004, 104,1629-1662.

Gaussian 03, Revision A.1, M. J. Frisch, G. W. Trucks, H. B. Schlegel, G. E. Scuseria, M. A. Robb, J. R. Cheeseman, J. A. Montgomery, Jr., T. Vreven, K. N. Kudin, J. C. Burant, J. M. Millam, S. S. Iyengar, J. Tomasi, V. Barone, B. Mennucci, M. Cossi, G. Scalmani, N. Rega, G. A. Petersson, H. Nakatsuji, M. Hada, M. Ehara, K. Toyota, R. Fukuda, J. Hasegawa, M. Ishida, T. Nakajima, Y. Honda, O. Kitao, H. Nakai, M. Klene, X. Li, J. E. Knox, H. P. Hratchian, J. B. Cross, C. Adamo, J. Jaramillo, R. Gomperts, R. E. Stratmann, O. Yazyev, A. J. Austin, R. Cammi, C. Pomelli, J. W. Ochterski, P. Y. Ayala, K. Morokuma, G. A. Voth, P. Salvador, J. J. Dannenberg, V. G. Zakrzewski, S. Dapprich, A. D. Daniels, M. C. Strain, O. Farkas, D. K. Malick, A. D. Rabuck, K. Raghavachari, J. B. Foresman, J. V. Ortiz, Q. Cui, A. G. Baboul, S. Clifford, J. Cioslowski, B. B. Stefanov, G. Liu, A. Liashenko, P. Piskorz, I. Komaromi, R. L. Martin, D. J. Fox, T. Keith, M. A. Al-Laham, C. Y. Peng, A. Nanayakkara, M. Challacombe, P. M. W. Gill, B. Johnson, W. Chen, M. W. Wong, C. Gonzalez, and J. A. Pople, Gaussian, Inc., Pittsburgh PA, 2003.

Keywords: BPMOs, Rh, PD, Ru, hemilability, theoretical study, bidentate, monodentate, DFT, B3LYP, B3PW91, ζ lanl2dz.

DFT Calculations of the Structural and Electronic Properties of Spinosyns A and D

K. Ouadah[1], K. Smail[1], N. Tchouar[1]

[1]Faculté des Sciences, Laboratoire LAMOSI, Université des Sciences et Technologie d'Oran USTO
B.P.1505, Oran, 31000, ALGERIA
biokarim2000phyto@yahoo.fr

The spinosyns, a novel family of insecticidal macrocyclic lactones, are active on a wide variety of insect pests, especially lepidopterans and dipterans. The biological activity of a mixture of the two most abundant spinosyns (spinosyns A and D) is an unsaturated tetracyclic ester with two sugar derivatives (forosamine and rhamnose sugars) attached through ether
Linkages. against pest insects is on a par with that of many pyrethroid insecticides [1]. The spinosyns also exhibit a very favorable environmental and toxicological profile, and possess a mode of action that appears unique, with studies to date suggesting that both nicotinic and gamma-aminobutryic acid receptor functions are altered in a novel manner. Being the two investigated spinosyns (spinosyns A and D), many of their properties are strongly dependent on the environment, i.e. the nature of the solvent and the pH of the solution. Therefore, this investigation has been extended to the forms spinosyns A and spinosyns D and the effects of the solvent have been taken into account. Despite the numerous experimental works on spinosyns, only a few theoretical studies have been reported to date on spinosyns A and spinosyns D [2]. In this work, the structural properties and chiralite of spinosyns A and spinosyns D are studied with ab initio methods in vacuum and in solution. Molecular structures have been optimized with MP2, RI-MP2 and DFT using different functionals and basis sets. Harmonic vibrational frequency calculations have been performed on the optimized structures to ensure that geometries obtained were real minima. The frontier molecular orbitals and the HOMO–LUMO gap of the different geometries have been computed and their changes have been thoroughly analyzed.

References:

Crouse, G. D. Sparks. T. C. (1998) *Rev. Toxicol.*, 2, 133-146.
De Amicis, C., Graupner, P. R., Erickson, J. A., Paschal, J. W., Kirst, H. A., Creemer, L. C., Fanwick, P. E. (2001) *J. Org. Chem.*, 66, 8431-8435.

Study of Non Linear Instability of Taylor in the Vicinity of its Appearance

M. Ouali[1], R. Bellatreche[1], A. Bouabdallah[1]

[1] Faculté de Physique, Laboratoire LTSE, Université des Sciences et de Technologie Houari Boumediene, Alger
BP EL ALIA 16111 – Bab Ezzouar - ALGER, ALGERIA
ouali_maamar@yahoo.fr

Introduction: The theoretical study proposed here is essentially limited to the nonlinear analysis of the evolution of Taylor instability in the vicinity of its occurrence. This domain of investigation has been abandoned for 30 years. In 1920, Lord Rayleigh attempted to conduct a study of linear stability in the event of a perfect fluid [1]. G.I. Taylor took over the problem in 1923, real fluid [2]. In 1958, J.T. Stuart made the first non-linear theory in hydrodynamics [3].

The question applies to a movement flow system confined between coaxial cylinders. These developments set the amplitude A(t) related to the instability of Taylor. In particular, it examines how the solution calculated from the linear theory to determine the evolution of the amplitude Ae equilibrium when the Taylor number Ta tends towards the critical value corresponding to Tc1 appeared. For this purpose all this theoretical approach based only on the data of steady laminar movement $\overline{V_0}$ as a variable of the problem considered. In general, the disturbance field (u, v, w) and the perturbed average field $\overline{V}$ will be considered as a distortion of the entire flow from the basic movement $\overline{V_0}$.

The movement considered applicable to a flow system confined between coaxial cylinders whose interior cylinder is rotating and the outer one is kept fixed in an upright position (Figure 1). It is assumed that the flow evolves infinity geometry such as aspect ratio Γ = H / d is Γ → ∞. For our study, will be selected, the system of cylindrical coordinates (r, θ, z) knowing that the radial positions r and z axial flow are defined respectively in the field:
r □ [R_1, R_2] et 0≤ z ≤H in function of the velocity components $\vec{V}$ (V_r=U, V_θ=V, V_z=W) respectively along the radial direction r, azimuth θ, and axial z.

We started by the system of linear equations of the instability of Taylor

$$\begin{cases} \frac{\nu}{\lambda^2}(DD^* - \lambda^2 - \frac{\sigma'}{\nu})(DD^* - \lambda^2)u = 2\frac{\overline{V}v}{r} \\ U(DD^* - \lambda^2 - \frac{\sigma}{\nu})v = (D^*\overline{V})u \end{cases}$$

Boundary conditions :

à $r = R_1$ $\quad U = R_1\Omega_1$ et $V = W = 0$

à $r = R_2$ $\quad U = R_2\Omega_2$ et $V = W = 0$

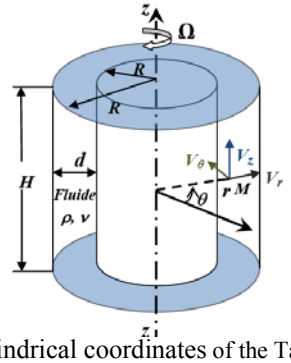

Figure 18: Cylindrical coordinates of the Taylor-Couette flow system

The expression of the average field in laminar disruption is written as follows:

$$\overline{V}(\overline{V_0}) = \overline{V_0} + 0.01_1 \,\mathrm{Re}\,\alpha_1\beta_1 Ae^2(7.06\,10^{-4}\,\overline{V_0} - 2.7\,\overline{V_0}^4 + 6.66\overline{V_0}^5 - 5.7933\overline{V_0}^6 + 1.8142\overline{V_0}^7 - 0.032\overline{V_0}^8 - 0.0194\overline{V_0}^9)$$

Under these conditions proposed, and with the application of the Galerkin method, it was able to assess the evolution of the equilibrium amplitude Ae from a calculation using the value of the mean field. The representation of the equilibrium amplitude Ae depending on variable factors α and β allowed us to optimized and adapted to the times following the theory, and experiment.

$$Ae^2 = \frac{1.18310^3}{\mathrm{Re}\,\alpha_1\beta_1}\left[1 - \left(1.038\frac{\alpha_1}{\beta_1} - 0.508\right)\frac{1}{T_s^*}\right]$$

This new formulation shows a more general and global instability of the approach and incorporated the key to assessing the degree of disturbance and disruption of the field and its distortion.

References:

Lord Rayleigh (1916), On the dynamic of revolving fluids, *Proc Roy. Soc. London, Ser A93, 148-154.*
Taylor, G.I. (1923), Stability of viscous liquid contained between tow rotating cylinders, *Philos. Trans. Roy. Soc. London Ser A223.*
Stuart, J.T. (1986), Taylor- Vortex flow, *A dynamical system SLAM Review. Vol28, No3, pp 315-342.*

Development of software for photonic crystal simulation and analysis using FDTD and PWE methods

A. Dekhira[1, 2], O. Ouamerali[1]

[1]Faculty of Chemistry, USTHB, Alia BAB EZZOUAR, 16111, Algiers, ALGERIA
ouameralio@hotmail.com
[2]Ecole Doctorale Physique Chimie Théorique Chimie Informatique
azedbox@yahoo.com

Abstract: This work describes the design of simulation software for photonic crystals modeling and analysis using the two most popular methods, FDTD and PWE. The software is implemented using C++Builder and developed using object-oriented scheme and modular approach, to enable code reuse and ease of upgrade in future.

Photonic crystals, in which the refractive index changes periodically, provide an exciting tool for the manipulation of photons and have made substantial progresses in recent years. Due to the complexity of synthesis and design of photonic crystals as well as the costs of systematic experimental analysis, Simulation of such structures has become of increasing importance. The FDTD (Finite Difference Time Domain) gives the electromagnetic field distribution inside the crystal and the PWE (Plane Wave Expansion) is to calculate the band structure and provide the dispersion diagram. Combining these two powerful methods into one package with Intuitive and flexible graphical user interface produces a virtual laboratory for photonic band gap materials investigations.

The figure below shows the basic modules of the software package. Windows interface module is to handle use interface, read and parse input data and set up the data types and variables in the program. The input module consists of graphical interfaces to set parameters of mesh generation, boundary conditions, excitation sources, media investigated and a cad-based interface to represent the photonic materials.

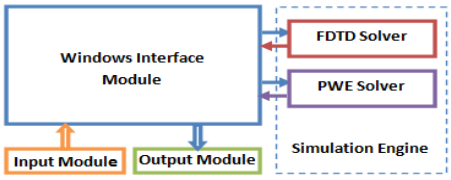

Figure 19: Major software blocks

The simulation engine, through the two solvers and the package of FDTD and PWE algorithms implemented, is to execute the operations and give back the results calculations. The output module is to recover the results of the simulations and display them graphically and numerically.

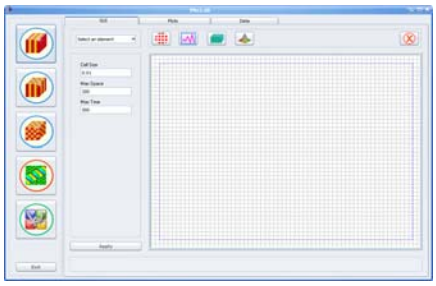

Figure 2: Graphical user interface view

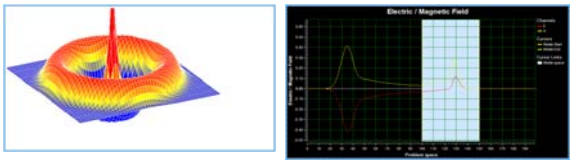

Figure 3: Graphical Output samples

we have calculated the band structure of a 2D photonic crystal based on $LiNbO_3$ material with air holes in triangular lattice. The TM polarization and the ratio r/a=0.43 were chosen. The result was the same as the one calculated using "MPB", the standard developed by MIT.

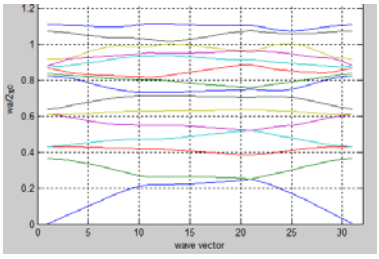

Figure 4: Band Structure of 2D phc based on $LiNbO_3$

References:

Berenger, J.-P., "*A perfectly matched layer for the absorption of electromagnetic waves*," *Journal of Computational Physics*, v. 114, pp. 185–200, 1994.

J. D. Joannopoulos, R. D. Meade, and J. N.Winn. *Photonic Crystals: Molding the Flow of Light*. Princeton University Press, Princeton, (2008).

Taflove, A. and Hagness, S. C., *Computational electrodynamics: the finite difference time-domain method*. Boston: Artech House, second ed., 2000.

Theoretical study of structural and thermal properties of Fe_2 (Zr, Nb) Laves alloys

L. Rabahi[1], A. Kellou[2], D. Bradai[1]

[1] Faculté de physique, Laboratoire physique des matériaux, Université des sciences et de la technologie Houari Boumediene *USTHB* B.P.32, El Alia, 16111, Bab Ezzouar, Alger, ALGERIA
rabahil@yahoo.fr
[2] Faculté de physique, Laboratoire physique théorique, Université des sciences et de la technologie Houari Boumediene *USTHB* B.P.32, El Alia, 16111, Bab Ezzouar, Alger, ALGERIA

Introduction:

Alloys based on the Fe-Al phases matrix represent a promising class of intermetallics with great potential for substituting stainless steels for applications at elevated temperatures. This is due to their high strength, excellent resistance against corrosion, low cost of the constituents and a lower density compared to that of many other iron-based materials. The principal shortcoming is their pronounced brittleness at ambient temperature which has been tried to be overcome by micro and macro alloying. Among the elemental addition are Zr and Nb that form intermetallics compounds named Laves phases.

The aim of this is to use ab initio calculations (with the (PP) Pseudopotential method) to give new insights on structural and thermal properties of binary and ternary C15-Laves Fe_2(Zr,Nb) alloys. The temperature effects have been obtained using the quasi-harmonic Debye model exploiting the total energy calculations of the PP method.

Compund	*Cell parameter a_0 (Bohr)*	*Bulk Modulus B (GPa)*
Fe_2Zr	13.347	139.5
$Fe_2(Zr_{0.75}Nb_{0.25})$	13.252	143.2
$Fe_2(Zr_{0.5}Nb_{0.5})$	13.152	152.3
$Fe_2(Zr_{0.25}Nb_{0.75})$	13.046	160.2
Fe_2Nb	12.940	166.1

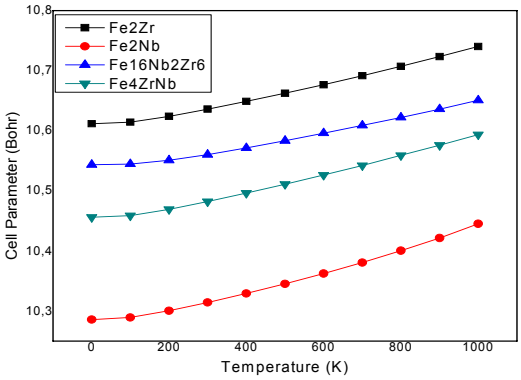

The main results show that:
1) The structural properties obey to the Vegard's law, meaning that Fe_2(Zr, Nb) are quite ordered alloys independent of the Zr/Nb ratio**.**
2) The use of the quasi-harmonic Debye model was successfully applied to determine the thermal properties of the Fe_2(Zr, Nb) alloys in the 0-1000 K temperature range. The effect of temperature on bulk modulii and volume expansions is important in Fe_2Nb while lesser in Fe_2Zr.

References:

A. Kellou, T. Grosdidier, C. Coddet, H. Aourag, (2005). acta materialia, Volume 53, Issue 5
F. Moret, R. Baccino, P. Martel, L. Guetaz, (1996), Journal de physique IV, Vol6,.
J. Adamiec, M. Kalka, (2006), Journal of Achievements in Materials and Manufacturing Engineering, Volume 18, Issue1-2.
L.Rabahi, Mémoire de Magister, (2010), USTHB Alger,
M.A.Blanco et al(2004), Computer Physics Communications I58.
M. Martinez Celis, Thèse de Doctorat, (2007), Institut National Polytechnique de Toulouse.

Ab initio calculations and structures properties correlation of SiO2 polymorphs

H. Sediki[1], A.Krallafa[1]

[1]Faculté des Sciences, Laboratoire LCPMM, Université D'Oran Es-sénia,
Campus Pr TALEB Mourad (ex-IGMO) niveau 1et2 département de chimie, 31000 Oran, ALGERIA
sedikih@yahoo.fr

Abstract: A series of static calculations and ab initio molecular dynamics in high temperature and high pressure have been undertaken to investigate the structural, electronic and optical properties of Si-O systems namely quartz, cristobalite and stishovite.
In this context, density functional theory DFT approach is used with different functional as the local density approximation LDA and generalized gradient GGA, based on the use of two types of pseudopotentials, ie the pseudopotential Ultrasoft and the standard norm-conserving.
Our study allowed us to determine from the geometry optimization, the most stable structure of these materials and their corresponding lattice parameters.
Our study allowed us to determine from the geometry optimization, the most stable structure of these materials and their corresponding lattice parameters.
The electronic properties such as densities of states, band structures have been described. As for the optical properties we became interested in determining the complex dielectric function that aims primarily to calculate the dielectric constant of the material and the optical gap.
The results obtained are in good agreement obtained by other previous work.

Table 1: Structural parameters, energies and charges for silica polymorphs.

Lattice parameters (A°)	Quartz Alpha	Quartz Beta	Cristobalite -high	Cristobalite -low	Stishovite
a	5.014132	5.025651	7.328912	5.177410	4.180847
b	5.014132	5.025651	7.328912	5.177410	4.180847
c	5.502759	5.497988	7.328912	7.295635	2.647977
Energy (eV)	-2972.07	-2972.05	-7925.56	-3962.81	-1979.67
Charge	Si 2.39	2.40	2.44	2.44	2.03
	O -1.20	-1.20	-1.22	-1.22	-1.01

Table 2: Energies bands of silica polymorphs.

Band gap (eV)	Quartz Alpha	Quartz Beta	Cristobalite-high	Cristobalite-low	Stishovite
ΓV – Γc	6.2119	6.2123	5.5894	5.5648	5.884

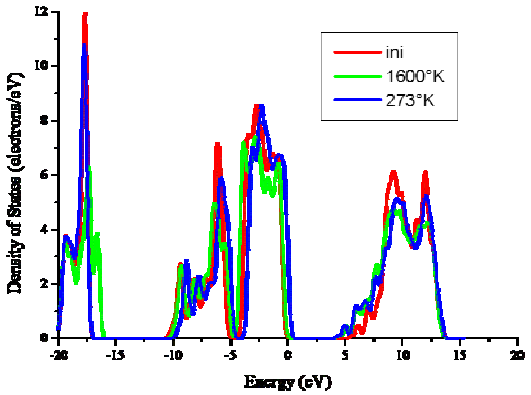

Figure 1 : Densities of states DOS for quartz α.

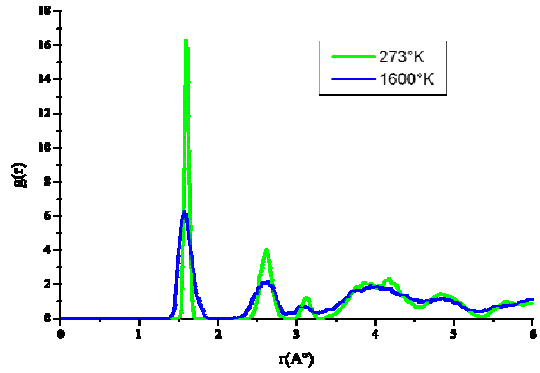

Figure 2 : Radial distribution functions g(r) for quartz α.

References:

S.Munetoh,T.Motooka,K.Moriguchi,A.Shintani (2006) Computational Materials Science 39 (2007) 334-339.
N.Garg and S.M.Sharma (2007) Journal of Physics:Condensed Matter 19 (2007) 456201.
K.Yamahara,K.Okazaki,K.Kawamura (2001) Journal of Non-Crystalline Solids 291 (2001) 32-42.
V.N.Sigaev,E.N.Smelyanskaya,V.G.Plotnichenko,V. V.Koltashev,A.A.Volkov,P.Pernice (1999) Journal of Non-Crystalline Solids 248 (1999) 141-146.
E.Görlich (1982) Ceramics International Vol 8 n 1 1982.

Structural and thermoelastic properties of the B2–YX (X=Cu, Mg and Rh) intermetallic compounds

A. Sekkal[1], A. Benzair[2], H. Aourag[1], H.I. Faraoun[1], G. Merad [1]

[1] Laboratoire d'Etude et Prédiction de Matériaux, Unité de Recherche Matériaux et Energies Renouvelables, Département de Physique, faculté des Sciences, Université Abou Bekr Belkaid B.P 119, 13000 Tlemcen, ALGERIA
asamad2002@yahoo.fr
[2] Département de Physique, faculté des sciences, Université Djillali Liabes. 22000 Sidi Bel Abbés, ALGERIA

Abstract

The study of rare earth intermetallic compounds have received great attention of the scientific world because of their unique mechanical properties, such as high tensile strength, good ductility, high corrosion resistance and thermal stability.

A new class of ductile intermetallic compounds was recently discovered. These intermetallics are made of equal atomic ratios of a rare-earth element and late transition metal or early p-element. The intermetallics have CsCl-type (B2) structure, of which the primitive unit cell is cubic, with one sub-lattice site occupying the corners of the cube and the other occupying the center of the cube. These intermetallics have high ductility and high fracture toughness at room temperature, with several of them exceeding a remarkable value of 21% tensile strain. The reason for the high ductility and strength is not entirely clear.

Studies indicate that the elastic behavior of these materials is significantly more isotropic than ''typical'' B2 intermetallics, and their bonding is less covalent than, for example, NiAl which also has B2 structure.

To understand some of the physical properties of these compounds **we** have investigated the structural, elastic and thermal properties of intermetallic B2–YX (X=Cu, Mg and Rh) compounds using the full-potential augmented plane wave (FP-LAPW) method, within the generalized gradient approximation. The calculated structural parameters, the bulk modulus and its pressure derivative are in agreement with the available data. The independent elastic constants and their related properties satisfy the requirement of mechanical stability, indicating that our compounds could be stable. Thermal effects on some macroscopic properties of YCu, YMg and YRh are predicted using the quasi-harmonic Debye model in which the lattice vibrations are taken into account. For the first time, the numerical estimation of the thermal properties are performed for these compounds and still await experimental confirmations.

Reference

A.M. Russell, Z. Zhang, K.A. Gschneidner Jr, T.A. Lograsso, A.O. Pecharsky, A.J. Slager, D.C. Kesse, Intermetallics 13 (2005) 565.

A. Sekkal, A. Benzair, H. Aourag, H.I. Faraoun, G. Merad. *Structural and thermoelastic properties of the B2–YX (X=Cu, Mg and Rh) intermetallic compounds.* Physica B: Condensed Matter, Physica B 405 (2010) 2831–2835

G. U˘gur, M. C- ivi, S- U˘gur, F. Soyalp, R. Ellialtio˘glu, J. Rare Earths 27 (4) (2009) 661.

I.R. Shein, A.L. Ivanovskii, Scr. Mater. 59 (2008) 1099.

J.R. Morris, Yiying Ye, Yong-Bin Lee, et al., Acta Mater. 52 (2004) 4849.

K. Gschneidner, A. Russell, A. Pecharsky, J. Morris, Z. Zhang, T. Lograsso, et al. Nat. Mater. 2 (2003) 587.

X. Tao, Y. Ouyang, H. Liu, Y. Feng, Y. Du, Z. Jin., Solid State Commun. 148 (2008) 314.

Determination of the density of states (DOS) of the amorphous semiconductors using Laplace Technics

F. Serdouk[1], M. L. Benkhedir[2]

[1,2] Laboratoire de Physique Appliquée et Théorique L P A T, Université de Tébessa, ALGERIA
[1]iserdouk@yahoo.fr
[2]benkhedir@gmail.com

Introduction: Spectroscopic techniques for mapping out localized-state distributions are of fundamental importance for understanding of electronic properties of amorphous semiconductors. An experimental technique often used for this purpose is that of transient photoconductivity (TPC). A method for the determination of density of states from TPC using Laplace transforms is described

Theory: The basic multiple trapping equations in case of monomolecular recombination are then

$$\frac{dn}{dt} = -\sum \frac{dn_i}{dt} - \frac{n}{\tau} + n_0 \delta(t), \qquad (1)$$

$$\frac{dn_i}{dt} = \omega_i n - \delta_i n_i, \qquad (2)$$

Theses equations can be solved using Laplace transforms. If we start with the Laplace transforms

$$n(s) = \int_0^\infty n(t) e^{-st} dt, \qquad (3)$$

We obtain

$$n(s) = \frac{n_0}{s + \frac{1}{\tau} + s\int_0^{E_f} \frac{\sigma\nu g(E)}{s + \nu e^{-\frac{E}{k_B T}}} dE}. \qquad (4)$$

Here, $g(E)$ is the localized-state distribution of amorphous semiconductors in question. With some algebra methods, we arrived at the theoretical form of $g(E)$ as follows

$$g(E) = \frac{1}{\sigma\nu k_B T}\left[\frac{d}{d\ln s}\left(\frac{I(0)}{I(s)}\right) - s\right]. \qquad (5)$$

Results The Laplace transform of $I(t)$ can be carried out by simple numerical integration over N sampling points

$$I(s) = \sum_{i=2}^{N-1}\left[I(t_{i+1})e^{-st_{i+1}} + I(t_i)e^{-st_i}\right]\frac{t_{i+1} - t_i}{2} \qquad (6)$$

The localized-state distributions can be obtained from Eq. (5). The physical quantities used in the computation were

$$\sigma\nu = 10^{-7}\ cm^3/s\ ;\ \nu = 10^{12}\ s^{-1}$$

We applied the LT method to the determination of the localized-state distribution in a-Se (Amorphous Selinium). The fig. 1 shows the TPC following flash illumination of a coplanar sample of a-Se. Fig. 2 shows the calculated localized-state distribution in some temperature.

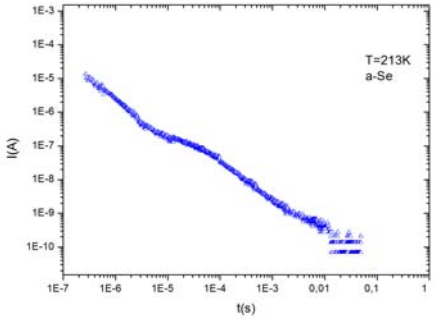

Fig. 1: Transient photocurrent of a coplanar sample of a-Se.

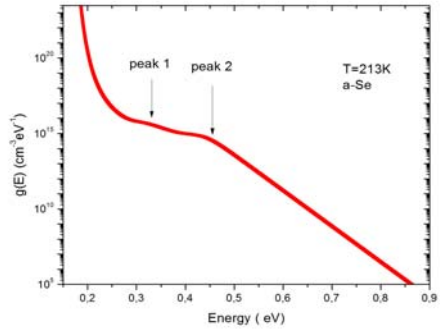

Fig. 2: The localized-state distribution $g(E)$ as computed from the data in the Fig. 1

References:

Naito. H, Nagase. T, Ishii. T, Okudo. M, Kawaguchi. T and Maruno. S, *Journal of Non-Crystalline Solids*, 198-200 , 1996.

Benkhedir. M L, Brinza. M, Adriaenssens. G and Main. C, *J. Phys.: Condens. Matter* 20, 21520, (2008).

COMPUTATION AND PREDICTION OF EXCHANGE AND CORRELATION ENERGY IN DENSITY FUNCTIONAL THEORY USING DATA MINING METHODS

N.Settouti[1], H.Aourag[1]

[1] Laboratory of study and prediction of materials (LEPM)
Unity of Renewable Energies and Materials, Department of Physics (U.R.M.E.R)
Faculty of sciences, University Abou Bekr BELKAID Tlemcen ALGERIA
B.P. 119 - 13000 Tlemcen - ALGERIA
nadera_settouti@ymail.com

Abstract

Data mining is predicted to be "one of the most revolutionary developments of the next decade " [2] , " it is the process of discovering meaningful new correlations, patterns and trends by sifting through large amounts of data stored in repositories, using pattern recognition technologies as well as statistical and mathematical techniques. " [1]

In this work we study the exchange and correlation energy in density functional theory, using data mining tools. As we know the exchange and correlation energy is a key quantity in DFT, it is very important in conception of new materials.

Principal component analysis (ACP), and partial least squares regression methods, computing techniques, were used here to predict the exchange and correlation energy of a 194 binary materials, which prove that the regression PLS is a powerful tool for prediction of materials.

Keywords: Exchange and correlation energy, density functional theory, data mining, principal component analysis, partial least squares regression.

References:

Daniel T. Larose, (2005), " Discovering knowledge in data : an introduction to data mining ", John Wiley & Sons, Inc,.
The online technology magazine *ZDNET News* (February 8, 2001).

First-principles calculations of Mo/ZrC interface and Re alloying effects on adhesion

H. Si Abdelkader[1], H. I. Faraoun[1]

[1]Laboratoire d'Etude et Prédiction des Matériaux. LEPM-URMER. Université A. Belkaid, Tlemcen. ALGERIA
shhayet@yahoo.fr , h_faraoun@mail.univ-tlemcen.dz

Abstract:
During the last decade, the metal/ceramic interface has been widely studied, as well on the experimental point of view as on the theoretical one, due to its numerous applications in coating, heterogeneous catalysis, microelectronics, thermal barriers, corrosion, and fabrication of composite materials, etc [5]

A particular case of metal/ceramic interface of interest in this study is cermets interfaces, those cermets consist of a ceramic material (such as carbides or carbonitrides) with a metal binder. Most of the time, the ceramic provides high hardness while the metal provides the toughness. First-principles density functional theory calculations have been used to study the adhesion of the cermet interfaces, Dudiy and Lundqvist [2-4] studied the Co/Ti(C,N) interfaces and Christensen et al. [1] compared Co/WC and Co/TiC interface adhesion. The present work considers another important situation of cermet interfaces, in particular the effect of Re alloying on adhesion of Mo/ZrC cermet.

Although Mo did wet the refractory carbides ZrC but for certain cermets, it is preferable to use additive elements which can improve wettability. Microscopic examination of the metal/ceramic interfaces showed that Mo-40%Re/ZrC has highly desirable wetting and solubility characteristics for making cermets [6].

In this work, we use first-principles density functional pseudopotential calculations to study the adhesion and the interfacial electronic structure of Mo(110)/ZrC(100) interface.

The work of adhesion (W_{ad}) was calculated for two different stacking sequences with respect to the ZrC surface structure and it was found that Mo atoms prefer to bind above the C atoms and the interfacial Mo and C atoms form strong covalent bonds. In addition, we examine the effects of Re alloying element at the interface, and find that Re atom addition improves the adhesion, as shown in table 1, the work of adhesion increases with 0.67 J/m^2, but does not affect the nature of the interface bonding.

Table1: Change in W_{ad} and d_0 due to the substitutional incorporation of Re at the Mo surface

	Segregation atom	***d0 (Å)***	***Wad (J/m2)***
Mo/ZrC interface	Clean	1.66	3.67
	Re	1.63	4.34

References:

Christensen, M., Dudiy, S. V., Wahnstrom, G., *Phys. Rev. B* 65 (2002) 045408.
Dudiy, S. V., Hartford, J., B. I. Lundqvist, B. I., *Phys. Rev. Lett*. 85 (2000) 1998.
Dudiy, S. V., Lundqvist, B. I., *Phys. Rev. B* 64 (2001) 045403.
Dudiy, S. V., Surf. Sci. 497 (2002) 171.
Finnis MW. *J Phys: Cond Matter*. 8 (1996) 5811.
Manning JR, C. R, Stoops, R. F, *J. Am. Ceram. Soc*. 51 (1968) 415.

Theoretical Study of the Structural and Electronic Properties of Luteolin

K. Smail[1], K. Ouadah[1], N. Tchouar[1]

[1]Faculté des Sciences, Laboratoire LAMOSI, Université des Sciences et Technologie d'Oran USTO
B.P.1505, Oran, 31000, ALGERIA
smailkh@yahoo.fr

Abstract:

Luteolin (3', 4', 5, 7-tetrahydroxyfavone) is one of the more common flavones. It is present in many foods including parsley, celery, peppers, olive oil, rosemary, lemons, and thyme. It play an important role in the human body as an antioxidant, a free radical scavenger, an anticancer, an agent in the prevention of inflammation and an immune system modulator.

Despite the numerous experimental works on flavones, only a few theoretical studies have been reported to date on luteolin [1-2]. To gain insight into the structural and electronic properties of luteolin, we report here a theoretical investigation of this system in vacuo.

The structural properties of luteolin in vacuo are studied with ab initio methods. Molecular structures have been optimized by MP2 and DFT using different functionals and basis sets. The frontier molecular orbitals and the HOMO–LUMO gap at the different geometries of luteolin have been computed and analyzed.

References:

Leopoldini, M., Pitarch, I., Russo, N., Toscano, M. (2004), *Journal of Physical Chemistry A,* 108, 92–96.

Van Acker, S., de Groot, M., van den Berg, D.J., Tromp, M., Donne-OpdenKelder, G., Van der Vijgh,W., Bast, A. (1996), *Chemical Research in Toxicology*, 9, 1305–1312.

Effective interaction and structure of charge-stabilized colloidal suspension

F.Smain[1], F. Ould-Kaddour[1]

[1]Faculté des Sciences, Laboratoire de physique théorique, Université Aboubakr Belkaid de Tlemcen.
PB 119 Tlemcen (13000) ALGERIA
fatiha_smain@yahoo.fr

Abstract: Charge-stabilized colloidal suspension exhibit rich thermodynamic phase behaviour and tuneable material properties that are the bases of many industrial, technological and biological applications. In this paper, we determine the radial distribution function for charge-stabilised colloidal suspensions for various volume fractions and various salt concentrations by mean of Ornstein Zernick Integral Equation Theories (IET) from a previous knowledge of the interactions (Levin Y 2004) between pair of particles. The pair potential is calculated using the Derjaguin-Landau-Verwey-Overbeek(DLVO) theory which reduces the original multicomponent colloidal suspension (formed by macroions -colloids-, microions -conterions and salt ions in case of added electrolyte- and solvent molecules) to an effective one formed by charged macroions dressed by strongly correlated microions. The DLVO theory (Derjaguin B and Verwey E J W) is based on the Poisson-Boltzmann (PB) equation of microions written in the framework of a given model (Dobnirar. J) (Cell, Jellium or modified Jellium model). The PB equation gives information on the pair interactions between macroions and provides an approximate equation of stat of the suspension. Interaction potential utilised as input in the IET scheme (Lomba. E) is effective (Trizac E 2002) and depend on the renormalized charge and the effective screening parameter. By neglecting the attractive part of the DLVO potential (the case of highly charge colloidal suspensions), the resulting interaction is repulsive and takes the Yukawa form. Because the interaction potential can be density-dependent, by mean of the screening parameter, the use of IE scheme must be applied using serious precautions. In our case we utilise a self integral equation theory, the so-called *double Self Consistent Verlet Modified* closure (SC2VM) which was adopted for the first time by us to solve the thermodynamic consistency(Smain F 2010) problem of charge colloidal suspensions. The SC2VM is a parametric form of the Verlet Modified closure considered as one of the most accurate closures for repulsive systems. The use of this closure can be justified by the important repulsions between highly charged like-colloidal surfaces.

We find that in the salt free case, when the screening is dominated by the counterions, the interaction potential is density-dependent, The consistency criteria is fixed by comparing the osmotic isothermal compressibility calculated both from IET and from PB equation (Trizac E 2007). In highly salt concentration, the screening is dominated by the salt ions, therefore the density dependence of the potential is week and the potential behaves like a hard core potential, in this case the standard IET scheme can directly be applied. The comparison of the renormalized parameters with experimental data show that the cell and the Jellium models reproduce only qualitatively the dance and the dilute suspensions, this is due to the fact that these imperial models neglect the effect of the correlation of macroions on the structure. In order to inject a good pair potential which take into account colloidal correlations in the IET we utilised the modified Jellium model (Castañeda-Piegro R).

Keywords Charge colloidal suspension, Structure, Effective interactions, Integrals Equations Theories.

References:

Castañeda-Piegro R, Rojas-Ochoa L F, Lobaskin, V and Mixteco-Sanchez C. (2006), Phys, Rev, E 74, 051408,2006.

Derjaguin B V and Landau L. (1941), Acta Physicochimica 14, 633.

Dobnirar. J, Castañeda-Piegro R, Grünberg H and Trizac E. (2006). New. J. Phys 8, 277,2006.

Levin, Y. (2004) Brazilian Journal of Physics 34, 1158 (2004).

Lomba. E, Alvarez M, Lee LL and Almanza N G. (1995) J. Chem. Phys 104, 41801995.

Smain F and Ould-Kaddour F. (2010) A macroion correlation effect on the structure of charged stabilized colloidal suspensions: A self integral equation study. In press in Colloid and polym Scien.

Trizac E, Boquet L, Aubouy M. (2002) Phys. Rev. Lett 89, 248301 17, 2002.

Trizac E, Dobnikar J, Belloni L, Von Grünberg H H and Castañeda-Piegro R. (2007) Phys. Rev. E 75: 011401, 2007.

Verwey E J W and Overbeek J T G (1948) Theory of the Stability of Lyophobic Colloids Elsevier, Amsterdam.

A Comparaison of Experimental and Theoretical Optical Constants of the ZnxCd1-xO (x=1-0.6 - 0.4 - 0) Thin Films

H.Tabet-Derraz[1], M. Boukhalfa[1], N. Benramdane[1], J-M. Frigerio[2]

[1]laboratoire d'Elaboration et Caractérisation des Matériaux, Département d'Electronique, Université Djillali Liabès, Sidi Bel Abbès, 22 000, BP. 89, ALGERIA
[2]Institut des Nano Sciences de Paris, Université Pierre et Marie Curie - Paris 6, CNRS, UMR 7588, Campus Boucicaut, 140 rue de Lourmel, 75015 Paris, FRANCE
htabet@univ-sba.dz
htabet05@yahoo.fr

Abstract:
In this work, we expose the fact that when we mixed two pure binary materials having different structure we can obtain a new material, not an alloy but a composite one. Those two pure binary materials are the ZnO with an hexagonal würtzite structure and the CdO with cubic (NaCl) structure. They are obtained by the spray pyrolysis technique at a temperature of deposition of 420°C by using respectively $Zn(NO_3)_2.6H_2O$ and $Cd(NO_3)_2.4H_2O$ solutions at 0.1 Mol/l. To obtain the $Zn_xCd_{1-x}O$ we mixed the solution respectively at 40 and 60% to obtain the $Zn_{0.4}Cd_{0.6}O$ and $Zn_{0.6}Cd_{0.4}O$. Them spectral RX diffraction indicate the co existence of the peacks of the ZnO and CdO materials with the grain size average of about 26.75 nm estimated from the preferential orientations (002) and (200) respectively. The evolution of the optical parameters of the $Zn_xCd_{1-x}O$ can be calculated from the measurements of the transmittance and the reflectance of the all samples and by using just of the ZnO and CdO in a model of the approximation of the effective medium (Bruggeman). From the evaluation of the dielectric function we can deduce the refractive index n around 1.7 and the extinction coefficient k and calculate optical properties of the obtained films. The results of the model are in agreement of the experimental ones as the gaps of the materials which vary between 2.26 and 3.26 eV.

Keywords:
Spray pyrolysis, binary materials, composites, model of Approximation of the Effective Medium, optical parameters.

Numerical Simulation of Thermodynamics, Structural and Transport Properties of Liquid Para-Hydrogen by the Quantum Molecular Dynamics

N. Tchouar[1], K. Bentayeb[1], M. Benyettou[1]

[1]Faculté des Sciences, Laboratoire LAMOSI, Université des Sciences et Technologie d'Oran USTO
B.P.1505, Oran, 31000, ALGERIA
lamosi2002@yahoo.fr

The hydrogen energy system represents a major challenge, scientific, environmental and economic. Liquid hydrogen consists of 99.79% parahydrogen, 0.21% orthohydrogen. Liquid para-hydrogen (p-H_2) is a typical quantum liquid, which exhibits strong quantum effects especially at low temperature. The objective of this research is to review the reliability of the method of molecular dynamics, namely the correlation of different thermodynamic properties calculated of para-hydrogen in liquid state at different state points in the phase diagram. Several fundamental transport properties (the radial distribution function, the total energy, pressure, potential energy, enthalpy, the diffusion coefficient and shear viscosity.) of liquid para-hydrogen (p-H_2) at different state points have been numerically evaluated by means of the quantum dynamics simulation called the Feynman-Hibbs molecular dynamics (FHMD) [1].

For comparison, classical molecular dynamics (MD) simulations have also been performed under the same condition. In accordance with the previous path integral simulations, the calculated static properties of the liquid agree well with the experimental results [2]. For the diffusion coefficient and shear viscosity, the FHMD predicts the values closer to the experimental ones though the classical MD results are far from the reality. The agreement of the FHMD result with the experimental one is especially good for the shear viscosity with the difference less than 5%.

References:

Voth , G. A., (1996) *New Methods in Computational Quantum Mechanics and Dynamics*, Adv. Chem. Phys, Wiley, New York.

Yoshiteru, Y., Kenichi, K., (2003) *Journal of Chemical Physics*, 119, 18, 2003

Simulation and optimization of photovoltaic parameters in single and tandem junction thin film silicon solar cells

B. Zebentout[1], Z. Benamara[1], Y. Bourezig[2], T. Mohammed-Brahim[3]

[1]Laboratoire de MicroElectronique Appliquée, Université Djillali Liabès, Sidi Bel Abbès (22000), ALGERIA
b_zebentout@yahoo.fr
[1]Laboratoire d'élaboration et de Caractérisation de Matériaux, Université Djillali Liabès, Sidi Bel Abbès (22000), ALGERIA
[2]Groupe Microélectronique, IETR, Université de Rennes 1, 35042 Rennes Cedex, FRANCE

Introduction: The actual aim of researchers is focusing to performing the efficiency of silicon solar cells based on amorphous materials. An important design that must give a good performance is the tandem solar cell (double or triple PIN junction).Optical and electrical analysis of a micromorph silicon solar cell is carried out using numerical simulations with AMPS-1D software intended for non crystalline materials simulation.We investigated the influence of various parameters for each layer top cell (a-Si: H) and bottom cell (µc-Si:H) in particular the thickness, the doping level and the Density of states (DOS).

The simulation analysis confirms that the combination of an a-Si:H PIN top cell and a µc-Si:H PIN bottom cell is the best structure to profit from a large range of the solar spectrum with a significantly higher stable efficiency compared to single a-Si:H PIN and µc-Si:H PIN cell.

The performances of micromorph cell obtained from simulation agree very well with the experimental results and confirm the importance of the combination a-Si/µc-Si as a double junction solar cell [1].

Simulation results: During our simulation under AMPS 1D[2], we have take fixed conditions of illumination 'One Sun' with the standard AM1.5G and the ambient temperature of 300 K. The model DOS (density of states) is used for the modeling of the amorphous materials which possess a strong density of defects such as the amorphous silicon and the microcrystalline silicon. We did not take into account the defects at the interfaces between various materials.

In tandem applications, we have chosen a-Si top cell with following thickness layer:

- Thinner layer a-Si doped p (L = 10 nm)
- Intrinsic layer a-Si, the thickness is 250 nm
- Thinner layer a-Si :H doped n (L' = 20 nm)

The microcrystalline cell is mainly constituted by:

- A film µc-Si doped p of thickness of the order of 30 nm with Eg = 1.4 eV
- An intrinsic µc-Si film with Eg = 1.4 eV
- A material µc-Si doped n of thickness of 30 nm approximately Eg = 1.4eV.

In accord with the importance which must be taken to the density of current in a tandem cell, in the follow work of simulation we have taken 900 nm thick intrinsic layer of the bottom cell.

e
r

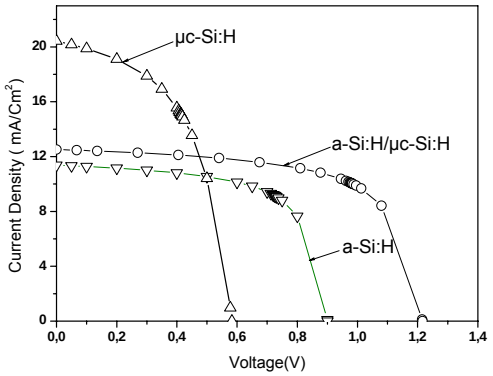

Figure1: Illuminated J-V characteristic of a-Si, µc-Si and combination a-Si/µc-Si solar cell.

The corresponding performances are mentioned in the following table:

Table 1: Photovoltaic parameters of a-Si, µc-Si single junction and a-Si/µc-Si tandem solar cell.

Structure PIN	a-Si:H	µc-Si:H	a-Si:H/µc-Si:H
Jsc (mA/cm^2)	11.675	20.436	12.58
Voc (V)	0.894	0.583	1.21
η(%)	5.968	6.244	9.85
FF (%)	57.2	52.4	64.75

References:

F. Meillaud, A. Shah, C. Droz, E. Vallat-Sauvin and C. Miaza, '*Efficiency Limits for Single-Junction and Tandem Solar Cells*', Solar Energy Materials and Solar Cells, Vol. 90, N°18-19, pp. 2952 – 2959, 2006.

H. Zhu, A.K. Kalkan, J. Hou, S.J. Fonash, '*Applications of AMPS-1D for Solar Cell Simulation*', National Center for Photovoltaics (NCPV), 15th Program Review Meeting, AIP

First principle prediction of half-metallic ferrimagnetism in the Heusler alloys Mn2TiZ(Z=Al,As,Bi,Ga,Ge,Sb,Si,Sn) in high ordered structure

H. Zenasni [1,2] , H. Faraoun[1], H. Aourag [1]

[1]LEPM, URMER, Department of Physics, University Abou Bakr Belkaid,Tlemcen 13000, ALGERIA
zhhocine1@hotmail.com

Abstract

Half-metallic ferromagnetisms(HFM), which have only one spin channel for conduction at the Fermi level, have attracted more and more attentions because of their potential applications in spin-based electronic devices.

The HMF has been found in many materials, for example in ferromagnetic metalic oxides, dilute magnetic semiconductors, binary transition metal pnictides, calcogenies with zinc-blende structure and Heusler compounds [1]. Since their first discovery by de Groot et al.[2]. Among them, half-metallic Heusler alloys are exepted to play a key role in realistic applications du their high Curie temperatures and their structural compatibility with the widely used binary semiconductors cristallizing in zing-blende structure.

Although the research on HMF is intense, half metallic ferrimagnetic materials are much more desirable than their ferromagnetic conterparts in magneto-electronic applications. This is mostly du to the fact that the small value of the total magnetic moment in these systems provides additional advantages, they do not give rise to strong stray fields in devices ans are less affected by external magnetic fields. Some perfect Heusler compounds like FeMnSb and Mn2Val are predicted to present half metallicity in conjunction with ferrimagnetis[3]

Using the first-principles plane wave pseudopotential method based on density fonctional theory and within the generalized gradient approximation framwork, we have investigater the electronic and magnetic structures $L2_1$ of the heusler alloyn Mn2TiZ (Z=Al, As, Bi, Ga, Ge, Sb, Si, Sn) with high ordered structure.

Table 1: The calculated equilibrium lattices of ferrimagnetic phase and spin magnetic moments.

Compound	*a(Å)*	μ_B
Mn2TiAl	5.967	3.06
Mn2TiAs	5.820	0.99
Mn2TiBi	6.201	3.06
Mn2TiGa	5.945	1.99
Mn2TiGe	5.875	1.02
Mn2TiSb	6.073	1.99
Mn2TiSi	5.782	2.05
Mn2TiSn	6.135	5.13

References

Heusler, F. ;Starck, W. ;Haupt, E. Verh Dtsch Phys Ges 1903, 5,219.

R.A. de Groot, F.M. Mueller, P.G. van Engen, K.H.J. Buschow, Phys. Rev. Lett. 50 (1983) 2024.

[R.A. de Groot, A.M. van der Kraan K.H.J. Buschow, J. Magn. Mater. 61 (1986)330.

Electronic structure of the tetragonal ternary iron arsenide $BaFe_2As_2$: Contribution of itinerant Fe 3*d*-states to the Fermi Level

R. Zine El Kelma[1], Z. Dridi[1], B. Bouhafs[1]

[1]Modelling and Simulation in Materials Science Laboratory
Djillali Liabès University of Sidi Bel-Abbès, Sidi Bel-Abbès 22000, ALGERIA
rachida.kelma@yahoo.fr

Abstract: Based on first-principles FP-LAPW calculations, we have investigated the electronic structure of the tetragonal ternary iron arsenide $BaFe_2As_2$ in the non-magnetic state using the local density approximation (LDA) and in the ferromagnetic state using the local spin density approximation (LSDA) and the LSDA+U (with Hubbard-U corrections). The obtained results reveal that from a structural point of view, the ferromagnetic case studied using LSDA is similar to the non-magnetic case. Using the LSDA+U, the Fe-3*d* states are located in the valence bands for majority spin, and around the Fermi level for minority spin. The electronic structure is characterized also by hybridization between Fe-3*d* and As-4*p* states which is responsible for covalent Fe-As bonding.

Introduction: The Superconductivity in iron-based oxyarsenides has recently become a hot topic in the condensed-matter physics community. The discovery of high-temperature superconductivity in oxypnictide phases, prototype LaFeAs(O,F) by Singh has sparked widespread interest in establishing the physical properties of these materials and especially the mechanism for superconductivity. de Jong et al. have presented high-resolution photoemission data taken with hard x-ray and VUV photon beams on single crystals of the undoped parent compound of the electron- and hole-doped pnictide high-temperature superconductor, $BaFe_2As_2$. From the line shape of the core levels it could be deduced that the near-EF electronic states are primarily of itinerant Fe 3*d* character.

Calculation: The calculations are based on the density-functional theory in the local spin-density approximation (LSDA) with additional Hubbard correlation terms describing on-site electron–electron repulsion associated with the 4*f* narrow bands (LSDA+U approach).

We first calculate the total energy as a function of the volume per formula unit for the ferromagnetic and anti-ferromagnetic states of $BaFe_2As_2$ compound (Fig. 1). We find that for all systems the anti-ferromagnetic phases have lower energies than the ferromagnetic phase. To find the ground state, several initial spin configurations were tried. In all cases, spin polarization of final configurations was nonvanishing, which demonstrates the presence of stable magnetic moments.

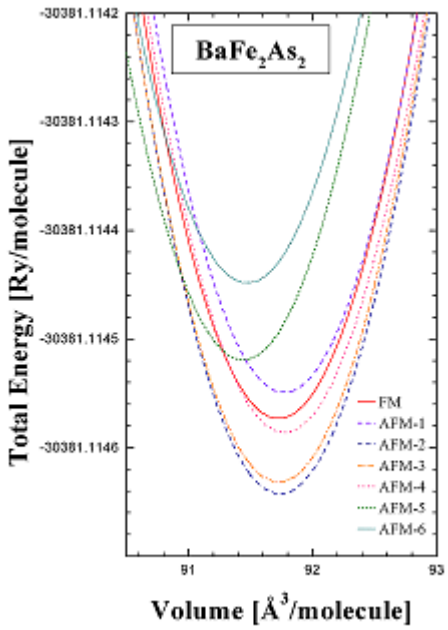

Figure 20: Total energy versus volume for $BaFe_2As_2$ in different magnetic configurations.

References:

Singh, D. J. (2008) Electronic structure and doping in $BaFe_2As_2$ and LiFeAs: Density functional calculations, *Physical Review B*, 78, 094511

de Jong, S., Huang, Y., Huisman, R., Massee, F., Thirupathaiah, S., Gorgoi, M., Schaefers, F., Follath, R., Goedkoop, J. B. and Golden, M. S. (2009) High-resolution, hard x-ray photoemission investigation of $BaFe_2As_2$: Moderate influence of the surface and evidence for a low degree of Fe 3*d*–As 4*p* hybridization of electronic states near the Fermi energy, *Physical Review B*, 79, 115125

Etude des résonances plasmons dans les Nano-fils en Ag

M.Z. Chekroun[1], L.Salomon[2], G. Bassou[1]. M. Youcef Mahmoud[1], A. Taalbi[1]

[1] Laboratoire de Microscopie, Microanalyse de la matière et Spectroscopie Moléculaire
Université Djillali Liabès de Sidi Bel-Abbès
[2]Groupe d'Optique de Champ Proche
Institut de Carnot de Bourgogne (ICB), UMR CNRS 5209, Université de Bourgogne,
09 Avenue Alain Savary, BP 47870, 21078 DIJON

Dans ce papier nous exposons une étude numérique de la réponse spectrale d'un réseau de nano-fils en Ag de dimension sub-longeur d'onde. L'outil de modélisation numérique utilisé, est la méthode différentielle avec sa nouvelle formulation développée grâce aux remarques de Li ainsi que l'utilisation de l'algorithme 'S-Matrix' **[1]** et le 'Redheffer's star product' **[2]**.

Ces calculs basés sur l'interaction de la lumière incidente avec un réseau de nano- fils, nous ont permit de suivre l'évolution du spectre d'extinction optique en transmission du réseau de nano-fils métalliques en ajustant les paramètres géométriques du réseau ainsi que l'indice du substrat. Les paramètres géométriques considérés sont similaires à ceux utilisés expérimentalement par Schider et al **[3].**

Les résultats que nous avons obtenus numériquement et qui tiennent compte du champ lointain ainsi que du champ proche optique, se sont avérés en bonne concordance avec ceux obtenus expérimentalement par Schilder. Nous exposerons ensuite le diagramme de rayonnement de ces structures nonométriques dans différentes conditions.

M. Nevière et E. Popov, Light propagation in periodic media: differential theory and design, Marcel Dekker, New York, 2003.

J. Tervo et al, *Optics Communications* 198 (2001) 265-272.

[3] G. Schider et al, Optical properties of Ag and Au nanowire gratings. *Journal of applied physics* volume 90, number 8 (2001) 3825 - 3830.

Full-potential study of structural and electronic properties of β-ZrNX (X = Cl,Br and I)

B. Benaffane[1], O. Benhelal[1], A. Chahed[1], A. Mokadem[1], B. Bouhafs[1]
[1]Modelling and Simulation in Materials Science Laboratory (LMSSM), Physics Department,
University of Sidi-bel-Abbes, 22000 ALGERIA

Abstract

The structural and electronic properties of β-ZrNX (X = Cl, Br and I) have been investigated using the full potential linearized augmented plane wave (FP-LAPW) method within density functional theory (DFT). We used the local density approximation (LDA) and the generalized gradient approximation (GGA) that is based on exchange–correlation energy optimization for calculating the total energy. The plane wave cut off of Kmax = 7.0/RMT (RMT is the smallest muffin-tin radius) is chosen for the expansion of the wave functions in the interstitial region while the charge density was Fourier expanded up to Gmax = 12, with special k-points equal to 65.

The equilibrium lattice constant for β-ZrNX (β-ZrNCl, β-ZrNBr and β-ZrNI) compounds agrees well with the experimental and theatricals results. We have investigated the lattice parameters, bulk moduli, band structures, total and partial densities of states, charge densities for β-ZrNCl, β-ZrNBr in the SmSI structure and β-ZrNI in YOF structure are presented. The results show that both ternary compounds possess an indirect and larger. Note, that Our results are in good agreement with theorical and experimental values.

Keywords: DFT, FP-LAPW, GGA, energy gap.

References:

F. D. Murnaghan, Proc. Natl. Acad. Sci. USA, 30, 5390 (1944).
G. K. H Madsen, P. Blaha, K.Schwarz, E. Sjostedt and L. Nordstrom, Phys. Rev. B 64, 195134(2001)
H.J.Monkhorst and J.D.Pack,phys.rev.B13,5188 (1976)
J. P. Perdew, Y. Wang, Accurate and simple analytic representation of the electron-gas correlation energy, Phys. Rev. B, Vol. 45, No. 23, 1992.
J. P. Perdew, K. Burke, M. Ernzerhof, Generalized Gradient Approximation Made Simple, Phys. Rev. Lett. , Vol. 77, No. 18, 1996.
L. Hedin, B. I. Lundqvist, Explicit local exchange-correlation potentials, J. Phys. C: Solid St. Phys. , Vol. 4, 1971.
L.J. Sham and W. Khon, Phys. Rev. 145, 561 (1965).
O.K.Andersen , phys.Rev.B12,3060(1975)
P. Blaha, K.Schwarz, J.Luitz, Wien2K, A Full Potentiel Linearized Augmented Plane Wave Package for Calculating Crystal Properties, Vienna University of Technology, Austria, 2001.
P. Hohenberg and W. Khon, Phys. Rev. 136, B864 (1965).
P. M. Woodward, T. Vogt, JOURNAL OF SOLID STATE CHEMISTRY 138, 207-219 (1998)
R. Juza, J. Hendersen, Z. Anorg. Allg. Chem. 332(1964).159.

Full-potential study of structural and electronic properties of metal nitride halide chlorides, β-MNCl (M = Ti,Zr and Hf)

A. Mokadem[1], O. Benhelal[1], S. Laksari[1], A. Chahed[1], B. Benaffan[1], B. Bouhafs[1]
[1]Modelling and Simulation in Materials Science Laboratory (LMSSM), Physics Department,
University of Sidi-bel-Abbes, 22000 ALGERIA
mokadem_az@hotmail.fr

Abstract

We present first-principals calculations concerning structural and electronic properties of, β-MNCl (M = Ti,Zr and Hf), In is studied by means of fully relativistic full-potential linearized augmented-plane wave (FP-LAPW) calculations within the formalism of the density functional theory(DFT) in the local density approximation (L.D.A) and the generalized gradient approximation (G.G.A) for the exchange correlations functional., with WIEN 2k package.

The equilibrium lattice constant for (β-TiNCl, β-ZrNCl and β-HfNCl) compounds agrees well with the experimental and theatricals results. We have investigated the lattice parameters, bulk modulus, band structures, total and partial densities of states, charge densities for β-ZrNCl, β-ZrNBr and β-ZrNI in the SmSI structure are presented. The results show that both ternary compounds possess an indirect and larger. Note that our results are in good agreement with theorical and experimental values.

Keywords: metal nitride chlorides, DFT, FP-LAPW, GGA, Electronic structure.

References:

A. Ino et al. / Journal of Electron Spectroscopy and Related Phenomena 144–147 (2005) 667–669
D. R Hamann, Phys. Rev. Lett. **212**, 662 (1979).
F. D. Murnaghan, Proc. Natl. Acad. Sci. USA, **30**, 5390 (1944).
G. K. H Madsen, P. Blaha, K.Schwarz, E. Sjostedt and L. Nordstrom, Phys. Rev. B 64, 195134(2001)
H. Kawaji, K. Hotehama, S. Yamanaka, Chem. Mater.9 (1997) 2127.
J. P.Perdew, S. Burke and M. Ernzerhof, *Phys. Rev. Lett.*, **77**, 3865 (1996)
J. P. Perdew, Y. Wang, Accurate and simple analytic representation of the electron-gas correlation energy, Phys. Rev. B, Vol. 45, No. 23, 1992.
J. P. Perdew, K. Burke, M. Ernzerhof, Generalized Gradient Approximation Made Simple, Phys. Rev. Lett. , Vol. 77, No. 18, 1996.
J. R.Chelikowsky and A. Jin, Phys. Rev. B **40**, 9644 (1989).
L. Hedin, B. I. Lundqvist, Explicit local exchange-correlation potentials,J. Phys. C: Solid St. Phys. , Vol. 4, 1971.
P. Blaha, K.Schwarz, J.Luitz, Wien2k, A Full Potentiel Linearized Augmented Plane Wave Package for Calculating Crystal Properties, Vienna University of technology, Austria, 2001
Perdew J. P. and Wang Y. 1992 *Phys. Rev.* B **45**, 13 244
P. M. Woodward, T. Vogt, JOURNAL OF SOLID STATE CHEMISTRY 138, 207-219 (1998)
R. Juza and J. Heners, Z. Anorg. Allg. Chem., 1964, 332, 159.
S.Ya. Istomin et al. Physica C 319(1999)219–228
S. Yamanaka, K. Hotehama, H. Kawaji, Nature 392 (1998) 580.

Vickers Indentation Method used for Elastic Properties Characterization of Porous Silicon Thin Films

K. Rahmoun[1], V. Keryvin[2, 3]
[1]Faculté des Sciences, URMER, Laboratoire L, Université Abou Bakr Belkaid, B.P.119, Tlemcen, 13000, ALGERIA
k_rahmoun@mail.univ-tlemcen.dz
[2]LARMAUR, EA 410, Université de Rennes 1, Campus de Beaulieu, 35042 Rennes cedex, FRANCE
[3]L.I.MA.T.B. EA 4250**,** Université de Bretagne-Sud, Campus de Saint-Maudé,Centre de Recherches Christiaan Huyghens, BP 9211656321 Lorient cedex, FRANCE

Abstract: Porous silicon is studied in recent years potential candidates for low-k applications. This paper reports on micro-instrumented indentation of a porous silicon structure obtained by anodisation of a p type doped (100) silicon substrate in function of the current density. Correlations between mechanical and microstructural properties of the films are discussed.

Keywords: Microindentation, mechanical properties, porous silicon

Experimentation: The porous silicon layers were obtained by anodisation of a highly p-type doped (100) silicon substrate (_ = 0.01_ cm). The electrolyte was composed of HF (27%): H2O (38%) ethanol (35%) during 2mn. The surface of porous silicon samples was observed under a Scanning Electron Microscopy (SEM), a Hitachi 2460N with variable pressure.

The measurements were performed with a Fischerscope H100 XYp micro-indenter (maximum load of 1 N, load resolution of 0.02 mN, depth resolution of 2 nm). Indentation tests consists in continuously applying a load to the specimen with a sharp Vickers pyramid indenter of face angle 136° and continuously monitoring the penetration depth in the sample.

Results and discussion:

Figure1 schows a micrographie picture of the top surface of two porous silicon layer obtained with the current density of 100 and 150mA/cm2. The mechanical properties are strongly influenced by their pore structures, such as porosity, pore size, pore orientation and interconnections between the pores.

The SEM pictures allowed the size and density of pores to be estimated [1]

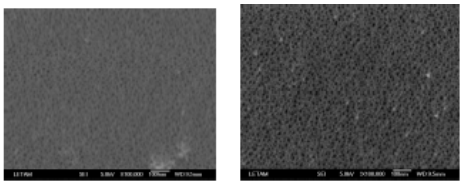

Figure1: SEM micrograph of the top surface of PSE6 and PSE7

Figure2,3, show the evolution of the reduce modulus of elasticity , it increases gradually with the increasing of the indentation depth and increasing applied load. It dependent on the substrate's Young's modulus, because elastic fields have longer ranges than plastic fields,

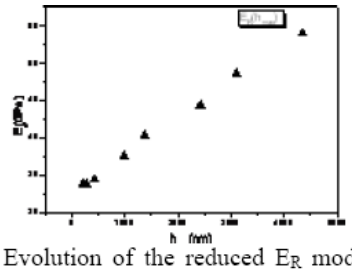

Figure2: Evolution of the reduced E_R modulus on the top surface of PSE6 with the indentation depth h_{max}.

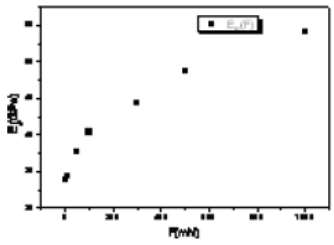

Figure3: Evolution of the reduced E_R modulus on the top surface of PSE6 with the indentation load F.

which are localized [2]. The same results are obtained for PSE7.

Conclusion:

Elastic modulus changes with the penetration depth. The porosity, pores sizes and thickness affect the mechanical properties of porous silicon. The substrate influence on the elastic properties.

References:

Rahmoun, K., Iost, A., Keryvin, V., Guillemot, G., Guendouz , M., Lazhar Haji., M., Chabane Sari , N.E., *Determination of Vickers Microhardness of Oxidized and Nonoxidized Porous Silicon,* Collogue sur l'indentation, **Indentation 2008**, Rennes 7-8 Octobre 2008

Rahmoun, K., Iost, A., Keryvin, V., Guillemot, G., Chabane Sari , N.E. Thin Solid Films 518 213– 221, (2009).

ABSTRACTS

Posters2
Chemistry

Theoretical Study of the Reaction of Rearrangement of 1,3 DIAZA-CLAISEN

S. ABDELKRIM[1], A.BOUYACOUB[1]

[1]Laboratoire de Chimie Physique Macromoléculaire LCPM.
Département de Chimie, Faculté des Sciences.
Université d'Oran Es-Senia. ALGERIA
abdelkrim_soumia@yahoo.fr

Abstract:
The reaction of claisen rearrangement is a sigmatropic reaction discovered in 1912 by Ludwig Claisen [1]. In this rearrangement there is migration of σ bond along a system π. This reaction is concerted where intervenes a state of transition from a cyclic structure to six links.

Figure 1 : Model on the claisen rearrangement

The replacement of the basic heteroatom oxygen (X=O) of a Claisen rearrangement by a nitrogen atom defines the so-called aza-Claisen rearrangement. This reaction presents a great interest in the organic chemistry [2].
We proposed to study the reaction de1,3 diaza-claisen between methyl isocyanate (A) and the azanorbornene (B).
These two reagents lead to two products (C) and (D). The compound (C) is the majority product and results from a nucleophilic attack of nitrogen. The product (D) results from a nucleophilic attack of oxygen. (Figure 2)

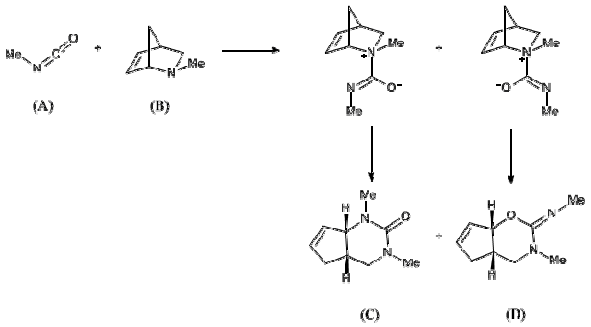

Figure 2: The reaction of methyl isocyanate and azanorbornene

We calculated, in gas phase, the geometrical properties and determined the reaction path for two products using an ab initio calculation MP2/6-31G*.
Our calculations are in good agreement with the experimental data.

References :

Claisen, L. Chem. Ber. 45, 3157, 1912.
Overmann, L. E. Angew. Chem. 96, 565, 1984.

Influence of Amino Acid Side Chain Preceding Azaprolyl Residue on β-turn Stabilization

H.Aliouat[1]; M.Zouikri[1]

[1]Laboratory of Molecular and Macromolecular Physical Chemistry
Faculty of Sciences, Department of chemistry
University Saad Dahlab of Blida. P.O.B 270-09000 Blida
aliouathf@yahoo.fr

Abstract:
One of the more exciting research areas in pharmaceutical and medicinal chemistry has been the design and synthesis of so-called peptidomimetic molecules. These latter are obtained by transforming the information found in natural peptide into low-molecular-weight nonpeptide structure. These compounds are expected to have the same therapeutic effects as natural peptide counterparts, with an added advantage of enhanced metabolic stability, a longer duration of action and high selectivity. Of particular interest has been the substitution in a given natural substrate of dipeptide pattern with a constrained rigidified counterpart that stimulates a so called β-turn. On the many peptide secondary structures, β–turns are at the centre of interest in drug design since they have been identified as bioactive conformations. Among peptides backbone modifications, replacement of α-carbon of an amino acid by a Nitrogen atom to give Azapeptide seems to be a powerful tool to limit conformational flexibility of the native peptide and improve its biological activity.

The Computational studies of For-AzaPro-NH2, Ace-Pro-NHMe, Ace-AzaPro-NHMe, carried out by ab-initio methods HF/3-21G*, HF/6-31G*, B3LYP/3-21G* and B3LYP/3-21G* showed that substitution of (CH)α by a nitrogen atom of proline induced very important local structural changes. The α-nitrogen atom is at the center of a sp3 pyramidal structure with a prochirality. The most important result was obtained with a potential energy surface E=f (φ, ψ) study of For-AzaPro-NH2 with a 30° step. This latter compound showed that unlike proline, the Azaprolyl residue favors a βVI-turn with the residue (i+1) preceding it.
In order to understand typical elements that influence stabilization of β–turn in Azapeptide and since the 3D-arrangement of amino acid side chain is essential for the interaction with recognition receptor, the theoretical studies of a set of Azapeptide model Ace-Xaa-AzaPro-NH2 with (Xaa= Gly, Ala, Phe, Cys) using DFT as calculation method is investigated.

Keywords: Computational chemistry; β-turn; Azaproline; Ab-initio calculations.

Theoretical Research of the Obtained Isomer in the Synthesis of New Derivative Pyrazolones: DFT Modelling

A. Amar [1, 2], H. Meghezzi [1], Z. Haddadi[1], K. Semar[3], Y.Rachedi[3], M. Hamdi[3]

[1]Laboratoire de Thermodynamique et Modélisation Moléculaire, Faculté de chimie, U.S.T.H.B BP 32 El Alia, 16111 Bab Ezzouar, Alger, ALGERIA
[2]Département de Chimie, Faculté des Sciences, Université Mouloud Mammeri, Tizi Ouzou
[3]Laboratoire de Chimie Organique Structurale, Faculté de chimie, U.S.T.H.B BP 32 El Alia, 16111 Bab Ezzouar, Alger, ALGERIA

Abstract:

Pyrazolones constitute a group of organic compounds that have been extensively studied due to their properties and applications [1, 2]. A great deal of attention has been paid to the analgesic and antipyretic properties of these compounds. Although the use of pyrazolones as drugs has warranted significant attention, many more applications have been devised for this group of molecules outside the pharmaceutical field. For example, they have been applied to the solvent extraction of metal ions and in the preparation of colorants. In the present work, the mechanism for the reaction of synthesis of new derivative pyrazolones has been characterized in detail by means of B3lyp/6-31g* method using Gaussian 03 program, in gas phase and solution. Calculations in ethanol were performed using PCM model [3, 4]. Our study indicates that the reaction can occur according to two approaches, leading to cis and trans product respectively. Full optimization using SCAN method first and followed by QST2 method is done for all the steps of the reaction in the two approaches considered. Vibrational frequencies were analyzed to determine the nature of the stationary points. Our study indicates that the approach 1 is kinetically and thermodynamically favored. In the presented results we explain witch isomer of the product is obtained, witch is impossible to determine experimentally.

Keywords: reaction mechanism, DFT, pyrazolone.

References:

M. L. Kuznetsov, A. I. Dement'ev, V. V. Zhornik, J. Mol. Struct. (Theochem) 571 (2001) 1-3

Jun Li, Li Zhang, Lang Liu, Guangfei Liu, Dianzeng Jia, Guancheng Xu, Inorganica Chimica Acta, 360 (2007) 1995-2001.

S.Miertus, E.Scrocco, J. Tomasi, J. Chem. Phys. 55 (1981) 117.

J. Tomasi, M. Persico, Chem. Rev.94 (1994) 2027.

The Molecular Conformation of 2-Ethylhexyl Acrylate, an Infrared and Abinitio Study

O. BELAIDI[1], T. BOUCHAOUR[1], U. MUSCHKE[2]

[1]Laboratoire de Recherche sur les Macromolécules, Faculté des Sciences, Université Abou Bakr Belkaid, B.P :119 Tlemcen 13000 ALGERIA
[2]Laboratoire de Chimie Macromoléculaire, UMR CNRS N°8009, Université des Sciences et Technologies de Lille, F-59655 Villeneuve d'Ascq Cedex, FRANCE
othmanblaidi@gmail.com

Abstract:

Esters of acrylic acid were widely used as monomers for acrylic polymers, which are further used for production of dyes, paper, textiles, glues, adhesives, paints etc. More than half of the world production of acrylic acid is used to synthesize various acrylic acid: mainly methyl, ethyl, n-butyl, and 2- ethylhexyl acrylates [1].

Introduction:

Extensive research, both experimental and theoretical, has shown that acrylates exist preferentially in two heavy planar structures (s-cis and s-trans). The preferred molecular conformation of these molecules may be of considerable significance in explaining and interpreting some of the proprieties and applications of these compounds [2].

Experimental:

2-ethylhexyl acrylate (purity greater than 99%) was purchased from Sigma-Aldrich and it was used without further purification. The FT-IR spectra of liquid films placed between the NaCl windows were registered within 4000-700 cm^{-1} range using "PERKIN-ELMER MODEL 2000" apparatus.

Computational:

Calculations of harmonic frequencies at fully optimized geometries of planar s-cis and s-tans rotamers at ground state have been performed with Density Functional Theory using B3LYP functional and extended basis sets 6-31G**and 6-311+G**. Scaled 6-311+G** anharmonic frequencies and potential energy distribution have been use as an aid to the assignment of the experimental spectrum over the region of 4000-700cm^{-1}.

A structural comparison is made between the 2-ethylhexyl acrylate and methyl acrylate[3], it shows a good agreement on heavy atoms.

The computed spectrum is in excellent agreement with the experiment and confirms the co-existence of the two planar rotamers (s-cis and s-trans) of nearly equal energy.

References:

Jamro´z MH, Jamro´z ME, Rode JE, Bednarek E, Dobrowolski JC. Vibrational spectroscopy 50 (2009) 231-244.

Tory E, Shouji M, Hideo F,Hiroshi T, Shigehiro K. Journal of molecular structure 352/353 (1995) 193-201.

Orgill M, Baker BL, Owen NL. Spectrochimica Acta Part A 55 (1999) 1021-1024.

Correlation Between Molecular Structure and Inhibition Efficiency Against Corrosion of Two Tautomers of 2-Mercapto 1-Methyl Imidazole

O. Benali[1], L. Larabi[2] et S. M. Mekelleche[2]

[1]Département de Biologie, Faculté des Sciences et de la Technologie, Université de Saïda
benaliomar@hotmail.com
[2]Département de Chimie, Faculté des Sciences, Université de Tlemcen

Abstract:

Several organic substances have been used extensively as a corrosion inhibitor for the past four decades. Among the latter, the heterocyclic compounds containing one or more nitrogen, oxygen and sulfur can affect the inhibition of corrosion of metals and alloys in acid solutions [1-2]. The inhibitory efficacy of a compound depends not only on its structure but also the characteristics of the environment in which it operates, the nature of metal and other experimental conditions. Under certain conditions, the electronic structure of organic inhibitors has a major influence on the effectiveness of corrosion inhibition vis-à-vis the material to be protected. Recently, the quantitative relationship of structure and activity (QRSA) has been a subject of intense interest to many disciplines of chemistry. The development of semi-empirical calculations give quantum chemical approaches to interest scientists involved in the selection of inhibitors by correlating the experimental data with quantum chemical properties.

The aim of this work is to establish a correlation between inhibition efficiency and molecular structures of the two tautomers of 2-mercapto 1-methyl imidazole.

Quantum-chemical indices, namely energy E_{HOMO}, E_{LUMO} energy, the difference $\Delta E=E_{HOMO} - E_{LUMO}$ and dipole moment were calculated. The reactivity of different sites of the molecules was evaluated using indices of Fukui.

The results obtained show that the difference in energy band favors the thione tautomer relatively to thiol, it indicates that the thione form of MMI molecule can be easily transferred electrons to empty d-orbitals of the metal. So a large values of E_{HOMO} and dipole moment μ facilitates the adsorption and consequently the inhibition by influencing the transport process in the adsorbed layer [3]. These results were confirmed by the indices of Fukui.

References:

Benali, O., Larabi, L., Tabti, B., and Harek, Y. (2005), Influence of 1-methyl 2-mercapto imidazole on corrosion inhibition of carbon steel in 0.5M H_2SO_4, *Anti-Corrosion Methods and Materials*, 52, *280-285.*

Benali, O., Larabi, L., Mekelleche S. M., and Harek, Y. (2006), *Journal of materials science, 41, 7064-7073.*

Larabi, L., Benali, O., Mekelleche S. M., and Harek, Y. (2006), *Applied Surface Science, 253, 1371-1378*.

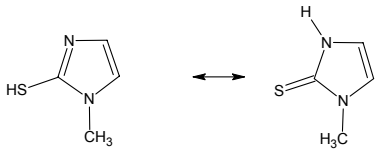

MMI (1) MMI (2)

Figure 1: Molecular structures of 2-mercapto-1-methylimidazole

Physicochemical properties, pollen spectra, and antimicrobial activity of few varieties of honeys harvested in western and central regions of Algeria

[1]Bendahmane M, [2]Oughilas A, [2]Amrani OK, [2]Belaskri G, [2]Bendimered FZ, [2]Koudache F, [2]Bousmaha L, [2]Benhassaini H

[1]Laboratoire LRES, CHU of Sidi-Bel-Abbès,
[2] Department of Biology, Faculty of Sciences, Djillali Liabès University of, Sidi Bel Abbés

Abstract- Honey is the natural food produced by the *Apis mellifera* bee from nectar flowers, and which has long been used by humans for its nutritional and therapeutic properties. The objective of our work is to study the physicochemical properties, pollen spectra, and antimicrobial activity of some varieties of honeys harvested in different parts of western and central regions of Algeria. Th results of physicochemical characteristics (p H, electrical conductivity, moisture, optical rotation), show that the values are consistent with international standards (Codex Alimentarius, EU). The pollen spectra analyses using light microscopy revealed that all samples of honeys are multifloral type, and the number and vegetal species of pollen grains vary from honey sample to another and this according to their floral origin. The study of antimicrobial activity was carried out on 4 different microorganisms (*E. coli, Candida albicans, Pseudomonas aeruginosa, Bacillus cereus*) at different concentrations of honey (10%, 25%, 35%, 50%, 75% and 100%). The results show that the E. coli species is the most sensitive, while *Candida albicans strain* was resistant to the antifungal activity's of all honeys samples tested whatever their botnical origin or concentrations

Keywords: Honey, physicochemical analysis, pollen spectra, antimicrobial activity.

Contribution of microscopic techniques to anatomical and morphological knowledge on *Pistacia atlantica* Desf. ssp. atlantica in Algeria

H. Benhassaini [1], M. Tires [1], K. Sail[2], G. Bassou[2]

[1]-Laboratoire de Biodiversité végétale: Conservation et valorisation
[2]- Laboratoire de Microscopie, Microanalyse de la matière et Spectroscopie Moléculaire
B.P.89, Sidi Bel Abbès, 22000, ALGERIA
ecoreve@yahoo.fr

Introduction: The arid climates have always selectioned a xerophytics plant species which presents a morphological and physiological variations permit to adopt a strategy survey against water deperdition.

The aim of this study was to precise anatomical and morphological features of the species *Pistacia atlantica* Desf. ssp. *atlantica* with the help of current microscopic techniques, those features being of interest as valuable taxonomic characters. Typical hairy structures were observed on all surfaces of the aerial organs and their location, density and size were specified. Both adaxial and abaxial leaf surfaces are covered with trichomes. The leaf surface contains two types of trichomes, covering hairs and glandular hairs. The glandular trichomes are sparsely distributed over the entire leaf surfaces. Unicellular glandular trichomes were recorded in this study. Moreover, we demonstrated the occurrence of stellate trichomes in the leaf blades, these structures were revealed for the first time for this species.

Keywords: Anatomy, morphology, scanning and optic microscopies, stellate trichomes, *Pistacia atlantica* Desf. ssp. *atlantica*.

Metcalf, C.R. Chalk, L. (1950) Anatomy of the dicotyledons: Vol.1. Oxford University Press.

Belhadj, S. Djerridi, A. Aigouy, T. Gers, Charles. Gauquelin, T. and Mevy, J.P. (2007) Comparative morphology of leaf epidermis in eight populations of atlas pistachio (*Pistacia atlantica* Desf., Anacardiceae). Microscopy research and technique, Wiley-Liss. 1-10.

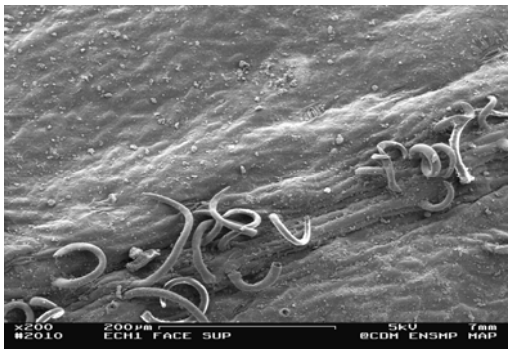

Figure 21: Ciliate trichomes near principal midrib

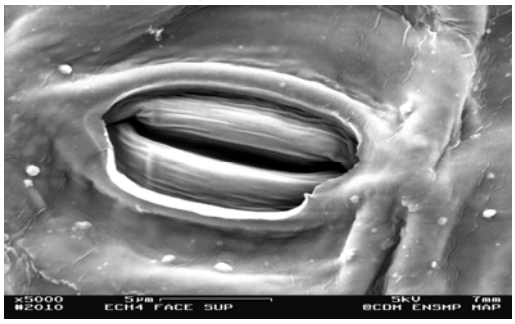

Figure 2: Stomatal type in the species *Pistacia atlantica* studied

Theoretical Study and Car Parrinello Molecular Dynamics (CPMD) Calculation Of The ν_{O-H} IR Spectra for Acetic Acid Cyclic Dimers

M. Benmalti[1,2] Abdelghani Krallafa[b]

[1]Laboratoire de Strusture, Elaboration et Application des Matériaux Moléculaires, Université de Mostaganem
malti23@yahoo.fr
[2]Laboratoire de Chimie-Physique Macromoléculaire, Université d'Oran (Es-Senia)

Abstract:
Both Car Parrinello Molecular Dynamics calculations and a quantum theoretical model are used in order to study the IR spectrum of the acetic acid dimer and its deuterated in the gas phase. The theoretical model is taking into account the strong anharmonic coupling, Davydov coupling, multiple Fermi resonances between the first harmonics of some bending modes and the first excited state of the symmetric combination of the two ν_{O-H} modes and the quantum direct and indirect relaxation. The IR spectra obtained from cpmd is compared with our theoretical lineshape. Note that in a previous work we have shown that our approach reproduces satisfactorily the main futures of the IR experimental lineshapes of the acetic acid dimer [1]

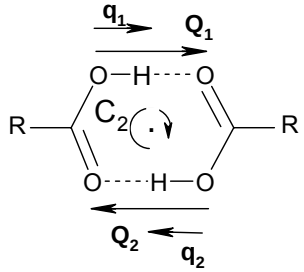

Figure 22: Cyclic H-bond dimer: q_1, q_2 are the coordinates of the high frequency modes and Q_1, Q_2 corresponding to the low frequency modes

References:

M. Benmalti, Paul Blaise, H. T. Flakus, Olivier Henri-Rousseau, Chem Phys, 320(2006) 267-274.

Molecular Dynamics Simulation of a Cold-adapted Enzyme

D. Benrezkallah[1], A. Krallafa[1]

[1]Faculté des Sciences, Laboratoire de Chimie Physique Macromoléculaire LCPM, Université d'Oran Es-Sénia, ALGERIA
berrezmanou@yahoo,fr

Abstract:
Adaptation to both high and low temperatures requires proteins with special properties. While organisms living at or close to the boiling point of water need to have proteins with increased stability, other properties are required at temperatures close to the freezing point of water.

In permanently cold habitats, low temperatures have constrained psychrophilic or cold-adapted organisms to develop enzymatic tools allowing metabolic rates compatible to life and comparable to those of temperate organisms at their respective optimum temperatures (1,2).

Enzymes isolated from cold-adapted organisms are generally characterized by higher catalytic efficiency (K_{cat}/K_m) at low temperature in order to cope with the reduction of metabolic fluxes and chemical reaction rates (3).

A general theory for cold-adaptation has not yet been formulated since different enzymatic families can follow different evolutionary strategies (4,5). Therefore, recently, the research community has focused on comparative structural investigations of homologous proteins adapted to different temperature conditions (6). It turns out, however, that a high intrinsic structural flexibility of cold-adapted enzymes is generally accepted as the main adaptive strategy at low temperatures.

In our study we investigate the role of structural flexibility in cold adaptation of Endonuclease I from psychrophilic Vibrio Salmonicida and mesophilic Vibrio Cholerae. Molecular dynamics simulations have been used to generate structural ensembles at 288 and 310K of the psychrophilic and mesophilic Endonuclease I. we carried out simulations for 10 ns, in the isobaric-isothermic NPT ensemble, applying periodic boundary conditions.

Based on the simulated structures, we find that very few salt-bridges are stable throughout the simulations, and provide little stabilization/destabilization of the proteins. In addition, the hydrophobic core of the two enzymes is almost identical, but the Vibrio Salmonicida Endonuclease has a slightly lower number of internal hydrogen bonds. this is likely to influence both the catalytic activity and the stability of the protein.

References:

D. Georlette, v. blaise, t. Collins, S. D'Amico, E. Gratia, A. Hoyoux, J. C. Marx, G. Sonan, G. Feller, C. Gerday, (2004) Some like it cold: biocatalysis at low temperatures, FEMS Microbiol. Rev. 28, 25-42.

A. O. Smalas, H. K. S. Leiros, V. Os, N. P. Willassen, (2000) Biotechnology Annual Review, vol. 6, Elsevier science B. V., Amsterdam.

P. A. Fiels, (2001) Comp. Biochem. Phys. A 129, 417-431.

G. Gianese, P. Argos, S. Pascarella, (2002), structural adaptation of enzymes to low temperatures, Protein Eng. 14, 141-148.

C. Gianese, F. Bossa, S. Pascarella, (2002), Comparative structural analysis of psychrophilic and meso- and thermophilic enzymes, Proteins 47, 236-249.

S. D'Amico, C. Gerday, G. Feller, (2003), Temperature adaptation of proteins : Engineering mesophilic-like activity and stability in a cold adapted alpha-amylase, J. Mol. Biol. 332, 981-988.

Spectrophotometric Studies of Complexes of Some Electron Donors with Ferric Chloride in Methanol

K. Bentayeb[1], N. Tchouar[1], A. H. Al-Taiar[2]

[1]Faculté des Sciences, Laboratoire LAMOSI, Université des Sciences et Technologie d'Oran USTO
B.P.1505, Oran, 31000, ALGERIA
k_bentayeb@yahoo.fr

[2]Faculté des Sciences, Département de Chimie, Université des Sciences et Technologie d'Oran USTO
B.P.1505, Oran, 31000, ALGERIA

The UV-visible absorption bands for complexes of some electron donors such as Phenylhydrazine, diethyl amine, ethyl diamine, benzyl amine, azobenzene and benzamide with Ferric Chloride and iodine as electron acceptors were obtained and studied in methanol solutions at 300.5 °K in methanol at 25°C. The values of some parameters such as: association constant K^{AD}, molar extinction coefficient ϵ^{AD}, and absorption band energy of the complex, $h\upsilon_{CT}$ were calculated.

The ionization potentials of the electron donors, I^D were calculated from iodine complex band energies. The free energy changes of the association reactions were also calculated. Finally, the kinetics of the above reactions were studied, from which the order of reactions; their half-life periods $t_{1/2}$ as well as their rate constants were obtained.

Theoretical Study of the [2+2]/ [4+2] Competitive Cycloaddition Pathways of Ketenes with Diazadienes

F. Berrahoui[1], B. Messaoudi[1], S. M. Mekelleche[1]

[1]Department of Chemistry, University of Tlemcen, PB 119, Tlemcen, 13000, Algeria.
(b_fethi2000@yahoo.fr ; sm_mekelleche@mail.univ-tlmcen.dz,)

Abstract:
Cycloaddition reactions represent one of the most powerful methods for the synthesis of cyclic and heterocyclic structures with pharmacological interest and for the preparation of natural products [1]. Cycloaddition reactions of ketene species (>C=C=O) with diazadienes [2] can yield to either four-membered or six-membered cycles (***scheme 1***). Our aim in this work is to analyze the substitutent effects on the reaction pathway of these cycloadditions by means of various theoretical approaches, namely, calculations of thermochemical quantities (ΔH, ΔG) for the study of the thermodynamic control, exploration and analysis of the potential energy surface for the prediction of the kinetic control and reaction mechanism.
The favored cyclization mode is predicted by the calculation of activations energies and by the use of DFT-based reactivity indices [3]. The calculations were performed at the DFT/B3LYP/6-31G* and ONIOM levels of theory using *Gaussian 03W* package.
The atomic electronic populations were calculated using Mulliken (MPA), natural (NPA) and electrostatic (MK algorithm) population analyses. The obtained results are in a good agreement with experimental outcomes.

Keywords: [2+2]/[4+2] cycloadditions; Ketenes; Reaction mechanism; Potential energy surface; Regioselectivity; Conceptual DFT.

References:

B. Alcaide, Y. M. Camtalego, J. Plumet, J. R. Lopez, M. A. Sierra, *Tetrahedron*, 1991, 32 803.
E. Rossi, G. Abbiati, E. Pini, *Tetrahedron*, 1999, 55, 6961.
P. Geerlings, F. De Proft, W. Langenaeker, *Chem. Rev*., 2003, 103, 1793.

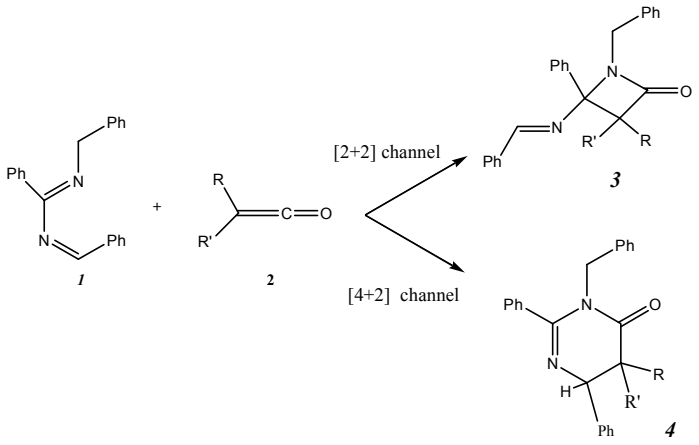

R	R'
H	CO2ET
H	Cl
H	PH
PH	PH
H	CH2=CH
Me	Me
H	Ome
Cl	Cl

Scheme 1

RELAXED ENERGETIC MAPS OF KAPPA-CARRABIOSE : A DFT STUDY

N. BERREKHCHI-BERRAHMA-BESTAOUI[1], M. SEKKAL-RAHAL[1], A. SAYEDE[2] , N. YOUSFI [1]

[1] Faculté des Sciences, Laboratoire L2MSM, Université Djillali Liabes de Sidi Bel Abbès, B.P.89, Sidi Bel Abbès, 22000, ALGERIA
nbesber@yahoo.fr
[2] Faculté des Sciences Jean Perrin, UCCS, UMR CNRS 8181, Université d'Artois, S.P.18, rue Jean Souvraz, Lens Cedex 62307, FRANCE

K-Carrageenan is a sulphated linear galactan[1] polysaccharides of D-galactose and 3,6-anhydro-D-galactose extracted from red seaweeds. It has been abundantly used in the food industry as thickening, gelling[2] and more recently in the pharmaceutical industry.[3]

Carrageenan structures are based on linear chains of alternating 3-linked β-D-galactopyranosyl units, and 4-linked α-D-galactopyranosyl (or 3,6-anhydro-α -D-galactopyranosyl) units, usually sulfated in different positions.[4,5]

The properties of these and other polysaccharides depend on their conformations and molecular flexibility, which is concentrated mostly on the glycosidic linkages.[4]

In this work, we studied the structure and the energy of one of the two repeating disaccharides constituting κappa-carrabiose(4-O-sulphated-α-D-(1→3)-3,6-anhydro-β-D-galactopyranose) shown in figure.1.

DFT calculations using the B3LYP functional and the 6-31G(d) basis set were carried out on the molecules of kappa-carrabiose, and performed with the Gaussian 03 program. The results have been explored using the Gaussview software. The maps have been plotted using the Surfer software.

Relaxed isopotential maps, often called Ramachandran plots, show where regions of low energy occur in the Φ and Ψ glycosidic bonds tortional space.[6]

These energetic contour maps were performed in the gas phase and then by simulating the presence of water as solvent using the Onsager model. We have considered the value of thedielectric constant 78.39 corresponding to polar solvent water. [7] Only one starting conformation has been considered to carry out all the calculations.

The conformational maps have been built as suggested by French and Dowd[8] by interpolating a set of data comprising 144 energy values, which were generated by varying each dihedral angle in increments of 30 deg. Once the set of the two specific values of Φ and Ψ angles fixed, they were kept frozen while optimizing all of the other geometrical parameters.

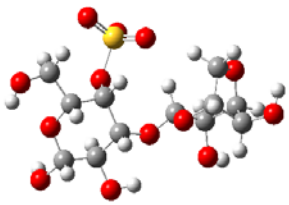

Fig.1: Kappa-carrabiose

Table 1: Φ and ψ (in degrees) and relative energies (Kcal/mole) in phase gas and in water.

Conformer	*Phase gas*		*water*	
	ΔE	*Φ, ψ*	*ΔE*	*Φ, ψ*
A	*0.00*	*85, 113*	*0.00*	*61, -168*
B	*0.35*	*115, 83*	*5.71*	*1, 72*

In each case we have obtained two minima corresponding to the lower energy conformers. In water the molecule is more stable and the energy is lower. Intra-molecular hydrogen bonding is formed and seems to contribute in the stability of the molecule.

References:

Routh Falshaw, Richard H. Furneaux and David E. Stevenson. Carbohydr. Res. 2005, 340, 1149-1158.
Vanessa Leiria Campo.; Daniel Fabio Kawano.; Dilson Braz da Silva Jr., Ivone Carvalho. Carbohydr. Polymers. 2009, 77, 167-180.
Fred van Velde.; Anna S. Antipova.; Harry S. Rollema.; Tatiana V. Burova.; Nataliya V. Grinberg.; Leonel Pereira.; Paula M. Gilsenan.; R. Hans Tromp.; Brian Rudolph and Valerij Ya. Grinberg. Carbohydr. Res. 2005, 340, 1113-1129.
Stortz. C. A. Carbohydr. Res. 2006, 341, 2531-2542.
Stortz. C. A. In Handbook of Carbohydrate Engineering; Yarema, K. J., Ed.; Taylor and Francis: Boca Raton, 2005, 211–245.
Schnupf U.; Willett J. L.; Bosma W. B.; Momany F. A. Carbohydr. Res. 2007, 342, 2270-2285.
7. Gonçalves, P. F. B.; Stassen, H. J. Comput.
8. French A. D.; Dowd M. K. J. Mol. Struct. (Theochem) 1993, 286, 183.

A Comparative X-ray Diffraction Study and Theoretical Calculation on a Nonlinear Optical Material

A. Chouaih[1], N. Benhalima[1], N. Boubegra[1], F. Hamzaoui[1]

[1]Laboratoire SEA2M, Université de Mostaganem, Mostaganem, ALGERIA
achouaih@gmail.com

Introduction:

In recent years an intense worldwide effort has been focused on the design and development of organic conjugated materials with large optical non-linearities due to their potential applications in various optical devices [1–5]. Materials with high non-linear optical (NLO) activities are useful as electro-optic switching elements for telecommunication and optical information processing.

We present here a comparative study of a quantum-chemical analysis and X-ray diffraction study of a new nonlinear optical material structure that belongs to the family of thiazole. The molecular optimized and experimental geometries are obtained via B3LYP/6-31G (d, p) level and X-ray diffraction respectively. The agreement between the experimental and theoretical results such as: bond distance and angle was satisfactory.

Figure below shows the molecule obtained from X-ray diffraction study:

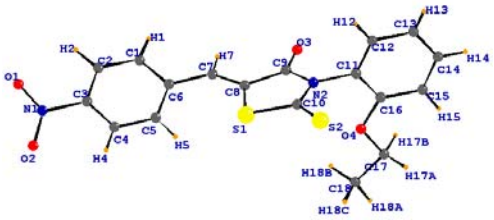

Figure 1: Structure of the molecule

References:

J. Zyss, *Molecular Nonlinear Optics: Materials, Physics and Devices*, Academic Press, New York, 1994.

H.S. Nalwa, S. Miyata (Eds.), *Nonlinear Optics of Organic Molecules and Polymers,* CRC press, Boco Raton, FL, 1997.

M.G. Mkuzyk, *Nonlinear Optical Properties of Organic Materials*, in: SPIE Proceedings, 1997. p. 3147.

K. Clays, B.J. Coe, *Chem. Mater*. 15 (2003) 642.

B.J. Coe, L.A. Jones, J.A. Harrs, B.S. Brunschwig, I. Asselberghs, K. Clays, A. Persoons, *J. Am. Chem. Soc*. 125 (2003) 862.

Design of Copolymeric Films Intended to be Employed in Nonlinear Optical Field: a DF study

S. N. Derrar[1], K. Guemra[2], M. Sekkal-Rahal[1]

[1] Faculté des Sciences, Laboratoire L2MSM, Djillali Liabès University of Sidi Bel-Abbès, ALGERIA
derrarsiham@yahoo.fr
[2] Laboratoire de Chimie Organique Physique et Macromoléculaire, Djillali Liabès University of Sidi Bel-Abbès, ALGERIA

Abstract:

Over the last past decades, many experimental and theoretical investigations have been achieved about creation of new materials serving for nonlinear optics. These devices are intended to be employed in several photonic and optical applications.

Materials are mainly classified upon their first hyperpolarizability β, according to the following equation:

$\mu_i = \mu_i^0 + \alpha_{ij}E_j + \beta_{ijk}E_jE_k + \gamma_{ijkl}E_jE_kE_l + \ldots.$

Where μ_i^0 is the dipole moment of the unperturbed molecule, α_{ij} is the linear polarizability, β_{ijk} and γ_{ijkl}, are the first and second hyperpolarizabilities, respectively.

Our work has been devoted to the study of a family of push-pull molecules, where OH group represents the donor extremity, and a series of acceptor groups has been tested in the other extremity, as well, a phenyl ring enhanced by an alkyl chain $(C=C)_n$ have been employed to ensure the electronic delocalization between the two sides .

Generation of monomers has been established from combination of these chromophores with acryloyle chloride. Grafting of these compounds has been done with methyl methacrylate, to form copolymeric films.

Optimization, calculation of dipole moment and dynamic first hyperpolarizability have been performed using Gaussian03 program package, through a DF study, where B3LYP functional and 6-31G(d) basis set have been selected to carry out this theoretical investigation.

Enhancement of alkyl chain improves gradually β values for all the acceptor groups studied.
Results of first hyperpolarizability magnitudes found for the monomers and the grafted copolymeric oligomers confirm that these systems still have good nonlinear optical properties.

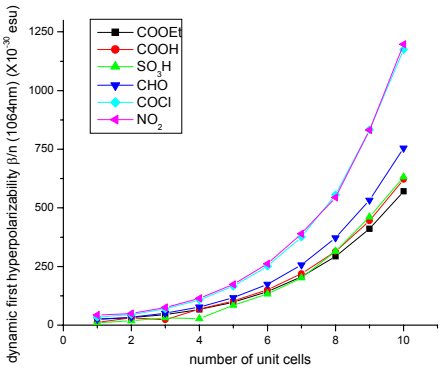

Figure 23: Evolution of dynamic first hyperpolarizability per unit cell (β/n) (1064nm) and chain length.

References:

Chemla, D. S.; Zyss, J. (1987) *Nonlinear Optical Properties of Organic Molecules and Crystals*, Academic Press, Orlando.
Prasad, P. N.; Williams, D. J. (1990) *Introduction to Nonlinear Optical Effects in Molecules and Polymers*, John Wiley and Sons Inc., New York.
Zyss, J. (1994) *Molecular Nonlinear Optics*, Academic Press, Boston.

Structure, Theoritical And Electrochemical Study Of A New Zwitterionic Schiff Base Derivative From DHA.

A.Djedouani[1,2], M.S. Zendaoui[3] A.Bendaas[2], B.Zouchoune[3], M.Allain[4]

[1] Laboratoire d'Electrochimie des Matériaux Moléculaires et Complexes,
[2] Ecole Normale Supérieure De Constantine
Djed_amelle@yahoo.fr
[3]Laboratoire de chimie moléculaire, du contrôle de l'environnement et des mesures physico-chimiques.
[4]Chimie de Coordination, SONAS, EA 921 Faculté de Pharmacie ; Université D'Angers ; 16 Boulevard Daviers, F-49045 Angers Cedex 01, FRANCE

Hydroxy Schiff bases have been extensively studied due to their biological, photochromic and thermochromic properties [Garnovskii, A. D., and al 1993]. They can be used as potential materials for optical memory and switch devices [Zhao, L., and al 2007]. Proton transfer in these compounds forms the basis for an explanation of the mechanisms of various biological processes where proton transfer is the rate-determining step [Lussier, L. S., and al 1987].
In general, *O*-hydroxy Schiff bases exhibit two possible tautomeric forms, the phenol-imine (or benzenoid) and keto–amine (or quinoid) forms. Depending on the tautomers, two types of intra-molecular hydrogen bonds are possible : O–H· · ·N in benzenoid and N–H· · ·O in quinoid tautomers. Another form of the Schiff base compounds is also their Zwitterionic form [Ogawa, K., and al 2003]. Zwitterions of Schiff bases have an ionic intra-molecular hydrogen bond (N^+–H· · ·O^-) and their N^+–H bond lengths are longer than the standard interatomic separations observed in neutral N–H bonds (0.87 Å).

The title Schiff base, $C_{15}H_{15}NO_4$, display a Zwitterionic form, the resulting iminium and hydroxy groups are linked by an intramolecular N–H…O hydrogen bond, and shows an E configuration.. C–H…O interactions, link the molecules into a tree-dimensional network. The compond has the following structural properties : Monoclinic, $P2_1/c$, a=11.739 (2)Å, b=12.107(2)Å, c = 12.521(2)Å, β = 107.590 (14)°, and Z = 4.

Theoretical calculations using DFT method reproduce the observed geometrical parameters and confirm the zwitterionic form.
Density functional theory (DFT) calculations were carried out using the Amsterdam Density Functional (ADF). DFT calculations are carried out without any symmetry constraints. A large HOMO-LUMO gap of 2.54 eV calculated for (I) is in agreement with the molecule stability.
The calculated N-H bond of the zwitterion form equal to 1.113 Å deviates slightly from the experimental one by 0.093 Å, which is longer than the standard interatomic separations observed in neutral N–H bonds (0.87 Å).

An electrochemical study, by cyclic voltammetry for the the compond, has been achieved in aprotic medium, DMF-TBAHFB 0.1M, on a platin electrode of 2 mm of diameter.
A cyclic sweep in the -1.8 to +1.8 V range show an cathodic peak at -1570V and two anodic peaks at 1170 V and -665 V.

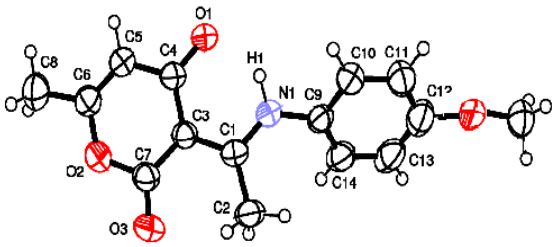

The molecular structure, showing the atom-labelling schema

References :

ADF 2007.01, Scientific Computing and Modelling NV, Theoretical Chemistry (Vrije Universiteit: Amsterdam , The Netherlands, http://www.scm.com.
Garnovskii, A. D., Nivorozhkin, A. L., & Minkin, V. I. (1993). *Coord. Chem. Rev,* 126, 1–69.
Lussier, L. S., Sandorfy, C., Le-Thanh, H. & Vocelle, D. (1987). J. Phys. Chem. 2282–2287, 91.
Ogawa, K., Harada, J. (2003). *J. Mol. Struct.* 211–216, 647.
Zhao, L., Hou, Q., Sui, D., Wang, Y., & Jiang, S. (2007). Spectrochim. Acta A, 1120-1125, 67.

Cys3 His-Zn2+ Interactions with SPC Water Molecules: Computational Study using GROMOS96 Force Field

N. Drici[1], A. Krallafa[1]

[1] Faculté des Sciences, Laboratoire de Chimie Physique Macromoléculaire LCPM, Université d'Oran, B.P. 1524 El M'Naouer Es-Senia, Oran 31000 Algérie
dricinedjoua@univ-mosta.dz, dricinajwa@hotmail.fr

Abstract: A large number of protein domains folds stably by binding a metal ion. In zinc activated proteins the folding phenomenon depends solely on the binding of Zn^{2+} ion and can be studied independently of the bulk protein. Metalloproteines [3] and their metal binding sites are promising targets for specific drug design. The theoretical and computational description of this binding site is a challenging task. A 5ns molecular dynamics simulation is used to explore in detail the structural stability and to gain deep insights on the cluster structure of CCHC–Zn^{2+} domain [4] with explicit SPC water molecules [2]. Such goal is achieved by employing the original structural parameter set and partial charges of GROMOS96 force filed [4] derived for the case of tree cysteinates Cys(-). Only Van Der Waals and Coulomb terms involving the zinc ion were included. The age of the simulation as well as the temperature effect on the dynamical behavior of this system is discussed through several aspects. In terms of radial distribution function (RDF), the divalent zinc ion [1] exerts a strong influence on its hydration shell, leading to a remarkable rearrangement from the initial CCHC coordination to a less stable square planar complex conformation that include SPC water molecules. The lack of explicit polarizability and charge transfer in the GROMOS96 force field leads to poor accuracy. However the results obtained here suggests that other electrostatic treatment methods available in GROMACS package should be tried.

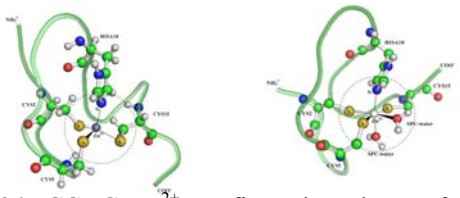

Figure 24: CCHC–Zn^{2+} configuration change from tetrahedral to square planar complex conformation.

References:

Emilie Cauët, S. B., John H. Weare, John L. Fulton, Gregory K. Schenter, and Eric J. Bylaska (2010), Structure and dynamics of the hydration shells of the Zn2+ ion from ab initio molecular dynamics and combined ab initio and classical molecular dynamics simulations, *J. Chem. Phys*, 132, 19450201-19450219.

H. J. C. Berendsen, J. R. G., and T. P. Straatsma (1987), The missing term in effective pair potentials, *J. Phys. Chem*, 91, 6269-6271.

Hanas, J. S., Hazuda, D.J., Bogenhagen, D.F., Wu, F.Y., Wu, C.W. (1983), Xenopus transcription factor A requires zinc for binding to the 5 S RNA gene *Journal of Biological Chemistry*, 258, 14120-14125.

M. F. Summers, L. E. H., M. R. Chance, J. W. Bess, Jr, T. L. South, P. R. Blake, I. Sagi, G. Perez-Alvarado, R. C. Sowder, 3rd, D. R. Hare (1992), Nucleocapsid zinc fingers detected in retroviruses: EXAFS studies of intact viruses and the solution-state structure of the nucleocapsid protein from HIV-1, *Protein Science*, 5, 563-574.

ab initio Conformational Maps for Lactulose in Gas Phase and Aqueous Solution

M.H.Gafour[1]; M. Bouterfas[1], I.N Taleb-Mokhtari[1], M. Sekkal-Rahal[1]

[1]Faculté des Sciences, Laboratoire L2MSM, Djillali Liabès University of Sidi Bel-Abbès, ALGERIA

Abstract*: ab initio* conformational maps for lactulose in both the gas phase and in aqueous solution using the Onsager model have been constructed at the HF/6-31G(d,p) level of calculation. Using quantum mechanical (QM) methods, the energies were plotted against the Φ and Ψ dihedral angles, These plots were compared to those obtained previously in the way of the usual 3D contour maps, which relate the energy with the two glycosidic angles (Φ and Ψ).

The effects of aqueous salvation upon the lactulose are investigated through comparison of the vacuum and aqueous solution free-energy surfaces.

The results of the gas-phase ab initio calculations allows us to conclude that a rigid conformational map is able to predict the regions of the minima in the potential energysurface of lactulose, in full agreement with those found in the relaxed conformational map. The solvation effects do not give rise to locals minima in the potential energy surface of lactulose.

Keywords: Lactulose; energetic relaxed maps; *ab initio* conformational map; HF; Lactulose conformers.

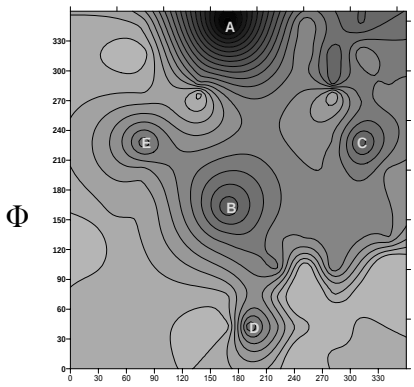

Figure1. Relaxed conformational map calculated for lactulose at HF/6-31G(d,p)
(144 points) using in the successive steps.
Energies are in cal/mol

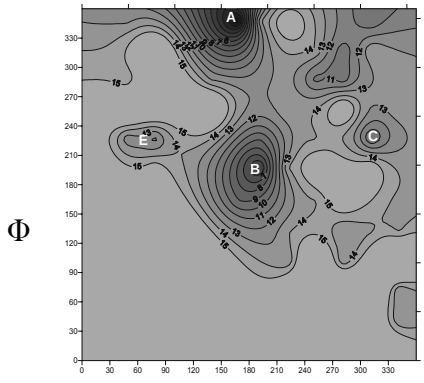

Figure2. Rigid conformational map calculated for lactulose at B3LYP/6-31G(d,p) level (144 points). The energy values are in kcal/mol

Modelling of the Diazepines' Synthesis by PM3 and DFT Methods

Z. HADDADI[1], H. MEGHEZZI[1], A. AMAR[1], R. KAOUA[2], B. KOLLI[2]

[1] Laboratory of Thermodynamics and Molecular Modelling, Faculty of Chemistry, U.S.T.H.B. B.P.N° 32 El Alia, 16111 Bab Ezzouar, Algiers, ALGERIA
haddadizehira@Yahoo.Fr
[2] Laboratory of Structural Organic chemistry, Faculty of Chemistry, U.S.T.H.B., B.P.N° 32 El Alia, 16111 Bab Ezzouar, Algiers, ALGERIA

Introduction:

Our work is to study the reaction of synthesis of diazepines by action of aliphatic amines on the pyrone ring, which presents very important pharmacological and biological properties [1]. Calculations were carried out in gas phase by semi empirical method PM3 [2] and DFT [3] method with B3LYP functional and 6-31G** basis using the chain of program G98 and G03. Above all, the research of the stability of the compounds studied and the results show that compound 2 is more stable with a value of -229.82898 a.u. in DFT and 78.2 kcal/mol by PM3 method. Then, we studied the reactivity of aliphatic diamines on DHA, using for this purpose, different indices of responsiveness in order to study, explain and identify the intermediate states and transition states. The nature of the reaction studied was identified by calculating the energy gap between the frontier orbitals. The study found that the electron transfer takes place from compound 2 (or compound 3) to the compound 1 with a value of chemical potential -127.8 kcal / mol in DFT. With the indices of hardness and softness , we show that aliphatic diamines are large relative hardness of the pyrone ring is a compound with a soft character and is the most electrophilicity index as found equal to 352.0 kcal / mol . The studied reaction is then hard and soft character. We were interested in the study of the stability of the tautomeric forms that are reactional intermediate met in this reaction. The results are in favour of way 1 of reaction path 1. We gave the energy profile to make the synthesis of diazepines [4].

The obtained results are in good agreement with the experimental values.

References:

B. Kolli (1982) thesis of doctor of state, Algiers.
J. J. P. Stewart (1989) *J. Comput. Chem*., 10, 209, ibid, 10, 221-264.
Yang W. Lee and R. G. Parr, *Phys. Rev. B*, 37.785, 1988.
Z. Haddadi, H. Meghezzi (2010) *Communication presented in the 9th Days of Theorical and Computational Chemistry (JCTC9*), Constantine.

Structure and Charge Distribution, Electronic and Vibrational (Hyper) Polarizabilities of Some Twist Intramolecular Charge Transfer Chromophores

M. Hadj Ben Ali[1], A. Saal[1,2], O. Ouamerali[1]

[1] Laboratoire de Physico-Chimie Théorique et Chimie Informatique,
faculty of chemistry USTHB university, Algiers 16111, ALGERIA
diakiti79@yahoo.fr
[2]Department of Chemistry, UMMTO university,Tizi-ouzou 15000, ALGERIA

Abstract:
Nonlinear optical materials are largely investigated by experiments and theorists as well because of their technological applications. At the microscopic level these nonlinear optical (NLO) properties are governed by the tensors hyperpolarizabilities.

Among the different material types which are candidate for the application in the field of nonlinear optics, the polyconjugated organic materials have attracted a particular interest. Due to the donor/acceptor ends capped conjugated system, the charges may move along the backbone and thus very easy to be polarized. It has been shown in many papers, that these materials always exhibit large nonlinear optical properties [1,2].

The push-pull considered molecules are represented in Chart 1. They are constituted of two rings: Nmethyl-(*p*-oxophenyl)-pyridine (PPP) and its derivatives. These derivatives are obtained by substituting a hydrogen atom in the positions R_{10}, R_{11}, R_{17}, and R_{18} by methyl radicals, Figure 1.

Chart 1

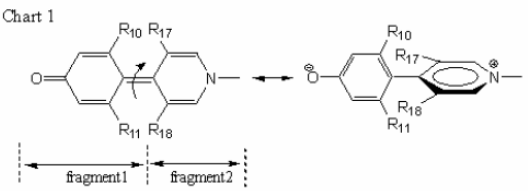

Molecule	R.10	R.11	R.17	R.18
I	H	H	H	H
II	Me	H	H	H
III	H	H	Me	H
IV	Me	Me	H	H
V	Me	H	Me	H
VI	Me	H	H	Me
VII	H	H	Me	Me
VIII	Me	Me	Me	H
IX	Me	H	Me	Me
X	Me	Me	Me	Me
XI	t-Bu	t-Bu	t-Bu	t-Bu

Figure25: Structure of push-pull molecules used in this letter

Dipole moment, vibrational and electronic isotropic polarizabilities and first hyperpolarizabilities have been determined for all the molecules under consideration at the HF/6-31G level.
The vibrational contributions to the (hyper)polarizabilities have been computed using the formulation of Bishop and Kirtman. The study have been mainly focused in the effect of the inter ring twist angle upon these quantities and upon the inter ring bond character and the BLA. It has been found that tuning the twist angle affects substantially both electronic and geometrical structures. The results show that ground state dipole moment, electronic (hyper)polarizabilities increases with the dihedral inter ring angle however the vibrational quantities $\Delta\alpha^v$ and β^v show a maximum value at ~78°.The calculations have been performed by using GAUSSIAN03 package.

References:

B. Champagne, B. Kirtman In Nalwa, H.S., ed. *Handbook of Advanced Electronic and Photonic Materials and Devices*, vol.9:*Nonlinear Optical Materials*; ©2001 by Academic Press.
D.S. Chemla, J. Zyss, Eds. *Nonlinear Optical properties of Organic Molecules and Crystals*; Vol.1 and Vol.2, Academic Press: New York, 1987.

QUINTET ELECTRONIC STATES OF N2

M. Hochlaf[1], H. Ndome[1] and D. Hammoutène[2]

[1]Université Paris-Est, Laboratoire Modélisation et Simulation Multi Echelle,
MSME UMR 8208 CNRS, 5 bd Descartes, 77454 Marne-la-Vallée, FRANCE
[2]Laboratoire de Thermodynamique et Modélisation Moléculaire, Faculté de Chimie,
USTHB, BP32 El Alia, 16111 Bab Ezzouar, Alger, ALGERIA

Introduction:

Two quintet electronic states of N_2 are known, namely the $A'^5\Sigma_g^+$ and the $C''^5\Pi_{ui}$. They were widely investigated theoretically and experimentally because of the $A'^5\Sigma_g^+$ involvement in the N_2 afterglow $B^3\Pi_g - A^3\Sigma_u^+$ and because of the eventual perturbation of the N_2 $^3\Pi_u$ states by the $C''^5\Pi_{ui}$. In addition, the $C''^5\Pi_{ui} - A'^5\Sigma_g^+$ system was predicted by Partridge et al. [1] to be responsible for the Hermann Infrared bands (HIR), which remained unassigned for more than thirty years. Later, Huber and Vervloet confirmed this theoretical prediction through the analysis of their high resolution emission spectra relative to this system [2,3].

In the literature, both theoretical and experimental studies suggested the existence of couplings between the close lying quintet and triplet electronic states via spin-orbit interactions. There are, however, no ab initio treatments of these non-diagonal couplings and nothing is said about the eventual existence of other bound quintet electronic states and of their influence on the dynamics of the valence-Rydberg states of N_2 (located well below the ionization threshold).

In this theoretical contribution [4], we present the potential energy curves of the quintets and other spin-multiplicity electronic states of N_2, which are lying in the 0 - 110 x 10^3 cm^{-1} energy range with respect to N_2 ($X^1\Sigma_g^+$). Using these highly correlated wavefunctions, we deduce their spin-orbit coupling evolutions. These curves and data are used later to derive accurate spectroscopic terms and the lifetimes of these quintets and to discuss their metastability.

References

H. Partridge, S. R. Langhoff, C. W. Bauschlicher, Jr. and D. W. Schwenke, *J. Chem. Phys*. 88, 3174 (1988).

K. P. Huber and M. Vervloet, *J. Chem. Phys*. 89, 5957 (1988).

K. P. Huber and M. Vervloet, *J. Mol. Spectrosc*. 153, 17 (1992).

M. Hochlaf, H. Ndome, D. Hammoutène, *J. Chem. Phys*. 132, 104310 (2010).

QUANTUM CHEMISTRY STUDY OF LANTHANIDE (III) COMPLEXES WITH TRI&BIDENTATE OXYGEN LIGANDS

D Hannachi,[1] N Ouddai[2] ,H Chermette[3]

[1]Faculté des Sciences, Département de Chimie, Université de Ferhat Abbas -Sétif- – ALGERIA
H_douniazed@yahoo.fr.
[2]Faculté des Sciences, Laboratoire de Chimie et Chimie de l'Environnement, Université El-Hadj Lakhdar - Batna – ALGERIA
[3]UNIVERSITE DE LYON; Université Lyon 1 et CNRS UMR 5180. Sciences Analytiques; Laboratoire de Chimie Physique Théorique, bât Dirac, 43 bd du 11 novembre 1918, 69622, Villeurbanne cedex, FRANCE

Kay words: Triflate; Prchlorate; Tridentate; Bidentate; Tricapped Trigonal Prismatic geometry (TTP); Trigonal Prismatic Geometry (TP).

Abstract : Density functional theory has been used to probe the electronic structure, coordination number, optical properties and the vibration spectra of monolanthanide trifluoromethane sulfonate Ln(OTf)3 and perchlorate lanthanide $Ln(ClO_4)_3$ complexes where Ln = La, Ce, Nd, Eu, Gd, Er, Yb and Lu. The study reveals that the OTf and ClO_4 groups are bonded to Ln as a bidentate ligand. TDDFT calculations show that, for $La(OTf)_3$, MLTC and HOMO–LUMO transitions in the UV-vis are strongly bathochromically shifted compared to those of $Lu(OTf)_3$.

Introduction: The trivalent lanthanide ions have a wide range of coordination numbers (CN = 3–12). The size of the ligand and the steric hindrance determine mainly the geometry, the coordination number and the ligand packing around the metal ions in a way to minimize ligand–ligand repulsion. Lower coordination numbers can be achieved with very bulky ligands such as $N(SiMe_3)_2$, whereas the highest coordination numbers are usually achieved with chelating ligands, which have small angles such as NO_3^-. Furthermore, the ligand can bond the metal in many ways; in particular, the triflate ligand [$CF_3SO_3^-$ = OTf⁻] may adopt different coordination modes in complexes (μ_1, μ_2, μ_3 or μ 0, the non-coordinating free anion);[1] for example, $[M(OTf)_3(terpy)_2]$ complexes where M is a lanthanide or a actinide are monodentate,[2] whereas the $[(U(OTf)_2(OPPh_3)_4)]$ complexes contain one monodentate and one bidentate [OTf-].[3]The same feature exists for the perchlorate [ClO_4-] group, which could act as a monodentate and bidentate ligand.[4]

Lanthanide triflates $Ln(OTf)_3$ are important in a wide variety of applications such as organic synthesis.[5] They are mild and selective catalysts, which have been used widely in carbon–carbon and carbon–heteroatom bond-forming reactions, including Mukaiyama,[6] Friedel–Crafts,[7] esterification, aromatic nitration,[8] and Diels–Alder[9] reactions. These catalysts are regarded as environmentally safe because of their low toxicity, ease of handling, stability in water, no corrosiveness and their ability to be reused.

In this paper we carry out a quantum calculation based on the density functional theory (DFT) of the lanthanide triflate and perchlorate (see Fig. 1 and Fig. 2 respectively). Our aim is to study the changes of the geometry with the variation of coordination number between six (TP geometry) and nine (TTP geometry), furthermore we report the computational study on $Ln(OTf)_3$ where Ln = La, Ce, Nd, Eu, Gd, Er, Yb and Lu.[10]

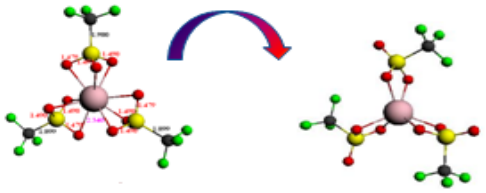

Figure 26: Structure of the $Ln(OTf)_3$ complex

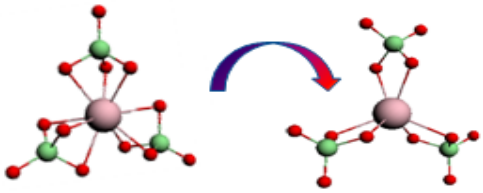

Figure 2: Structure of the $Ln(ClO_4)_3$ complex

References

Hitchcock, P. B., Hulkes, A. G., Lappert, M. F., Protchenko, A. V. (2006) Journal of Inorganica Chimica Acta, 359, 2998.

Berthet, J. C., Nierlich, M., Miquel ,Y. (2005) Journal of Dalton Trans, 369.

Berthet, J. C., Lance, M., Nierlich, M., and Ephritikhine, M. (1999) Journal of *European Journal* of Inorganic *Chemistry*, 2005.

Brandàn, S.A. (2009) Journal of THEOCHEM, **908**, 19.

Kobayashi, S., Sugiura, M., Kitagawa, H., Lam, W. W. L. (2002) *Chemical* Reviews, 102, 2227.

Kobayashi, S., Hachiya, I. (1994) Journal of Organic Chemistry, 59, 3590.

Kawada, A., Mitamura, S., Kobayashi, S. (1996) Journal of Chemical Communications, 183.

Theoretical Studies (DFT and TDDFT) on Structures and Spectroscopic Properties of Series of Novel iridium complexes

A. Kadari[1,2], C. Adamo[3], M. Brahimi[1]

[1]Laboratoire Physico-chimie Théorique et Chimie Informatique, Faculté de Chimie, U.S.T.H.B, BP 32 Al-alia ; Babezzouar ; Alger ALGERIA
[2]Département de Chimie, Université Mouloud Maamri, Tizi Ouzou ALGERIA
Amel_kadari@yahoo.fr
[3]Laboratoire d'Electrochimie et Chimie Analytique, Ecole Nationale Supérieure de Chimie de Paris (ENSCP) FRANCE

Introduction: The obvious main energy source for renewable energy is coming from the sun. Dye-Sensitized Solar Cells (DSSC) is considered as being the most promising solution for harnessing the energy of the sun and converting it into electrical energy. Among phosphorescent metal complexes, iridium (III) complexes appear to be the most intensively explored owing to their easy syntheses and excellent color tunability (Chang, C.-J and al. Evans, RC and al.) They are attracting wide spread interest because of their unique photophysical properties and applications in organic light-emitting diodes (OLEDs) (Lowry, M.S. and al.). Geometries, electronic structures, and spectroscopic properties of a novel series of neutral iridium (III) complexes with cyclometalated ligands were investigated using density functional theory (DFT).
The UV-Visible absorption and phosphorescence spectra in CH_2Cl_2 environment are simulated with the TD-DFT level with IEFPCM models. The calculated results are in good agreement with the experimental ones.

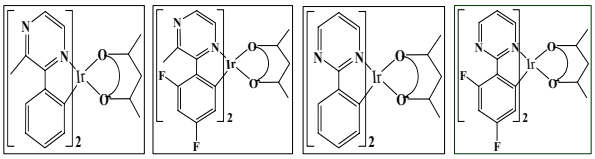

(MPPZ)$_2$ Ir (acac) I | (DFMPPZ)$_2$ Ir (acac) II | (PPM)$_2$ Ir (acac) III | (DFPPM)$_2$ Ir (acac) IV

Figure 1 : O1-O2 = acetylacetone (acac)
N1-C1 ≡ N1'-C1' = 2-Methyl-3-PhenylPyrazine (MPPZ) (I)
= 2-(2,4-DiFluoroPhenyl)-3 -MethylPyrazine (DFMPPZ) (II)
= 2- PhenylPyrimidine (PPM) (III)
= 2-(2,4-DifluoroPhenyl)-Pyrimidine (DFPPM) (IV).

Content: In this work, we report a theoretical study of the structures and the photophysicals properties of new iridium (III) diazine complexes. The first is the iridium (III) pyrazine complex and the other is the iridium (III) pyrimidine with H and F different substituents, respectively. These complexes are prepared and studied experimentally by Ge, G. and al. and showed in figure 1.

The goal is to study the structure, the absorption and emission spectra of the $(OL)_2Ir$ (acac) complexes. Density Functional Theory (DFT) and Time Dependent DFT (TD-DFT) have used to investigating and predicting electronic properties in both the ground and excited states. The Polarized Continuum Model (PCM) is used to simulate bulk solvent effect. The combination of the DFT methods with the PCM model, for inclusion of environmental effect, leads to a reasonable agreement with the experimental data.

Computational Details: All calculations were carried out using the Gaussian03 package. To calculate state geometries and excitation energies the DFT and TDDFT were employed.
The geometries of the investigated complexes were optimized using a Perdew-Burke-Enzerhof hybrid Functional model (abbreviated PBE1PBE).
Both of the electronic properties and structural optimizations calculation, for all atoms were described by the valence double-ξ basis set 6-31G (d, p), excepted the Iridium ones that is described by the pseudo-potential LANL2DZ basis set. In this work, only the 40 lowest singlet-singlet excitations at the S_0 optimized geometries will be discussed. At the optimized geometries we performed TD-DFT calculations at the same level of theory with the same basis set in gas phase and in Dichloromethane (CH_2Cl_2) solvent by means of the IEFPCM model.

References:

Chang, C.-J. Yang, C.-H. Chen, K. Chi, Y. Shu, C.-F. Ho, M.-L. Yeh, Y.-S. Chou, P.-T. *J. Chem. Soc*., Dalton Trans. 1881, (2007).
Evans, RC. Douglas, P. Winscom, C.J. Coord. *Chem. Rev*. 250, 2093 (2006).
Ge, G. He, J. Guo, H. Wang, F. Zou, D. *J. of Organometallic Chemistry* 694 (2009) 3050-3057.
Lowry, M.S. Bernhard, S. Chem. Eur. J. 12 (2006).
Tsuzuki, N. Shirasawa, T. Suzuki, S. Tokito, *Adv. Mater.* 15, 1455 (2003).

A DFT study of the mechanism, regio- and stereoselectivity of 1,3-dipolar cycloaddition of phosphorylated nitrone with substituted alkenes

A. khorief Nacereddine[1], A. Djerourou[1]

[1]Laboratoire de Synthèse et Biocatalyse Organique, Département de Chimie, Faculté des Sciences, Université Badji Mokhtar Annaba
B.P.12, Annaba, 23000, ALGERIA
a.khoriefnacereddine@lsbo-univ-annaba.dz

Abstract:

1,3-Dipolar cycloaddition (1,3-DC) are important processes in synthetic chemistry and are widely used for obtaining five-membered heterocyclic compounds[3]. Reactions between nitrones and alkenes leading to isoxazolidines are among the best known processes of this kind,[2]as substituted isoxazolidines have been found to exhibit antimicrobial activity[1], numerous applications as enzymes inhibitors,[6] intermediates in the synthesis of a variety of compounds after cleavage of the N-O bond.[4] A significant amount of theoretical and experimental work has been devoted to the study of the selectivities of 1,3-dipolar cycloaddition.

Piotrowska[5] found, experimentally that the 1,3-DCs of *C*-diethoxyphosphoryl-*N*-methyl nitrone with allyl alcohol and methyl acrylate were regiospecific and stereoselective (scheme) affording the corresponding 1,5-*trans*-cycloadduct as the major regio- and diastereoisomer (Table).

We have study theoretically the mechanism, the regio- and stereoselectivity of these reactions using DFT method at the B3LYP/6-31G(d,p) level of theory. The FMO analysis and DFT based reactivity indices confirmed the experimental *ortho* rgioisomeric pathway. Potential energy surface analysis shows that these 1,3-dipolar cycloaddition reactions favored the formation of the *ortho-trans* cycloadduct in both cases. Bond order and charge analysis show that the studied reactions are undergoing through concerted synchronous mechanism.

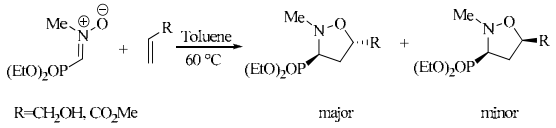

Figure**:** 1,3-Dipolar cycloaddition of *C*-diethoxyphosphoryl-*N*-methyl nitrone with alkenes

Table: Experimental regio- and stereoselectivity Ratios

Reaction	*R*	*ortho:meta*	*trans:cis*
1	CH2OH	100:0	62:38
2	CO2Me	100:0	90:10

References:

Ding. P., Miller. M., Chen. Y., Helquist. P., Oliver. A. J., Wiest. O. (2004) Org. Lett, 6, 1805-1808. 2004.

Gothelf. K. V., Jørgensen, K. A. (1998**)** Chem. Rev, 98, 863-909, 1998.

Padwa. A. (1984) *1,3-Dipolar Cycloaddition Chemistry*; Wiley: New York, 1984 .

Padwa. A., Pearson. W. H. (2002) *Synthetic Applications of 1,3-Dipolar Cycloaddition Chemistry Toward Heterocycles and Natural Products*; Wiley & Sons:New-York,2002.

Piotrowska. Dorota G. (2006) Tetrahedron Letters, 47, 5363-5366, 2006,

Wess. G., Kramer. W., Schubert. G., Enhsen. A., Baringhaus. K. H., Globmik. H., Müller. S., Bock. K., Klein. H., John. M., Neckermann. G., Hoffmann, A. (1993) Tetrahedron Letters, 34, 819-822, 1993.

Modeling stability conditions the different structures of Gas Hydrates

S. M. Messabih[1], N. Tchouar[2]

[1]Faculté des Sciences, Département de chimie, Laboratoire de la Chimie de l'Environnement,
Université Djillali Liabes de Sidi Bel Abbès, ALGERIA
newsbox2005@yahoo.fr
[2]Faculté des Sciences, Laboratoire de Modélisation et Simulation des Systèmes Industriels (LAMOSI),
Université des Sciences et Technologies d'Oran (USTO),
PB 1505 el Menaouer Oran- ALGERIA
lamosi2002@yahoo.fr

Abstract: The main objective of the study of gas hydrates or clathrates is to determine the conditions of pressure and melting temperature of these systems in one of the already known crystal structures (structures sI, sII and structure and structure H) [1].

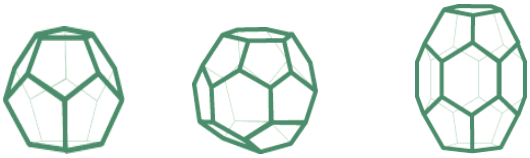

Structure sI Structure sII Structure H

However, the complexity of a mathematical model and physical chemical does not allow easy calculations for gas hydrates. In addition, the large number of thermodynamic intensive variables, independent, and therefore, different theoretical models used to describe these systems, make computer programming inevitable. Many models rely on numerical methods due to the complex equations of state included.
Computer programming is an essential means to organize codes Modeling and Simulation dedicated to physical phenomena such as gas hydrates.
These codes of Bakker [2] are designed using programming languages like C++ that allow you to insert all sorts of data or formulas (equations, chemical formulas, values ...) and create a database used in the calculations.
The various results are established and recorded in a file at the end of each calculation. The main objective of our work is to study the structural and thermodynamic properties in different conditions of temperature and pressure of gas hydrates such as methane, carbon dioxide, ethane and nitrogen.

Keywords: Gas Hydrates, Structure sI, Structure sII, Structure H, Bakker codes, structural and thermodynamic properties.

References:

Sloan E.D., "Gas Hydrates: Review of Physical/Chemical Properties", Energy & Fuels, Vol. 12, No. 2, 1998.
Bakker R.J., Computer andt Geosciences, 23, 1-18, 1997.

Theoritical Studies of Phosphirine Polyanions Using Density Functional Theory DFT

A. SADI[1], S. MOUSSI[1,2], O. OUAMERALI[1,2]
[1] Ecole Doctorale Physique Chimie Théorique Chimie Informatique
Faculté de Chimie USTHB BP N°32 El Alia BAB EZZOUAR
chantyqui@gmail.com
[2]Laboratoire de Physico-Chimie Théorique et Chimie Informatique.
Faculté de Chimie, USTHB, BP 32, ElAlia 16111 BabEzzouar, Alger. ALGERIA
Sofiane_moussi@yahoo.fr

Introduction: The phosphirines aroused the interest of many researchers, because of their applications in several fields: in chemistry of coordination To study the hyper valence of phosphorous[1,2], in chemistry containing organo-phosphorous for their synthesis and their reactivity[3] and too the homogenous catalysis while being used as ligands stabilizing of the gold nanoparticules4,5.

The 2,4,6- triphenyl-λ3-phosphinin belongs to the family of λ3-phosphabenzenene, homologous with pyridines which are heterocyclic and planar aromatic systems. The –CH fragment of the arylic part of benzene is substituted by a phosphorous atom (see figur1).

Our work consists to the theoretical study of the fundamental state of the phosphirine and its ion: the cation and the mono, di and tri anions in order to highlight the chemical properties of each structure.

For this study we used the density functional theory DFT, because of the convincing results which it gives. The calculations were carried out using Gaussian (GW 03) to the level of hybrid functionel B3lyp with 6-31(D,P) and 6-31+G (D,P).

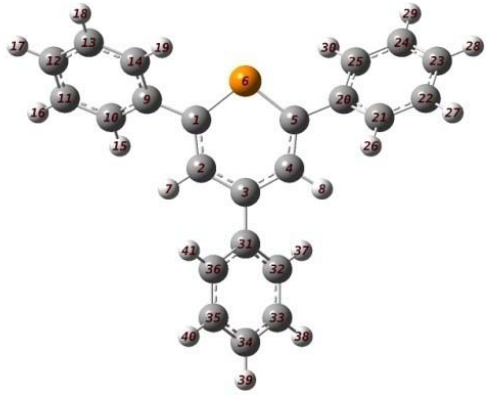

Figur1: 2, 4,6-triphényl-λ^3-phosphinine

Key words: Phosphinine, DFT, Polyanions, Phosphorous.

References:

Märkl G (1990) Multiple bonds and low coordination in phosphorus chemistry, .Georg
Mathey F, Le Floch P (2004) Science of synthesis, vol. 15, Thieme Verlag, p. 1097
Le Floch P (2006) Coord Chem Rev 250: 627
Weber L (2002) Angew Chem Int Ed 41: 653
Müller C, Vogt D (2007) Dalton Trans 47:5505

Physico-chemical study Microbiological some varieties of Local honey

A. Oughilas[1], M.Bendahmane[2], H.Benathmane[2], F.Ba[2.]

[1]Faculté des Sciences, Laboratoire LMC, Université Djillali Liabes de Sidi Bel Abbès, B.P.89, Sidi Bel Abbès, 22000, ALGERIA
oughilasahmed@yahoo.fr
[2] Faculté des Sciences Laboratoire de microbiologie Université Djillali Liabes de Sidi Bel Abbès, B.P.89, Sidi Bel Abbès, 22000, ALGERIA

Summary

Honey is the only food on earth produced by insects and consumed by humans. Given the therapeutic and nutritional quality, we process to physic-chemical, microbiological and sensory analyses of eight samples, five of them are local honeys and three others are imported honey.
The results obtained showed that all the honey samples meet the required standards of Codex Alimentarius (2001) and they are natural. In addition, a diversity of values of viscosity, water content and conductivity is observed.
The microbiological analyses have shown a total absence of pathogen germs with the exception of the sample from Mali origin.

Key words:

Honey, physic-chemical, microbiological, sensory tests, pathogen germs.

References:

ANCHLING. F, (2001) : Raconte-moi le miel..., l'abeille de la France. Revue autorisées par Apicervices françaises.
ANDRIEN, (2006): Fabriquer carburant et composé organique à partir du fructose. Extrait du BE U.S.A N°43. 1p.
BARBIER M, (1968): Biochimie de l'abeille. Biologie et physiologie générale in traité de biologie de l'abeille .tome ². Ed Masson et Cie. 536p
BOGDANOV S, (1999): Stockage - cristallisation e liquéfaction du miel. Centre suisse de recherche apicoles .05p.
BOGDANOV S, RUOFF K, ODDO PL, (2004): physicochemical methods for the characterization of unifloral honeys .apidologie 35. 17p.
CHAUVIN. R (1968) : Actions physiologiques et thérapeutiques des produits de la ruche, in Traité biologique de l'abeille, Tome 3. Edition Masson de Cie, Paris. Pp : 116-155.
ZIEGLER. H, (1968) : La sécrétion du nectar, in Traité biologique de l'abeille, Tome 3. Édition Masson de Cie, Paris. Pp : 218-247.

Interactions Between κ-Carrabiose and Some Ions of Alkali Metals

C. REGUIEG[1], N. YOUSFI[1], M. SEKKAL-RAHAL[1] A. SAYEDE[2], ILHEM N.TALEB[1]

[1;] Faculté des Sciences, Laboratoire L2MSM, Université Djillali Liabes de Sidi Bel Abbès, B.P.89, Sidi Bel Abbès, 22000, ALGERIA
reguiegc@yahoo.fr
[2] Faculté des Sciences Jean Perrin, UCCS, UMR CNRS 8181, Université d'Artois, S.P.18, rue Jean Souvraz, Lens Cedex 62307, FRANCE

Introduction: In this work, we were interested in a theoretical study of the electronic and molecular structures for the κ-carrabiose in both, vacuum and solvent cases and of its complexes (interactions) with alkali metal cations : Li^+, Na^+, and K^+. For this goal, the calculations of quantum chemistry were carried out with the Gaussian03 program.
Then geometry optimizations at the level of theory B3LYP/6-31G(d) were performed with all the conformers of lower energies.
Among the methods of quantum chemistry for the evaluation of the macrocyclic ligands, the density functional theory (DFT), with hybrid B3LYP has certain advantages. It can be an appreciable tool by providing a precise conformational analysis,[4-6] and has much less problems of convergence[2] than those usually met for pure methods DFT.
Moreover, the 6-31G(d) basic set reproduced the experimental data often better than other several basic sets [1,3,7]
full optimizations of geometry of A and B conformers, and all the complexes were carried out on the level B3lyp/6-31G (d).

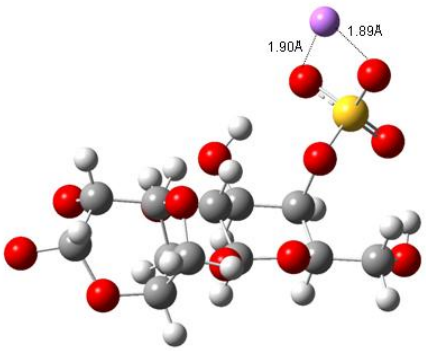

Figure 01: Optimized structure of the conformer corresponding to A minimum of (κ-carrabiose) calculated at B3LYP/6-31G(d) in vacuum, (ϕ,ψ) fixed $[Li^+]$ ion

The first general result that one can draw from the various tables is that the complexes κ-carrabiose--Li^+ form the shortest bonds compared to the complexes with Na^+ and K^+ cations. This is due probably to the small size of the ions Li^+ which can approach more the κ-carrabiose molecule.

Conformer	(φ,ψ) fixed	ΔE	Bond Length (Å) Alkali Ion - O	
			O1	O2
A	(171, 151)	2,16	1.89	1.90
B	(51, -178)	-	-	-
C	(-69, 91)	0,00	1.89	1.89
D	(81, 91)	1,82	1.90	1.89
E	(-69, 151)	0,95	1.88	1.89

Table 01: Various local minima calculated at B3LYP/6-31G(d) correspondent to κ-carrabiose-ion in the vacuum, ΔE in (kcal/mol).¶

Concerning energies of the different conformers, we note, such as one would have thought it a priori, that the value of energy becomes increasingly low with the increase in the size of the studied complex, energy of Li^+ until K^+.

References:

Francl, M. M.; Petro, W. J.; Hehre, W. J.; Binkley, J. S.; Gordon, M. S.; DeFree, D. J.; Pople, J. A. *J Chem Phys* 1982, 77, 3654.

Lee, C.; Yang, W.; Parr, R.G. Development of the Colle-Salvetti correlation-energy formula into a functional of the electron density. *Phys. Rev. B.* 1988, 37, 785-789.

Nicholas, J. B.; Hay, B. P.; Dixon, D. A. *J Phys Chem* 1999, 103, 1394.

Su, C. C.; Lu, L. H.; Liu, L. K. *J Phys Chem* A 2003, 107, 4563.

Su, C. C.; Lu, L. H. J Mol Struct 2004, 702, 23.

Hsieh, T. J.; Su, C. C.; Chen, C. Y.; Liou, C. H.; Lu, L. H. J Mol Struct 2005, 741, 193.

Rassolov, V.; Pople, J. A.; Ratner, M.; Windus, T. L. *J Chem Phys* 1998, 109, 1223.

Theoretical Study of The Transition State of The Cyanidobis (Cyclooctatetraenyle) Compound in DFT / Zora Relativistic

B. Teyar[1], L. Belkhiri[1], M. Ephritikhine[2], A. Boucekkine[3]

[1] Research Unit Environmental Chemistry and Molecular Structural (URCHEMS) University Mentouri Constantine, Constantine 25017, ALGERIA
billel_teyar@yahoo.fr
[2]CEA Saclay, DSM, IRAMIS, UMR 3299 CEA / CNRS SIS2M, 91191 Gif-sur-Yvette cedex.
[3]UMR CNRS 6226 chemical Sciences-Rennes, University of Rennes1, Campus Beaulieu 35042 Rennes Cedex, FRANCE

Introduction:

Since the synthesis in 1968 of the first complex sandwich uranocène (η^8-$C_8H_8)_2U$ by Streitwezer and Müller-Westerhoff [1], many more compounds derived reagents have been characterized. These mono-sandwich structures (η^n-C_nH_n) M (X) x (L) 4-x (n = 7, 8 and 9) [2] which are better organometallic precursors for the synthesis of elements f such as inverse sandwich shaped uranium L_nU (η^n-C_nH_n) UL_n(n=7,8)[3].

The chemistry of f elements currently raises an increasing interest both experimental [4] and theoretical [5]. Among these compounds, those actinide 5f show interesting molecular properties including a large structural flexibility and responsiveness of single metal - ligand.

On a structural level, these particular molecules are characterized by a coordination sphere of the central ion more open and therefore more reactive. Other $COTAn^{III}Cp$ mixed sandwich complexes of trivalent actinides were also synthesized in recent years [6], and were more reactive than their counterparts sandwich (η^n-C_nH_n) $2An^{IV}$. We offer a few examples fairly representative of this class of compounds; theoretically study their structural and electronic properties. Technically, we implement the Theory of Density Functional Relativistic [7] which has proved particularly advantageous and well suited for calculating large molecular systems. We will use the code ADF2009 (Amsterdam Density Functional) [7b], and the relativistic ZORA basis (TZP) [7] coupled with functional exchange and correlation BP86 whose performance in the study of organometallic systems of heavy elements is well established.

Figures:

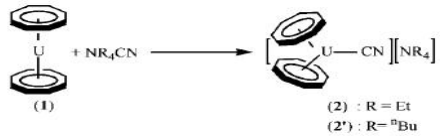

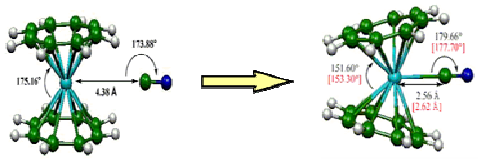

Figure 27: cyanido complex bis (cyclooctatetraenyle $((\eta^8$-$C_8H_8)_2U$ CN

Table: Optimization of molecular geometries and linear bent

$U^{+4}COT_2$ CN	U-C1	U-COT_1	U-COT_2	C1-N	C1-U-COT_1	C1-U-COT_2	COT_1-U-COT_2	U-C1-N
Coudée	2,56	2,06	2,06	1,18	104,15	104,23	151,60	179,66
Linéaire	4,38	1,96	1,96	1,18	92,34	92,44	175,16	173,88
X-Ray	**2,62**	**2,03**	**2,03**	**1,16**	**102,50**	**104,20**	**153,30**	**177,70**

References:

Streitwieser, A., Jr.; Müller-Westerhoff, U. *J. Am. Chem. Soc. 1968, 90, 7364.*

D. Baudry, E. Bulot, M. Ephritikhine, M. Nierlich, M. Lance, J. Vigner, *J. Organomet. Chem., 1990, 388, 279.*

P. L. Diaconescu, P. L. Arnold, T. A. Baker, D. J. Mindiola, C. C. Cummins *J. Am. Chem. Soc. 2000, 122, 6108-6109.*

(a) D. Seyferth, *Organometallics 23* (2004) 3562-3583 (b) M. Ephritikhine, *Roy. Soc. Chem. Dalton Trans.*, (2006) 2501–2516.

(a) Kaltsoyannis, N. *Chem. Soc. Rev.* 2003, *32*, 9–16. (b) Evans, W. J.; Kozimor, S. A.; Ziller, J. W.; Kaltsoyannis, N. *J. Am. Chem. Soc.* 2004, *126*, 14533. (c) Belkhiri, L. ; Lissillour, R ; Boucekkine. A., *J. Mol. Struct*. (*theochem)* 757 (2005) 155.

T. Arliguie, M. Lance, M. Nierlich, M. Ephritikhine. *J. Chem. Soc*., *Dalton Trans*. *1997, 2501–2504.*

(a) van Lenthe, E.; Ehlers, A.; Baerends, E. J. *J. Chem. Phys.* 1999, *110*, 8943.(b) ADF2009 release, SCM, Theoretical Chemistry, Vrije University, Amsterdam, The Netherlands; http://www.scm.com.

Conformational DFT Study of κ-Carrabiose in gas phase and aqueous solution

N. YOUSFI[1] M. SEKKAL-RAHAL[1] A. SAYEDE[2], C. REGUIEG[1], I.N.TALEB[1], M. SPRINGBORG[3]

[1] Faculté des Sciences, Laboratoire L2MSM, Université Djillali Liabès de Sidi Bel Abbès, B.P.89, Sidi Bel Abbès, 22000, ALGERIA
nordyp@gmail.com
[2] Faculté des Sciences Jean Perrin, UCCS, UMR CNRS 8181, Université d'Artois, S.P.18, rue Jean Souvraz, Lens Cedex 62307, FRANCE
[3] Physikalische und Theoretische Chemie, Universita¨t des Saarlandes, Postfach 15 11 50, Saarbruecken 66041, GERMANY

Introduction: κ-Carrageenan is a linear polyoside abundantly used as a texturing agent for various applications in food, chemical, and pharmaceutical industries, this is due to its physical property to form thermoreversible gels[6] that are related to its conformation. The structure of one of the two repeating disaccharides constituting κ-carrageenan; the 4-O-sulfated-b-D-galactopyranosyl (1,4) 3,6-anhydro-β-D-galactopyranose (see Fig. 1) is studied in this work.

During these two last decades, many works dealing with conformational studies of carbohydrates have appeared; most of them used classical methods to explore the structure of the conformers, such as molecular mechanics.[1–5]. More recently, a number of articles, using ab initio or density functional theory (DFT) studies, have begun to appear.[5–13]

The B3LYP density function was used with the 6-31G(d) basis set to perform relaxed energetic contour maps of the charged form of κ-carrabiose in the gas phase and for the neutral form first in the gas phase and then by simulating the presence of water as solvent using the Onsager model. Only one starting conformation has been considered to perform all the calculations. Rigid energetic maps have been then constructed either by addition of diffuse or polarization functions to the basis set obtaining in that way 6-311G(d)//6-31G(d), 6-311G(d,p)//6-31G(d), and 6-31111G(d,p)//6-31G(d) energetic maps that have been carefully examined. The obtained structures corresponding to the lower energy conformers have been then fully optimized using different basis sets with the B3LYP method, a reversion in term of energy has been observed for the two first minima in the case of the charged disaccharide in the gas phase, this was attributed to the large grid of 30° that could lead to the exclusion of an intermediate value corresponding to the real minimum of energy. We thus suggest that after establishing potential energy maps it is essential to proceed to full optimizations of the lower energy conformers. Calculations using the more accurate correlated method MP2 with the 6-31G(d) basis set have also been performed for conformers of the two disaccharides in the gas phase.

Figure 1: Structure of κ-carrabiose disaccharide, dihedral angles Φ and Ψ around the glycosidic linkage, and exocyclic angles of the hydroxymethyl group and hydroxyls groups.

References:

Csonka, G. I.; Sosa, C. P.; Csizmadia, I. G. *J Phys Chem A* 2000, 104, 3381.
Da Silva, C. O.; Nascimento, M. A. C. Carbohydr Res 2004, 339, 113.
French, A. D.; Kelterer, A.-M.; Johnson, G. P.; Dowd, M. K.; Cramer, C. J. *J Mol Graph Model* 2000, 18, 95
French, A. D.; Johnson, G. P.; Kelterer, A.-M.; Dowd, M. K.; Cramer, C. J. *J Phys Chem A* 2002, 106, 4988.
Gould, I. R.; Bettley, H. A.; Bryce, R. A. *J Comput Chem* 2007, 28, 1965.
Moir,A.; Smith,D.A. A. Rev Microbiol 1990,44, 531.
Melberg, S.; Rasmussen, K. Carbohydr Res 1979, 27.
Navarro, D. A.; Stortz, C. A. Carbohydr Res 2008, 343, 2292.
Momany, F. A.; Willet, J. L. *J Comput Chem* 2000, 21, 1204.
Stortz, C. A. Carbohydr Res 1999, 322, 77.
Stortz, C. A. Carbohydr Res 2006, 341, 2531.
Tvaroska, I. *Biopolymer*s 1982, 21, 1887.
Wang, Z. X.; Duan, Y. *J Comput Chem* 2004, 25, 1699.

Sandwich Complex Containing Ge Atoms: Comparative Studies With Ferrocene

S. ZAATER [1], A. RAHMOUNI[2], M. BRAHIMI[1,2,3]

[1]Laboratoire de Physico Chimie Théorique et de Chimie Informatique.
Faculté de Chimie. USTHB. BP N° 32 El Alia, Alger. ALGERIA
[2]Laboratoire de Modélisation et de Méthodes de Calcul. Centre Universitaire
Docteur Moulay Tahar de Saïda.
[3] Chercheur Associé au Centre de Recherche en Analyses Physico Chimiques.
C.R.A.P.C. BP 248 Alger RP 16004 Alger
sihemzaater@yahoo.fr

Abstract:

We perform, at the DFT/B3LYP level, a theoretical studies of different conformations of new sandwich complex **$(GeC_4H_5)_2Fe$** and compared them to the ferrocene ones **(figure 1) [1]**. The results show that the reaction of formation of the ligands $GeC_4H_5^-$ anion would be as favourable as $C_5H_5^-$. The1-ferrogermene **$(GeC_4H_5)_2$ Fe** has four stables structures **(figure 2)**, Contrary to the ferrocene **$(\eta^5\text{-}H_5C_5)_2Fe$** ones, so that we can obtain some possible reactivities for the 1-ferrogermene. The **IR** spectra shows a little resemblance with the ferrocene and the **$(GeC_4H_5)_2$ $Fe_{1\text{-}1'Hin}$** structure. In the ferrocene IR spectrum appear two vibrations, induced by iron-π CPD cycle interactions, noted $\zeta_{Fe} \longrightarrow$ and $\zeta_{Fe}\uparrow$ which not appear in the 1-ferrogemene. Whereas, in the 1-ferrogermene spectra, appear some vibrations, induced by sigma interaction from the Fe and the Ge atoms and the hydrogen ones, respectively.

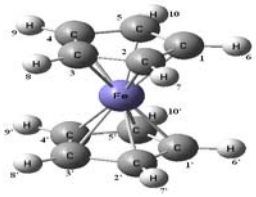

Figure 1: Eclipsed structure of ferrocene

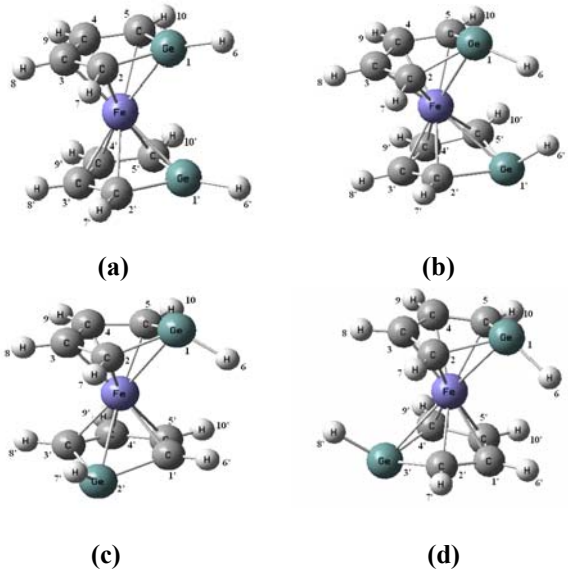

Figure 2: Structures of (a) **$(GeC_4H_5)_2Fe_{1\text{-}1'Hex}$** (b) **$(GeC_4H_5)_2$ $Fe_{1\text{-}1'Hin}$**, (c) **$(GeC_4H_5)_2$ $Fe_{1\text{-}2}$**, and (d) **$(GeC_4H_5)_2$ $Fe_{1\text{-}3'}$,** obtained at the B3LYP/6-31G* level.

Keywords: ferrocene, 1-Ferrogermene, DFT.

References:

S. Coriani, A. Haaland, T. Helgaker, P. Jorgensen. Chem. Phys. Chem. 7 (2006) 245-249.

Prediction of New Solid Catalysts by the Technique of Datamining

Z. Djelloul[1], H.AOURAG [2]

[2]LEPM, URMER, Department of Physics, University Abou Bakr Belkaid,
Tlemcen 13000, ALGERIA

Abstract:
The reasonable choice of solid catalysts for the synthesis of various inorganic and organic compounds at low cost is a challenge for decade's futures. Although empirical approaches are widely used in the manufacture of catalysts, modeling methods such as calculating the first principle should be explored and developed.(1-5)

We present a new approach based on data mining, for designing new materials for industrial use as heterogeneous catalysts more efficient and this by using the structural properties, thermodynamics and elastic new transition metal alloys and other metals of the periodic table bit exploited. The principal component analysis (PCA) (6-9) and partial least square regression (PLS) (10) , computer techniques has been applied to predict new materials.

Trends of the hardness and ductility of these materials are identified using physical and empirical criteria, and validated with experimental observations. The B / G the shear modulus (G) and compressibility (B) are used to evaluate the behaviors: fragility and ductility of alloys of transition metals.

Applying these trends to the selection of materials to design more efficient catalysts shows that this approach can be used not only to interpret existing experimental observations, but it could also be used to predict new materials with desired properties .

Keywords: Physical properties; heterogeneous catalysts, transition metal; Datamining

References:
Davids JR, Allen P, Lampman SR et al., *(ASM International, Metals Park, OH, 1990), Vol.(1997) 217-231 Catalytic combustion of diesel soot over metal oxide catalysts.*
V. Ponec, G. Bond;Metals *Catalysis by metals alloys,handbook, 10 th ed., editedby*
Elsevier 1995
G. ERTL , *Heterogeneous Catalysis on the Atomic Scale, Fritz-Haber-Institut der Max-Planck-Gesellschaft, Faradayweg* 4–6, D–14195 Berlin, Germany
Received 26 June 2000; accepted 11 July 2000
Hagen J-*Industrial Catalysis*
A Practical Approach, 2006, Wiley ed.
MATHIAS B. GUNTHER, *heterogeneous catalysis research progress*, 2008
Carlos Henriques *Heterogeneous Catalysis – II,* , 2009
M.A. Chikh, *"Analyse du signal ECG par les réseaux de neurones et la logique floue :Application à la reconnaissance des battements ventriculaires prématurés"*, Thèse présentée devant l'Université de Tlemcen, 2005.
I.T. Jolliffe *"Principal component analysis"*, Springer-Verlag, New York, 1986.
K.I. Diamantaras, S.Y . Kung, *"Principal component neural networks. Theory and*
applications", John Wiley and Sons , 1996.
P. Bastien, V. Esposito. Vinzi, M. Tenenhaus, *" PLS generalised linear regression"*,Computational Statistics Data Analysis 48 (2005) 17-46.

RESENTATION DU LOGICIEL DE CALCUL ADF : APPLICATION A L'ETUDE DE REACTION D'INTERCONVERTION DES ISOMERES DU CLUSTER $Fe_4N_2(CO)_{12}$.

N. Guechtouli[1, 2], H. Meghezzi[2], J.-Y. Saillard[3], S. Kahlal[3]

[1]Université de Mouloud Mameri UMMTO, Tizi Ouzou

[2]Laboratoire de Thermodynamique et Modélisation Moléculaire (LTMM), Faculté de chimie, USTHB, Alger, ALGERIA

[3]Unité sciences chimiques de Rennes (UMR – CNRS 6226), 35042 Rennes Cedex, FRANCE

Nabila_gue@yahoo.fr

Le programme ADF (Amsterdam Density Functional) est un programme de Fortran pour des calculs sur des atomes et des molécules (dans la phase gazeuse ou en solution), pour tous les éléments du tableau périodique. Il a été développé à l'Université de Vrije à Amsterdam par Baerends et collaborateurs [1]. Il peut être employé dans la spectroscopie moléculaire, la chimie organique et inorganique, la cristallographie et la chimie pharmaceutique. Une BANDE séparée de programme est disponible pour l'étude des systèmes périodiques: cristaux, surfaces, et polymères.
Le programme de COSMO-RS est employé pour calculer les propriétés thermodynamiques des fluides. Il se base sur l'approche de Kohn-Sham à la théorie de la fonctionnelle de la densité(DFT).
Pour les systèmes moléculaires contenant des éléments lourds, des effets relativistes (ZORA et Spin-Orbite) sont implémentées, en utilisant des orbitales de Slater parfaitement adaptées pour le traitement de ces composés.
Ce logiciel existe en plusieurs versions.

Dans le cas de notre travail, nous nous intéressons à l'étude de réaction d'interconversion des clusters organométalliques contenant des éléments du groupe principal, à 8 PES de formule $M_4E_2(CO)_{12}$. Nous prenons M=Fe, et E= N.

Le cluster $Fe_4N_2(CO)_{12}$ présente quatre isomères de squelette possibles ; la géométrie A(C_{2h}) correspond au composé octaédrique closo, les géométries B(C_{2v}) et C(C_{2v}) correspondent aux composés nido avec soit la rupture d'une liaison E-E, soit la rupture de la liaison M-M et la structure octaédrique distordue D(C_2).

Afin d'étudier la stabilité relative de ces clusters, une optimisation de géométrie a été faite pour chaque isomère suivi de calculs de fréquences des modes normaux de vibration, en DFT/BP. Les deux composés B(C_{2v}) et D(C_2) sont les plus stables par rapport aux

autres isomères. De ce fait, nous avons envisagé leur interconversion hypothétique.

Le chemin choisi est celui qui nécessite le déplacement minimum des atomes. Un axe de symétrie C_2 est conservé durant la transformation D(C_2) → B(C_{2v}) qui implique une rotation et une ouverture de vecteur N…N. Une courbe d'énergie sera déterminée. La caractérisation d'un intermédiaire de réaction nécessite un temps de calcul très important.
Les résultats obtenus sont comparés aux données trouvées dans la littérature.

Mots clé : ADF, clusters, DFT, stabilité, interconvertion.

Harmonic dynamics of β-D- RHAMNOSE in the crystalline state.

N .BEKHTI-BENSALEM[1], M. SEKKAL-RAHAL[1], M.H. GAFOUR[1].

[1]Faculté des Sciences, Laboratoire L2MSM, Université Djillali Liabes de Sidi Bel Abbès, B.P.89, Sidi Bel Abbès, 22000, ALGERIA
nabilachimie@yahoo.fr

Abstract: Throughout this work we have reproduced the vibrational spectrum of Rhamnose monohydrate using the calculation of normal modes of vibration of this monosaccharide in the crystalline state. A basis adjustment of frequencies from the potential function Urey-Bradley-Shimanouchi the principal enunciated by T. Shimanouchi is confirmed.

Keywords: Rhamnose; Crystalline state; Urey-Bradley - Shimanouchi.

Introduction: The method used to determine the frequencies and normal modes of vibration is adapted from the Wilson and *al*. GF method (E. Wilson, J. Decius, 1958) and it uses the local symmetry coordinates developed by Shimanouchi (T. Shimanouchi, 1963)

The frequency calculation of the internal intermolecular vibration has been accomplished using the CVOA (Crystalline Vibrations Optically Active) program. This program has been written by Takeuchi (Takeuchi H, 1975).

Crystallographical data, infrared and Raman spectra used in the normal mode analyse of the β-D-Rhamnose in the crystalline state.

β -D-Rhamnose monohydrate crystallises in a monoclinic system, the spatial group is then $P2_1$, with number of cells is 25 and 2 molecules per cell. The unit cell parameters are: a = 7.906, b = 7.921 and c = 6.673 Angstroms.

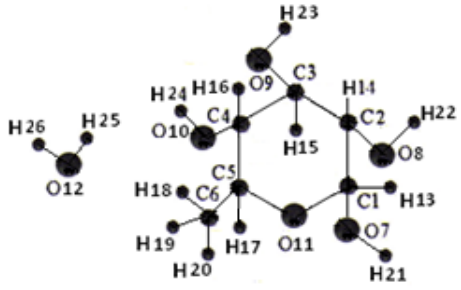

Figure 1: β-D-Rhamnose monohydrate and atomic numbering used in calculations.

The initial set of parameters is derived from the alpha-L-Fucopyranose forces field previously established (Taleb Mokhtari I.N and al, 2003).

Results and discussion: The differences in the values of force constants are mainly due to the methyl group and the Hydrogen bonds. The vibrational spectrum of Rhamnose monohydrate is reproduced. A good agreement between calculated and observed frequencies is achieved after fitting the initial force field.

We shall now discuss the assignments for different spectral regions:

The 3600-2500 cm^{-1} range: These frequencies are related to the contribution of the OH bonds of water molecules, the liability of the hydroxyl groups in solution and CH streching modes.

The 2800-1600 cm^{-1}range: Just one band is observed and calculated in this range is due to vibration of the molecule of water.

The 1700-1200 cm^{-1}range: Topically, the infrared, as well as the Raman, spectra of sugar molecules exhibit many bands in this range. These bands are due to the coupling of vibrations involving the hydrogen atoms (HCH, CCH, HCO and COH).other interesting band are observed in this range, corresponding to the endocyclic hydroxyl-methyl group.

The 1200-950 cm^{-1} range: The interpretation of results in this region is difficult because of strong coupling between a lot of modes of ring bonds: attractive and repulsive bending (COH, OCH, CCH, and HCH) also stretching bands (C-O and C-C).

The 950-750 cm^{-1}range: Although few bands are observed in this range, their coupling is an important point to consider.

The 750-200 cm^{-1}range: In this part of the spectrum, the vibrational modes are generally tortional C-C, C-O modes and CCO, CCC, OCO, COC bending modes.

The range below 200 cm^{-1}: These bands are due to the intramolecular vibrations as well as the lattice vibrations.

Conclusion: The vibrational spectroscopic data of the β-D-Rhamnose molecule have been well reproduced from the modified Urey-Bradley-Shimanouchi force field. So, the principle of transferability is conserved since the initial force field of Fucose was modified only for the groups for which the geometry or the configuration is different. This new parameters are needed for future calculations on di and oligo-saccharides including the Rhamnose as a unit.

References:

Shimanouchi T. (1963) Pure Appl. Chem. 71 131.
Taleb Mokhtari I.N., Sekal-Rahal M. and Vergoten G. (2003) Spectrochimica Acta Part A 59, 607-616.
Takeuchi H. (1975) Ph D thesis, Tokyo, Japan.
Wilson E., Decius J. and Cross P. (1958) Molecular Vibrations (Chapter 4), McGraw Hill, New York, 1958, pp. 54-76 (Chapter 4).

Structure, dynamics and ligand binding of the DEAF-1 MYND domain by NMR

Fatiha Kateb [1,2], Helene Perrin[3], Konstantinos Tripsianes[1,2],Peijian Zou[1,2], Roberta Spadaccini[4],Matthew Bottomley[5], Stephane Ansieau[3], Michael Sattler[1,2]

[1] Institute of Structural Biology, Helmholtz Zentrum München, Ingolstädter Landstr. 1, 85764 Neuherberg, Germany
[2] Lehrstuhl für Biomolekulare NMR-Spektroskopie. Department Chemie, Technische Universität München, Lichtenbergstr. 4, 85747 Garching
fatiha.kateb@tum.de
[3] INSERM U590, Centre Leon Berard; Universite Claude Bernard Lyon I, Lyon 69373.
[4] Dipartimento di Chimica, Università degli Studi di Napoli "Federico II", Via Cintia, 80126 Napoli, Italy
[5] Merck, 126 E. Lincoln Ave., Rahway, NJ 07065

The characterization of the structural and dynamical properties of biomolecules plays a central role in the study of biological functions. NMR is a method of choice not only because it enables the determination of the 3D structure of biomacromolecules such as proteins or nucleic acids, but also because it provides unique tools to study the dynamical aspects of molecular functions. The human transcriptional regulator DEAF-1 is involved in embryonic development and implicated in clinical depression and suicidal behavior (Gross and McGinnis 1996; Lemonde, Turecki et al. 2003). It contains a MYND domain, a cysteine-rich region that is organized in a C4-C2HC motif enabling the binding of two Zn ions. Its transcription regulation activity is mediated through interactions with co-repressors such as NCoR and SMRT

We report the solution structure, dynamics and ligand binding of the MYND domain of the human transcriptional regulator DEAF-1. The structure reveals a cross-brace topology for the C4C3H zinc binding motif, common to other MYND domains as expected from the high sequence similarity observed among this protein family[3]. ^{15}N NMR relaxation data and analytical ultracentrifugation data reveal an oligomerization tendency at high micromolar concentrations.
The binding to 10-residue peptides derived from SMRT and NCoR co-repressors has been characterized by NMR titrations. The binding site mapped by the chemical shift perturbations agrees well with the one reported for the ETO MYND domain for related peptides. A dissociation constant in the mM range was estimated from the NMR titration. We show that DEAF-1 MYND domain also behaves as a protein-protein interaction domain that can recruit co-repressors, and thus confirmed its transcriptional function.

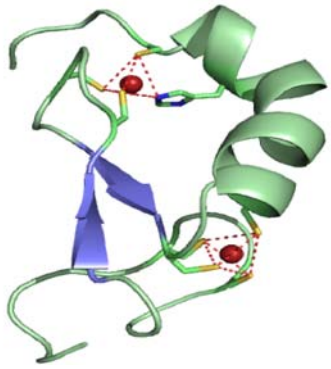

Figure 28: Ribbon representation of the DEAF-1 MYND domain. Side-chains of the residues coordinating the zinc atoms are shown as sticks. Zinc coordination geometry is highlighted in red dots and reveals a perfect tetrahedron

References:

Gross, C. T.; McGinnis, W., DEAF-1, a novel protein that binds an essential region in a Deformed response element. *EMBO J.* **1996,** *15* (8), 1961-1970;
Lemonde, S.; Turecki, G.; Bqkish, D.; Du, L.; Hrdina, P. D.; Bown, C. D.; Sequeira, A.; Kushwaha, N.; Morris, S. J.; Basak, A.; Ou, X.; Albert, P. R., Impaired Repression at a 5-Hydroxytryptamine 1A Receptor Gene Polymorphism Associated with Major Depression and Suicide. *J. Neurosci.* **2003,** *23* (25), 8788-8799.
Liu, Y.; Chen, W.; Gaudet, J.; Cheney, M. D.; Roudaia, L.; Cierpicki, T.; Klet, R. C.; Hartman, K.; Laue, T. M.; Speck, N. A.; Bushweller, J. H., Structural Basis for Recognition of SMRT/N-CoR by the MYND Domain and Its Contribution to AML1/ETO's Activity. *Cancer Cell* **2007,** *11*, 1-15.

Theoretical study of tautomerization and iomerization of methylphosphino- and Phenylphosphino-substituted cyclic azaphospholines, oxphospholines and thiaphospholines in gas and aqueous phases

S. Abdalla[1], M. Springborg[1]

[1] Physical and Theoretical Chemistry, University of Saarland, 66123 Saarbrücken, Germany
s.abdalla@mx.uni-saarland.de

The effect of solvation on tautomeric equlibrium of five member ring heterocyclic system has been subject to many studies[1-4]. Through studies in the tautomerization in different environment it has been found that the environment is important for relative stability of various tautomers. Results of several study on compounds containing amidine group-NH-C(R)=N- have been reported[5-12]. As natural of those we have recently started a theoretical study of the isoelectronic systems containing the -PH-C(R)=N- group by replacing a single nitrogen atom by phosphous atom[13,14]. The present work is a continuation of this work by investigating system containing -PH-C(R)=P- , group.

Different isomers and tautomers of methylphosphino-and phenylphosphino-substituted cyclic azaphospholine, oxaphospholine and thiaphospholine have been investigated theoretically in gas and aqueous phases. Special emphasis is put on the relative energies and on the changes in the order of stability due to substitution or solvation. The calculations were carried through using the B3LYP/6-31+G(d,p) method. The calculations in the aqueous media were done by considering two different models, i.e. the PCM–SCRF and the Microsolvated/SCRF model. The solvent affects strongly the relative stability and the order of stability of different tautomers and isomers.

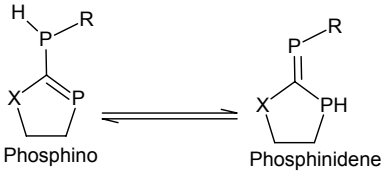

Figure 29: Structures isomers and tautomers of methylphosphino-and phenylphosphino-substituted cyclic azaphospholine, oxaphospholine and thiaphospholine

References:

[1] Karelson, M. M. , Katritzky, A. R. , Szafran, M. (1990) Zerner, M. C. , J. Chem. Soc. Perkin Trans. 2. 1990, 195, 1990.
[2] Woodcock, S. , Green, D. V. S. ; Vincent, M. A. , Hillier, I. H. , Guest, M. F. , Sherwood, P. (1992) J. Chem. Soc. Perkin Trans. 2. 1992, 2151, 1992.
[3] Luque, F. J. , Lŏpez-Bes, J. M. , Cemeli, J. , Aroztegui, M. , Orozco, M. (1997) Theor. Chem. Acc. 96, 105, 1997.
[4] Nagy, P. I. , Tejada, F. R. , Messer, Jr. , W. S. (2005) J. Phys. Chem. B 109, 22588, 2005 .
[5] de Vries, A. H. , van Duijnen, P. Th.(1992) Biophys. Chem. 43, 139, 1992.
[6] Raczynska, E. D. , Taft, R. W.(1998) Polish J. Chem. 72 , 1054, 1998.
[7] Caminiti, R. , Pieretti, A. , Bencivenni, L. , Ramondo, F. , Sanna, N.(1996) J. Phys. Chem. 100 , 10928, 1996.
[8] Remko, M. ,Walsh, O. A. , Richards, W. G.(2001) Chem. Phys. Lett. 336 , 156, 2001 .
[9] Remko, M. , Walsh, O. A. , Richards, W. G. (2001) Phys. Chem. Chem. Phys. 3, 901, 2001.
[10] Marchand-Geneste, N. , Carpy, A. (1999) J. Mol. Struct. Theochem 465 , 209, 1999.
[11] Remko, M. , Walsh, O. A. , Richards, W. G.(2001)J. Phys. Chem. A 105 , 6926, 2001.
[12] Remko, M. , van Duijnen, P. Th. , Swart, M. (2003) Struct. Chem. 14 , 271, 2003.
[13] Abdalla, S. , Springborg, M. (2010) J. Phys. Chem. A 114 , 5823, 2010.
[14] Abdalla, S. , Springborg, M. , J. Mol. Struct. (THEOCHEM) (2010) doi:10.1016/j.theochem.2010.09.024.

Author Index

Acknowledgement

The organizing committee thanks all of the sponsors of this Conference and particularly the main one:
The Alexander Von Humboldt-Stiftung,
Bonn, Germany
www.avh.de

Alexander von Humboldt
Stiftung/Foundation